RENSIT:
RadioElectronics. NanoSystems. Information Technologies

Journal "Radioelectronics. Nanosystems. Information Technologies" (abbr. RENSIT)
publishes original articles, reviews and brief reports, not previously published, on topical problems in **radioelectronics (including biomedical) and fundamentals of information, nano- and biotechnologies and adjacent areas of physics and mathematics.**

Designed for **researchers, graduate students, physics students of senior courses and teachers**.
It turns out **2 times a year** (that includes 2 issues)

Authors of journal are academicians, corresponding members and foreign members of Russian Academy of Natural Sciences (RANS) and their colleagues,
as well as other russian and foreign authors on presentation of their manuscripts by the members of RANS, which can be obtained by authors before sending articles to editors.
And also after its receiving - on recommendation of a member of editorial board of journal, or another member of Academy of Natural Sciences, that gave her opinion on article at request of editor.
The editors will accept articles in both **Russian and English** languages.

Articles are internally peer reviewed (**double-blind peer review**) by members of the Editorial Board.
Some articles undergo external review, if necessary.

Journal RENSIT is included in the **DB SCOPUS, EBSCO Publishing,** in the international abstracts database - **Ulrich's International Periodicals Directory**,(USA, New York, http://www.ulrichsweb.com), in the **AJ and DB VINITI RAS** (http://www.viniti.ru), and DB **Russian Science Citation Index (RSCI** http://elibrary.ru/project_risc.asp).
Full-text content is posted in the DB of the **Russian Scientific Electronic Library**
- information resource on the Internet http://elibrary.ru and is available for registered users.
And also - in Open Access **CyberLeninka NEB** of Russian Federation http://cyberleninka.ru.
On journal's website http://www.rensit.ru posted metadata publications
and **RENSIT: Radioelectronics. Nanosystems. Infomation Technologies - english version** (cover-to-cover translation) of journal, which is a party to **CrossRef.**

The founder - the **Russian Academy of Natural Sciences**
Publisher - Publishing Center of the Russian Academy of Natural Sciences
Publisher Address: 119002 Moscow, per. Sivtsev Vrazhek 29/16

CONTENTS

RUSSIAN ACADEMY OF NATURAL SCIENCES

DEPARTMENT OF RADIOELECTRONICS, NANOPHYSICS AND INFORMATION TECHNOLOGIES PROBLEMS

RENSIT:

RADIOELECTRONICS. NANOSYSTEMS. INFORMATION TECHNOLOGIES.
2018, VOL. 10, № 2

FOUNDED IN 2009
2 ISSUES PER YEAR
MOSCOW

ISSN 2414-1267 online

The journal is registered by the Ministry of Telecom and Mass Communications of the Russian Federation. Certificate El. no. FS77-60275 on 19.12.2014

EDITORIAL BOARD ADDRESS
218-219 of., 7 b., 11, Mokhovaya str.,
125009 MOSCOW, RUSSIAN FEDERATION
TEL. +7 495 629 3368
FAX +7 495 629 3678 FOR VLADIMIR I. GRACHEV

From the Editorial Board

This issue of the journal RENSIT, 2018, 10 (2) is devoted to the Anniversary of the Kotelnikov Institute of Radioengineering and Electronics of the Russian Academy of Sciences is his 65th birthday. In this connection, the Editorial Board considered it appropriate to publish materials of the 60-80s of the 20th century, software for such areas of research as radar, dynamic chaos, biomedical radio electronics and information technology. Modern research, continuing this topic, are presented in issue by the work of the current staff of the Institute.

KOTELNIKOV INSTITUTE OF RADIOENGINEERING AND ELECTRONICS OF RUSSIAN ACADEMY OF SCIENCES - 65 YEARS OLD

Yuri V. Gulyaev

Kotelnikov Institute of Radioengineering and Electronics of Russian Academy of Sciences, http://www.cplire.ru/
Moscow 125009, Russian Federation
gulyaev@cplire.ru

Abstract. **Information is presented on the establishment of the institute, on the initiators of its education, on the leaders of the first scientific divisions, on the composition of the leading staff - doctors and candidates of science, on the branches of the Institute in the Moscow region and Russia. 17 scientific directions in the field of radio engineering, radiophysics, electronics and informatics, realizing the main task of the Institute, are listed. The main achievements of the IRE are also listed. IRE RAS for the 65-year period of activity and the most significant scientific results of the Institute received in recent years, also listed. The evaluation of the activity of the IRE from the side of the Government of our country, its Academy of Sciences and foreign scientific organizations, expressed in the awards of both the Institute as a whole and a large number of its employees - orders and medals, higher state ranks, numerous awards, incl. international.**

Keywords: **institute, initiators of creation, heads of divisions, achievements, awards**

PACS 01.10 Fv

Bibliography - 5 references *Received 03.09.2018*

RENSIT, 2018, 10(2):133-146 **DOI: 10.17725/rensit.2018.10.133**

Kotelnikov Institute of Radioengineering and Electronics of Russian Academy of Sciences (Kotelnikov IRE RAS) was formed by the decision of the Council of Ministers of the USSR of August 29, 1953 and the corresponding resolution of the Presidium of the USSR Academy of Sciences on September 18, 1953 to investigate the generation, propagation and channeling of electromagnetic energy for the analysis of physical processes and the development of the theory of phenomena in semiconductor materials and electronic devices, the development of new methods for measuring magnetic and electric quantities, and also to search for new applications of radio pecifications methods in science, economy and defense techniques [1]. For its placement in the same year, the building of the physical institute and the physical faculty of the Lomonosov Moscow State University on

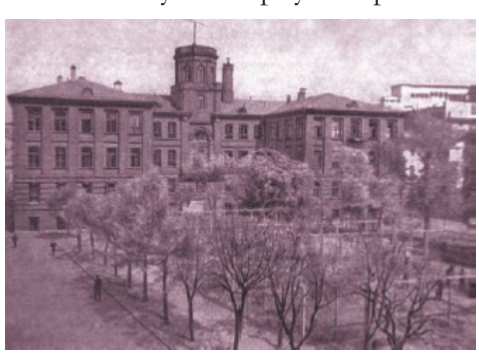

Fig. 1. *Physics Faculty of Lomonosov Moscow State University, photo 30-ies of the 20th century.*

Fig. 2. *Kotelnikov Institute of Radioengineering and Electronics of Russian Academy of Sciences.*

Mokhovaya Street, house 11 (**Fig. 1**), where the Institute is located at the present time (**Fig. 2**).

The initiators of the Institute's formation and the leaders of the first scientific divisions were the prominent scientists: academicians A.I. Berg (director-organizer), B.A. Vvedensky, N.D. Devyatkov, Yu.B. Kobzarev, V.A. Kotelnikov (director of the IRE from 1954 to 1987), V.V. Migulin, Corresponding Members of the USSR Academy of Sciences D.V. Zernov, V.I. Siforov, A.A. Pistolkors.

The heads of the first scientific divisions were also Doctors of Sciences A.G. Arenberg, N.A. Armand, A.E. Basharinov V.I. Bunimovich, G.S. Gorelik, M.I. Elinson, M.E. Zhabotinsky, L.A. Zhekulin, SG Kalashnikov, B.Z. Katsenelenbaum, M.A. Kolosov, T.M. Lifshitz, R.V. Matveev, Ya.E. Monosov, V.B. Sandomirsky, A.V. Sokolov, Z.S. Chernov, B.M. Tsarev, N.L. Yasnopolsky.

Hereinafter, academicians Yu.V. Gulyaev (director from 1987 to 2014), A.S. Bugaev, N.A. Kuznetsov, V.I. Pustovoit, V.Ya. Shevchenko; corresponding members of the RAS V.G. Mokerov, S.A. Nikitov, Ya.E. Pokrovsky, D.I. Trubetskov, V.A. Cherepenin, as well as numerous detachment of doctors and candidates of sciences of the Institute made a great contribution to the its formation and development.

In order to develop large-scale research, strengthen the material and technical base of the Institute and accelerate the introduction of research results into industry, in Fryazino, Moscow Region, in 1955, according to the resolution of the USSR Council of Ministers, the Fryazino part of the IRE was formed (now the Fryazino branch of IRE RAS, director of the branch Dr. V.M. Smirnov), and in 1958, by the decree of the Presidium of the USSR Academy of Sciences, the Special Design Bureau (SDB) of the IRE was created (now the director is chief designer of the SDB IRE RAS V.V. Abramov). Later in 1979, on the initiative of Academician Yu.V. Gulyaev created the Saratov branch of IRE RAS, headed by Ph.D. G.T. Kazakov (now the director of the branch is DrSci Yu.A. Filimonov), and in 1990 - the Ulyanovsk branch of IRE RAS, headed by Ph.D. A.A. Shirokov (now the director of the branch is Dr of Techn. Sci. V.A. Sergeev).

Currently, the IRE RAS, including 3 branches, employs more than 1000 employees, including 3 academicians, 4 corresponding members of the RAS, about 130 doctors and more than 280 candidates of science. Director of the Institute is a laureate of the Government of the Russian Federation Prize, Corresponding Member of the RAS Sergei Apollonovich Nikitov.

The main task of the Institute is to conduct fundamental and applied research in the field of radio engineering, radiophysics, electronics and computer science in the following 17 scientific areas:

- radiophysical studies of planets and outer space;
- Remote sensing of terrestrial cover and atmosphere;
- propagation of radio waves and electrodynamics of various media and structures;
- statistical radiophysics;
- generation of electromagnetic oscillations;
- nonlinear dynamics and dynamic chaos;
- biomedical radio electronics and informatics;
- optoelectronics and fiber optics;
- physical acoustics and acoustoelectronics;
- Physics of magnetic phenomena and magnetoelectronics;
- condensed matter physics;
- physics of semiconductors and semiconductor electronics;
- molecular electronics;
- technology of new materials and structures for radio engineering and electronics;
- physics of low-dimensional structures, micro- and nanoelectronics;
- superconducting electronics;
- informatics, telecommunications, radar.

The Institute prepares scientific personnel of the highest qualification through postgraduate and doctoral studies, three doctoral dissertational councils work at the Institute.

To the most important achievements of Kotelnikov IRE RAS for the 65-year period of activity can be attributed the following.

- Radiolocation of the planets Venus, Mars, Mercury and Jupiter in the period 1961-1982.
- Mapping the surface of Venus with spacecraft Venera-15 and Venera-16
- Asteroid radiolocation
- Investigation of natural resources by radiometric methods
- Sonar and oceanic sonar location
- Studies of atmospheres, ionospheres of planets and near-solar plasma by radiophysical methods
- Propagation of millimeter and submillimeter waves in the Earth's atmosphere
- Development of supersensitive quantum paramagnetic amplifiers for planetary radar and radio astronomy studies
- Investigations in the field of generation of powerful electromagnetic oscillations by electron beams
- Studies on the nonthermal effect of powerful electromagnetic pulses on rocks
- Development of scientific foundations and devices of biomedical radioelectronics
- Development of scientific foundations and devices of EHF-therapy
- Development of broadband telecommunications and information technologies based on dynamic chaos
- Pioneering work in the field of acoustoelectronics, including theoretical prediction and experimental detection of a new fundamental type of surface acoustic waves (Gulyaev-Blyusteynov waves)
- Fundamental work in the field of acousto-optics, magnetoelectronics (including spinwave electronics and spintronics), superconductor electronics
- Pioneering work on the study of carbon nanotubes, graphenes and other low-dimensional electronic systems
- Pioneer work in the field of semiconductor physics.

The following outstanding scientific results of the Institute, received in recent years and noted in the annual reports of the Russian Academy of Sciences, can be noted.

- A superconducting integrated spectrometer for monitoring the 450-650 GHz atmosphere on the basis of tunnel nanostructures Nb-AlN-NbN was created and tested. Successful launch of the on-board integrated spectrometer at the "Esrange" range (Sweden) (noise temperature of 120 K, spectral resolution is better than 1 MHz). During the flight on a high-altitude balloon, the spectra of various gas components, including ClO and BrO, responsible for the destruction of the ozone layer of the Earth, their distribution in the altitude range 12-36 km during the sunrise (IRE RAS, Institute of Physics of Microstructures of RAS, National Institute Space Research of the Netherlands (SRON)).
- Based on the Ni-Ti-Cu alloy with shape memory effect (EPR) coated with a platinum layer, samples of composite microinstruments, in particular nanopincetes and nanoscraps, with overall dimensions of 1-15 microns were made. A prototype system for manipulating nanoobjects was created on the basis of a nanopinket with an EPF docked with an Omniprobe nanomanipulator and a semiconductor injection laser controlled by a beam. Three-dimensional manipulation of stacks of graphene sheets, bundles of carbon nanotubes and microfiber of biological nature is demonstrated. The size of the captured and manipulated object is 10-1000 nm (IRE RAS, Moscow Engineering Physics Institute, Moscow Institute of Steel and Alloys, FTI RAS).
- A superconducting integrated spectrometer of the 450-650 GHz range based on Nb-AlN-NbN tunneling nanostructures for atmospheric monitoring was created and tested. Successful launch of the on-board integrated spectrometer at the "Esrange" range (Sweden) (noise temperature of 120 K, spectral resolution is better than 1 MHz). During the flight on a high-altitude balloon, the spectra of various gas components, including ClO and BrO, responsible for the destruction of the ozone layer of the Earth, their distribution in the altitude range 12-36

km during the sunrise (IRE RAS, Institute of Physics of Microstructures of RAS, National Institute Space Research of the Netherlands (SRON)).

- Based on the Ni-Ti-Cu alloy with shape memory effect (SME) coated with a platinum layer, samples of composite microinstruments, in particular nanopincetes and nanoscraps, with overall dimensions of 1-15 microns were made. A prototype system for manipulating nanoobjects was created on the basis of a nanopinket with an SME docked with an Omniprobe nanomanipulator and controlled by a beam of a semiconductor injection laser. Three-dimensional manipulation of stacks of graphene sheets, bundles of carbon nanotubes and microfiber of biological nature is demonstrated. The size of the captured and manipulated object is 10-1000 nm (IRE RAS, Moscow Engineering Physics Institute, Moscow Institute of Steel and Alloys, FTI RAS).
- The state induced by a strong magnetic field with a charge density wave in graphite is revealed. This state is explained by the charge density wave arising in graphite due to the one-dimensionalization of its electronic spectrum under the action of a magnetic field. The possibility of its existence was predicted theoretically by Yoshioka and Fukuyama more than 30 years ago to explain the anomaly of the magnetoresistance of graphite in strong fields at low temperatures. (Institute for Physics and Technology of RAS, Institute of Neel, Grenoble, France and the National Laboratory of Pulsed Magnetic Fields, Toulouse, France).
- The principles of building wireless ultra-wideband communication networks and sensor networks with energy-saving functions are developed. Specifically designed, manufactured and tested experimentally low-power ultra-wideband direct-chaotic transceivers with various energy-saving modes; Network management algorithms have been created that allow the self-organization and self-diagnosis functions of the network to be realized, taking into account the power-saving modes of the transceivers; created algorithms for data transmission over the network, taking into account energy-saving modes; implemented and experimentally explored the mock-up of a wireless voice transmission system based on a self-organizing network. (IRE RAS).
- A new method for evaluating the wavelet spectrograms of the brain's electroencephalogram (EEG), focused on the search for signs of Parkinson's disease (PD) at an early stage. The essence of the method is the analysis of the statistics of the frequency-time distribution of local extrema of the EEG wavelet spectrograms, since the interhemispheric asymmetry of the frequency-temporal distribution of the local maxima of the wavelet spectrograms is noted when comparing the wavelet spectrograms of the EEG symmetric cortical regions in patients with the first stage of the PD (IRE RAS, IHNA&NPh RAS, Scientific Center of Neurology of RAMS).
- For the first time, chains of bolometers have been created on cold electrons that are record-sensitive to terahertz radiation and insensitive to cosmic rays. For the first time in Russia, optical sensitivity values at the level of 20 $aW/Hz^{1/2}$ were obtained under background radiation conditions at the level of 3 K (IRE RAS, IPP RAS, Chalmers University, University of Rome)

In the State Register of Discoveries of the USSR 8 discoveries made by the Institute's employees were registered.

For 65 years of its existence, the Institute's works have been awarded two prizes of the European Physical Society, two Lenin Prizes, 24 State Prizes of the USSR, six State Prizes of the Russian Federation, four Prizes of the Council of Ministers of the USSR, three Prizes of the Government The Russian Federation, 3 Lenin Komsomol Prizes, 2 State Prizes of the Ukrainian SSR, the First Prize of the Government of the Russian Federation in Education and the First State Prize of the Russian Federation named after Marshal of the Soviet Union G.K. Zhukov in the field of military science.

For success in scientific activities, the IRE was repeatedly praised by the Council of Ministers of the USSR and the Government of Russia, as well as by the Academy of Sciences of the USSR, the Russian Academy of Sciences and foreign scientific organizations.

In 1969, the IRE Academy of Sciences of the USSR was awarded the Order of the Red Banner of Labor. A number of the Institute's employees were awarded the title Heroes of Socialist Labor (academicians ND Devyatkov, Yu.B. Kobzarev, VA Kotelnikov (twice)). Many employees of the Institute were awarded orders and medals for fruitful scientific and public activities. Academician V.A. Kotelnikov was awarded the Order of Merit for the Fatherland, I degree, and Academician Yu.V. Gulyaev - orders Order of Merit for the Fatherland, IV and III degrees.

A number of the Institute's employees for scientific achievements were awarded prestigious international prizes awarded by the International Institute of Electrical and Electronics Engineers (IEEE): Academician V.A. Kotelnikov - Gold Medal of A.G. Bell (and also the prize of the Eduard Raine Foundation (Germany)), academician Yu.V. Gulyaev - Rayleigh Award, Dr.Sc., Prof. G.D. Mansfeld - Cady's award, Dr.Sc. M.A. Tarasov - the award to them. Van Duser.

A number of employees of the Institute were awarded prestigious prizes and awards from the Academy of Sciences of the USSR and the Russian Academy of Sciences: A.S.Popov Prize (M.I. Elinson, A.G. Zhdan, A.N. Vystavkin, T.M. Lifshits, M.E. Zhabotinsky), the B.P. Konstantinov Prize (Yu.V. Gulyaev), a gold medal named after A.S. Popova (V.A. Kotelnikov, Yu.B. Kobzarev, N.D. Devyatkov, Yu.V. Gulyaev), a gold medal named after M.V. Lomonosov (V.A. Kotelnikov), a gold medal named after MV Keldysh (VA Kotelnikov).

14 employees of the Institute were awarded the honorary title of "Honored Worker of Science and Technology".

APPENDIX

Directors of V.A. Kotelnikov IRE RAS

The first director of the IRE was **AKSEL IVANOVICH BERG**, an engineer-admiral, doctor of technical sciences, an academician of the USSR Academy of Sciences in the Division of Technical Sciences (**Fig. 3**), deputy minister of defense of the USSR in those years, served as director of the IRE in 1953-1955 [2].

Axel Ivanovich was born on November 10, 1893 in Orenburg, in the family of Russian general Johann Alexandrovich Berg, a Swede by birth, and Italian Elizabeth Camillovna Bertholdi, whose ancestors moved to Russia. At the birth of his son, he, according to the Lutheran custom, gave a double name Axel-Martin.

After four years in St. Petersburg Petrishul Axel studies in the Alexander Cadet Corps, after which he graduated in 1908 in the Naval Cadet Corps, which ends in 1914 with the rank of midshipman. In the same year he married Nora Rudolfovna Betlingk, the daughter of a famous Petersburg therapist. Serves two years in Finland, in Helsingfors (Helsinki) on the battleship "Tsesarevich", where he goes as a company commander, after which - almost a year navigator of a submarine that took part in the fighting of the First World War. After studying in the winter lull of military operations, in February 1917 he received the rank of lieutenant.

Fig. 3. *Aksel Ivanovich Berg - the director-organizer of the Institute of Radioengineering and Electronics of the USSR Academy of Sciences.*

During the October Revolution, Berg was at sea and heard about it only after the submarine returned to the base. Soon there was a separation of Finland from Russia, Bergu and his wife succeeded in the last train to go to Petrograd. Here, after a brief service on the destroyer, Berg gets to the fleet command headquarters, takes out submarines from Finland, directs the restoration of damaged submarines.

At the same time he studies at the Petrograd Polytechnic Institute. After deduction from the active fleet on health, he studies at the Higher Naval Engineering College (electrical and radio engineering), then at the Naval Academy, teaches radio engineering (the first textbooks, including the "General Theory of Radio Engineering"), after its completion in 1925 he teaches at the College. In 1928, he disagreed with Nora (a childless marriage) and married Marianna Ivanovna Penzin

In 1928-32 he was sent to purchase hydroacoustic instruments in Germany, the United States, Italy. It organizes a scientific and testing ground (1927), then - the Maritime Institute of Communications (1932), develops and implements a system for the radio equipment of the fleet. In 1936 the appraisal commission awarded A.I. Berg holds a doctorate in engineering. In 1937 he was awarded the Order of the Red Star.

At the end of 1937 he was arrested on suspicion of participating in the "Tukhachevsky case", for 2.5 years in prisons of Kronstadt and Moscow he communicated, among other things, with Marshal Rokossovsky, designer Tupolev, academician Lukirsky and others, in 1940 was released "for insufficient evidence. " All ranks and academic degrees to Axel Ivanovich were returned, appointed as the head of the departments at the Naval Academy, with which in 1941 engineer-Rear Admiral Berg was sent to evacuation to Astrakhan, then to Samarkand.

In the first years of the war, a new trend in radio electronics was born - radar. At the end of 1942 Axel Ivanovich sent to Moscow his project for the development of radar operations in the USSR and, being summoned to the capital, walked around the offices of officials with his posters on radar, which ended in 1943 with the resolution of the State Committee for Defense "On Radar" and the creation of a Council for radar with the inclusion of all the color radar thought of Russia in those years. Berg himself was the seventh item of the decree approved by the deputy commissar of the electrical industry by radar, and then by deputy. Chairman of the Council on radar in the GKO USSR.

In August 1943 Berg was also entrusted, among other things, with the duties of the head of the "radar institute" designated in the decree "On Radar." In September, the institute was given the name "VNII №108" (today - CIARTI named after Academician AI Berg). Thanks to Axel Ivanovich, who was actively engaged in the selection of specialists, by the end of 1944 eleven laboratories were created at VNII-108. Director of the Institute, Berg worked until 1957. Under his leadership in the "one hundred and eighth" were started work in the field of electronic warfare.

In 1953, Berg was appointed Deputy Minister of Defense of the USSR for radio equipment. This was the highest point in his career - being the second person in the "power" ministry he could influence the solution of the most diverse issues of the country's defense industry. Possessing the appropriate powers and knowing perfectly well that his "one hundred and eighth" institution is littered with works of a defensive nature and is unable to deal with the vital issues of radio electronics productively, Berg decided to organize the Institute of Radio Engineering and Electronics at the Academy of Sciences of the USSR in the capital of the country. In September 1953 a corresponding decree of the Presidium of the Academy of Sciences was issued, and Axel Ivanovich was appointed as the director-organizer of the new institution.

Painful work began - selection of scientists, correspondence with the Ministry of Culture on the allocation of new premises to the new institute, the creation of the first orders. In August 1955, Berg was awarded the title of Engineer-Admiral. Unfortunately, the enormous burden on the posts of the Deputy Minister of Defense of the USSR, which Axel Ivanovich combined with participation in the Radio Council of the Academy of Sciences

and the leadership of the Central Research Institute-108, undermined his iron health. A bilateral infarction in July 1956, three months in the hospital, a year and a half in sanatoria. In one of them, he met with a nurse Raisa Glazkova. She was younger than Axel Ivanovich for thirty-six years, but this difference because of the "motor" nature of Berg was not strongly felt. Soon the radio engineer decided to marry for the third time. Raisa Pavlovna, a large, sedate and skillful woman, was very different from the other companions of his life - the morbid Nora Rudolfovna and the tiny Marianna Ivanovna, who agreed to divorce only after the birth of Margarita - daughter of Berg from Raisa Pavlovna in 1961. "Young father" Axel Ivanovich became at the age of sixty-eight.

In May 1957, in connection with the state of health, Berg was relieved of his post as Deputy Minister of Defense and concentrated his forces at work in scientific research institutions of the Academy of Sciences. In January 1959, the Presidium of the Academy of Sciences instructed him to form a commission for the preparation of a report titled "Basic Problems of Cybernetics." In April this year, following the discussion of the report, the Presidium of the Academy of Sciences adopted a resolution to establish the Scientific Council for Cybernetics. The main structural subdivision of the Council was its sections, to the work of which on a voluntary basis attracted more than eight hundred scientists (including eleven academicians), which corresponded to the size of a large scientific research institute.

Gradually, through the efforts of Berg and a number of his associates, cybernetic ideas were widely disseminated among Russian scientists. Symposiums, conferences and seminars on cybernetics, including at the international level, have been held every year. Publications were published: "Cybernetics for the service of communism" and "Problems of cybernetics", ten or twelve collections of "Problems of Cybernetics" were published annually. In the sixties institutes of cybernetics appeared in all the Union republics, in universities - laboratories and departments, in the branch institutes of the laboratory. Also new fields of cybernetic science appeared: artificial intelligence, robotics, bionics, situational management, theory of large systems, noise-immune coding. The priorities in mathematics also changed, because with the presence of a computer, it became possible to process large amounts of information. In 1963, Berg was awarded the title of Hero of Socialist Labor.

Berg paid a great deal of attention to the propaganda of knowledge among the masses, mainly to radio amateurs. Axel Ivanovich possessed an outstanding oratorical talent. His speeches left an indelible impression on the listeners and were remembered for life. Non-standard presentation, free operation of statistical data, the breadth of problems, witty aphorisms and replicas - all this captivated, amazed the listener. Axel Ivanovich was the initiator of the founding of the publishing house of the "Mass Radiobility", which produces radio amateur works. The publishing house began to function in 1947, Axel Ivanovich headed his editorial board until his death.

Axel Ivanovich died at the age of eighty-five years on the night of July 9, 1979 in the hospital ward. Buried at the Novodevichy Cemetery.

The second director of IRE RAS, Academician **VLADIMIR ALEKSANDROVICH KOTELNIKOV**, held this post in 1954-1988.

V.A. Kotelnikov is an outstanding scientist, engineer, teacher and organizer, one of the founders of radiophysics, radio engineering,

Fig. 4. *Vladimir Alexandrovich Kotelnikov - director of the Institute of Radioengineering and Electronics of the USSR Academy of Sciences from 1954 to 1988.*

computer science, radio astronomy and domestic cryptography. His pioneering work laid the foundation for the development of new areas of science and technology: informatics and the digital method of signal transmission, statistical radiophysics, planetary radar, domestic cryptography and large-scale space exploration [3].

V.A. Kotelnikov was born 110 years ago, on August 24 (September 6), 1908 in Kazan. His grandfather and father were professors of Kazan University. By the age of six Volodya already read, wrote, mastered the initial courses of arithmetic, algebra, geometry. During the First World War, revolutions and the Civil War, the family moved from town to town, and Volodya continued his education independently according to the books available in their house. At school he studied only the last three classes, and finished it in 1925.

Remaining faithful to his childish and youthful enthusiasm for radio engineering, Vladimir wanted to enter the Electrotechnical Faculty of the MVTU. N.E. Bauman, but there they accepted only "persons of worker-peasant origin" after the rabfak, and in his documents it was "from the nobility." It took a year to study in the technical school of communication, but in 1926 the MVTU announced a "free reception", and Vladimir easily entered there. Simultaneously with his studies at the Moscow Higher Technical University, he attended courses at the Physics and Mathematics Department of Moscow State University. In 1930 he graduated from the Moscow Power Engineering Institute (MEI), which was graduated from the Moscow Higher Technical School just in the year of graduation. After graduation he worked at the Research Institute of Communications of the Red Army. In 1931 he enrolled in the graduate school of Moscow Power Engineering Institute (1931-1933) and simultaneously worked as a laboratory assistant, then as assistant, assistant professor (1931-1938), head of the department of Radio Engineering of the Moscow Power Institute (1938-1941). The Central Institute of Communications of the People's Commissariat of Posts and Telegraphs (CNII CNS) is the engineer, chief engineer of the institute on radio, head of the laboratory (1933-1941). State Union Industrial and Experimental Institute No. 56 - head of the laboratory, Ufa (1941-1943), Department of Government Communication of the People's Commissariat of Internal Affairs of the USSR Moscow (1943-1944). MEI - professor, head. Department of Radio Engineering, Dean of Radio Engineering Faculty (1944-1980). IRE USSR Academy of Sciences - Deputy Director (1953-1954), Director (1954-1987), Honorary Director (1987-2005). Presidium of the USSR Academy of Sciences - acting. vice president (1969), vice president (1970-1988).

The creative path of Vladimir Aleksandrovich Kotelnikov covered 78 years. He began in 19 years, the creation of the first in our country device "triple character". This work was carried out after the first course of the MVTU during the summer holidays at the Nizhny Novgorod Radio Laboratory (1927). It was published in 1928.

At the age of 24 he was the first to formulate mathematically and proved, in the aspect of communication technologies, the mathematical "Sample Counting Theorem" ("Kotel'nikov's Theorem"), which initiated the theory of information, digital systems for the transmission of messages, control, coding and processing of information (MPEI, 1932).

At the age of 27, under his leadership and with his participation, the first multi-channel letter printing machine for radio work was set up in our country, which significantly exceeded foreign analogues in its parameters and was subsequently widely used in our country (1935).

At the age of 30 he was awarded the degree of candidate of technical sciences without defending a thesis (1938, Leningrad Electrotechnical Institute), head. Department of Radio Engineering MEI.

At the age of 31, a unique multi-channel telephone and telegraph equipment for radio communications was created, using for the first time one sideband, which was installed on the Moscow-Khabarovsk (1939) line. This highway was the largest achievement of domestic and world radio engineering of that time.

At the age of 32, for the first time, the fundamental in the development of cryptography was formulated and proved a theorem that

clearly defined the criteria for a mathematically undecipherable system (1941, NIIS NCC). In the same years, a new class of Russian-language speech encoding systems for private radio communication (1941-1943, Ufa) was not deciphered at that time. The systems were successfully used in the active army, as well as during the acceptance of Germany's surrender to link the Soviet delegation to Moscow (1943-1945). Subsequently, improved systems of this type have been successfully used for government communications up to the 1970s.

At the age of 36, he recreated and headed the Department of Theoretical Foundations of Radio Engineering at the Radio Engineering Department of the Moscow Power Engineering Institute, which he subsequently directed for 36 years (1944-1980). In 1944-47 years. under his leadership, telemetric equipment for aircraft was developed.

In 38 years, the "Theory of potential noise immunity" (doctoral dissertation), one of the main branches of information theory, in which the foundations of a new scientific direction - statistical radiophysics were laid - was created. This work, far ahead of its time, later became one of the cornerstones of modern communication theory (1946, MPEI).

In 39 years - created and headed the "Sector of special works for scientific research in the interests of reactive weapons" (subsequently OKB MEI) - one of the leading organizations that developed radio electronic equipment for rocket and space programs (1947, MPEI). As the chief designer of the Special Sector in 1947-1953. He was part of the interdepartmental Council of Chief Designers, which was headed by S.P. Korolev. Elected Dean of the Radio Engineering Faculty of the Moscow Power Engineering Institute (1947-1953).

At the age of 45 he was elected a full member of the Academy of Sciences of the USSR, bypassing the degree of corresponding member (1953), appointed deputy. Director of the Institute of Radio Engineering and Electronics (IRE) of the USSR Academy of Science.

At the age of 46, he became the director of the IRE of the Academy of Sciences of the USSR, which he created, which in a very short time became one of the leading scientific institutions in the field of radio electronics, both in our country and abroad. He headed the institute for 33 years (1954-1987), remaining then an honorary director and continuing to head the scientific council of the Institute for another 18 years, until the end of his life.

With the name of VA. Kotelnikova connected a new direction in the exploration of outer space - planetary radar, a new page in radio astronomy was opened: on his initiative, under his leadership and direct participation, unique experiments were carried out for the radiolocation of Venus (1961-1964), Mercury (1962), Mars (1963) Jupiter (1963). As a result of these studies, the value of the astronomical unit was determined with high accuracy, a new theory of the motion of the inner planets of the solar system was created and experimentally confirmed. The astronomical unit specified by him together with his colleagues made it possible to provide the necessary accuracy of control over the movement of space vehicles. An outstanding worldwide achievement was the radar survey of Venus, carried out in 1983-84. with the help of the onboard complex radar system AMS "Venera-15 and -16", thanks to which it was possible to obtain an image of the northern part of the planet with an area of 115 million km2 with a resolution of 1 km. As a result of the analysis of these unique data, the first in the history of science, "The Atlas of the Surface of Venus" (M., MIIGAiK, 1989) was created and subsequently published; Kotelnikov. (1961-1989, IRE).

In 88 and 89 years - published his latest articles, closing the circle of his work in the field of radiophysics (1996, 1997).

The creative path of Vladimir Alexandrovich was completed on the 97th year of his life, the almost finished but not published work "Model Quantum Mechanics" (published in 2008, after the departure of Vladimir Alexandrovich from life).

Vladimir Alexandrovich Kotelnikov was a talented teacher. In MEI he was the first to introduce the teaching of courses in theoretical physics and to establish a new specialty "Radiophysics". In 1949, he developed the "Program on the theoretical fundamentals of radio engineering" for the specialty "Radio Engineering", for which

for many years the students of this specialty were trained in all universities of our country. He was a brilliant lecturer (1931-1941, 1944-1955). His course of lectures "Fundamentals of Radio Engineering" was published in the form of a two-volume textbook with the same title (in 1950 and 1954) and enjoyed immense popularity. Vladimir Alexandrovich organized and for a long time headed the Department of Electromagnetic Waves at the Moscow Institute of Physics and Technology (1968-1999).

Along with the solution of scientific problems and pedagogical activity, Vladimir Aleksandrovich was engaged in great scientific and organizational activities. In the years 1969-1988. V.A. Kotelnikov was acting president, vice president, first vice-president of the USSR Academy of Sciences.

Vladimir Alexandrovich headed a number of scientific councils, including the Scientific Councils of the USSR Academy of Sciences on the complex problem "Radio Astronomy" (1961-1989) and "Radiophysical Methods of Studies of the Seas and Oceans" (1978-2005). In 1980-2005, he is the vice-president of the Scientific Council on Space and headed the Council for International Cooperation in the field of exploration and use of outer space Intercosmos. Actively worked as chairman of the section of radio electronics for the Lenin and State Prizes of the USSR in the field of science and technology under the Council of Ministers of the USSR.

Vladimir Alexandrovich was the founder and editor-in-chief of the journal "Radio Engineering and Electronics" (1956-80), the editor-in-chief of the "Bulletin of the Academy of Sciences of the USSR" (1974-88), and also a member of the editorial board of the journal "Radiotekhnika".

Academician V.A. Kotelnikov enjoyed deserved authority not only in our country, but also abroad. He was a member of many scientific organizations, including: 16 Russian, international and foreign academies, vice-president of the International Academy of Astronautics (1983-95), a member of the International Institute of Electronics and Electrical Engineers IEEE (elected in 1964, since 1987 Honorary Member), a member of the International Scientific Radio Union (1957-2005). Vladimir Alexandrovich was elected to the Supreme Soviet of the RSFSR (1971-80), Chairman of the Supreme Soviet of the RSFSR (1973-80), deputy of the Supreme Soviet of the USSR (1979-89).

For his scientific merit VA. Kotelnikov was awarded the 31st state award, among which - two Orders "For Services to the Fatherland" - 1st degree (No. 4) and 2 nd degree; two stars of the Hero of Socialist Labor, six Orders of Lenin; two State Prizes (Stalin Prizes 1st degree); The Lenin Prize, the Council of Ministers Prize. He was awarded with high scientific awards - a gold medal named after A.S. Popova (1974), a gold medal named after M.V. Lomonosov and the Gold Medal with the MV Keldysh Prize for a series of works on the study of outer space. The international scientific community noted his scientific achievements with 17 international and foreign medals and prizes. International Institute IEEE awarded Vladimir Alexandrovich in 1973 with the medal. Hernand and Sozenes Ben for his outstanding contribution to the development of the theory and practice of radio communications, in 1999 the highest annual award - Alexander Graham Bell for his fundamental contribution to the theory of signals, in 2000 the highest medal of honor - the Gold Medal in honor of the III-th millennium for outstanding achievements in the fields of his scientific activity. In 1998 the International Academy of Astronautics awarded V.A. Kotelnikov with his highest annual award - the Von Karman Award. The International Science Foundation Eduard Rein (Germany) in 1999 awarded VA. Kotelnikov's main prize for the first time was mathematically precisely formulated and proved in the aspect of communication technologies the sampling theorem.

VA Kotelnikov is an honorary professor at the Moscow Power Engineering Institute and St. Petersburg Electrotechnical University. For the adjuncts of the Institute of Cryptography, Communications and Informatics of the Academy of the Federal Security Service, two scholarships have been established for them. V.A. Kotel'nikov.

In the name of VA Kotel'nikov is named the Small Planet No. 2726 (in the International Catalog

Circular No. 9214). His name is a naval vessel, the Institute of Radioengineering and Electronics of the Russian Academy of Sciences (Decree of the Presidium of the RAS No. 274 of December 18, 2007) and also an institute within the MEI University.

February 1, 2005 V.A. Kotelnikov died, was buried at Kuntsevo Cemetery in Moscow

The third director of IRE RAS - academician **YURI VASILYEVICH GULYAEV,** held this post in 1988-2014.

Academician of the Russian Academy of Sciences Yuri Vasilievich Gulyaev is an outstanding Russian scientist in the field of solid state physics, radiophysics, electronics and computer science, one of the founders of new scientific and technical directions - acoustoelectronics, acousto-optics, spin-wave electronics, and biomedical radioelectronics [4].

Yuri Vasilyevich Gulyaev was born in the village. Tomilino, Lyubertsy district, Moscow region. Father Gulyaev Vasily Sergeevich, an economist, fought from the first day of the war and until the very end, was shell-shocked, had many military awards. Mother Anisimova Eugenia Dmitrievna, worked as a doctor all her life, went through the whole war.

In 1952 r. Yuri Gulyaev finished with a silver medal Luberetskaya secondary school and entered the Moscow Institute of Physics and Technology, which graduated in 1958 r. with Honours. In 1962 r. he defended his thesis, in 1970 r. - doctoral.

Fig. 5. *Yury Vasilievich Gulyaev - Director of IRE RAS from 1988 to 2014.*

Since 1960 Yu.V. Gulyaev works at the V.A. Kotelnikov Institute of Radioengineering and Electronics of Russian Academy of Sciences (IA Kotelnikov Institute of RAS) as a junior researcher, senior research fellow, head of the laboratory, deputy director (from 1972 to 1988), director (from 1988 to 2014 r.r.). At present, he is the scientific director of the Institute, the chairman of the Academic Council.

Since 1972 r. Yu.V. Gulyaev heads a department at the Moscow Institute of Physics and Technology, the modern name of which is the Department of Solid State Electronics, Radiophysics and Advanced Information Technologies.

For the years of his creative work Yu.V. Gulyaev prepared over 80 candidates of science, 20 of whom became doctors of science, with one of his pupils elected a corresponding member of the Russian Academy of Sciences, the other an academician of the Russian Academy of Sciences. Yu.V. Gulyaev is a laureate of the RF Government prize in the field of education (2009). Total Yu.V. Gulyaev alone, together with his students and employees, published more than 700 scientific articles in the most prestigious domestic and foreign scientific journals, received more than 80 patents for inventions. He is the co-author of 11 monographs. He is also a co-author of the discovery - the so-called acoustomagnetoelectric effect (diploma No. 133).

Yu.V. Gulyaev is one of the creators of a number of the most promising trends in modern radio electronics, such as acoustoelectronics and acoustooptics, spin-wave electronics and spintronics, and biomedical radioelectronics. His name and works are world famous. In 1968 r. simultaneously with the American scientist J. Bluesstein and independently of him, he discovered the existence in piezoelectrics of a new type of surface acoustic waves called "Bluesstein-Gulyaev waves" in the world literature, which in some cases are more preferable for practical use in comparison with known types of waves.

In 1979 r. Yu.V. Gulyaev was elected a corresponding member of the Academy of Sciences of the USSR, and in 1984 r. - full member (academician) of the USSR Academy of Sciences. Since 1992 r. Yu.V. Gulyaev is elected a member of the Presidium of the Russian Academy of Sciences. Yu.V. Gulyaev - President of the Russian Union of Scientific and Engineering Public Organizations, President of the Russian Scientific and Technical Society of Radio Engineering, Electronics and Communications. A.S. Popova, president of the Academy of Engineering Sciences. A.M. Prokhorov, Academician of the Russian Academy of Natural Sciences, a foreign member of the Polish and Moldavian National Academies of Sciences, a foreign member of the Chinese Academy of Engineering Sciences, a member of the Advisory Scientific Council of the Development Fund for the Center for the Development and Commercialization of New Technologies in Skolkovo.

Yu.V. Gulyaev is the editor-in-chief of six prestigious domestic scientific journals (Radio and Electronics, Radio Engineering, Biomedical Radio Electronics, Science in Technology and Industry, News of Higher Educational Institutions, Applied Nonlinear Dynamics, Journal of Radioelectronics), five of them which are included in the List of VAK, and a member of the editorial board of more than ten domestic scientific journals.

On the initiative of Yu.V. Gulyaev established branches of the Institute of Radio Engineering and Electronics of the Russian Academy of Sciences in Saratov and in Ulyanovsk, the Scientific Center of Electronic Diagnostic Systems (Center "Eldis"), the department of microelectronics technology, which later was separated into a separate Institute of Microwave Semiconductor Electronics of the Russian Academy of Sciences. Yuri Vasilievich was the director-organizer of the Institute of Nanotechnology of Microelectronics of the Russian Academy of Sciences. He is one of the organizers and the permanent leader of the Saratov Scientific Center.

Contribution of Academician Yu.V. Gulyaev was awarded with high awards and prizes in the development of science and technology: the European Physical Society Award (1979), the USSR State Prizes (1974, 1984), the State Prizes of the Russian Federation (1993, 2007) B.P. Konstantinov RAS (1991), the Gold Medal of the Russian Academy of Sciences. A.S. Popova (1995), as well as a number of orders and medals, including the Order of Merit for the Fatherland IV (1995) and III (1999) degree. Work Yu.V. Gulyaev are important for enhancing the country's defense capability and security, as evidenced by the USSR Council of Ministers' Prize in 1989, two Commendations of the Supreme Commander-in-Chief of the Armed Forces of the Russian Federation (2000, 2002) and the State Prize of the Russian Federation named after Marshal of the Soviet Union G. TO. Zhukov in the field of military science (2013).

Yu.V. Gulyaev was one of the first to suggest and organize systematic studies of physical fields (thermal, microwave, optical, acoustic, chemical, etc.) at the Eldis Center and the characteristics of bioobjects and humans. Based on these studies, numerous methods and devices of early (usually non-invasive) medical diagnostics of the state of organs (heart, brain, lungs, mammary glands, etc.) and the entire human body were developed. Work to ensure traffic safety in railway transport using the developed means of diagnosing the driver's condition, carried out under the guidance and with the participation of Yu.V. Gulyaeva, was awarded in 2012 by the Government of the Russian Federation.

Recently, Yu.V. Gulyaev is actively engaged in the development and research of new methods in biomedical radioelectronics, in particular, quasi-static tomography of man. On his initiative, an electrical impedance mammogram was developed for a wide application in personal medicine as a household appliance. The first results in electric field tomography are obtained. Under his leadership, the development of a fundamentally new method of targeted delivery of drugs in the human body has begun. These results correspond to the world level or exceed it.

Currently, Yuri Vasilyevich Gulyaev is the scientific director of IRE them. V.A. Kotelnikov RAS and the chairman of its Academic Council.

The fourth director of Kotelnikov IRE RAS - Corresponding Member of the Russian Academy of Sciences **SERGEY APOLLONOVICH NIKITOV**, occupies this post from 2014 to the present.

Dr.Sc., Prof., Corresponding member of RAS Nikitov Sergey Apollonovich - specialist in the field of solid-state micro- and nanoelectronics, solid state physics, computer science and elemental component base [5].

Born April 23, 1955 in the city of Berdichev, Zhytomyr region, Ukrainian SSR. In 1979 he graduated from MIPT (Faculty of Physical and Quantum Electronics), in 1982 - his postgraduate studies with the thesis of the candidate of technical sciences, since 1982 he works at the Kotelnikov Institute of Radioengineering and Electronics (research associate, senior research fellow), in 1991 defended the thesis of the doctor of physical and mathematical sciences, since 1995 professor, from 1991 to the present time the head of the laboratory of magnetic and optical methods of information processing, since 2003 the deputy director for science in IRE RAS.

Fig. 6. *Sergey Apollonovich Nikitov - director of V.A. Kotelnikov IRE RAS from 2014 to the present.*

May 22, 2003 he was elected Corresponding Member of the Russian Academy of Sciences in the Department of Informatics and Computer Systems of the Russian Academy of Sciences, since 2014 - Director of Kotelnikov IRE RAS.

Awards: 1981 - Komsomol Prize of the Moscow Region, 1984 - Lenin Komsomol Prize, 2009 - Russian Government Education Prize, 2010 - winner of the First competition of scientific megacities. In 1993-1994 he was a scholar of the A. von Humboldt Foundation, the Ruhr University in Bochum, Germany, 1999 - a scholarship of the Landau-Volta Foundation (natural sciences), Rome, Italy.

Since 1985 S.A. Nikitov visited various universities as a senior researcher or as an invited specialist in various countries: England, France, Germany, Brazil, USA, Korea, Italy, Netherlands, Spain, Japan, Bulgaria, Poland, etc.

He was the organizer of several international meetings in various countries, in particular, he was the co-director of NATO ARW in Italy in 1995. Member of the Russian Physical and Magnetic Societies, Russian Academy of Engineering Sciences, IEEE, member of the Materials Research Society (USA), Vice-President of the Russian Section of the IEEE, member of the Popov Russian Scientific and Technical Society of Radio Engineering, Electronics and Communications, Honorary Doctor of the University of Toulouse (France).

Member of the editorial boards of the journals "Radio Engineering and Electronics", "Nonlinear World", "Micro- and Nano-System Engineering.

S.A. Nikitov is the author and co-author of more than 400 scientific publications, incl. more than 170 articles in peer-reviewed scientific journals, co-author of 6 patents, co-author of books "The Newest Imaging Methods" (2008), "Shell fibers fiber modes and long-period fiber gratings" (2012), "One-dimensional microwave photonic crystals."), more than 200 invited papers at international conferences and leading scientific centers around the world.

From 2007 to the present, Professor and Head Department of Information Security of the Russian New University (RosNOU). In 2012,

under his leadership, the Metamaterials laboratory was opened in Saratov Chernyshevsky State University.

Under his leadership, 15 candidate dissertations and 2 doctoral dissertations were defended. As an expert, he is a member of the Board of Directors of Unique Fiber Instruments LLC, the Russian Board of Reviewers of Nanotechnology Corporation, the Russian Foundation for Basic Research, the Council of Experts of the Information Technology Agency of the Russian Federation, the Board of Directors of Engineering Center LLC.

For about 30 years he has been the head of research and R&D in the framework of research programs of the Russian Academy of Sciences, RFBR, the Ministry of Education and Science, the Ministry of Industry and Trade, the Ministry of Telecommunications and Informatics of the Russian Federation.

Sergey Apollonovich is the deputy chairman of the Scientific Council of the Russian Academy of Sciences on the problem of "Physics of Magnetic Phenomena", a member of the Scientific Council of the Russian Academy of Sciences on the problem of "Scientific foundations of building computing, telecommunication and location systems", the RAS Commission for Working with Youth, the Scientific Secretary of the Presidium of the RAS Commission for the Improvement of the Structure of the Russian Academy of Sciences, director of the Institute of Physics and Materials of the Saratov Chernyshevsky State University.

REFERENCES

1. Chusov II. V.A. Kotelnikov IRE RAS (to the 60th anniversary of the Institute). *Radiotekhnika,* 2013, 9:1-4 (in Russ.).
2. Erofeev YuN. *Axel Berg* (series LWP). Moscow, Molodaya gvardiya Publ., 2012, p. 240.
3. Kotelnikova NV. To the 100th anniversary of Academician VA Kotelnikov. http://www.ras.ru/news/shownews.aspx?id=59dc9c27-d249-486e-b537-2edfb02a0ede&_Language=ru.
4. Academician of the Russian Academy of Sciences Yuri Vasilievich Gulyaev (on the occasion of his 80th birthday). *Radiotekhnika,* 2015, 8:4-10.
5. Nikitov Sergey Apollonovich. http://www.ras.ru/win/db/show_per.asp?P=.id-53831.ln-en.

RADAR LOCATION ASTRONOMY

Vladimir A. Kotelnikov, Gennady M. Petrov

Institute of Radioengineering and Electronics of the USSR Academy of Sciences, http://www.cplire.ru
Moscow 125009, USSR
info@cplire.ru

Abstract. **A review of the work on planetary radar performed at the Institute of Radioengineering and Electronics of the USSR Academy of Sciences from the 1960s to the early 1980s of 20th century is presented. The works were stimulated by the practical cosmonautics requirements that arose after 1957 and required a more accurate knowledge of the distances and motions of the planets of the solar system than what the optical telescopes developed in classical observational astronomy provided. Along with the refinement of the basis of all calculations - the astronomical unit and the construction of the theory of the motion of inner planets certain basic parameters of these planets and their orbits-the radius and nature of the rotation of Venus, its surface, and also the surfaces of Mercury and Mars, were refined. The size and composition of the particles of Saturn's rings are also studied. The work was carried out with the help of the planetary radar designed for them, and the methods and ground-based echo-signals processing software.**

Keywords: **astronomy, radar, echo-signals, astronomical unit, theory of motion of inner planets, characteristics of planets, planetary radar**

UDC 621.396.967

Bibliography - 12 references *Received May 25, 1981*[1]

RENSIT, 2018, 10(2):147-166 **DOI: 10.17725/rensit.2018.10.147**

Content

INTRODUCTION

In the last two decades, a new direction of observational astronomy has successfully developed, using physical principles and methods of radar to study the celestial bodies of the solar system: their positions, movements, rotat The knowledge of the dimensions of the planetary orbits, expressed in kilometers, was especially inadequate, since direct measurements of distances to the planets are inaccessible to the optical means of classical observational astronomy. Indirect methods, based on measurements of the difference in the angular positions of the planets in the celestial sphere with observations from different points of the Earth, led to large errors - hundreds of thousands of kilometers. ion, sizes, physical properties of the constituent rocks, relief and other characteristics of the surface.

The rapid development of radar astronomy was stimulated and supported by the practical needs of astronautics, since for the flights of space stations to planets more precise information was needed on the position and motion of the planets. Observations of the planets and the Sun, conducted over two centuries with the help of optical telescopes, made it possible to construct very perfect theories of their motion, however, the accuracy of calculating the position of the planets on their basis still did not satisfy the high requirements of astronautics.

Unlike indirect optical methods, radar allows you to determine the distance to the planet directly from direct measurements of the time interval during which radio waves propagate to the planet and after reflection from it back to the radar. The speed of propagation of radio waves, equal to the

speed of light, is known with high accuracy, and therefore the accuracy of measuring the distance is also high. In addition, radar makes it possible to determine directly and with high accuracy from the Doppler shift of the frequency of reflected radio waves the rate of change in the distance to the planet (radial velocity).

In modern planetary radars, the distance to the nearest sections of the planets is measured to within a few hundred meters, the speed is up to several centimeters per second. For example, our planetary radar (wavelength 39 cm), located in the Crimea, allows you to measure the distance to Venus to within 300 m, the speed of the planet - up to 0.8 cm/s. At the same time, it is possible to separate and measure the radio signals reflected from the individual parts of the planet being studied, since these signals come with different delay and have different Doppler frequency shifts caused by the rotation of the planet.

The radar of the Moon was carried out in the first years after the Second World War; The radars created by that time had sufficient power for this. However, due to the fact that the power of the reflected radio waves returning to the locator decreases proportionally to the fourth power of the distance to the object to be detected, it was necessary to raise the radar power tens of millions of times or to increase the antenna size and sensitivity of the receivers in order to successfully locate the planets.

The first successful radar of the planet was Venus - in the USSR, the USA and England it was carried out in April 1961, when it was at the minimum distance from the Earth (40 million km). In 1962, the radar of Venus was repeated in the USSR, Britain and the USA, and in 1964 - in the USSR and the United States.

In the observations of 1962, the sensitivity of the radar of the USSR was increased sixfold - at that time it was the most sensitive (the sensitivity of the radar depends on the radiated power, the dimensions of the antenna, and the sensitivity of the receiver). The increase in sensitivity made it possible to measure the distance to Venus for two months and to reduce their errors by a factor of 70 compared with 1961. The distance in 1962 was determined with an accuracy of 12-15 km, speed - 6 cm/s.

For the first time, the energy distribution of the echo signal was obtained from the delay time with high resolution (**Fig. 1**), which allowed to draw conclusions about the nature of the reflecting surface of Venus. At the same time, for the first time (in the USSR and the USA), the direction and period of rotation of Venus was determined. The main result of observations of Venus in 1961, 1962 and 1964. was a cardinal (almost 1000 times) refinement of the astronomical unit - the average distance from the Earth to the Sun. In addition to great scientific value, this fundamental result was of utmost practical importance for the solution of navigational problems during flights of interplanetar.

The increase in the sensitivity of the radar of the USSR made it possible in June 1962 for the first time to conduct a successful radar of Mercury. The first experiments on the radar of Mars and Jupiter were conducted in 1963 in the USSR and the USA.

In January-February 1966, joint Soviet-British radar observations of Venus were carried out, in which radio waves to the planet were emitted from the Center for Remote Space Communications in

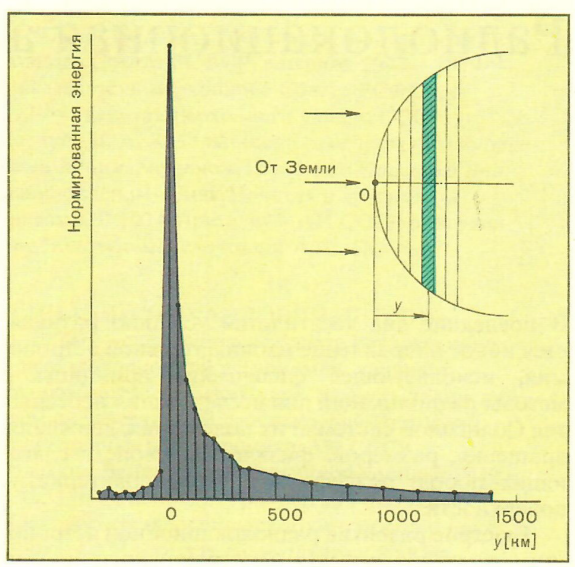

Fig. 1. *The energy distribution of radio waves reflected by Venus in terms of range (delay) (USSR, 1962). A sharp maximum at point 0 (the closest point of the planet to the Earth) says about mirror reflection in the center of the disk of the planet.*

the Crimea, and signals reflected from the planet were received and recorded on a magnetic tape at the Jodrell Bank [2]. Their processing was carried out independently in the USSR and England. The analysis of the obtained frequency spectra of echo signals made it possible to specify the period of rotation of Venus and to supplement information on the reflecting properties of its surface.

Since 1969, the planetary radar of the USSR performed regular measurements of the distance and radial velocity of Venus in order to predict the position of the planet at the final stage of flights to it of interplanetary stations. In the process of preparing for observations, the equipment and methods of observations were continuously improved in order to improve the accuracy of measurements.

Thanks to the increase in the transmitter power, the improvement of the antenna and the receiver, and also the improvement of the methods for processing echoes using computers, the radar sensitivity in the USSR was increased 70 times by 1971. This allowed during the great confrontation of Mars[1] 1971 (the minimum distance to Earth - about 56 million km) during two months to measure its distance from the Earth, which was necessary to ensure flights to it of the interplanetary stations "Mars-2" and "Mars" -3 ".

In 1979, a full-rotating parabolic antenna with a mirror diameter of 70 m (**Fig. 2**) was constructed at the Center for Far-Eastern Space Communications in the Crimea, on the basis of which a more perfect planetary radar was created (at the same wavelength). The use of a high-efficiency antenna, increasing the transmitter power and improving the sensitivity of the receiver made it possible to increase the sensitivity of the USSR radar by a factor of 50, which increased the radar range of the planets by more than 2.5 times.

With the help of this radar in the period from February to April 1980, radar observations of

[1]In oppositions, Mars is visible in the sky in the constellations opposite to the Sun ("standing against the Sun"). In this case, the distance between Mars and the Earth is minimal, unlike the other positions of these planets in orbits.

Fig. 2. *The receiving and transmitting full-rotating antenna with a diameter of 70 m of the Center for Remote Space Communications in the Crimea, used for the USSR's planetary radar since 1980.*

Venus, Mars and Mercury were made on significant sections of their orbits, with the largest distances being 161 million km - to Venus, 135 million km to Mars, 139 million km - up to Mercury (these distances are not limiting for the locator). A new high-precision astrometric information has been obtained for three planets, which, together with the results of observations of previous years, made it possible to construct a unified theory of the motion of inner planets (Mercury, Venus, Earth and Mars). In addition, new information was obtained on the relief and reflective properties of the surface of these planets.

As a result of observations of Venus, Mars and Mercury, which were regularly conducted in the USSR and the USA for two decades, extensive astrometric information was accumulated, on the basis of which the orbits of these planets were substantially refined and more advanced numerical theories were constructed to predict their motion.

The sensitivity of modern radars is increased several thousand-fold compared with 1961, which makes it possible to radar the inner planets at all sections of their orbits. It was also sufficient to conduct observations of the rings of Saturn, four Galilean moons of Jupiter and five minor planets (asteroids).

2. DETERMINATION OF THE ASTRONOMICAL UNIT AND THE RADIUS OF VENUS

The main result of radar observations of Venus, which is of paramount importance for astronautics,

is a cardinal refinement of the astronomical unit[2]. Through the astronomical unit, all distances in the solar system are expressed, so the task of determining its absolute magnitude in kilometers has always been of great cognitive interest and has been in the center of attention of astronomers.

Its values, obtained by different optical methods in the period 1940-1960 r, ranged from 149.4 to 149.7 million km, i.e. the spread was about 300 thousand km. Prior to the beginning of radar measurements, the most reliable value was 149527000 ± 10,000 km, obtained in 1950 from observations of the movement of the small planet Eros during the period 1926-1945. The value of 149 545 000 ± 20 000 km, obtained in 1960 from measurements of the radial velocity of the Pioner-5 automatic station, was coordinated with it. However, as shown by radar measurements, these values were 50-70 thousand km less than the true value.

Such a mistake would lead to inevitable misses in the flights of spacecraft to the planets. Thus, when flying to Mars, the ship would have passed away from the planet at a distance of 15 of its radii, and when flying to Venus - at a distance of three of its radii.

The classical theory of planetary motion made it possible to calculate interplanetary distances through an astronomical unit with an accuracy of 10^{-5}-10^{-6}. Measuring the interplanetary distance in kilometers using a radar, obviously, it was possible to determine with the same accuracy and astronomical unit.

Even the first radar observations of Venus in 1961 made it possible to refine the value of ac: rronomic unit by approximately 50 times. Its values, obtained in different countries and at different wavelengths, were in good agreement with each other, which indicated a high reliability of measurements.

A significant reduction in the errors in measuring the distance to Venus, achieved in the USSR in 1962 and 1964, made it possible to

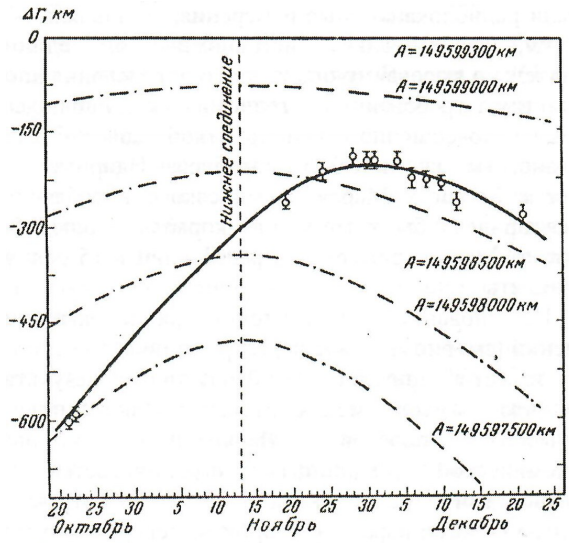

Fig. 3. *Deviations (points) of the measured values of the distance from the calculated values from the observations of Venus in 1962 (in calculations it was assumed that the astronomical unit is 149599300 km, the radius of Venus is 6100 km). The curve (solid line) passing through these experimental points was calculated for astronomical values of 149597900 km, corrections for the difference between the longitudes of Venus and Earth +0 ", 5 and the radius of Venus of 6020 km.Dashed lines-curves calculated for other values of the astronomical unit (are shown on the right), but without taking into account the correction to the longitude and the radius of Venus*

increase the accuracy of the determination of the astronomical unit. However, for this purpose, it was required to refine the parameters of the orbits of Venus and the Earth, as well as the radius of Venus, but this could be done only on the basis of radar measurements over a longer time interval spanning several synodic periods of the Venus rotation (the synodic period is the time interval between the two lower connections, in which the distance between the Earth and Venus is minimal).

The possibility of refining the elements of the

Table

The values of the astronomical unit and the average radius of Venus, obtained in the USSR in different years

Observation interval	Astronomical unit (km)	Venus radius (km)
1961	149599300 ± 1000	-
1962	149597900±250	6020±50
1964	149598000 ± 130	-
1962-1964	149597886 ± 80	6046±15
1962-1975	149597888.9 ± 0.7	6052.3±0.3
1962-1980	149597889.0± 0.3	6050.1±0.1

Note. The astronomical unit values in the table are given at the speed of light 299792.5 km / s. If we use the refined value of the speed of light 299792458 ± 1.2 m / s, then the magnitude of the astronomical unit in the last definition will be equal to 149597868 ± 0.7 km.

[2]The astronomical unit of length is the average distance of the center of gravity of the Earth-Moon system from the center of the Sun.

orbits was demonstrated already in the processing of the results of 1962 (**Fig. 3**). Then, along with the correction to the astronomical unit, corrections were also found to the position in the orbit and the radius of Venus (Table).

The radius of Venus on optical observations was determined at the level of the upper edge of the cloud layer and according to the estimates of astronomers was 6120 ± 8 km, the height of the cloud layer above the surface was unknown. For an accurate determination of the astronomical unit, it is very important to know the radius of the reflecting surface of Venus, as the distance to the front sections of this surface is measured radar-wise, and the theory of the motion of the planets gives the position of their center of mass, which is further by the radius value.

The processing of two cycles of measurements performed in the USSR in 1962 and 1964 made it possible to find corrections to the elements of the orbits of Venus and the Earth, which led to a further refinement of the astronomical unit and the radius of Venus.

Work on the simultaneous refinement of the astronomical unit, the parameters of the orbits of Venus and Earth, and the radius of Venus was carried out by the Lincoln Laboratory in the USA in 1966. As a result of the joint processing of the radar measurements of the USA and the USSR for the period 1962-1966, and optical measurements of the USA for the period 1950-1966. for the astronomical unit at a speed of light 299792.5 km / s, the value of 149597892.3 ± 1.5 km was obtained; for the radius of Venus is 6055.8 ± 1.2 km.

Subsequent measurements and analysis of radar data obtained before 1969 at the Lincoln Laboratory gave a value of 6050 ± 0.3 km.

The most accurate values of the astronomical unit and the radius of Venus in the USSR were obtained in 1976 and 1980. thanks to the construction of a more perfect theory of the motion of Venus and the Earth (see Table).

3. THE THEORY OF MOTION OF INNER PLANETS

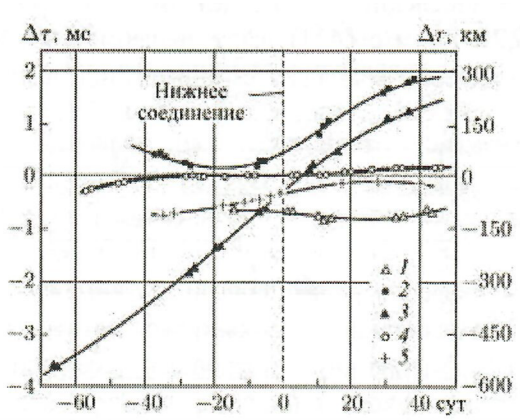

Fig. 4. *Deviations of the delayed echo signal from Venus and the corresponding distances from the calculated values calculated in accordance with the classical theory (calculated in the calculation: astronomical unit -149597890 km, radius of Venus-6050 km), measured in different years in the USSR.*

Radar observations of the planets have shown that even after the astronomical unit is refined, there are noticeable discrepancies between the measured distances and their values calculated by classical theories. The discrepancies reached several hundred kilometers (**Fig. 4**). Such errors in predicting the motion of planets according to classical theories made it difficult to solve the navigational tasks of astronautics, especially such complex ones as landing of the descent vehicle into a pre-selected area of the surface or the removal of an artificial satellite of the planet with given parameters of its orbit.

In connection with this, during the flights of automatic interplanetary stations, along with trajectory measurements of the position of the station, radar observations were also needed to determine the position of the planet.

It was necessary to create new, more accurate theories of planetary motion based on radar information.

Numerical theory of the motion of Venus and the Earth on the basis of radar observations of Venus in the interval 1962-1975. was built by the Institute of Radio Engineering and Electronics of the USSR Academy of Sciences and the Institute of Applied Mathematics of the Academy of Sciences of the USSR together with a number of organizations in 1976-1978.

At the same time, the data of optical observations of Venus and the Sun made by the Nikolayev Observatory of the USSR Academy of Sciences and the US Naval Observatory were used, and the parameters of the movement of Venus-9 and Venus-10 artificial satellites in Venus in 1975

The problem was solved by numerical integration on the computer of a system of differential equations describing the motion of eight bodies in their gravitational field. The bodies were the Sun, Mercury, Venus, the Earth-Moon system, Mars, Jupiter, Saturn, Uranus. Estimates have shown that the influence of Neptune and Pluto in solving this problem can be neglected. Twelve elements of the orbits of Venus and the center of mass of the Earth-Moon system, as well as the astronomical unit and the radius of Venus, were included in the number of parameters to be determined.

The experimental verification of the constructed numerical theory, performed with the next radar of Venus in 1977, 1978 and 1980, showed that deviations of the measured distances from Venus from their predicted values in the numerical theory do not exceed 3-6 km (**Fig. 5**). At the same time, deviations of the measured distances from the forecast according to the classical theory, even with the specified astronomical unit, reached 500 km in this period.

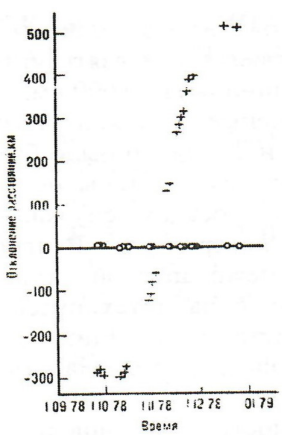

Fig. 5. *Deviations measured in 1978 in the USSR distances to Venus from the calculated values, calculated on the basis of a new numerical theory (circles) and classical theory (crosses); in the calculation it was accepted: the astronomical unit is 149597888.9 km, the radius of Venus is 6052.3 km.*

At the launch of the stations "Venus-11" and "Venus-12" in 1978 r. All navigational calculations were carried out on the basis of a new numerical theory. Measurements of the parameters of the movement of the stations, in turn, confirmed the high accuracy of this theory: the measured distances to them differed from those predicted by no more than 3 km.

In 1979, the Institute of Radioengineering and Electronics of the Academy of Sciences of the USSR jointly with other organizations processed radar observations of Mars in 1964-1971 and optical observations of Mars and the Sun for 1960-1975.

The determination of the orbits of Mars and the Earth was carried out by the same method used in the processing of observations of Venus. The determined parameters were 12 elements of the orbits of Mars and the center of mass of the Earth-Moon system. The accuracy of the forecasting of the motion of Mars on the basis of the solution obtained was verified by its radar observations in the USSR in 1980. The error in predicting the distance relative to the mean surface level of the planet on a two-month interval of observations varied monotonically from 13.6 to 21 km.

As a result of radar observations of Venus, Mars and Mercury in large sections of orbits in 1980, a new high-precision astrometric information was obtained in the Soviet Union. It substantially supplemented the results of previous radar observations of the planets, in particular Mercury and Mars. Thus, a real basis was created for constructing a unified theory of the motion of inner planets, i.e. for the simultaneous determination of the orbits of Mercury, Venus, Earth and Mars along the entire set of available radar and optical observations.

In 1980, the Institute of Radioengineering and Electronics of the Academy of Sciences of the USSR jointly with a number of organizations developed and software implemented a computer method and algorithms for constructing such a theory on the basis of the general theory of relativity. In this case relativistic differential

equations were used to describe the motion of inner planets. Among the planets, whose motion is described by a system of differential equations, Neptune was additionally introduced. When processing observations in the calculated values of the delay time of the reflected signal, relativistic corrections were introduced.

On the basis of the developed methodology, a unified relativistic theory of the motion of inner planets was created.

This problem was independently solved at the Institute of Applied Mathematics of the USSR Academy of Sciences and the Institute of Theoretical Astronomy of the USSR Academy of Sciences.

The construction of this theory was carried out on the basis of radar and optical observations of Venus and Mars, used earlier in the construction of particular theories of their motion; radar observations of Venus, made in the USSR in 1977 and 1978; the above-mentioned radar observations of Venus, Mars and Mercury in 1980; radar observations of Mercury in Arecibo in 1964-1965; optical observations of Mercury performed by the Nikolaev Observatory of the USSR Academy of Sciences, the United States Marine Observatory and the Greenwich Astronomical Observatory in 1960-1976. A total of 3.768 radar measurements of the delay time of the signal reflected from the planets and 7193 optical (angular) measurements were processed.

During processing, 28 parameters were determined: the elements of the orbits of Mercury, Venus, the center of mass of the Earth-Moon system, Mars, the astronomical unit, the radii of Mercury, Venus, Mars. For the radii of Mercury and Mars the values were respectively 2434.9±1.1 km and 3394.6±0.3 km.

The root-mean-square deviations of the measured distances from their values calculated from this theory are: for Venus (in the period 1970-1980) - 0.9 km; for Mars (in the period 1967-1980) - 2.5 km; For Mercury (in 1980) - 2 km. These deviations are largely due to the influence of the surface relief of the planets. Deviations of optical measurements from the forecast according to this theory range from 0.6"-1.2".

In order to estimate the limits of the applicability of Newtonian mechanics in the construction of such theories, all information was also processed without taking into account relativistic corrections. As might be expected, the coordination of the measured and calculated ranges has deteriorated markedly, systematic deviations have appeared in some sections of the orbits, reaching 390 km for Mercury, 12 km for Mars and 8 km for Venus.

The good agreement between the measured and calculated data achieved in the construction of a single relativistic theory of the motion of inner planets can be considered as an additional experimental test of the general theory of relativity.

It should be noted that radar observations of planets over a 20-year period (together with optical observations of planets and the Sun) made it possible to reduce the uncertainty of knowledge of the astronomical unit by almost 50,000 times and to increase the accuracy of the theory of motion of inner planets by one and a half to two orders, predict their mutual position with an error of less than 15 km. These fundamental results are a major contribution to the study of the dynamics of the solar system

4. ROTATION OF VENUS AND MERCURY

Among the fundamental discoveries of radar astronomy are the results of a study of the rotation of Venus and Mercury. Three unexpected natural phenomena were discovered.

The first - Venus, unlike all other large planets, rotates in the opposite direction, opposite to its orbit in orbit. The second - the reverse rotation of Venus is regulated not by the Sun, but by the Earth, and so that at each approach to the Earth Venus almost exactly faces the Earth with the same side. Third - Mercury for every two orbiting makes almost exactly three turns around its axis. Previously, it was mistakenly believed that Mercury makes one revolution around its axis

during one revolution in orbit, i.e. he always faces the Sun with the same side.

Before the radar observations, the period of rotation of Venus was estimated from 15 hours to 225 days. (the definition was complicated by the cloud cover of Venus). The width of the frequency spectrum of the echo signal at the first radar of Venus in 1961 showed that the planet rotates very slowly - with a period of more than 100 days.

More definite information was obtained with the next radar in 1962, when due to a significant increase in radar sensitivity, the duration of observations was increased to two months. At that time, the Institute of Radioengineering and Electronics of the Academy of Sciences of the USSR and the Jet Propulsion Laboratory of the United States independently established that Venus rotates in the opposite direction (in comparison with the direction of orbit around the Sun), the period of its rotation around the axis lying within 200-300 Earth days. In these observations, the rotation was investigated from measurements of the width of the frequency spectrum of radio waves reflected from the planet upon irradiation with a monochromatic signal.

The width of the frequency spectrum is proportional to the magnitude of the angular velocity of the total relative rotation that could

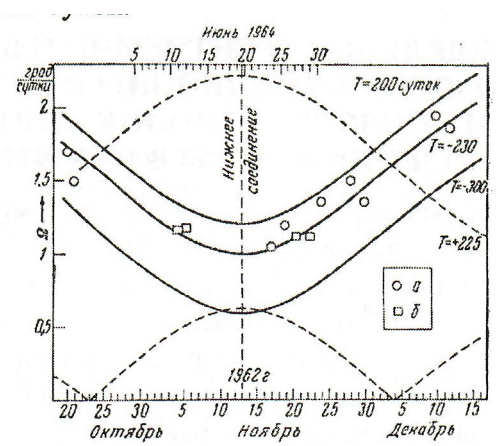

Fig. 6. *Determination of the period and direction of rotation of Venus from observations in the USSR (circles) and in the USA (crosses) in 1962. The curves show how the total angular velocity of Venus's apparent rotation relative to the radar should vary with different values of the period T. The measurements indicate reverse rotation with a period of 200-300 days.*

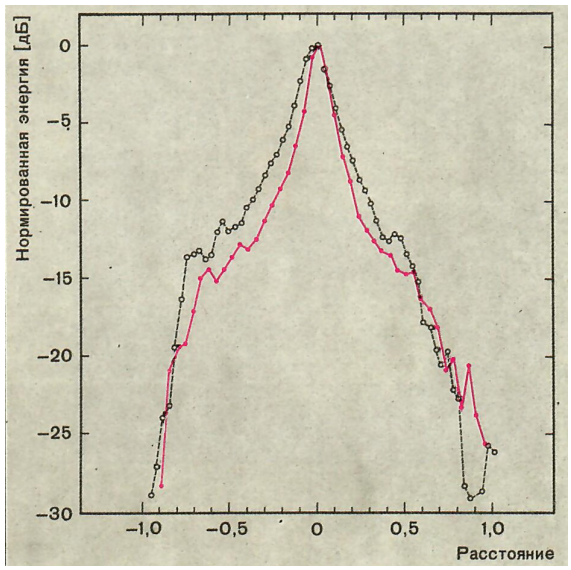

Fig. 7. *Energy distribution of echo signals from Venus along the equator with monochromatic irradiation at a wave of 39cm (Crimea-Jodrell Bank, 28.01.1966, solid line) and 3.8cm (Heystek, 01.02.1966, dashed line). The distance from the center of the visible disk of the planet in fractions of its radius is plotted horizontally.*

be seen from the Earth. This "visible" rotation consists of two components: own (sidereal) rotation and apparent, which is a consequence of the change in the mutual position of Venus and the Earth. The magnitude and sign (direction) of the second component vary with time; its values, depending on the dates of observations, are calculated on the basis of the known motion of the planets. In the lower connections, it is maximal (about 0.6 degrees per day) and has a positive sign; 21 days before the lower connection and 21 days after it the sign changes to the opposite one.

The character of the change in the total angular velocity of the visible rotation will be different depending on which sign has the angular velocity of the planet's own rotation. If it were positive, corresponding to a direct rotation, then the angular velocity of the total apparent rotation of Venus in the lower connections would be the largest and would decrease with departure from them. In fact, in all measurements near the lower connections, the opposite picture is observed; therefore, the direction of the proper rotation of Venus is the opposite (**Fig. 6**).

In subsequent observations, the rotation of Venus was investigated by other, more accurate methods, based on tracking the movement of the

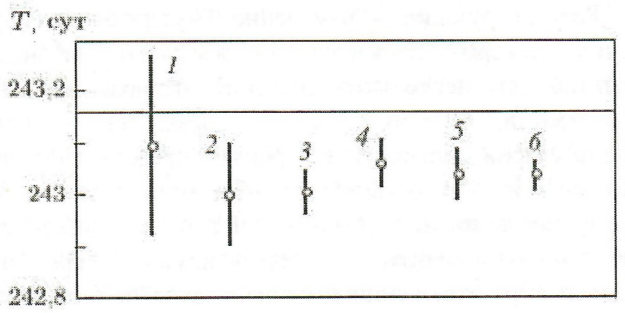

Fig. 8. *Intervals of possible values of the period of rotation of Venus by radar observations in the USSR and the USA in different years.*

abnormally reflecting radio waves detected on its surface. They appear on the frequency spectrum in the form of characteristic details with an increased spectral density (**Fig. 7**). Their position in the spectrum is determined by the ray velocities of the regions at the time of observation. Tracking the change in the position of parts in the spectrum over a long time allows us to determine not only the period, but also the direction of the axis of the planet's own rotation and specify the coordinates of the regions. In the joint Soviet-English observations of Venus in 1966, this method yielded a value of 243.9 ± 0.4 days for the period.

More precise values of the period of rotation of Venus were obtained by identifying the details of the spectrum from the anomalously reflecting regions in the lower compounds of different years.

In 1972, in 1975 and in the years of 1977, in the USSR, the moments of passage through the center of the visible disk of Venus were measured for two abnormally reflecting regions whose coordinates on the surface of the planet were determined by observations of 1964. The processing of these measurements gave a value of 243.04 ± 0.03 days. Similar results were obtained in the USA (Arecibo, 1964, 1967 and 1969 - 243.9 ± 0.1 days, Goldstone, 1962, 1964, 1966, 1967 - 242.98 ± 0.04 days).

These measurements show that the period of rotation of Venus in the opposite direction is very close to the synchronous (243.16 days), in which it would face the Earth exactly the same side in each lower junction (**Fig. 8**). The duration of a solar day on Venus is 117 earth days. As shown by the analysis of radar observations, the axis of rotation of Venus is almost perpendicular to the plane of its orbit: the deviation from the perpendicular does not exceed 2°.

Before carrying out radar studies of Mercury, as already mentioned, astronomers believed that the period of its rotation around the axis is equal to the period of revolution around the Sun (88 days) and that it always faces the Sun with the same side as the Moon to the Earth. However, the radar observations of Mercury performed in Arecibo in 1965 with different positions in orbit showed the fallacy of such a statement.

It was found that the period of rotation of Mercury is 59±3 days. Subsequent detailed analysis of old sketches and photographs of the surface of Mercury led astronomers to a more accurate value of the period - 58.65 ± 0.01 days, which corresponds to orbital-rotational synchronization-2 orbiting Mercury makes 3 turns around the axis.

It is necessary to explain that the previous error of astronomers was caused by the objective difficulties of observing Mercury by optical means, namely proximity to the Sun and small angular dimensions. Because of proximity to the Sun, astronomers were forced to observe Mercury once a year, during the period of its greatest angular distance from the Sun, when the conditions for observations are most favorable.

During the year, Mercury makes about four hits in orbit and, as now established, about six revolutions around the axis, rather than about four, as astronomers mistook earlier. At the same time, the earlier sketches and photographs of the surface of Mercury within their rather crude resolution are consistent with both the new and the old, erroneous, value of the period

.

5. SURFACE OF VENUS

Venus is surrounded by a dense cloud cover, opaque in visible, ultraviolet and infrared rays, so its surface is not available for observation even by the most sophisticated telescopes. Radio waves of the entire decimetric and adjacent part of the

centimeter range, used in radar, freely pass through the entire atmosphere of the planet. Due to this, its surface was accessible ("visible") for observations by radar.

Two decades ago nothing was known about it. The hypothesis of a continuous ocean of water covering the entire planet seemed quite plausible. The hypotheses about a continuous ocean of oil and a continuous sandy desert were not rejected either.

The first reliable information about the surface of Venus was obtained only from the results of radar observations of 1961 and 1962.

Then for the first time it was found out that it is composed of hard rocks, the dielectric permittivity and density of which is about the same as that of terrestrial rocks on a silicate basis. This conclusion follows from the measurements of the coefficient of the back reflection of radio waves and the dependence of the scattering pattern on the angle of incidence on the planet's surface (the coefficient of back reflection is defined as the ratio of the energy of the received echo from the planet to the energy that would have been assumed had the planet been a smooth ideally conducting ball of the same size).

The average reflectance at 12.5, 39, and 68 cm wavelengths was within 11-16%, and its value during averaging over large areas changed very little from day to day (for example, in a two-month interval of observations in 1962 in the USSR, the change was not went beyond 11-18%), which indicated an isotropic structure of the surface on a global scale. The values of the reflection coefficient corresponded to the values of the permittivity 4-6, which are characteristic for soil density of 2-3 g / cm3. It is pertinent to note that the average reflection coefficients of the surfaces of Mars, Mercury and the Moon are about half that of Venus.

If the first observations of Venus were aimed at obtaining integral characteristics of reflection and elucidating the global properties of the surface, then later the main focus was already on identifying the distinguishing features of different regions. Abnormal areas of increased reflection were discovered back in 1962, and then re-examined in 1964. At the same time, a venereocentric coordinate system was introduced, whose zero meridian passes through the brightest region called the α-region (the latitude of the α-region is -30°). In this system, it was possible to determine the coordinates of other detected anomalous regions, thereby creating a framework for constructing radar maps.

The first, still rather rough map of the reflective properties of a limited region with a resolution of hundreds of kilometers was compiled from observations in Heystock (USA) in 1969. A map of a larger region with a resolution of 50x50 km^2 was obtained from observations in Goldstone in 1969 and 1970. These maps show some large-scale continental formations of limited areas. Studies with a resolution of 10x10 km^2 of individual regions measuring about 1500 km in the equatorial belt of Venus began at Goldstone in 1972. In one of these regions, more than 10 ring craters with a diameter of 35 to 150 km were found. Works on the mapping of individual parts of Venus with a resolution of about 20 km were carried out in 1976 also in Arecibo.

Great attention was paid to the studies of its relief during the radar observations of Venus.

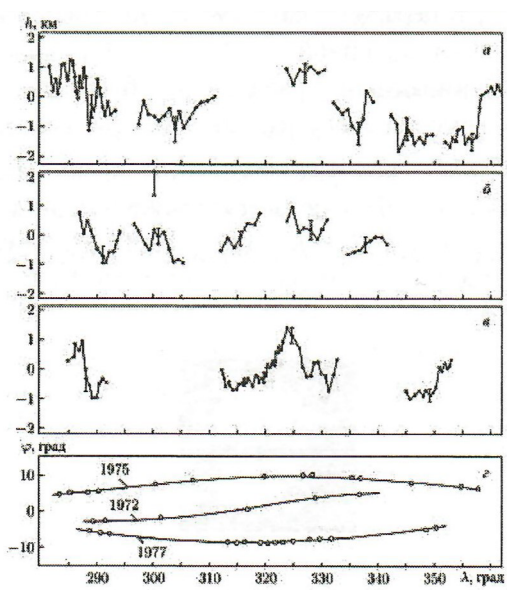

Fig. 9. *Profiles of the heights of the surface of Venus, obtained in the USSR in 1972, 1975 and 1977. Below: the tracks along which measurements were taken.*

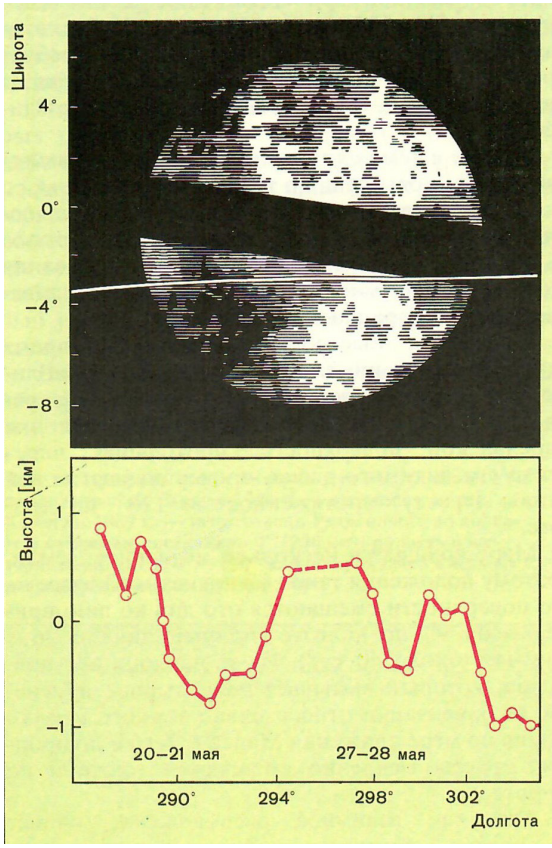

Fig. 10. *Comparison of the profile of the altitudes of the surface of Venus (USSR, 1972) (bottom) with the results of the study of the relief of the circular section, along which the profile measurement trajectory passed (Goldstone, USA, 1973) (top). The track is marked by a white stripe. In the upper figure, high brightness corresponds to a large brightness; all brightness gradations - four (after 500 m)*

For such studies, the equatorial belt of Venus is available in the latitude interval ± 10°. The measurements of the surface heights profiles in this belt, performed at the Haystack and Arecibo stations in 1967-1970, covered eight complete revolutions of Venus relative to the Earth.

The height profiles were obtained from measurements of the delay time of signals reflected as the planet rotates from the closest parts of its surface to the Earth. The resolution along the traces was 200-400 km, the accuracy of measuring the altitude variations was 0.2-1 km. There are two mountainous areas with a length of 4 and 2.5 thousand km, the elevations of which are respectively about 4 and 3 km. On the other longitudes, elevations do not exceed 2 km.

In the USSR measurements of height profiles were carried out in 1972, 1975 and 1977. The length of the traces was about 10 thousand km,

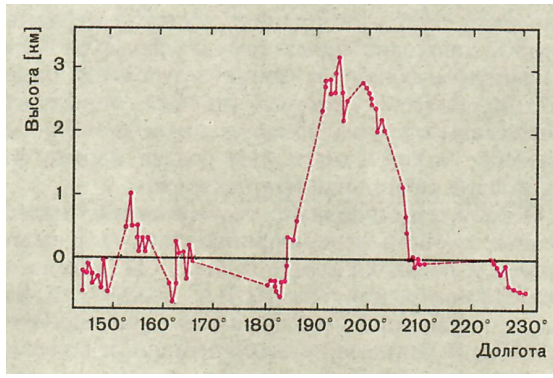

Fig. 11. *Profile of the heights of the surface area of Venus (USSR, 1980). The measurement route runs from 2.4 ° S. (left) to 3.7 ° S. (on right).*

the surface resolution along the traces was 40-200 km, the accuracy of the altitude measurements was 150-300 m (**Figs 9, 10**).

Simultaneously with the heights profiles along the slopes, the surface slopes (by the nature of the radio wave scattering) and the permittivity of the soil (from the reflection coefficient measurements) of individual regions were determined - an analysis of these parameters together with altitude variations gives a more complete picture of the investigated areas.

The measured altitude differences on all routes do not exceed 2 km. Areas with a strongly cut profile are detected (for example, in the longitude interval 280°-290°), where altitude differences of 1-2 km are observed on the basis of 100-200 km, and extensive flat areas with a length of more than 1000 km (for example, in the vicinity of 305 ° longitudes and 350° at latitude + 10°). The mountain range at longitude 325° also has a length of more than 1000 km and a width of several hundred kilometers. The plain at longitude 350° resembles a giant basin composed of less dense material than its slope at a longitude of 355°. The surface characteristics of different regions vary within wide limits: the permittivity is from 2.7 (which corresponds to dry, sandy deserts on the Earth) to 6.6 (hard rocks), the average surface slopes are from 2.5° to 5°.

In the observations of Venus in the USSR, carried out in 1980 at a distance of 161 million km, the research route lay in another interval of longitudes and had a length of about 14 thousand

km. It passed through the two mountain regions mentioned above. The greatest height of the first of them at the latitude of the route was about 4 km (at a longitude of 90 °), the height of the second - about 3 km (at a longitude of 193 °). For the second region, a detailed elevation profile with a longitude resolution of about 40 km was obtained (**Fig. 11**).

6. SURFACE OF MARS

To realize the radar of Mars is much more difficult than the radar of Venus because of its greater distance from the Earth, smaller dimensions and relatively fast rotation. The speed of rotation of Mars is approximately 400 times greater than the speed of visible rotation of Venus in the lower connection. In most of the confrontations (with the exception of the great ones, which repeat only after 17 years), it approaches the Earth by only 80-100 million km. The detection of an echo from Mars at such distances requires approximately 500 to 1000 times more sensitive radars than from Venus in the lower connections.

However, if the sensitivity of the radar is already increased to the required value, then due to the rapid rotation of Mars and the greater inclination of its axis to the plane of the ecliptic (about 25 °), the possibilities for a detailed study of its surface are much better than for the study of slowly rotating Venus.

Due to the rapid rotation during one night cycle of observations (when you approach the Earth, Mars is only visible at night), say for 8 hours, the points of the Martian surface nearest to the Earth passing through the center of its visible disk draw a line (route) of 120° in longitude.

Mars rotates somewhat slower than the Earth, so the positions of such (one-day) traces on its surface are shifted from day to day by about 9° in longitude (a full cycle of 360° takes about 40 days). Due to the inclination of the axis of rotation, which causes a continuous change in its orientation relative to the terrestrial observer as Mars and Earth move in orbits, the traces slowly move also in latitude.

Since the mutual arrangement of planets in orbits in oppositions of different years varies, the traces of observations pass through different latitudes, the possible interval of which is ± 25° from the equator.

The first series of radar observations of Mars at different wavelengths was performed in the 1960s: in the Crimea (1963, 39 cm), Goldstone (1963, 1965, 1969, 12.5 cm), Milestone (1965, 23 cm), Arecibo (1965, 70 cm), Heystack (1967, 1969, 3.8 cm). Traces closest to the Earth points in these observations were in the northern hemisphere of Mars.

Studies have shown that the coefficient of back reflection of radio waves does not depend on the wavelength. Its average value is 0.07. It is about the same as that of the Moon, but somewhat larger than that of Mercury, and half as much as that of Venus. At the same time, local parts of the surface of Mars are differentiated in their properties much more than in Venus and Mercury. For example, the reflection coefficient varies depending on the coordinates on the surface in a wide range - from 0.03 to 0.14.

The most intense echoes are due to mirror reflection from smooth surface areas in small neighborhoods of the nearest point. For these sites, the reflection coefficient values (12-14%) are approximately the same as for terrestrial rocks with a dielectric constant of about 4.5, which corresponds to a density of about 2.5 g/cm^3.

The low reflectivity of some regions of Mars can be caused either by their large roughness (irregularities in the wavelength scale lead to a decrease in specular reflection), or by the low density of the surface material (greater absorption of radio waves and a smaller reflection coefficient) or by the combined action of these causes-a weak echo level Signals did not allow to find out the true reason.

It should be noted that a small reflection coefficient (3-4%) corresponds to a matter density of only 0.8-1.0 g/cm^3. Such a density can, for example, have fine dust covering these areas of the surface. This dust, even under conditions of rarefied · Martian atmosphere, can be suspended

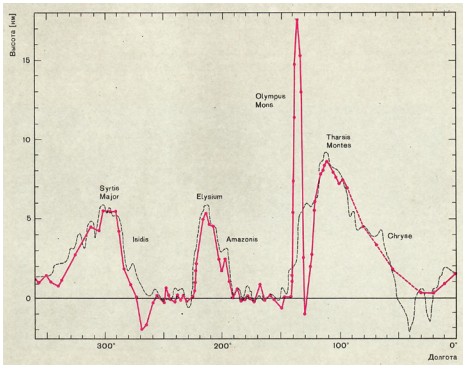

Fig. 12. *Profile of the heights of the Martian surface along the 21st parallel of the north. (Crimea, 1980 - solid line, Haystack, 1967 - dashed line). The longitude resolution was mainly 4° (240 km); the region in the longitude interval 120° -150° was analyzed in the Crimea with a resolution of about 1.5 ° (90 km).*

for a long time and can be a source of Martian dust storms.

Mars compared with other inner planets and the Moon has the smoothest surface.

The root-mean-square value of the slopes of the irregularities on a scale of several dozen radio wavelengths varies for different regions in wide ranges - from 0.5 to 6°, but its average value is about half that of Venus and 3 times less than in Mercury and the Moon .

The first radar measurements of the profile of the altitudes of the Martian surface along the 21st parallel of the north. were performed at Heystek in 1967. The hardware resolution by distance was 9 km, but the relative changes in altitude were measured to within 1 km.

Favorable conditions for radar observations of Mars were available during the great confrontation of 1971. Radar in this period was conducted in the Crimea, Heistek and Goldstone. The research routes passed in the southern hemisphere of the planet and covered the latitude from -14° to -23°. Along the traces were obtained profiles of heights and characteristics of reflection of radio waves by local areas of the surface. The total height difference from the highest mountains (about 8 km) to the lowest basins (about 8 km) in the investigated belt of latitudes was about 16 km.

Radar studies of reflective and physical characteristics in the southern hemisphere of the equatorial belt of Mars, performed in the 1970s,

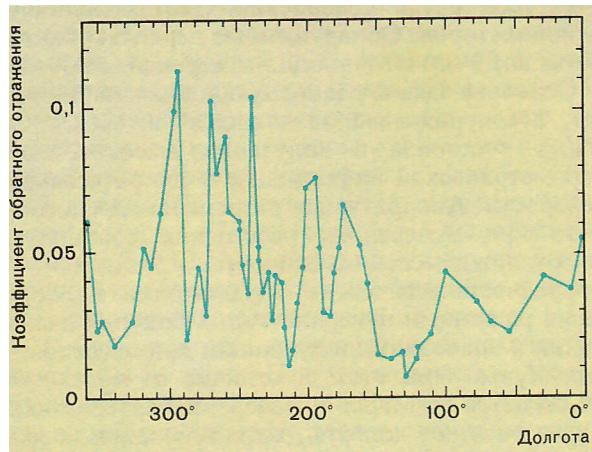

Fig. 14. *Variations of the Mars backscattering coefficient along the 21st parallel of the north latitude. (USSR, 1980).*

showed that the parameters of local sections of the surface vary within the same wide limits as in the northern hemisphere.

Interesting new information on the surface of Mars was obtained by its radar in the USSR in 1980. Along the 21st parallel of the northern latitude, passing through the Tharsis, Olympus Mons, Elysium, Syrtis Major massifs, measurements of the surface profile were made (**Figs 12, 13**) and the reflection coefficient of radio waves (**Fig. 14**). The distance to Mars (100-135 million km) was measured to within 0.6 km.

The measurement route passed along the northern slope of the mountain Olympus Mons, where the maximum at this latitude was measured - 17.5±1.5 km. The average steepness of the slopes of the mountain, estimated from the ratio of the height to the half-width of the foot at the zero level, is 3.6°. It is found that the western slope of the mountain is separated from the Tharsis mountain massif by a depression whose depth is 1 km below the average surface level. Another depression, up to 2 km deep, is at a longitude of 270° in the region of Isidis. Mount Olympus Mons and these depressions were not previously recorded on the height profile obtained at Heistek at the same latitude (see Fig. 12).

The reflection coefficient of Mars along the path varies by more than an order of magnitude - from 0.01 to 0.12 (see Fig. 14). An abnormally low value in the mountainous regions of Olympus Mons and Elysium can be associated with a special structure of their surface: they have a small fraction

of the areas oriented perpendicular to the incident ray of radio waves. Its greatest importance is on the Syrtis Major plateau; there is a strong mirror image from large-scale smooth regions.

7. SURFACE OF MERCURY

The radar of Mercury is almost as difficult as the radar of Mars. The minimum distances to Mercury in different lower connections vary within the limits of 80-100 million km, as in most of the oppositions of Mars. The geometric area of its cross-section is 2 times smaller than that of Mars, the surface is several times more rough, as a result of which the fraction of mirror reflection of radio waves from its surface decreases. True, compared with Mars, it rotates 60 times slower, so that the allocation of its echoes from the receiver's noise is simplified.

The first radar observations of Mercury at different wavelengths were performed in the Crimea (1962, 39 cm), Goldstone (1963, 12.5 cm), Arecibo (1964, 70 cm), Heisteke (1966, 3.8 cm) . The main task of these and subsequent observations in the 60's was to obtain astrometric information about the speed of the planet and the distance to it. This information was necessary for the independent determination of the astronomical unit and the refinement of the orbits of not only Mercury, but also of Venus and the Earth, since Mercury exerts a noticeable gravitational influence on their motion, depending on its position in orbit.

Simultaneously with the astrometric data, the average (global) characteristics of the reflection of radio waves by the Mercury surface were obtained: the reflection coefficient and the energy distribution of the echo signals by delay and frequency.

The hardware resolution in the observations of the 1960s was insufficient to measure the height profile and to study in detail the characteristics of the local sections of the Mercury surface. Such studies with a resolution of the surface at the equator of about 40 km and an altitude of about 1 km were achieved only in the early 1970s after increasing the sensitivity of radar. The observed

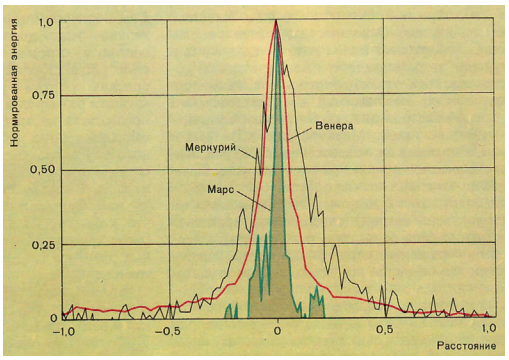

Fig. 15. *Distribution of the energy of echo sialals from Mercury, Venus and Mars along the equator at a wavelength of 39 cm (USSR, 1980). The normalized distance from the center of the visible disk of the corresponding planet in fractions of its radius is plotted along the horizon. The averaging time of the echo-signal energy is about 12 min. For Venus and Mars, the distributions have a smaller width than for Mercury, which suggests greater surface rareness of the two planets.*

altitude differences reach 3 km with an accuracy of ± 500 m.

The main task of radar observations of Mercury, performed in the USSR in 1980, was to obtain high-precision astrometric information about its distance and speed: The instrumental resolution for distance measurements was 1.2 km, with a velocity measurement of 5 cm/s.

The average statistical characteristics of the reflection of radio waves by the surface of Mercury are very close to the values obtained during the studies of the Moon. In this case, in contrast to what is observed on Mars and Venus, the characteristics depend little on the longitude, although the changes in the reflection coefficient by a factor of 2 depending on the longitude are also observed. Its average values at different wavelengths are in good agreement with each other and lie in the range 0.055-0.065 (for the Moon in the same range of radio waves they vary within 0.065-0.075).

Surfaces of Mercury and the Moon are similar in degree to their unevenness (roughness): as in the case of the Moon, the average slopes of the surface of Mercury increase monotonically with a decrease in the wavelength from 6° at 70 cm to 9.7° at 3.8 cm. The slope is about 1.5 times more than that of Venus, and 3 times more than that of Mars. The relative degree of roughness of these planets is clearly shown in **Fig. 15**.

8. THE RINGS OF SATURN

In the last century, it was theoretically and experimentally proved that the rings of Saturn consist of a huge number of particles that independently revolve around the planet along Keplerian orbits with different velocities. As for the size and composition of the particles, there was no definite answer to this question. On the basis of numerous observations near the infrared frequency range, it has recently been concluded that the rings of Saturn consist of the smallest particles of ice with a diameter of about 70 μm. However, there were arguments in favor of the fact that the ring is a conglomerate of ice fragments (or another substance covered with ice) of various sizes (from several meters to a centimeter or less).

More definite conclusions about the size and composition of the particles could be made only by the results of the radiolocation of the rings of Saturn.

The first echoes from the rings of Saturn were obtained with the help of radar in Goldstone at a wavelength of 12.6 cm in 1972-1973. A big surprise for the researchers of this planet was the unexpectedly large magnitude of the total area of particles participating in the reflection of radio waves back to the locator: it turned out to be equal to 68% of the geometrical ring of the rings visible from Earth. Such a value could only be obtained if the particle sizes in the rings were greater than 1 cm, which was in contradiction with the previous conclusions.

In late 1974 and early 1975, the radiolocation of Saturn's rings at Goldstone was performed at 3.5 and 12.5 cm wavelengths. In the latter case, the sounding signal was emitted from Arecibo, and the echoes were received at Goldstone.

From the analysis of all observations it follows that the reflection from the rings of Saturn is completely depolarized and does not depend on the wavelength. The joint processing of these results with radio astronomical and optical observations showed that the particles in the rings of Saturn are very rough, polyhedral pieces of water ice with an average transverse dimension of about 4 cm. The total echo signal from Saturn's rings is formed by repeated reflection of radio waves (almost lossless)) from the particle surfaces.

Fig. 16. *Antenna of the Center for Remote Space Communications, used in the USSR's planetary radar prior to 1980.*

New information was provided by the radiolocation of Saturn's rings in January 1976, conducted in Arecibo at a wavelength of 12.5 cm. The use of a modulated signal made it possible to separate the echo signals simultaneously by delay and frequency and to obtain a radial distribution of the particles along the annular zones. An appreciable number of particles was also found in the optically dark ring near the planet.

The localization of echo signals by delay and frequency showed the absence of an echo signal from the space occupied by the planet itself (radio waves are absorbed by the vast atmosphere of Saturn).

9. CAPTIVE RADAR

In the Soviet Union, radar studies of planets are conducted by the Institute of Radio Engineering and Electronics of the USSR Academy of Sciences in conjunction with a number of organizations. Planetary radar at a wavelength of 39 cm was created in 1961 on the basis of the antenna (Figure 16) and the transmitter of the Center for Remote Space Communications in the Crimea. Subsequently, as already noted, radar was continuously improved to improve its sensitivity and measurement accuracy.

In 1962, the radar sensitivity was increased mainly due to the application of a low-noise paramagnetic amplifier (maser) on a ruby crystal

cooled to liquid helium at 4 K (-269° C) at the input of the receiver. In the future, its increase was achieved by increasing the transmitter power, upgrading the antenna, applying more advanced methods for processing echoes using computers and improving the measuring equipment complex. Radar sensitivity was radically increased in 1980 due to the use of a new antenna with a mirror diameter of 70 m (see Fig. 2) and more powerful transmitters.

In comparison with conventional planetary radar has a number of distinctive features.

The received echo signals from the planet are very weak, long-term accumulation and averaging are required to separate them from the fluctuation noise interference of the receiving equipment, which can reach tens of hours with a very weak signal (the ratio of the echo-signal energy to the fluctuation noise at the output of the accumulator increases in proportion to the square the root of the accumulation time).

The reception of the signal reflected from the planet takes place after its emission through a considerable time, unusual for ordinary radiolocation, during which the radio waves propagate to the planet and back (for example, for Venus it ranges from 4.5 to 29 min, and for Mars reaches 45 min). In connection with this, the radar observation session of the planet includes two time intervals: in the first one, the probing signal is continuously radiated to the planet, in the second, the receiving return signal reflected from it is received.

The position and motion of the planet relative to the radar can be calculated with great accuracy in advance, even before the beginning of the observation session. When the first radar of Venus was conducted, the distance to it could be predicted with an accuracy of ± 20 thousand km. Now, after clarifying the astronomical unit and constructing a more accurate theory of the motion of inner planets, the distance to them is predicted to within 10-15 km.

High accuracy of the preliminary calculation allows measuring the delay and Doppler shift of the echo frequency based on the hardware reference (playback) of their predicted values and determining deviations from the forecast, which drastically reduces the measurement interval when processing echoes.

Finally, it must be specially noted that the relative accuracy of measurements in the planetary radar required and already achieved is several orders of magnitude higher than in conventional radar; for example, the distance to the planets is now measured with relative accuracy up to $2 \cdot 10^{-9}$, while the accuracy required for conventional radiolocation does not exceed 10^{-6}.

Further, we explain in more detail the principle of construction and operation of the radar.

The radar is built on the principle of a coherent-synchronous system: in it all the oscillations necessary for the formation of the emitted signal, the receiver's heterodyne signals, reference signals in the processing system of the received echo signals, as well as signals for counting the time intervals in the program-time device are synthesized from one highly stable reference signal of the master oscillator by multiplying, dividing and converting frequencies.

The frequencies and phases of all oscillations with such a locator structure are related to each other by precisely known relationships and have a high stability, determined by the stability of the reference signal, which allows obtaining a high accuracy of frequency-time measurements. As a

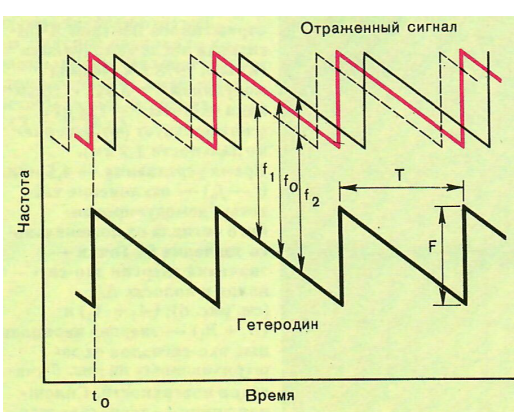

Fig. 17. *Frequency change with linear frequency modulation (LFM) of the reflected signal at the receiver input (top) and the heterodyne signal (bottom). t_0 is the calculated delay time of the echo signal; f_0 - rated frequency; f_1 - frequency below the nominal, and f_2 - above the nominal; T is the modulation period; F is the frequency deviation.*

master oscillator in the 1960s, a precision quartz oscillator with a frequency stability of about 10^{-9} was used, and in the 70s a hydrogen standard of frequency with stability was better than 10^{-12}. The true value of its frequency is also known with the same accuracy, which is especially important for determining the exact time intervals for measuring the delay of echoes.

The program-time device (chronizer) allows to count the predicted delay for the delay of echoes with a duration of up to 10.000 s with a resolution of 0.1 μs by counting the number of periods of the reference signal with a frequency of oscillations of 10 MHz.

A digital synthesizer with programmable frequency variation gives the calculated Doppler shift with an accuracy of 0.01 Hz in the range of ± 300 kHz.

For the simultaneous measurement of the delay and the frequency of echo signals in the radar of the USSR, linear-frequency-modulated radio signals (LFM signals) have been applied since 1962, the frequency of oscillations of which periodically varies according to a sawtooth linear law (**Fig. 17**). In the United States, signals with phase-pulse code modulation are used for these purposes. The use of linear frequency modulation turned out to be very effective after the development of a special generator in 1962, providing a strict linearity of frequency variation.

It was suggested to synthesize a modulated oscillation from sufficiently short sinusoid segments of an increasing or decreasing frequency that are fused at times of simultaneous zero crossing. A set of fused sinusoidal oscillations is formed from a reference signal, which results in high stability and repeatability of the synthesized signal form. In the new radar system, the LFM signal is formed on the principle of direct digital synthesis using integrated microcircuits.

The motion of the planet relative to the locator leads to a change in the delay of the echo signal. An original way of taking into account the motion of the planet was proposed, which consists in the fact that the correction for the predicted value of the Doppler shift, reduced to this frequency, is introduced into the frequency of the standard oscillations from which the modulated signal is formed. In this case, each period of the radiated signal varies according to the expected current velocity of the planet, and the period of the received reflected signal remains constant as from the fixed target, which allows it to accumulate and averaging without degrading the accuracy of the delay measurement.

The beginning of modulation of the probing chirp signal emitted in the direction of the planet is "tied" to the signals of a single universal time. During the reception of the echo, the chirp signal is repeatedly generated and fed to the receiver heterodyne, where it is used as the reference heterodyne oscillation for demodulating the received signals; while the beginning of its modulation is delayed by the predicted propagation time of radio waves to the planet and back.

The surface of the planet can be considered as a set of independent point-like reflectors, which are located at different distances from the locator and have relative to it a different speed of motion, caused by the rotation of the planet. Therefore, the echo signal from the planet is the sum of the partial echoes with different delays and Doppler frequency offsets.

The change in the frequency of each of the partial echoes at the input of the receiver (see Fig. 17) repeats the change in the frequency of the emitted chirp signal with a delay determined by its propagation time. The frequency of the heterodyne signal varies according to the same law - the beginning of its modulation corresponds to the calculated instant t0 of the arrival of the echo signal from the closest parts of the planet's surface to the Earth. The frequency of the signal at the output of the receiver is equal to the difference between the frequencies of the echo signal and the local oscillator; it depends both on the actual lag of the partial echo signal and on its Doppler bias. If the actual lag and Doppler offset values are equal to the predicted values, the frequency at the receiver output is equal to the nominal value f_0.

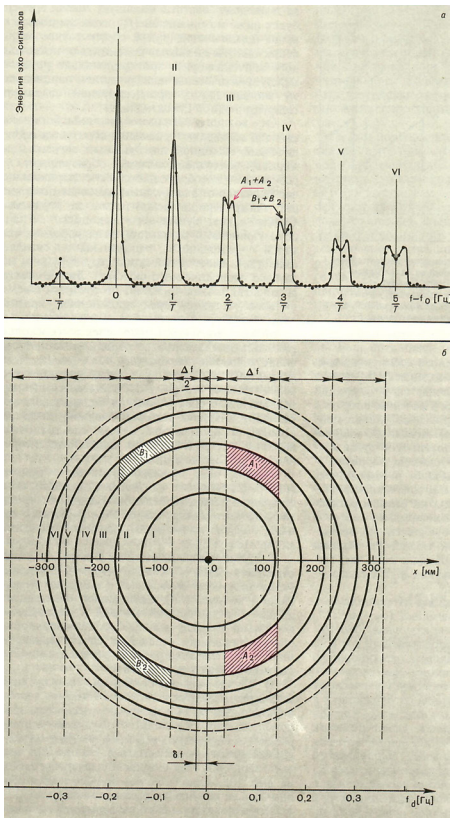

Fig. 18. *a is the spectrogram of the Venus reflected LFM signal after demodulation (Crimea, 1978). The modulation period is T = 0.512 s. The frequency deviation is F = 128 kHz (corresponds to a resolution of 1.2 km). The averaging time is 4.5 min. ($f - f_0$) is the deviation of the frequency f of the demodulated signal from the nominal value f_0. Points are the energy values of the echo signals in the Δf bands (see Fig. B); ($A_1 + A_2$) and ($B_1 + B_2$) - the energy of the partial echo signals from the shaded in Fig. b surface areas. The solid line is a theoretical spectrogram for an isotropic-reflecting surface. Roman numerals are the numbers of echo-signal sub-spectra from individual ring ranges of range (see figure b). Vertical lines are half the total energy of the echo signal in each of the subspectra. b - the central part of the visible disk of Venus, responsible for the reflection of the echo signal, the spectrogram of which is shown in Fig. a. Circles - boundaries of resolved ring zones (Roman numerals), separated by 1.2 km (in range). Vertical dashed lines are the boundaries of bands separated by frequency with a resolution of Δf = 0.122 Hz, x is the distance in the equatorial direction, f_d is the Doppler shift caused by the rotation of the planet. δf is the group shift of the subspectrums in frequency due to inaccurate compensation of the Doppler shift caused by the motion of the planet in orbit. A_1 and A_2 (B_1 and B_2) are parts of the surface that are solvable by delay and echo frequency together (see Fig. a).*

If the echo comes a little earlier, the output frequency will be much lower than the nominal frequency (f_1); if later, then above the nominal (f_2). In general, the frequency deviation at the receiver output from the nominal value will be proportional to the difference between the actual delay of the partial echo and the predicted latency of the LFM signal.

From each input partial echo at the output of the receiver, a periodic output partial signal is generated. The total output signal resulting from the conversion of all partial echoes from disparate points on the surface is also periodic (with the same period). The spectrum of the frequencies of the total output signal, formed as a result of interference of the spectra of individual partial signals (**Fig. 18**a), has a line structure (as in any periodic signal). The spectral lines are located at frequencies that are separated from the nominal frequency at intervals that are multiples of the frequency of repeating the sawtooth modulation.

It may seem that the spectrum (since the lag of individual partial echoes changes continuously) must also be continuous. However, as the detailed examination shows, this is not so. It turns out that when the spectrum is expanded into a spectrum, the energy of the partial echoes, whose frequency should fall in the interval between the spectral lines, is distributed to the nearest discrete spectral lines.

In Fig. 18a shows, as an example, the spectrum of signals reflected from Venus after heterodyning. If Venus did not rotate, then this spectrum, as from a periodic signal, would be ruled (vertical lines in Fig. 18a).

In the case of a "nonrotating" Venus, the left spectral line is due to echo signals reflected from the zone of Venus closest to us (zone I in Fig. 18b). Next, the spectral line - from the ring zone II, located somewhat further, etc. Strictly speaking, the zones that cause individual spectral lines are not separated by a sharp boundary: they overlap one another in part.

In the case of the rotation of Venus, the spectral lines are blurred due to the fact that the frequencies of the partial echoes from the elements of the zone approaching the locator will increase somewhat due to the Doppler shift, and the retreating ones will decrease. In Fig. 18b show the values of these displacements for the case of the spectrum in Fig. 18a. Clearly, the larger the

number of the zone, the greater the extension of the line.

Studying the spectrum, it is possible to separate the reflections from different parts of the planet: Thus, the reflection from the shaded elements in Fig. 18b causes the spectral components shown in Fig. 18a with arrows.

In the case when the axis of rotation of the planet is exactly perpendicular to the direction of the locator, it is not possible to divide the signal from the surface elements symmetrically lying relative to the equator. When, however (as is the case with Venus), the axis is not perpendicular, the separation can be made by location of the planet in different parts of the orbit.

The average frequencies of all subspectra correspond to reflections from the points of the surface for which the Doppler shift caused by the rotation of the planet is zero. Therefore, by group shifting of the average frequencies of the subspectra from their nominal positions, known with high accuracy (better than 0.01 Hz), it is possible to determine the uncompensated part (deviation from the prediction) of the Doppler shift caused by the motion of the orbiting planetary. In this case, an unambiguous determination can be obtained only if the deviation from the forecast does not exceed half the frequency of the repetition of the modulation.

In the radar of the planets, two deviation values (the total deviation of the frequency) were mainly used: 128 kHz, at which 8 μs delay resolution (1.2 km in range) is provided, and 32 kHz, at which it is 32 μs (4.7 km in range).

The modulation period is selected in such a way as to ensure the separation of the spectra of the individual zones. With the radar of Venus and Mercury, modulation periods from 0.06 to 4 s were used, with Mars radar from 0.008 to 0.064 s.

The system for processing the echo signal using probing chirp signals is simpler than using other types of modulation (pulse, phase-pulse, etc.), since it reduces to a single-channel system of spectral analysis. Other types of modulation require multi-channel processing systems.

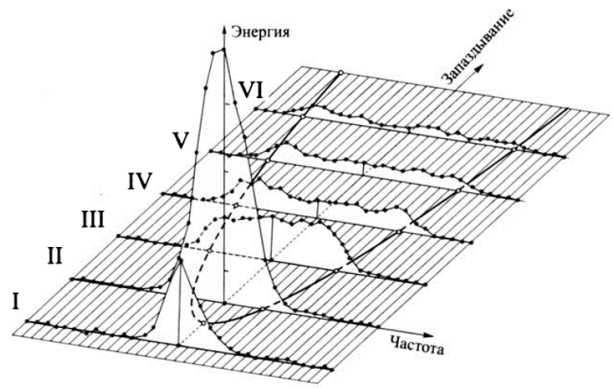

Fig. 19. *Two-dimensional distribution of the energy of Venus reflected radio waves by delay (range) and Doppler frequency shift (along the equator) (USSR, 1970).*

Operative processing of signals reflected from the planet during their reception for the purpose of controlling the operation of the radar and correcting the predicted delay is performed by a specialized digital device that allows analyzing the current spectrum of the received signal in the entire frequency band with a resolution of 0.25 to 16 Hz.

Complete processing of the received signals is carried out with the help of a general-purpose computer. For this, in the reception process, they are first recorded on magnetic tapes in analog and digital forms. In the analog version, simultaneously with the signal, a reference reference oscillation is also recorded, by means of which time and frequency calibration is performed while processing the registered echoes.

At the first stage of full processing in the computer, a spectral analysis of signals with a frequency resolution of 0.122 Hz is performed for the radar of Venus, 0.5 Hz for Mercury and 16 Hz for Mars. As a result, 256 (or 512) coefficients of the Fourier expansion of the energy spectrum are obtained and a two-dimensional energy distribution f the reflected signals is determined from the delay and frequency (**Fig. 19**).

At the second stage, the resulting two-dimensional distribution is analyzed in order to extract the information of interest to us.

10. CONCLUSION

At the Institute of Radioengineering and Electronics of the USSR Academy of Sciences

in the period 1961-1982, a new direction of observational astronomy-planetary radar-was developed. The work was carried out with the help of a specially designed planetary radar (λ = 39 cm) of appropriate sensitivity, as well as developed methods and an echo signal processing program. The first successful radar of Venus made it possible to drastically clarify the basis of all calculations - an astronomical unit approximately 100 times, the value 149597889.0±0.3 km was obtained. A new high-precision astrometric information was received on Venus, Mars and Mercury, which together with optical observations allowed the construction of a single relativistic theory of the motion of inner planets (Mercury, Venus, Earth and Mars). In addition, new information was received on the relief and reflective properties of the surface of these planets, the radius and nature of the rotation of Venus, its surface, as well as the surfaces of Mercury and Mars. The size and composition of the particles of Saturn's rings are also studied. These fundamental results are a major contribution to the study of the dynamics of the solar system.

REFERENCES

1. Kotelnikov VA, Petrov GM Radar location astronomy. In: "Science and Humanity", Moscow, Znanie Publ., 1982, p. 202-223.
2. Lovell B. Radio Astronomy Observatory in the Jodrell Bank. Science and humanity, 1968, 284.
3. Kotelnikov VA, Dubrovin VM, Morozov VA, Petrov GM, Rzhiga ON, Trunova ZG, Shakhovskoi AM Results of the radar of Venus in 1961. Radio Engineering and Electronics, 1962, 7 (11): 1860.
4. Kotelnikov VA, Dubrovin VM, Dubinsky BA, Kislik MD, Kuznetsov BI, Lishin IV, Morozov VA, Petrov GM, Rzhiga O .N., Sytsko GA, Shakhovskoi AM Radar observations of Venus in the Soviet Union in 1962. DAN USSR, 1963, 151 (3): 532.
5. Kotelnikov VA, Dubrovin VM, Kuznetsov BI, Petrov GM, Rizha ON, Shakhovskoy AM Advances in planetary radar. Nature, 1964, 9: 3.
6. Kotelnikov VA, Aleksandrov Yu.N., Apraksin LV, Dubrovin VM, Kislik MD, Kuznetsov BI, Petrov GM, Rizha ON, Franceson A B.V., Shakhovskoy A.M. Radar observations of Venus in the Soviet Union in 1962 DAN USSR, 1965, 163 (1): 3.
7. Kislik MD, Kolyuka Yu.F., Kotelnikov VA, Petrov GM, Tikhonov V.F. Determination of the orbits of the Earth and Venus, the astronomical unit and the radius of Venus on the basis of radar observations of Venus in 1962-1877. DAN USSR, 1978, 214 (5): 1046.
8. Kotelnikov VA, Rzhiga ON, Aleksandrov Yu.N., Dubrovin VM, Morozov VA, Petrov GM, Shakhovskoi AM, Franceson AV Development of radar studies of planets in the Soviet Union. In: Problems of modern radio engineering and electronics. P / p Kotelnikova V.A. M., Science, 1980.
9. Petrov G.M. Radar studies of Venus. Earth and the Universe, 1982, 1: 8.
10. Kaevitser VI, Zakharov AI The main directions of the work of G.M. Petrova. In the book. Petrov and his team. M., Editus, 2018, p. 112-140.
11. Rzhiga ON A new era in the study of Venus (radar imagery using spacecraft "Venus-15" and "Venus-16"). M., Knowledge, 1988, 64 p.
12. Vasiliev MB, Vyshlov AS, Kolosov MA, Savich NA, Samovol VA, Samoznav LN, Sidorenko AI, Aleksandrov Yu.N., Danilenko A .I., Dubrovin VM, Zaitsev AL, Petrov GM, Rzhiga ON, Stern D.Ya., Mesterton A.P. Detection of the night ionosphere of Mars. DAN USSR, 1974, 218 (6): 1298-1301.

RADAR OBSERVATIONS OF PLANETS WITH RT-70 PLANETARY RADAR IN EVPATORIA

Alexander I. Zakharov, Lyudmila N. Zakharova, Alexander S. Nabatov, Viktor P. Sinilo, Mark V. Sorochinskii

Kotelnikov Institute of Radioengineering and Electronics of RAS, Fryazino Branch, http://fire.relarn.ru
Fryazino 141190, Moscow Region, Russian Federation

aizakhar@ire.rssi.ru, zakharova@ire.rssi.ru, nabatov@ire.rssi.ru, sinilo@ire.rssi.ru, sorochinskii@ire.rssi.ru

Abstract. **In 2012, after a 20-year break, radar observations of the planets in Evpatoria were resumed with a use of upgraded planetary radar with RT-70 antenna. One of the features of radar operations in 2012 was a new scheme of correction the Doppler distortion of sounding signal. The correction was implemented in digital form after wide band registration of the echo signal. This correction was performed in a form of monotonous adjustment of signal sampling frequency in accordance with nonlinear law of two-way delay variations estimated from the model of the planet motion with respect to radar. The sequence of further signal processing stages included chirp heterodyning, filtering into a narrow frequency band with reduction of the signal sampling frequency, calculation and incoherent accumulation of power spectra. The technique of the spectra analysis in the range measurements procedure utilized precalculated reference radiophysical spectra of the signal scattered by the planet. Measurements of the distance to Venus near the interior conjunction were made, and 3.8 km discrepancy with a forecast was found. Because of too large distance to Mars (more than 180 million km), signal scattered by this planet was discovered only in one session with carrier signal. The results of radar observations confirm the operability of the RT-70 radar instrument in Evpatoria and ground-based signal processing software.**

Keywords: **radar astronomy, chirp signal, signal spectrum, planet orbit**

UDC **621.396.967; 621.396.962**

Bibliography - 4 references *Received 10.09.2018*

RENSIT, 2018, 10(2):167-174 **DOI: 10.17725/rensit.2018.10.167**

Content

1. INTRODUCTION

Radar studies of the planets were started in the Institute of Radioengineering and Electronics of the Academy of Sciences of the USSR in 1960 on the initiative of the director of the institute, Academician V.A. Kotelnikov [1]. The use of radar methods in space research, which is the essence of radar astronomy, provides new opportunities for studying the celestial bodies of the solar system, new information on their position, motion, rotation parameters, dimensions, physical properties of the surface composing rocks, and much more. The increased practical interest in the development of radar methods in the interest of studying the planets in the early 1960s, among other things, was caused by the need to ensure the navigation of spacecraft during the planned interplanetary flights.

The most outstanding result of radar astronomy in the early 1960s was the acquisition and analysis of echoes from Venus, Mars,

Mercury and Saturn. Pioneer work on radar observations of the planets of this period of observations was highly appreciated - a group of IRE staff members of the Academy of Sciences of the USSR, headed by Academician V.A. Kotelnikov (VM Dubrovin, VA Morozov, GM Petrov, ON Rzhiga, A. Shakhovskoy) received in 1964 the Lenin Prize.

Accumulation of the actual measuring material over the time interval from 1961 to 1980 made it possible to significantly clarify the parameters of the motion of the terrestrial planets and begin to create a new theory of planetary motion. The unified relativistic theory of the motion of the planets Earth, Venus, Mars and Mercury, created by the IRE Academy of Sciences of the USSR in collaboration with a number of other organizations on the basis of domestic and foreign radar and optical measuring material, made it possible to predict their relative position 50-100 times more accurately than the classical theory forecast movements of planets. The deviations of the measured distances from the planets from their calculated motion, calculated according to a unified theory, do not exceed the values: for Venus, 0.9 km in 1970-1980; for Mars - 2.5 km for 1967-1980; Mercury - 2.0 km in 1980. For a series of works on the creation of a unified relativistic theory of planetary motion, a group of Soviet scientists in 1982 was awarded the USSR State Prize. Among the awarded are the IRE staff of the USSR Academy of Sciences: Academician V.A. Kotelnikov and head of the Laboratory of Radar Research of the Planets of the Institute of the Academy of Sciences of the USSR, G.M. Petrov.

2. USE OF COMPLEX SIGNALS IN THE RADAR PLANET

The method of measuring the planetary radar of the Center for Long-range Space Communication in Evpatoria in classical works on the radar of the planets of 1960-1980 was a well-established idea of using linear frequency modulation of the probe signal. The use of signals with complex modulation allows for a more detailed study of its surface by separating the signals reflected from the surface of the planet by delay and the Doppler frequency shift. The basis of the method is that selection by frequency allows you to isolate a signal reflected from a surface strip located at a certain distance from the axis of rotation of the planet, and selection by delay allows you to isolate the signal reflected from the annular band on the visible disk of the planet whose center coincides with the discontinuous point. The intersection of the bands of equal Doppler frequency shift and equal delay allows us to identify small areas on the planet's surface and achieve a high resolution on the surface, unattainable only due to the terrestrial antenna in the case of Venus from the Earth. As a rule, the sounding signal is a long premise of successive repeating probing pulses with intrapulse modulation (in our case - chirp), the duration of the signal on the radiation is equal to the time of the signal passing to the planet and back.

When probing the planet with a long radio pulse, its shape and carrier frequency are distorted due to the displacement of the reflecting surface during the arrival of the pulse. Specially created equipment made predistortions in the radiated signal so that at reception it was free from Doppler distortion of frequency and duration [2]. For this, the frequency of the emitted signal and the period of its sampling at the output of the LFM signal generator were continuously adjusted so that when receiving the signal it was at the nominal frequency and the duration of the chirp pulse was nominal and constant during the radar session. Chirping the receiving echo at the reception and further narrowband filtering made it possible to record the signal in a narrow band and successfully conduct further digital processing by then modest computing tools. Thus, the echo signal of Venus was digitized in

the 4 kHz band. The Mars signal was recorded in the 32 kHz band. LFM heterodyning of the received signal at reception made it possible to simplify further processing, reducing it to calculation and accumulation of signal spectra, which did not require the construction of a multi-channel receiver for processing signals with different delay and frequency.

At the beginning of the work on the planetary radar in 2012, after almost a 20-year hiatus, the hardware of the planetary radar was profoundly modernized, as a result of which the technology of measurement and processing of measurements was changed, in particular, another method for correcting Doppler distortions of the signal was adopted. To clarify the features of the radiolocation of a new stage, let us consider the scheme for performing the measurements in **Fig. 1** [3]. If, at the moment of radiation, the radar is at point *A*, the planet at the moment of arrival of the signal is at point *B*, and the reception occurs at point *C* (see), then the total retardation time τ will be equal to:

$$\tau = 0.5\,|\,r_{12} + r_{23}\,|, \qquad (1)$$

where r_{12} and r_{23} are the distances from the emitter to the planet and back, equal in turn:

$$r_{12} = |\,\dot{r}_2(t_2) - \dot{r}_1(t_1)\,|,$$

$$r_{23} = |\,\dot{r}_3(t_3) - \dot{r}_2(t_2)\,|.$$

When using a monochromatic signal, the movement of the reflecting surface leads to a change in the frequency of the radio signal. Taking the relativistic effects as insignificant

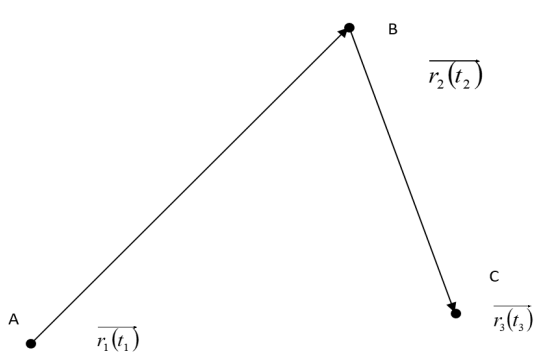

Fig. 1. *Scheme of signal passage in the radar session of the planet.*

(the velocity of the planet is much less than the speed of light), we find that the frequency of the signal arriving at the surface of the planet is

$$f_2 = f_1\left(1 - \frac{V_{12}}{c}\right),$$

where f_1 is the frequency of the radiated signal, V_{12} is the relative velocity of the radar and the reflecting surface as the signal passes to the planet, c is the speed of light. The reflected signal comes to the radar with a frequency f_3 equal to

$$f_3 = \frac{f_2}{\left(1 + \frac{V_{23}}{c}\right)},$$

where V_{23} is the relative velocity of the planet and the radar when the signal is received. The frequencies of the radiated and received signals are related by the following relation:

$$f_1 = f_3 \frac{\left(1 + \frac{V_{23}}{c}\right)}{\left(1 - \frac{V_{12}}{c}\right)} = \eta f_3.$$

The Doppler frequency shift at reception is

$$f_d = f_3 - f_1 = f_1\left(1 - \frac{1}{\eta}\right).$$

Consider the distortion of a narrow-band probing pulse, in which the carrier frequency *f* and the envelope *a*(*t*) can be distinguished. If the radiated pulse on the time scale of the radiator ttr can be described by expression

$$s_{tr}(t_{tr}) = a(t_{tr})\cos(2\pi f_1 t_{tr}), \qquad (8)$$

then on the receiving side the expression for the signal will have the form

$$s_r(t_r) = a(t_r)\cos(2\pi f_3 t_r). \qquad (9)$$

An example of distortion of a pulse with a chirp filling by a reflector approaching the radar is shown in **Fig. 2**. Here, along the abscissa, are the numbers of the signal samples.

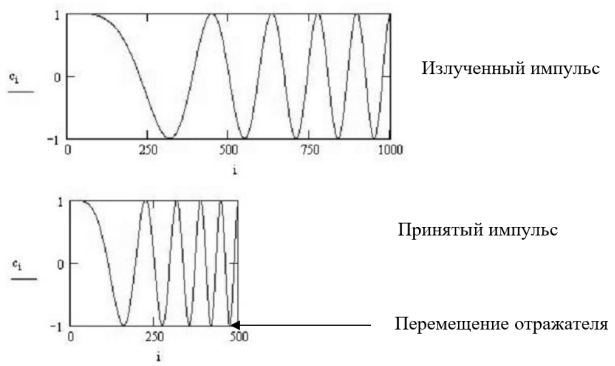

Fig. 2. *Deformation of the probe pulse reflected by the moving object.*

The coefficient η from (6) is actually the scale factor of deformation of the time structure of the probing signal:

$$f_1 t_{tr} = \eta f_3 t_{tr} = f_3 t_r. \quad (10)$$

Therefore, by introducing a distortion in the time scale tr, we can compensate for the Doppler distortion of the pulse shape/duration. Introducing a new time scale at the reception tint = trη, we obtain

$$s_r(t_{int}) = a(t_r\eta)\cos(2\pi f_1 t_r \eta). \quad (11)$$

A new algorithm for eliminating the Doppler effect was to emit a signal with fixed parameters and deform the time scale in the received signal. The deformation of the time scale was that the elementary step in time for sampling successive samples of the deformed signal was taken equal to dtrn, not to the interval between samples dt_r. The number of the k-th count of the deformed signal is the integer part of $k\eta dt_r$. Deformation of the timeline can be performed by skipping or duplicating some samples of the received signal. Note that η is not a constant. It changes during the session due to changes in the relative velocities of the planet and the radar (see (6)).

Since skipping or duplicating samples leads to phase distortions, this effect should be minimized. For this, the frequency of the signal quantization in the receiving path must be significantly higher than the frequency band. Estimates show that, with an eightfold increase, phase errors with this time scale deformation method result in a signal/noise ratio (SNR) reduction of less than 1 dB.

The next important point in eliminating the Doppler effect at the reception was the fact that before recording the signal in the receiving path is transferred from the carrier to some intermediate frequency in the low-frequency region, and therefore, instead of (11), we write

$$s_r(t_r) = a(t_r)\cos(2\pi(f_3 - f_g)t_r) = a(t_r)\cos(2\pi f_i t_r), \quad 12$$

where f_g is the frequency of the heterodyne oscillation, and f_i is the intermediate frequency, in the simplest case containing the Doppler correction to the carrier. The correct sequence of actions includes, as a first stage, the transfer of a signal from frequency fi to zero frequency (elimination of Doppler by a carrier), and the second is the elimination of Doppler by the envelope $a(t_r)$.

3. MATHEMATICAL MODEL OF SIGNAL, REFLECTED BY THE SURFACE OF THE PLANET

The planet is an extended goal with a strongly intersected relief, and therefore the reflected signal has a rather complex shape, which makes it difficult to measure the distance to the planet. As noted above, the rotation of the planet around its axis leads to a Doppler blur of the reflected signal spectrum. In **Fig. 3** shows the position of the components of the reflected signal in terms of range and

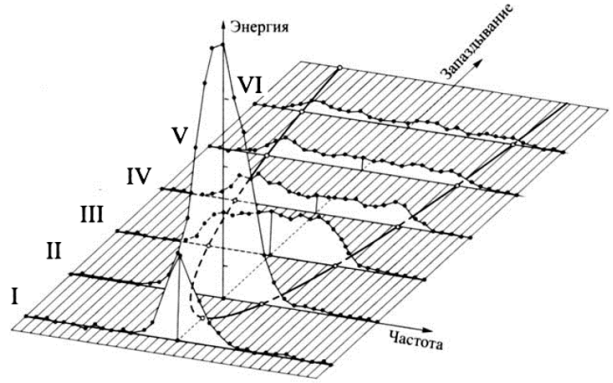

Fig. 3. *Distribution of the reflected signal by delay and frequency.*

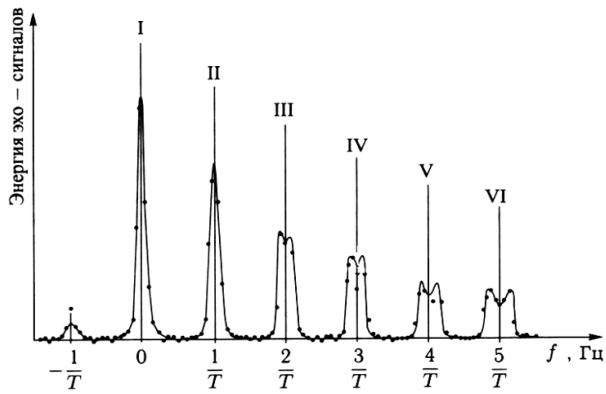

Рис. 4. *Распределение отраженного сигнала после ЛЧМ-гетеродинирования на приеме.*

frequency. Here, Doppler sub-spectra of different range zones follow one after the other along the axis of the delay. When a processing scheme with LFM heterodyning and calculation of the signal spectrum is applied, the subspectra of different range zones are located on one frequency axis with a shift to the repetition rate of $1/T$ pulses (see **Fig. 4**). Roman numerals in the figure indicate ranges of range 1-6 in Fig. 3.

Since the processing scheme with LFM heterodyning is the simplest in the computational plan, we take its basic one and give an expression for the spectrum of the model reflected by the surface of the planet when probing with periodically repeating pulses with a chirp filling.

The shape of the signal spectrum with linear frequency modulation (LFM signal) reflected by the surface of the planet and its position on the frequency axis are the basis for measuring the range, the velocity of the planet and the physical characteristics of its surface.

To obtain a mathematical model of the energy spectrum, we use the formula for the integral of elementary echoes over the surface of the planet, proposed by A.F. Khasyanov [4]:

$$T(m) = B\iint_S \sigma_0(r, C) A_m(x, y) ds.$$

Here m is the spectral reference number, B is a proportionality factor that takes into account the area of the radar antenna, the power and wavelength of the emitted signal, and the distance to the planet. Integration proceeds over the area of the resolution element s on the surface of the planet. Specific Effective Scattering Area where r is the radius vector from the observation point to the point of the planet's surface, is described by the formula:

$$\sigma_0(\theta(\vec{r})) = \frac{\rho_0 C}{2}(\cos^4\theta + C\sin^2\theta)^{-1.5},$$

where ϱ_0 is the specular reflection coefficient, C is the roughness parameter in the Hagfors formula describing the backscattering diagram of the planet's surface, θ is the angle of incidence of the radio wave on the planet's surface, $A_k(x,y)$ is the hardware function of the probing periodically repeating chirp signal in rectangular coordinates $\{x,y\}$ on the surface of the planet. A cumbersome expression for the hardware function can be found in [4].

4. SEQUENCE OF PRIMARY PROCESSING OF SIGNALS OF PLANET RADAR

The primary processing covers the steps of converting the reflected radar signal from the raw signal sample array to measuring the corrections to the delay and the speed of the probed planet, as well as the radiophysical parameters of the reflecting surface.

For the variant of shooting with pulse emission with fixed parameters, the first stage of processing after recording the echo was the elimination of signal distortion due to the Doppler effect (Doppler on the carrier and envelope). The next stage is chirp-heterodyning and filtering into a narrow frequency band. Next, the calculation and incoherent accumulation of power spectra, which is the input material for model processing, occurred. Extremely small values of the signal-to-noise ratio are characteristic for experiments on planetary radar, and therefore an obligatory stage of processing is incoherent accumulation of a mixture of signal power and noise and the

subsequent subtraction of the noise pedestal. In our processing scheme, the form of the additive noise spectrum was approximated by a polynomial of the 12th degree, the smooth approximation was subtracted from the signal-to-noise mixture. The models of the reflected signal spectra, calculated taking into account the survey parameters for the set of values of the Hagfors roughness parameter and the delay error, were used in the correlation procedure to determine the corrections to the ephemerides provided by the IPM RAS.

5. RESULTS OF 2012 RADAR MEASUREMENTS

The main series of work on the calibration of the equipment of the modernized planetary radar based on the RT-70 antenna and the development of radar measurement techniques was conducted during the period from 11 to 18 June 2012, in the region of the lower connection of Venus with the Earth. A month earlier, on April 27, a one-day series of radar observations of Venus and Mars was carried out as part of the testing of the software. On each of the days of observations, work was carried out on Venus and Mars.

A typical measurement session consisted of a radiation cycle, a reception cycle, and a pause needed to prepare for the next session. The sessions differed from each other by the duration of the radiation cycle, the object of measurement (Venus, Mars) and the type of the emitted signal (carrier, LFM signal with different parameters - deviation and repetition period). A total of about 50 sessions were conducted. The signal-to-noise ratio estimated from the radar-bearing sessions of Venus with the carrier was ~30 dB, which is close to the theoretical estimates for this planet at a distance of 44 million km with a Hagfors C roughness parameter of 400, reflectivity of the surface $\varrho = 0.05$ at a transmitter power of PRL 100 KW and noise temperature of the receiving system is 30º.

Measurements of the range to Venus were conducted in sessions with a chirp signal with a deviation of 100, 200, 400, 500 kHz and a repetition period of 20 and 30 ms. Since the unknown hardware delay of the transmit-receive path can be a source of errors in measuring the parameters of the motion of the planet, at the beginning of each session, a sounding signal was recorded in the "ring" mode. The hardware delay was calculated from the mutual position of the time of the onset of the formation of the chirp signal for radiation and the position of the chirp pulse during reception.

The results of the primary processing, the spectra of the reflected signal of Venus (**Fig. 5**) after correction of the Doppler effect and the chirp filtration are given below for various parameters of the probe signal. With the received processing parameters, the signal spectra in the 12 kHz band with a resolution of ~0.4 Hz were formed. Due to the high signal-to-noise ratio, a signal of several hundred zones can be observed in range. For greater clarity, we give only a portion of the spectrum near the nominal frequency, containing the first 10-15 zones in range. One can see a noticeable broadening of the far-band signal spectrum. The graph below shows the signal power in dimensionless units along the vertical axis, and the horizontal frequency in Hertz. An example of the combination of the real and model spectra for the session №7 from 11.06.12 is shown in **Fig. 6**. On the horizontal axis here are the numbers of the spectrum filters.

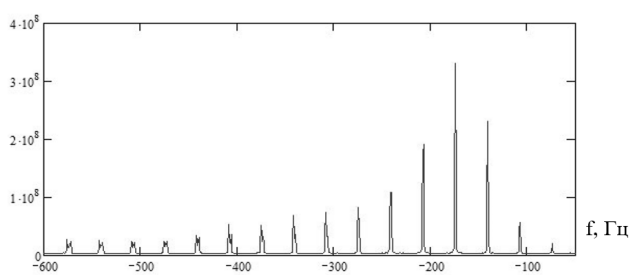

Fig. 5. *Spectrum of the signal reflected by Venus LFM signal 11.06.12 in the session number 3 near the face value. The frequency deviation is 195 kHz, the period is 30 ms.*

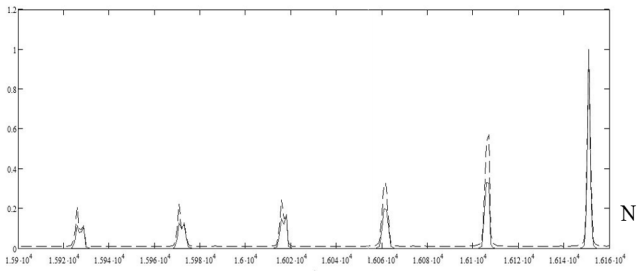

Fig. 6. *Combination of real and model signal spectra for the session №7 from 11.06.12.*

The solid line in Fig. 6 - model spectrum, discontinuous - the spectrum of the real signal. The difference in spectra is due to inaccuracies in the scattering parameters in the model, as well as by the features of the surface relief of the planet. In particular, the asymmetry of the band spectra in the left part of the graph is due to the presence of more strongly reflecting objects on one of the edges of the annular range zone. Model spectra were used to estimate the correction to the distance to the planet. To improve the accuracy of the delay measurements, the signal spectrum was compared with a set of model spectra of the signal reflected by the planet, calculated in advance for several values of the Hagfors parameter. For most range measurements, it is obtained that the surface of the planet is 3.8 km further than the predicted value.

In **Fig. 7** shows the height profile of the surface of Venus relative to the mean local radius of 6051 km according to the data of Magellan satellite in the equatorial region in the longitude range 336°-354°. The asterisks mark the position of the substitute point on June 11 (left) and June 13 (right).

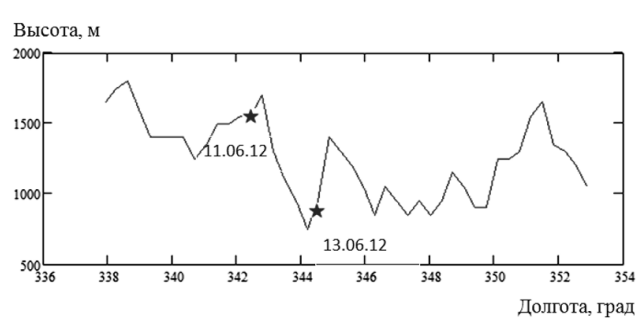

Fig. 7. *Profile of the heights of the surface of Venus according to the data of the radar-profilograph of the Magellan spacecraft with the position of the substitute point in the sessions 11.06.2012 and 13 .06 2012*

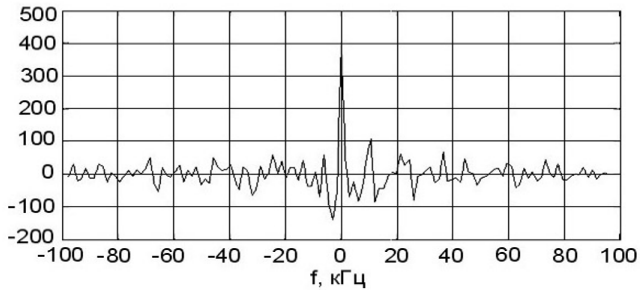

Fig. 8. *Spectrum of the carrier signal after subtraction of noise for Mars in the session of 13.06.12.*

It can be seen that on June 13, 2012, the tapping point hit the low relief area 0.6 km lower than the June 11th 2012 measurement, which made the measured range longer and, instead of 3.8 km, measured 4.2 km. Measured corrections to the range to Venus, predicted by the Institute of Applied Mathematics. M.V. Keldysh RAS (IPM), show that this planet in June was 3.8 km further than the forecast.

In the Mars radar sessions, a carrier and a chirp signal with a deviation of 32 kHz and a repetition period of 1 kHz were also used. Due to the long range to Mars in June 2012 (more than 180 million km), the signal with a signal-to-noise ratio of ~ 10, close to the theoretical one, was detected only in one session with the emission of the carrier signal. In **Fig. 8** shows the spectrum of the echo signal from Mars with a frequency resolution of 800 Hz, obtained after subtracting the noise pedestal in the form of a smooth approximation of a mixture of signal and noise by a polynomial of the 12th degree.

6. CONCLUSION

Work on the radar of Venus in 2012 was carried out using modernized planetary radar based on the RT-70 antenna in Evpatoria. In these works, a new scheme for correcting Doppler distortion of a signal was first used, which consisted in the fact that this type of distortion was eliminated after recording the echo signal in a wide band on the Earth. Measurements of the distance to Venus in the area of the lower connection with the Earth in June 2012 were obtained, which showed that the planet was at that time 3.8 km further than the predicted value. The results of the

work confirmed the readiness of the equipment of the planetary radar and mathematical support for the processing of signals to regular work on planetary radar.

REFERENCES

1. Kotelnikov VA. *Collection of works. T.2. Space Radiophysics and Astronomy.* M., Fizmatlit, 2009, 396 p.
2. Bakytko RV, Vasiliev MB, Vinitsky AS, Zaitsev AL, Grishmanovsky VA. *Radio systems of interplanetary space vehicles.* Moscow, Radio i svyaz Publ., 1993, 326 p.
3. Aleksandrov UN, Kuznetsov BI, Petrov GM, Rigga ON. Method of radar astrometric observations. *Astronomich. Zhurnal*, 1972, 49 (1): 175-185 (in Russ.).
4. Khasyanov AF. Radar studies of profiles of heights and reflective characteristics of the surfaces of Venus and Mars. *Dis. Cand. fiz-mat. sciences. Moscow*, 1981.

PETROV AND HIS LABORATORY "PLANETARY RADAR SYSTEMS"

Oleg N. Rzhiga, Alexander L. Zaytsev, Alexander I. Zakharov, Vladlen I. Kaevitser, Nataly V. Rodionova

Kotelnikov Institute of Radioengineering and Electronics of RAS, Fryazino Branch, http://www.cplire.ru
Fryazino 141190, Moscow Region, Russian Federation
info@cplire.ru, zaytsev@mail.ru, aizakhar@ire.rssi.ru, kaevitser@mail.ru, rnv1948123@yandex.ru

Abstract. **Some book fragments of the former 127 laboratory Kotelnikov FIRE RAS scientific researchers are presented. They include information about Petrov G.M. - the laboratory head, the solar system planet radar works in the 60-80s last century by Petrov and his colleagues, Venus surface atlas and so on.**

Keywords: **planetary radar, astronomical units, mapping**

UDC 621.396.967; 621.396.962

Bibliography - 3 references *Received 10.09.2018*

RENSIT, 2018, 10(2):175-192 **DOI: 10.17725/rensit.2018.10.175**

PETROV GENNADY MIKHAILOVICH (1.06.1924-2.12.2008) is a specialist in radio engineering and radar astronomy, PhD Phys.-Math., laureate of the Lenin Prize, head of the laboratory of the Institute of Radioengineering and Electronics of the USSR Academy of Sciences. Member of the Great Patriotic War from 1942. In 1955 he graduated from the Radio Engineering Department of the Moscow Power Engineering Institute and began working at the Institute of Radioengineering and Electronics of the USSR Academy of Sciences; since 1972 - Head of the Laboratory of Planetary Radar Systems. Since 1968 he defended his Ph.D. thesis on the specialty "Radio Astronomy".

GM Petrov is one of the leading specialists in the field of radar research of planets, the author of more than 90 publications. Under his leadership a large complex of planetary radar equipment was created. His thesis is devoted to the definition of an astronomical unit based on the results of radar observations of Venus, Mars and Mercury, performed in the Soviet Union in 1961-1964. The team led by GM. The extensive program of radar observations of planets and radiophysical studies in space with the help of automatic interplanetary stations "Mars-4, -5, -6", "Venera-9, -10, -11, -12" and an artificial moon satellite "Luna" -22 ".

G.M. Petrov was awarded the Order of the Badge of Honor, the Medal for Military Merit and five more medals.

--

Gennady Mikhailovich was born June 1, 1924 in the village Dorogorskoe Mezensky district of the Arkhangelsk region. In 1940 he entered the technical school. Since October 1941 - on the construction of fortifications near Moscow - he rebuilt the destroyed buildings in Moscow. He was drafted into the Red Army in August 1942, a cadet in the school of the anti-aircraft artillery regiment in Moscow, and from November 7, 1942, to the end of the war, as part of the 130th Independent Air Defense Armored Trains, where he fought in the South, West and South-fronts, from Kalach at Stalingrad to Peremyshl in Poland. His battle path, he began gunner guns and finished commanding guns.

In 1955, after graduating from the MEI radio department, a young engineer Petrov was sent to the Institute of Radioengineering and Electronics of the USSR Academy of Sciences, where he worked for almost half a century, from 1956 to

2004. At first he dealt with the problems of noise immunity of radars and the development of a technique for trajectory measurements of the first Earth satellites.

But the main business of G.M. Petrov became radar astronomy. With his direct and largely determining participation, the first domestic planetary radar was created. This unique instrument worked in the decimeter (39 cm) radio wave band and used two eight-mirror antennas of the Center for Remote Space Communications in the Crimea near Evpatoria. One of the antennas was transmitting, the second - the receiving room.

Very much then it was necessary to create for the first time. Gennady Mikhailovich developed and created a software-temporary device, the so-called "chronizer", for this radar. The range of time was previously unseen - up to 10 thousand seconds - after all, the delay of echo signals from the planets was tens of minutes. At the same time, the instrumental measurement error should be no worse than 1 microsecond. But then everything was done on antediluvian radio tubes and each trigger required a separate lamp.

An even more unique device is the first parallel digital spectrum analyzer. He, for decades ahead of his time, was developed by Petrov and created under his leadership.

The point is that the radar transmitter sends continuous coherent signals with periodic frequency modulation. The signals reflected from the planet have a ruled and extremely narrow spectrum, and therefore the optimal harmonic filter is precisely the parallel harmonic analyzer.

It was in the mid-1960s. The analyzer had 15 parallel channels with a frequency resolution of 0.25 to 16 Hz. It was made in the size of half a room on finger lamps, double triodes 6N3P (total 600 lamps), consumed several kW.

With the help of this first planetary radar, planets of the terrestrial group were successfully investigated, unique high-precision measurements were obtained, on the basis of which the Astronomical unit was radically refined. It was these measurements that made it possible to "get" to Venus to our first interplanetary stations.

From the TASS report of April 22, 1964: "For the radar studies of the planets Venus, Mars and Mercury, the Lenin Prize was awarded to the Director of the IRE of the USSR Academy of Sciences, the head of the work, Academician VA Kotelnikov, the staff of the same institute, VM Dubrovin, MD Kislik , VA Morozov, GM Petrov, ON Rzhige, AA Shakhovsky, the head of the laboratory GNII MOD of the USSR VP Minashin.

A detailed analysis of the long-term series of radar astrometry made it possible to create a highly accurate theory of planetary motion.

In 1982, G.M. Petrov as a member of the team of authors for the series of works "Creation of a single relativistic theory of motion of inner planets" was awarded the State Prize of the USSR.

The fundamental contribution of Gennady Mikhailovich Petrov to the national and world science was the active participation already as the head of the laboratory of the Institute of the Far East of the Russian Academy of Sciences "Planetary Radar Systems" created by him in 1982-1984 in the pioneering experiment on radar mapping of the planet Venus, which was carried out with the help of artificial satellites "Venus-15 "and" Venus-16 ". He made a significant contribution to the creation of the world's first "Atlas of the planet Venus".

Having already left the position of the head of the laboratory for health reasons, Gennady Mikhailovich continued to work fruitfully at the FIDE of the Russian Academy of Sciences. To him went for the qualified help and consultations, for wise advice and memories

THE BIRTH OF A LABORATORY 127

127 laboratories of the "Planetary Radar Systems" were born in 1972 from the group of 127. All information about the employees of the laboratory. 127 was in the famous barn book, which was mastered by G.M. Petrov. In this book there are records of more than 80 people who worked at one time or another in 127 laboratories. A general photo of the laboratory staff was preserved, made in 1975 on the stage of the Institute's assembly hall.

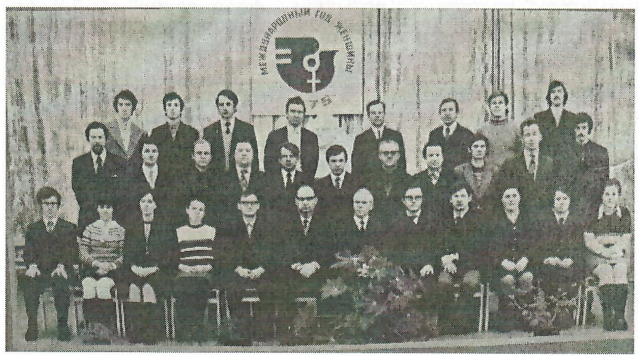

In this photo - the bottom row (from left to right): L.N. Samoznayev, N.V. Rodionova, L.V. Vyshlova, V.Z. Sukhoverkhova, Yu.N. Aleksandrov, V.M. Dubrovin, G.M. Petrov, V.M. Smolyaninov, E.G. Nazarenko, L.V. Abramova (our mother is responsible), V.I. Kaevitser, I.V. Turusina; average number: A.C. Vyshlov, A.S. Maksimov, B.I. Kuznetsov, E.A. Razumny, A.I. Sidorenko, Yu.V. Feofanov, N.A. Savich, P.V. Chernov, V.E. Zimov, V.K. Golovkov, V.A. Samovol; upper row: A.B. Kalinin, V.A. Ivanov, A.L. Zaitsev, A.F. Khasyanov, M.V. Sorochinsky, S.M. Baraboshkin, M.V. Labutin, V.I. Churkin.

PETROV'S GROUP

The main directions of work of Petrov's group are told by Dr.Sc. V.I. Kaevitser and Dr.Sc. A.I. Zakharov.

Radar studies of planets in IRE RAS

Radar studies of planets in the IRE RAS were started in 1960 on the initiative of the director of the Institute, Academician VA. Kotelnikov. The use of radar methods in space research, which is the essence of radar astronomy, provides new opportunities for studying the celestial bodies of the solar system, new information on their position, motion, rotation parameters, dimensions, physical properties of the surface composing rocks, and much more. The increased practical interest in the development of radar methods in the interest of studying the planets in the early 1960s, among other things, was caused by the need to ensure the navigation of spacecraft during the planned interplanetary flights.

Optical observations of planets and the Sun, which measure the angular position of objects on the celestial sphere, were conducted in the world for two hundred years. On the basis of these observations, quite advanced theories of planetary motion were constructed, but the accuracy of the forecast of their position was insufficient for the high requirements of astronautics. The point is that the accuracy of measuring the angular position in optical observations does not exceed a tenth of an angular second and is determined, in the main, by random deviations of the beam in the Earth's atmosphere. Because of this, for example, the error in measuring the position of the planet Venus in the picture plane at the moment of its closest proximity to the Earth is 40 km. The range to the planet is measured indirectly, by measuring the position of the planet in different parts of its orbit, and may have an error of tens of thousands of kilometers. This is completely inadequate for interplanetary flights, since the diameter of any of the terrestrial planets does not exceed 12.000 km.

Unlike indirect optical, the radar methods give direct measurements of distance based on the time of passage of the radio signal to the planet and back. In addition, the value of the Doppler frequency shift of the reflected signal makes it possible to estimate the radial velocity of the reflecting object, and the Doppler frequency band is the rotation speed around the axis. Modern radar facilities allow you to measure the range to the planets of the Earth Group with an accuracy of several hundred meters, and the speed - a few centimeters per second. Due to radar measurements of distance and speed, it is possible to determine the position of planets in space with an accuracy several orders of magnitude higher than on the basis of optical observations of their angular position.

The first experiments on the radiolocation of celestial bodies were carried out shortly after the war in the US and Hungary were then military radar. It turned out that with their help it is possible to reach only to the Moon, since by the level of the reflected signal this satellite of the Earth is comparable to the plane for them. To locate more distant objects like Venus, it was required to improve the radar parameters. For example, to increase the radiated power by 10 million times, because the power of the reflected signal coming to the radar is inversely proportional to the fourth power of the distance to the reflecting object.

The possibility of radarization of the planets of the Solar System appeared in the world only by the beginning of the 1960s due to the creation of antennas with a larger area, more powerful transmitters and sensitive receivers, as well as to improved methods for separating signals from interference.

Radar studies of planets in the Soviet Union was decided to be carried out on the basis of a set of receiving and transmitting antennas ADU-1000 receiving complex "Pluton" Center for long-range space communications in Evpatoria, which was established at that time for communication with interplanetary ships. Thanks to the use of ready-made nodes and solutions, two receiving and one transmitting antenna complexes were created in a short time.

The antenna systems of these complexes consist of 8 dural parabolic antennas with a diameter of 16 m, fixed in the form of a grill to the hull of a diesel submarine fixed to a railroad bridge farm, which in turn rests on a turnbuckle device from the gun battleship of the battleship's main caliber (cm Fig. 16, Article 2 of this issue).

Built in just one year, these antennas provided deep space exploration in the Soviet Union until the late 1970s, when the RT-70 system with a 70-meter antenna was put into operation (Fig. 2, article 2 of this issue).

About the first radar contacts with Venus abroad was reported back in 1958, but later it was established that the echo signal from Venus was taken as a noise emission. Reliable recording of the signal reflected by Venus was made in early 1961 at the time of the lower connection almost simultaneously in the USA, the Soviet Union and England, when the distance to the planet was about 40 million km.

The domestic radar operated at a frequency of 768 MHz, the power flux density was 250 MW per steradian, so that the entire visible surface of Venus hit 15 watts. The emitted signal had the form of telegraphic parcels and pauses lasting 128 or 64 msec (amplitude modulation). A signal was also used in the form of alternating telegraphic parcels at two frequencies, offset by 420 kHz, each with a duration of 64 msec (frequency modulation). The frequencies of the carrier signal and its manipulation were corrected for displacement due to the Doppler effect caused by a change in the distance between the Earth and Venus, as well as the rotation of the Earth. The transmission was conducted by sessions during the time the signal passed to the planet and back. Session management was conducted with the help of a specially developed high-precision chroniser. To ensure the possibility of detailed analysis of radar data with a review of various processing algorithms, magnetic recording of the received signal was realized. The analysis of the echo signal was carried out using an analyzer, which was a line of filters.

As a result of a series of observations from April 18 to 26, 1961, measurements were made of the distance to Venus, which made it possible to significantly clarify the value of the astronomical unit (the distance from the Earth to the Sun). Accurate knowledge of the astronomical unit - the distance from the Earth to the Sun - is important because in astronomy through this unit all other distances are determined. If before the radar observations the most significant was the value of the astronomical unit of 149527000 ± 10.000 km, obtained from optical observations of the small planet Eros, after the first radar observations it turned out that it is equal to 149599300 ± 2000 km, which is 73 thousand km more than was thought in astronomy.

In June 1962, after upgrading the equipment of the complex, which consisted of using a more sensitive receiving apparatus (a paramagnetic amplifier was used on a helium-cooled ruby crystal at the input of the receiver, which increased the sensitivity by a factor of 6), the radar was first conducted in the world for the planet Mercury. The emitted signal consisted of alternating parcels at two frequencies, differing by 62.5 Hz. The duration of the parcels and pauses at each frequency was 1024 msec. Estimates of the astronomical unit, based on measurements of the range to Mercury, were in good agreement with the estimates obtained in the radar of Venus. Due to the calibration of the sensitivity of the receiving equipment for the radiation of the

extraterrestrial radio source Cassiopeia A, the reflection coefficient of the Mercury surface was measured equal to 3-7%. Similar measurements in the US were conducted a year later.

In the fall of 1962, the radiolocation of Venus was repeated. In these works, for the first time, a signal with periodic linear frequency modulation was first used to measure the distance to the planet (in the US in subsequent years a signal with phase-shift manipulation was used), and corrections were made to the modulation parameters to compensate for the frequency variation due to the Doppler effect caused by the motion of Venus and the Earth. Thanks to the improvement of equipment and methods of signal generation and processing, measurements of the distance to the planet, obtained in each separate session, had an error of less than 15 km. The reflection coefficient of Venus was equal to 12-18%, and by broadening the spectrum of the reflected signal it was found that Venus rotates around its axis in the opposite direction compared to the Earth and at a very low speed: one revolution for 200-300 days. In optical observations, this could not be done because of the opaque, powerful cloud cover of the planet. The increase in the radar potential in these studies made it possible to conduct an amusing experiment on radiotelegraph communication using Venus as a repeater. The words "MIR", "USSR", "LENIN" were transmitted by the radio telegraph code in the direction of Venus. After a total distance of 85 million km, the signal was received on the Earth (see the fragment of the signal recording in **Fig. 2**).

In the first half of February, 1963, at the moment of confrontation, the first radar-tracking of Mars was made. The general parameters of the radar were the same as in the radar sessions of Mercury, and a signal was also used in the form of alternating rectangular pulses with different

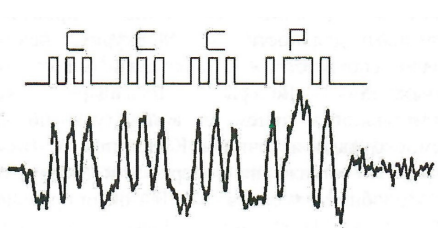

Fig. 2. *The word "USSR", transmitted by the telegraph code and reflected from Venus on November 24, 1962.*

frequencies. The reflected signal was reliably detected in 48 sessions on the night of 7 to 8 February and from 8 to 9 February. The reflection coefficient in various parts of Mars was less than that of Venus, but at times reached 15%.

In September-October of the same year, thanks to a further increase in radar sensitivity, it was possible to obtain reflections from Jupiter at a time when it was located at a distance of 600 million km from the Earth. The reflected signal was so weak that for its detection it was necessary to carry out the accumulation of energy for 20 hours. The reflection coefficient was 10%. At the same time conducted at the same time in the US attempts to radar Jupiter did not yield any results.

Pioneer work on the radar of the planets was highly appreciated - a group of staff of the IRE RAS, headed by Academician V.A. Kotelnikov won the Lenin Prize in 1964 (VM Dubrovin, VA Morozov, GM Petrov, OI RyzhA, AM Shakhovskoy).

In January-February 1966, the radar observations of Venus, jointly with the British Jodrell-Bank Observatory, were conducted, in which the monochromatic signal emitted from Evpatoria after being reflected from Venus was received by a large radio telescope in England. The signals recorded on the magnetic tape were digitized and analyzed at the Institute of Physics and Technology of the Russian Academy of Sciences. Due to the diversity of the transmission and reception points, the accumulation time of the signal was increased and the potential of such a radar system was improved. The data processed on a computer in the IRE RAS made it possible to reveal anomalies of the reflective properties of the surface, to specify the orientation of the rotation axis of the planet and the period of its rotation.

Radar observations of planets in the Institute of Radioengineering and Electronics of the Russian Academy of Sciences were regularly held in the following years. Further improvement of the parameters of the equipment and improvement of the processing methods led to an increase in the sensitivity of the planetary radar by an average of 70 times. This made it possible, for example, to increase the accuracy of measurements of the

distance to Venus from 1000 km in 1961 to 0.3 km in 1978, and its radial velocity from 40 cm/s in 1961 to 0.8 cm/s in 1978.

In 1978 a unique radio telescope RT-70 with a mirror diameter of 70 meters, one of the largest in the world, was built in Evpatoria. The new antenna, more powerful transmitters and low-noise receivers increased the potential of the planetary radar by 50 times, which further enhanced the capabilities of radar observations. With the help of this radar, observations of Mercury, Venus and Mars were carried out in February-April 1980 on large areas of the orbit of these planets: 139° of the arc of the orbit in the region of the lower compound for Mercury, 82° of the arc of the orbit in the region of maximum elongation for Venus and 29° of the arc of the orbit in the area of confrontation for Mars. The long-term radar observations of 1980 made it possible to obtain detailed profiles of the surface heights at the subscore point and to clarify the available data on the relief of the planets.

Accumulation of the actual measuring material in the time interval from 1961 to 1980 made it possible to start creating a new theory of planetary motion. The unified relativistic theory of the motion of the planets Earth, Venus, Mars and Mercury, created by the IRE RAS in collaboration with a number of other organizations on the basis of domestic and foreign radar and optical measuring material, made it possible to predict their relative position 50-100 times more accurately than the forecast for the classical theory of motion planets. The deviations of the measured distances from the planets from their calculated motion, calculated according to a unified theory, do not exceed the values: for Venus, 0.9 km in 1970-1980; for Mars - 2.5 km for 1967-1980; Mercury - 2.0 km in 1980.

For a series of works on the creation of a unified relativistic theory of planetary motion, a group of Soviet scientists in 1982 was awarded the USSR State Prize. Among the rewarded are the staff members of the IRE RAS: Academician V.A. Kotelnikov and head of the laboratory of radar research of the planets of the Institute of Far Eastern Studies of the Russian Academy of Sciences, G.M. Petrov.

The high accuracy of the created theory of planetary motion made radar observations unnecessary for a certain period of time. As a result of the soon-to-come social and economic transformations in society and the associated financing problems, this period has dragged on to the present day. New domestic plans for the exploration of outer space lead now to the need to resume radar observations of the planets and to refine the parameters of their motion.

Radar mapping of the northern hemisphere of the planet Venus with spacecraft Venus-15 and Venus-16

Radar studies of planets from the Earth are limited in detail of the measurements and the area of the planet under investigation. Surface heights profiles are measured along the trajectory of the displacement of the discontinuous point along the surface of the planet. As a rule, the profile of measurements of the reflecting characteristics of a surface is limited by this trajectory. The most successful experiment on mapping the planet Venus from Earth was conducted from Arecibo (Puerto Rico), using a unique radar with a mirror diameter of 300 m. In this experiment, using radio waves, it was possible to slightly open the cloud veil of Venus and see its surface. A radar image of a small area on the surface of Venus was constructed (see the fragment, an image of the region of the Maxwell mountains with a resolution of about 10 km in **Fig. 3**). In this figure, a lighter background is transmitted to the Maxwell mountain range system, which has an increased reflection coefficient against the background of more radio-dark smooth lava plains. The double

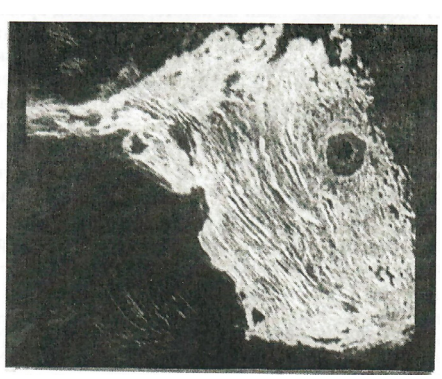

Fig. 3. *Radar image of the Maxwell Mountains region obtained by the radar in Arecibo.*

ring structure on the right side of the mountain range is Cleopatra's Pater, 100 km in diameter.

By 1980, the most detailed map of the surface of Venus was a map of the heights of the planet in the range from 60° S up to 75° N, built with the help of an altimeter of the American spacecraft Pioneer-Venus. Despite a relatively large step of measurements on the surface of ~ 50-150 km, this map reveals details of a continental scale - Ishtar's Land, Aphrodite's Land, Beta Area, etc. Smaller details - ridges, rift valleys, impact craters were not visible. Meanwhile, the absence of such details did not allow us to judge the age of the surface of the planet, about the geological activity of Venus.

In order to obtain a more detailed and important information for geologists, an experiment was conducted in the Soviet Union on radar mapping of this planet from the spacecraft Venera-15 and Venera-16, performed in 1983-1984 by Soviet scientists and deservedly a world-class achievement. For the first time in the world, a detailed radar survey of the planet's surface was carried out from the spacecraft, closed by a dense atmosphere, inaccessible to observations in the optical range. The area of the surveyed territory located north of 30° N is 115 million km^2, which is a quarter of the entire surface of Venus and only one-third less than the terrestrial land area.

The successful carrying out of the experiment became possible thanks to the close cooperation of domestic organizations, such as the Research Center named after G.N. Babakin (artificial satellites of the "Venera" series, satellite control during the experiment), OKB MEI (onboard radar system), NII KP (development of a radio link, receiving information at the Center for Remote Space Communications in Crimea), IPM. M.V. Keldysh (processing trajectory measurements), Central Research Institute of Geodesy, Aerial Photography and Cartography (mathematical foundations of cartographic support, preparation of maps), Vernadsky GEOKHI (geological and morphological analysis). The idea of carrying out the experiment and its scientific and methodological basis was developed at the Institute of Physics and Technology of the Russian Academy of Sciences. A computer center was set up in the Fryazino

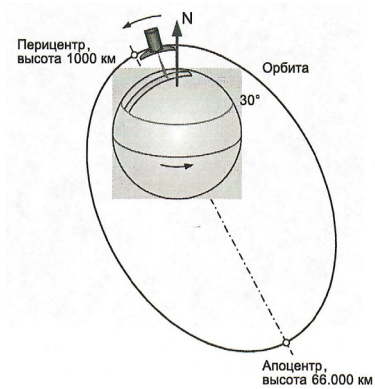

Fig. 4. *Survey scheme of the polar region of Venus from the spacecraft Venus-15/16.*

branch of the IRE RAS, all processing of the received material was carried out and digital maps of Venus were created. It should be noted that all the equipment used in the work in space and on Earth was created in the Soviet Union.

A synthetic aperture radar with a viewing angle of 10°, mounted on a spacecraft, provided a side-by-side image of the surface image strip with a spatial resolution of 1-2 km. The radio altimeter-profilograph made measurements of the surface heights in the nadir. The measurement scheme is shown in **Fig. 4**. The spacecraft, which is in an elliptical orbit with a period of revolution of one day, conducted a survey of the band of the radar image of a surface 150 km wide and 7000 km long in the vicinity of the pericentre of the orbit. In the area of the apocenter there was a drop of the received information on the radio link to the Earth. It should be noted that the radio telescope RT-70 in Yevpatoria was used as the receiving device for information on the Earth. During the time between successive shots, Venus rotated relative to the plane of the orbit of the device, which provided an increase in the area to be taken. The use of complex sounding signals and the aperture synthesizing method gave a relatively high spatial resolution in the images.

The achieved resolution of 1-2 km was sufficient for the discovery of all the main geological structures characteristic only of Venus (tesserae, arachnoids, crowns, lava plains and domes, etc.), and conducting a sufficiently detailed geological and morphological analysis. More than 100 impact craters measuring from 8 to 146 km were found, the density of their location along the

Fig. 5. *An example of a radar image of the Maxwell Mountains region.*

planet made it possible to estimate the age of the surrounding surface. The airborne radio altimeter of the OKB MEI design gave measurements of the relief height with an accuracy of about 30 m in height, over which the topographic map of the investigated territory was constructed.

In **Fig. 5** shows an example of an image on the junction area of the Lakshmi plateau (lava plain on the lower left) and the Maxwell mountains with the 100-kilometer Cleopatra's patron (top right). At the center of this unusual kilometer of depth, located on the eastern slope of Maxwell's mountains, a second dip of 1 km deep is clearly visible (see combined surface image and height profile in **Fig. 6**). According to geologists, the internal failure is not the result of a meteorite impact, but the result of a collapse of the bottom of the pater. In the middle of the image in Fig. 6 there is also the highest point of the surface on Venus - a peak 11.5 km high above the middle sphere, which is higher than the highest mountain peak on Earth.

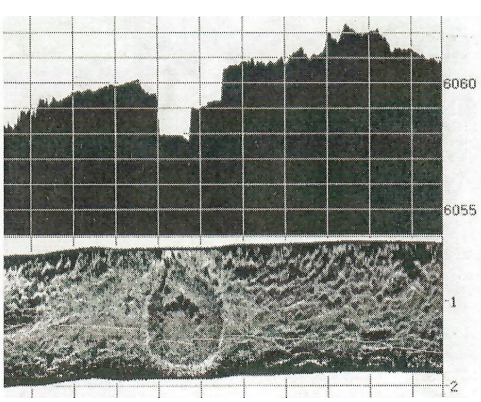

Fig. 6. F*ragment of the image band and height profile Cleopatra's fathers. The white line in the image shows the position of the height measurement track.*

As a result of the experiment, not only the first detailed surface maps were obtained, but the main forms of the geological structure of Venus were also revealed. It was established that the neighboring planet, close to the Earth in size and remoteness from the Sun, lives its geological life. For example, it does not have such an important mechanism for the formation and renewal of the earth's crust as plate tectonics, and the processes of erosion of the surface are extremely slow, which keeps the details of the relief unchanged for millions of years.

The results of radar mapping of Venus received in the Soviet Union were widely analyzed by the world scientific community and were used in the preparation of the US space experiment Magellan on global radar mapping of the surface of Venus, conducted 8 years after our experiment. Despite the globality of the radar images obtained by Magellan and an order of magnitude greater spatial resolution, the main geological discoveries on Venus were made according to the data of the Soviet apparatus Venera-15 and Venera-16.

For the work on radar mapping of Venus in 1985, the young employees of the FIRE RAS were awarded the Lenin Komsomol Prize (Zakharov A.I., Zimov V.E., Sinilo V.P., Shubin V.A.). The main ideologists and performers of the FIRE RAS were awarded in 1986 with the Lenin Prize (Alexandrov Yu.N., Sidorenko A.I.) and State Prizes in 1986 (Rzhiga ON), in 1989 (Zagorodni S.F., Zakharov A.I., Krymov A.A.).

Remote sensing of the seabed by sonar systems with complex sounding signals

The experience of radar studies of planets in IRE RAS has allowed to create a new direction of work - remote mapping of extended objects with the help of high-energy probing signals and digital methods of coherent echo signal processing. The digital methods of synthesizing and signal processing used in the location of the Earth and planets were proposed at the end of the seventies at the FIRE RAS to create a new generation of sonar systems for surface seabed mapping. The problem of distance studies of the seabed and bottom sediments by remote methods is related to the fact that only acoustic waves propagate in

water with low attenuation. In this case, the lower the frequency of oscillations, the less attenuation. The second feature is the propagation velocity of about 1500 m/sec, which along the propagation path can vary within a few percent. And the third problem is the preservation of the coherence of the probe signal during propagation and scattering by inhomogeneities. In this regard, the methods of radio vision, developed in the radio range, can not be used directly in an acoustic vision, additional research and technical developments are required. The first acoustic systems - side-scan sonar, echo sounders and profilographs, developed in the 1960s, emitted tone impulse messages in the frequency range 3-500 kHz. In this case, at low frequencies, the systems were provided with large-several km of sensing range, but with a low resolution in range because of the narrow band of the acoustic radiators-about 10% of the radiated frequency. High-frequency systems allow obtaining a high resolution up to 5 cm, but at distances up to 50-100 m. Increasing the range of the sonar systems by increasing the radiated power is limited by cavitation on the surface of the radiator. The contradiction is removed by using complex sounding signals with a large base and correlation processing of echoes. However, the implementation of this method implies preservation of the coherence of the signal during propagation and scattering, which was negatively perceived by marine acoustics at the beginning of our work.

These were the years of discovery on the ocean floor of rich stocks of precious metal ores. The task of estimating ore reserves of ferromanganese nodules was supposed to be solved by sonar on the power of reflected acoustic signals. For these purposes, the Shirshov Institute of Oceanology developed a side-scan sonar of the range of 6 kHz, using the traditional tonal impulse in those years, but the limited energy potential provided a range of up to 6 km. Since the deposits of iron manganese ores are located at depths of more than 5000 m, the efficiency of the device tested on the second voyage of the R/V "Akademik Keldysh" turned out to be low, comparable with the echo sounding device. However, it was possible to confirm a significant increase in the level of echoes during scattering from ore sites on the bottom surface. By this time, at the FIRE RAS under the direction of Kaevitser V.I. an experimental sample of a side-scan sonar with linear frequency modulation (LFM) of a sounding signal was created and tested in cooperation with NIPI "Oceangeophysics" in Gelendzhik. The results of the work made it possible to modernize the long-range IORAN in a short time, increasing its energy potential by more than 100 times due to the use of the chirp signal and digital correlation processing of echoes. The device was tested on the fourth voyage of the R/V "Akademik Keldysh" in the Pacific Ocean and the sixth voyage in the Indian Ocean. The experimental sonar had a survey on one side, while at a depth of 5-7 km a 12-15 km mapping strip with a detail of about 5 m was provided. As a result, a technique was developed for detecting and measuring the productivity of the fields of ZMK.

The conducted experiments confirmed the important advantages of our developments in comparison with traditional sonars using tonal sounding impulses. This increase in energy potential and resolution, increasing noise immunity and associated electrical and acoustic compatibility of various devices, increasing the ability to automate the sonar systems for various purposes.

In order to create an industrial long-range GBO in FIRE RAS in the mid-1980s, a laboratory was created which, on the instructions of Mingeo, the USSR developed and, together with the NIPI, Oceangeophysics, created a towed side-scan sonar for the long-range Okean-D, operating in the frequency range 10 kHz and providing a shooting strip for the acoustic image of the seabed at depths of up to 6 km in the 30 km band. The device was released in a small series and was widely used for exploration of ore formations on the seabed at NPO Yuzhmorgeologiya. The works carried out at the FIRE RAS were supported by the Main Navigation and Oceanography Directorate (GUNIO MO USSR) and the State Committee for Science and Technology of the USSR (Minnauka). As a result, several hydroacoustic systems were developed and tested at the FIRE RAS on new principles using long-duration probing signals

with intrapulse modulation and a correlation system for digital processing of echoes. These include: on-board sonar complexes of the surface survey of the topography and the bottom of the seabed - AGKPS-200 (80 kHz) and Coral-300 (80-240 kHz), towed by AGKPS-1500 (30 kHz) and AGKPS-5000 (12 kHz), high-frequency sonar "Kedr" (400 kHz, onboard and towed variants), profilographs (5-15 kHz, onboard or towed (the latter in a single module with HED "Kedr.") All systems use digital methods of signal generation and processing, LFM probing signals (corresponding correlation processing, coordinated and the calibration of the received signal, and in AGKPS-200/1500/5000 and "Coral" -300 and phase processing.) The complex AGKPS 1500 during the tests made it possible to detect the sunken submarine "Kursk", to determine the exact coordinates of the bow and stern parts. modular principle and in operation can be combined in various combinations.The navigation data comes in complexes from any satellite receiver and digital sensors for determining the spatial position. Abroad, such developments appeared only in the mid-1990s.

At present, acoustic sonar systems of coherent sounding have become the main instrument for remote measurements of the seabed relief and the structure of bottom sediments. For simultaneous measurements of the relief and obtaining of acoustic images of the bottom surface, two main, to some extent competing, class of systems have been formed: interferometric side-scan sonar and multi-beam echo sounders. If one survey antenna usually contains one antenna per board, interferometric HBO - two, three, then multi-beam echosounders are a more complex complex consisting of a much larger number of receiving elements of the order of 100 and higher. Low-frequency acoustic profilographs are used to study the subsurface structure of the seabed. This, as a rule, single-channel systems, providing continuous profiling of the soil along the route of the vessel.

The lateral survey methods are based on the sequential formation of data on the seabed during the movement of the vessel (**Fig. 8**).

The pulse radiated by the transmitting antenna is sequentially reflected from the individual elements of the bottom at different ranges. Reflected echoes are received by one or more receiving antennas. A cycle consisting of transmission and reception forms one implementation (one horizontal row of the acoustic image). The set of sequential realizations formed during the movement of the vessel contains information on the reflective characteristics of the seabed in the survey band and represents an acoustic image of the bottom - an analog of the optical and radar images. Such images are intended for visualization and classification of objects. The line of sight is determined by the directivity pattern of the receiving elements, the energy characteristics, the shape of the seabed relief, is usually set in the depths H_0 "below itself" and is 4-10 H_0. The use of antennas with narrow directional patterns in the lateral direction provides a certain two-dimensionality of measurements in the plane of the side-view. The seabed is considered as a spatial medium with a backscattering coefficient that depends on the distance L and the angle θ between the vertical and the direction of arrival in the lateral survey plane R = R (L, θ).

The processing task is to estimate the reflection coefficient $R(u,\tau)$ from the set of measurements $Z_n(t)$ and the subsequent determination of the seabed parameters. Depending on the number of receiving antennas in different systems, various methods for estimating the reflection coefficient

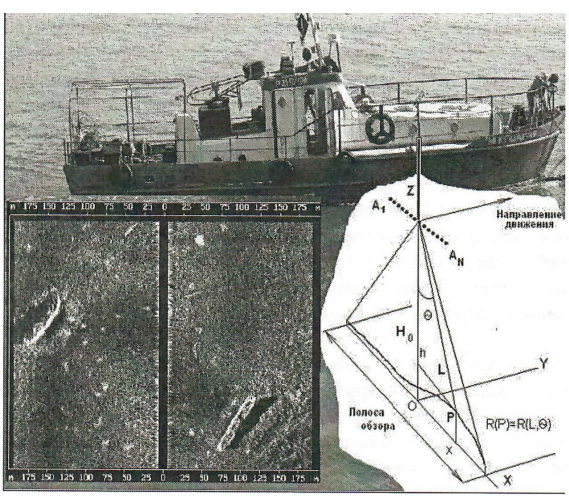

Fig. 8. *The geometry of the side scan and a fragment of the resulting acoustic image of the bottom with wrecks.*

R and the parameters of the seabed are used, as well as various restrictions on the assumed shape of the seabed relief.

The dependence of the reflection coefficient modulus R on the distance is the basis for constructing maps of the acoustic image of the bottom. The absence of angular selectivity in single-channel survey HBO is not an obstacle when using this class of systems to study relatively flat areas of the seabed, search for small objects, details of relief such as furrows, trenches, and stones. Usually the survey HBO is a single-channel sonar on the right and left sides, with independent transmit-receive antennas having a narrow (about 1°) directional pattern along the carrier line and, as a rule, a digital system for the formation, processing and recording of signals. The type of radiated pulses are tonal and chirp sending. Operating frequencies from 10 to 500 kHz. In the tonal mode, the pulse duration is a fraction of milliseconds, in the LFM mode it reaches several seconds. Interferometric methods are used to calculate the depths in the survey strip. For analysis of the bottom relief in the survey strip, interferometric HBO complex includes additional receiving channels with a set of antennas in the vertical plane. Signal processing in interferometric HBO is based on the calculation of the arrival angle and is performed by measuring the phase Ψ of the complex-conjugate product of a pair of samples of two channels (an interferometer).

One of the single-channel instruments, where chirp signals are widely used to increase the energy potential, are acoustic linear profilographs. The long experience of using a low-frequency profiler with chirp sounding signals, developed at the IRE RAS, confirmed its high operational capabilities and allowed to reveal some features of the interpretation of the results obtained. The working frequency of the profilograph is 5 kHz, the frequency band is about 4 kHz, the radiated power is about 3 kW. The profilograph includes: a nine-element antenna system (**Fig. 9**), an electronic system for generating sounding parcels (a digital synthesizer), a power emitter, and an input interface for information in the PC. The device contains a digital system for collecting, displaying and processing data. It is designed for examining the bottom relief and bottom sediments at depths from 20 m to 3000 m. Data collection programs provide coherent input of echo signals, input of navigation information from GPS sensors and the spatial position of the vessel, display of information in real time and archiving of the received data.

In **Fig. 10** shows a fragment of profiling the seabed in the ice conditions of the Chukchi Sea. The depth is about 70 meters. The result of the profiling shows the high noise immunity of the device, which made it possible to realize a high resolution of bottom sediments. The above fragment is also interesting in that a hollow is clearly visible, filled with sediments. This kind could well have been the bed of the ancient river after the descent of the land and the onset of the sea. High energy potential with the use of chirp sounding signals allows the profiling of bottom sediments at large depths of the sea. In **Fig. 11** shows the result of profiling from a ship in the Sea of Japan at depths ranging from 1200 m to 1.400 m. The area is characterized by a changing terrain with a thick layer of plastic deposits. The first reflection corresponds to the depth and is confirmed by the results of the measurement by single-beam and multi-beam echo sounders. The horizontal distance is the distance traveled in meters, and the vertical axis is the depth in meters. As can be seen in the figure, the profiling depth is 100 and more meters, the nature of the deposits on the slopes has a layered structure characteristic of silty clays. In the hollow, the profile of the profilogram is more uniform in depth, which is characteristic of sandy loam.

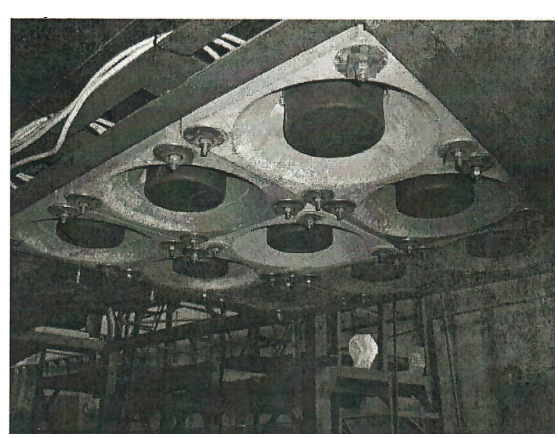

Fig. 9. *Acoustic antenna echo sounder profilograph.*

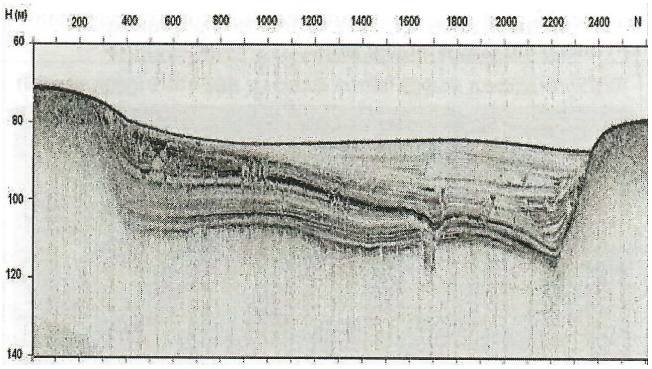

Fig. 10. *A fragment of the profiling of the seabed in the Chukchi Sea.*

A fragment of the acoustic image obtained during the survey of the route of laying the optical cable in the Arctic ice conditions is shown in **Fig. 12**, where the traces of ice ex-coverage from a large iceberg on the sea floor are clearly visible.

Long-term research of IRE RAS staff in the development and application of new methods of synthesis and signal processing for the solution of location problems is widely used at present in remote sensing of the Earth from space, as well as other scientific and technical applications.

From a brochure by Ryzhga Oleg Nikolayevich [2].

As the scientific leader of the space experiment on radar mapping of the planet Venus, the author remembers the stages of the creation of the unique space complex "Venus-15" and "Venus-16". This was an example of the creative cooperation of industrial enterprises and scientific institutions. The work was conducted by an interdepartmental team, under the leadership of the Vice President of the Academy of Sciences of the USSR, Academician V.A. Kotelnikov, where everyone did his work. The Academy of Sciences developed a

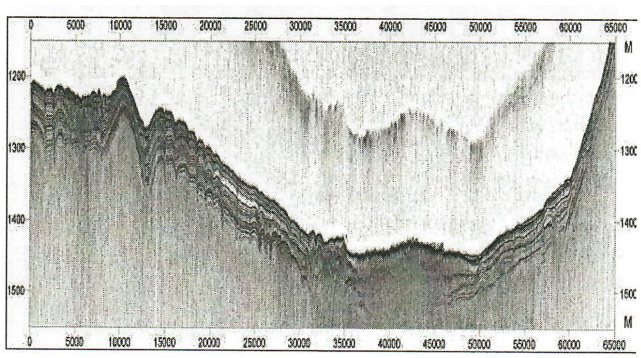

Fig. 11. *Fragment profiling the seabed in the Japan Sea.*

methodology for the experiment and carried out data processing. The OKB MEI of the Ministry of Higher Education developed the radar system equipment, and the cooperation of industrial enterprises created the spacecraft and ensured its management.

The idea of the experiment arose in the IRE of the Academy of Sciences of the USSR in the autumn of 1972. It was directly developed by Yu.N. Alexandrov, G.M. Petrov and the author. In November 1975, the author was received by the president of the Academy of Sciences of the USSR Academician. M.V. Keldysh. Shortly thereafter, an experiment on radar mapping of Venus was included in the program of space research. For the development of radar equipment, the director of the OKB MEI, A.F. Bogomolov. In OKB MEI was such a man GA. Sokolov, who immediately imbued with the task and set the goal of his life to carry out the experiment. Through him, a connection was made between the IRE of the USSR Academy of Sciences and the OKB MEI. He enjoyed great authority, and everything that we agreed with him was put into practice.

The equipment, including antennas, was first tested autonomously at the OKB MEI Medvezhye Ozera range. Guided this responsible work GA. Podoprigora. Then, during the year preceding the flight, tests were carried out together with data transmission equipment to the Earth and processing equipment. Signals reproducing reflections from point targets were fed to the input of the radar system receivers. Test equipment, developed under the leadership of M.N. Meshkov, allowed to automatically change the level of signals, their lag and the frequency of a certain program. Magnetic tapes with the recording of signals that passed through the receiving and recording equipment of the radar system were transmitted for processing and analysis at the Institute of Nuclear Physics of the USSR Academy of Sciences. These tests made it possible to identify 2-3 serious defects, after the elimination of which the equipment worked impeccably. Great work in the organization of tests is enclosed by V.G. Timonin.

To test the operation of the radar in conjunction with the new radio link, the tests were continued in

flight. The information recorded in advance on the Earth on magnetic storage devices was reproduced. The transmitter of the radar was switched on, its antennas were alternately sent to Earth, and the power of the sounding signal, its frequency and the modulation structure were measured on the Bear Lake. Slowly turning the device according to the program.

IRE USSR AS staff engaged in radar observations of planets in the Center for Long-Distance Space Communication, has a tradition to create with their own hands. In this connection, it is indicative to create a complex of equipment (Venus-15) and Venus-16 for the processing of radar information of spacecraft. In the creation of the Center and in the organization of information processing, his leader A.I. Sidorenko.

The development of a processor for accelerated execution of the Fourier transform on the reflected signals was started at the IRE of USSR Academy of Sciences under the direction of Yu.N. Alexandrov. Then this work was carried to the Institute of Electronic Control Machines of the Ministry of Applied Sciences, where B.Ya. Feldman, and the scientific leadership was carried out by Yu.N. Alexandrov. A specialized Fourier processor (SPF-SM), developed specifically for the processing of reflected signals during the survey of Venus using Venera-15 and Venera-16 spacecraft, is currently produced by the industry for research and economic purposes.

The methodology, algorithms and programs of information processing were created entirely in IRE USSR AS. For a year and a half before the experiment began, it turned out that programs written in the standard Fortran language work too slowly. For example, it turned out that one of the 6 main programs for processing information received in one shooting session (the program for building a radar image strip) requires 26 hours of computer time. Since it is impossible to make the machine faster, it was necessary to apply "small tricks", such as the switch to the language of assembler, the use of integer arithmetic, the decomposition of complex functions into finite series, interpolation. All, taken together, reduced the counting time by about 10 times.

Mathematical programs were supposed to provide complete processing of incoming information, including the construction of radar images and the measurement of the high-altitude relief of the surface of Venus. In addition to the speed of the account, they required independence in making decisions in the event of information distortions. During the processing, the characteristic values of the parameters of the reflected signals, such as power, frequency, delay, were to be calculated in order to promptly judge the operation of the radar and the processing progress. The complexity of programs is judged by the number of elementary operations into which the program falls. Some programs had up to 4000 such operations, and their total number in all programs reached 50.000!

In May 1983, several months before the start of the experiment for various reasons, several people left among the staff of the IRE of the USSR Academy of Sciences, who were preparing algorithms and programs. In the situation that emerged, when those who had been taught "little tricks" for several years were lost, no one could help. There was only one way out - to work more intensively, with maximum dedication. Some worked during their holidays, on weekends. In the last two months worked from 8 am to 8 pm, but no more to regain strength.

As a result, all major programs were debugged at the time of the receipt of magnetic tapes with the recording of the information of the first shooting session. Now we were at the last stage of a long chain, which began with the creation of a radar and a spacecraft. From our work depended on how successfully the work of many thousands of people participating in the experiment would end. This was the main stimulus in the work.

An experiment of such complexity was carried out for the first time, and when in early June 1983 spacecraft started to Venus, there were many fears in its success. Will the equipment work? Does the image distort the atmosphere of Venus? Do we correctly understand how radio waves are reflected by the surface of Venus? After all, after the first low-quality radar images obtained in the US, some

thought that Venus is as smooth as a billiard ball, and there's nothing to shoot!

And then came the landmark days. On October 16, 1983, the Venera-15 spacecraft made the first radar survey of the planet Venus. On October 18, magnetic tapes with the recording of the information of the first shooting session by an early train were delivered to Moscow by E.P. Molotov, who led the development of reception equipment and noise-resistant registration of spacecraft information. On October 20, about 15 h, a fragment of the first image of the surface of Venus appeared on the display screen (**Fig. 14**). Everything worked perfectly.

When the regular daily shooting of Venus began, the backlog in processing began to grow. Then in late 1983 it was decided to switch to two-shift work, including Saturday and Sunday. All the employees involved in the processing were divided into 3 brigades. One of them worked during the day, the other in the evening, and the third on these days rested. In the creation of a complex set of programs, the development of the equipment of the Center and the processing of information, a large role belonged to young researchers A.I. Zakharov, V.E. Zimov, A.P. Krivtsov, I.L. Kucheryavenkova, N.V. Rodionova, V.P. Sinilo and V.A. Shubin.

Every week, 100-150 photo prints with images and profiles of the surface heights of Venus were transmitted to the GEOCHI Academy of Sciences of the USSR and Central Research Institute of Geodesy, Aerial Photography and Cartography. To speed up the issue of maps, it was decided to build maps using digital methods using the equipment of the Center. By the middle of 1987 for the removed territory of Venus all 27 maps in four variants were constructed. They are transmitted on magnetic tapes to Central Research Institute of Geodesy, Aerial Photography and Cartography for preparation to the publication. Two maps of them were published in a small print run in 1986. In November 1987, A.A. Krymov and O.S. Shamparova completed the construction of a complete map of the removed territory of Venus, which included all the material obtained with the help of spacecraft "Venus-15" and "Venus-16".

The nomenclature of details of the surface of Venus for published maps was approved by the XIX General Assembly of the International Astronomical Union, held in November 1985 in Delhi. In the preparation of the nomenclature, Soviet specialists A.T. Bazilevsky, G.A. Bourba, M.Ya. Marov, Yu.S. Tyuflin, etc. The nomenclature contains over 250 items. It is widely represented by Russian women's names, women's names of the peoples of the USSR and the socialist countries. On the maps of Venus, we meet the names of famous women scientists, poetesses, actresses, public figures. So, on the first published map "Plateau Lakshmi" we see the craters of the name of Ekaterina Dashkova, Anna Akhmatova, Polina Osipenko, Ezheni Cotton. The publication of maps of Venus continued in 1987.

The results of radar survey of Venus with the help of spacecraft "Venus-15" and "Venus-16" aroused great interest not only in the Soviet Union. Preparing to repeat the radar studies of Venus from the orbit of an artificial satellite on the project "Magellan", American scientists asked the Academy of Sciences of the USSR to transmit the materials of the radar survey of Venus. Transmission of magnetic tapes with images and elevation profiles of Venus' surface is carried out regularly through the Intercosmos board. In turn,

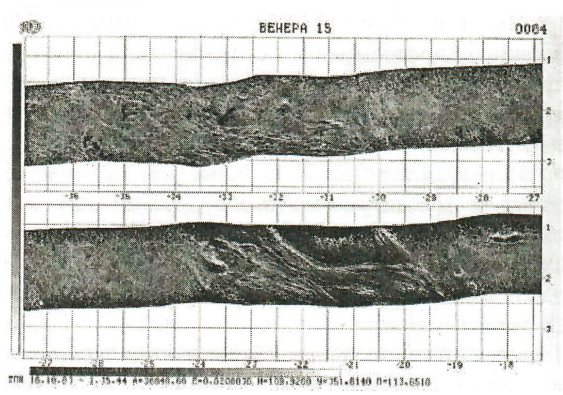

Fig. 14. *Part of the strip of the image of the surface of Venus, obtained in the first session of shooting on October 16, 1983 with the Venera-15 apparatus. The orbital longitude, measured from the pericenter of the orbit, is vertically in degrees, and the orbital latitude, measured from the plane of the orbit, is vertically in degrees. The spacecraft moved from left to right, its route passed above the band. Regular displacements of the strip relative to the orbital plane are associated with a change in the height of the apparatus moving in a highly elongated elliptical orbit, irregular - caused by local relief.*

we received all the data from the radar survey of Venus with the help of the Pioneer-Venus spacecraft, as well as detailed maps of Mars, based on the results of television surveys using the Mariner 9 and Viking spacecraft.

The flight of the spacecraft "Venus-15" and "Venus-16" opened a new era in the study of this planet. In an address by the General Secretary of the CPSU Central Committee, M.S. Gorbachev to members of the congress delegation of the Nobel Peace Prize laureates in November 1985, this experiment was put on a par with the launch of the first satellite, the first manned space flight and landing on the moon, the landing of automatic stations on Venus and Mars. The map of Venus is called beautiful!

SMOLYANINOV'S GROUP

The main theme of the Smolyaninov Vyacheslav Mikhailovich's group was the interference-proof transmission and reception of signals in various environments.

Currently, there is an intensive development of various digital data transmission systems. All systems use wireless channels for data transmission, in which interference of a different physical nature acts on the transmitted signal. This leads to the fact that the received data with a high probability will contain errors. At the same time, for many practical applications only a very small fraction of the errors in the discrete data being processed are allowed. As a result, the problem arises of ensuring the reliable transmission of digital information through channels with noises.

The most important contribution to the solution of this problem is made by the theory of noise-immune coding. On its basis, methods of error protection are developed, based on the use of noise-immune codes. The use of these codes makes it possible to obtain the energy gain of the coding, which characterizes the degree of possible reduction in transmission power when encoding as compared with the absence of coding, if the reliability of the transmission in both cases is the same. This gain can be used to improve the parameters and characteristics of many important properties of data transmission systems, for example, to reduce the size of very expensive antennas, increase the communication range, increase the data transfer rate, reduce the required transmitter power, etc

The development of noise-immune encoding has been going on for half a century. If at first it relied on algebraic methods, later it was replaced by the methods of majority coding and, as a more efficient, exhaustive algorithm of Viterbi. The disadvantage of the latter is the exponential increase in complexity for long codes. The next stage was cascade codes based on convolutional codes and Reed-Solomon codes. Cascade codes provided higher noise immunity characteristics with less decoding complexity, but were far from theoretically possible limits (Shannon's theorem for channels).

The turbo codes, discovered in 1993, made it possible to almost completely use the capacity of digital communication channels and approached codes with speeds close to the bandwidth of the channels, which is especially important nowadays with increasing communication range.

SAVICH'S GROUP

The group of Nikolai Alexandrovich Savich stood out from 117 laboratories in 1972, having joined the 127th laboratory. In June 1978, the Savich group was formed into a separate group 114. The main direction of the Savich group's work is connected with the study of the ionospheres of the planets of Venus and Mars.

Detection of the nocturnal ionosphere of Mars [3]

During the passage of the Mars-4 station near the planet Mars on 10.2.1974, the atmosphere of the planet was radarized by two coherent monochromatic signals in a decimeter ($\lambda \approx 32$ cm) and centimeter ($\lambda \approx 8$ cm) wavelength bands with a frequency ratio of 4 , which were emitted from the station and were received on Earth.

The problem consisted in detecting a plasma over the surface of Mars unenlightened by the Sun and determining the profile of the electron concentration in the nocturnal ionosphere. At the ground receiving point, each signal was separately received and processed simultaneously

by two independent systems of a dispersion interferometer. Both treatment systems produced identical results. According to the data obtained, under the assumption of the spherical symmetry of the ionosphere, the altitude distribution profile of the electron concentration in the night ionosphere of Mars was calculated (**Fig. 15**). The graph clearly shows the main ionization maximum at an altitude of about 110 km above the surface with a particle concentration of $N_m \approx 4.6 \cdot 10^3$ cm^{-3} and a half-thickness of the layer of the order of 35 km. The measurement error in the region of the maximum is of the order of 5%.

Multiple single-frequency transmission of the night ionosphere of Mars was carried out using the Mariner 9 station. However, the measurement errors inherent in the single-frequency method in the incoherent mode when the on-board transmitter is operating from the quartz generator do not allow us to detect the nocturnal ionosphere of Mars without a priori information.

Measurements of two-frequency radio luminosity allowed obtaining a reliable distribution of electron concentration in the night ionosphere of Mars and determining its main characteristics: the height of the main maximum and the value of the electron concentration.

Investigation of the ionosphere of Venus by the method of two-frequency radio transmission using Venus-9, 10.

Before the flight of spacecraft to Venus, information about its atmosphere was limited, mainly, to ground and radio-astronomical observations. The estimation of Venus ionospheric parameters was based on analogies with the terrestrial and had a hypothetical character.

The first experimental data on the parameters of the Venus ionosphere were obtained by the radiophysical method during the passage of the Mariner 5 apparatus in 1967. Two-frequency radiolocation was carried out on the Earth-to-space communication request line by two coherent signals of 49.8 MHz and 423.3 MHz, and the results of measurements of the reduced Doppler frequency difference, as well as the signal amplitudes, brought the first information on the electron concentration $N(h)$ distribution in the daytime and the nocturnal ionosphere of Venus. The main conclusions of this work are: 1. The daily ionosphere has a main ionization maximum at an altitude of ~ 140 km with a particle concentration $N_m \sim 5.5 \cdot 10^5$ cm^{-3} and a secondary ionosphere at ~130 km with $N_m \sim 2 \cdot 10^5$ cm^{-3}. 2. The night ionosphere has a main ionization maximum at an altitude of ~ 142 km with $N_m \sim 2 \cdot 10^4$ cm^{-3}.

In 1974, during the flight of the Mariner-10 apparatus near Venus, a two-frequency radio transmission of the day and night ionosphere of Venus was again carried out, but at higher frequencies (~ 2295 MHz and ~ 8415 MHz) via the Earth-to-space communication line. As a result, it was shown that: 1) The daytime ionosphere has a principal ionization maximum $N_m \sim 3 \cdot 10^5$ cm^{-3} at an altitude of ~ 145 km. 2) The night ionosphere has two ionization maxima.

To clarify the structure of the day and night ionosphere of Venus, systematic experimental data were needed on the altitude profiles of the electron concentration, which could be obtained with the help of a long-lived satellite of the planet. Therefore, when creating satellites "Venera-9, 10", it was envisaged to perform a multiple radio transmission of the ionosphere and the atmosphere of Venus by the method of a dispersion interferometer.

The conclusion in October 1975 of the automatic interplanetary stations "Venus-9" and "Venus-10" into the orbits of artificial satellites of Venus opened for the first time the possibilities for carrying out a multiple two-frequency radio

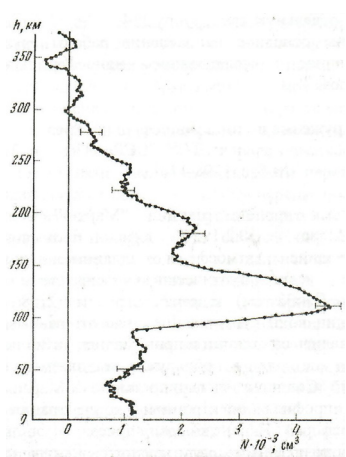

Fig. 15. *The distribution of electron concentration in height in the night ionosphere of Mars.*

transmission of the atmosphere of Venus. At both stations, in addition to a standard transmitter of a decimeter (32 cm) range, a coherent centimeter radio transmitter (8 cm) was designed and manufactured at the SKB IRE of the Academy of Sciences of the USSR. As a result, during the period from 24.10.76 to 7.12.76, 22 sessions of radio transmission of the night and 13-day ionosphere of Venus were successfully carried out using the dispersion interferometer.

It is established that in the night ionosphere of Venus, as a rule, the altitude distribution of ionization has two maxima (16 cases) and very rarely one (2 cases). The electron concentration in the upper maximum of the night ionosphere of Venus lies within N_m ~(2.9±16.0)·10^3 cm^{-3}, and its height in most cases is ~140±5 km. The lower maximum of the concentration has the parameters N_m ~(1.8±11.2)·10^3 cm^{-3} and a height of 120±13 km. It was shown for the first time that the electron concentration distribution in the Venus night ionosphere is characterized by considerable variability in time both in the density of ionized layers and in the shape of the profile.

In the daytime ionosphere of Venus (zenith angles from 10° to 87°), the electron concentration at the main maximum, located at altitudes 140±166 km, lies within N_m ~(1.25±4.4)·10^5 cm^{-3}. In addition, the existence of a lower ionized layer with a maximum concentration of N_m~(4.6±13)·10^4 cm^{-3} at altitudes of 125±138 km and an additional upper layer at altitudes of 180±210 km, which is observed at low zenith angles of the Sun at zenith angles ≥74°.

MAKSIMOV'S GROUP

One of the directions of the work of the staff of Maximov Alexander Stepanovich was the creation and research of semiconductor analogues of inductance. The fact is that in devices that work well. at low frequencies, when tuning them to infra-low frequencies, a number of specific features begin to appear: an increase in noise, a decrease in the Q-factor of reactive elements, an increase in the dimensions and weight. The problem of reducing the dimensions and weight of reactive elements for infra-low frequencies is particularly acute both in microminiaturization of equipment and in the creation of super-powerful reactive elements.

The IRE of the USSR Academy of Sciences proposed new principles for the creation of miniature elements with a large equivalent inductance (10^3 ÷ 10^6 H) and, accordingly, with a large time constant when using both thin-film and solid-state technology. The principle of operation of these devices is based on the phenomena of capture and release of charge carriers by slow surface states. It has been shown that the use of solid-state technology to create inductive elements is more promising. On the basis of *p-n-* and *p-n-p-n-* germanium and silicon structures with a specially treated surface, the possibility of their reproducible production, the stability of the parameters in time, and practical implementation in a number of radio engineering devices was demonstrated.

CONCLUSION

In conclusion, we list a list of all the laboratory workers 127 who worked in it at one time or another and who made their contribution to its glory and pride at the Institute of Radioengineering and Electronics of Russian Academy of Sciences: Abramova L.V., Azarov V.V., Aleksandrov Yu.N., Baraboshkin S.M., Belitsky M.R., Berezina S.I., Burkov V.D., Vasiliev M.B., Vyshlov A.S., Vyshlova L.V., Gavrik A.L., Gatilova M., Gerasimov S.V., Golovkov V.K., Dolotov S.A., Dubrovin V.M., Zaitsev A.L., Zaitseva O.S., Zakharov A.I., Zimov V.E., Zyablov A.B., Ivanov V.A., Kaevitser A.V., Kaevitser V.I., Kalinin A.V., Kovtun V.V., Kopnina T.F., Koroleva T.S., Krivtsov A.P., Krylov G.A., Krymov A.A., Kuznetsov A.A., Kuznetsov B.I., Kuznetsov O.O., Kuznetsova L.V., Kukushkin A.S., Kucheryavenkova I.L., Kushchenko E.F., Labutin M.V., Maksimov A.S., Margachev V.V., Metelskaya Z.T., Moiseenko V.Yu., Nazarenko E.G., Nazarov L.E., Nekrasov A.Ya., Pervushin S.A., Perfilova N.I., Petrov G.M., Prokofiev I.V., Prokuronov V.V., Razumnyi E.A., Rzhiga O.N., Rodionova N.V., Romanova G.V., Ryabova N.V., Savich N.A., Salnikov V.P., Samovol V.A., Samoznayev L.N., Semaev V.N., Semiletnikov V.V., Sidorenko A.I., Sinilo V.P., Sknarya A.V., Smolyaninov V.M.,

Sorokin V.K., Sorochinsky M.V., Suhoverhova V.Z., Turusin I.V., Feofanov Yu.V., Khasyanov A.F., Khlebnikov M.N., Tsarfin D.L., Chalikov S.F., Chelyshev N., Chernov P.V., Churkin V.I. Shatalova L.I., Shubin V.A., Shumilova L.V., Yurkova V.I.

REFERENCES

1. Rodionova NV (compiled and edited). *Petrov and his team*. Moscow, Editus Publ., 2018, 220 p.
2. Rzhiga ON. A new era in the study of Venus (radar imagery using spacecraft "Venus-15" and "Venus-16"). Moscow, Znanie Publ., 1988. 64 p.
3. Vasiliev MB, Vyshlov AS, Kolosov MA, Savich NA, Samovol VA, Samozavayev LN, Sidorenko AI, Alexandrov UN, Danilenko AI, Dubrovin VM, Zaitsev AL, Petrov GM, Rigga ON, Stern DY, Mesterton AP. Detection of the night ionosphere of Mars. *DAN USSR*, 1974, 218(6):1298-1301.

MULTI-FREQUENCY RADAR LOCATION OF THE "EFFECTIVE" SOIL MOISTURE

Anatoly A. Kalinkevich, Boris G. Kutuza, Vasiliy N. Marchuk, Vladimir M.Masyuk

Kotelnikov Institute of Radioengineering and Electronics of Russian Academy of Sciences, http://www.cplire.ru/
Moscow 125009, Russian Federation

Viktor A. Plyushchev

Radio Engineering Corporation "Vega", http://www.vega.su/
Moscow 121170, Russian Federation
kalinkevich@newmail.ru, marchuk@ms.ire.rssi.ru, masyuk77@mail.ru, mail@vega.ru

Abstract: **The review of studies on subsurface sensing topsoil radar method is presented, as well as on the development of an algorithm and techniques for combined interpretation of radar images using side-scan radar systems with a synthesized antenna operating over a wide range of wavelengths, including decimeter and meter bands. A method for constructing a deep profile of the "effective" moisture of the upper layer of the earth's surface is proposed. Ground experiments were conducted to determine the characteristics of the " diversity " of moisture and soil cover heterogeneities. The special attention was focused to using of ground penetrating radar for investigations of upper ground layer heterogeneities. The ground experiments were dictated by the need to justify the proposed algorithm for deep sounding of agricultural fields in the winter period at a low temperature with the help a synthetic antenna radar.**

Keywords: **synthetic antenna radar, ground penetrating radar, subsurface sensing, deep profile of the "effective" moisture, the "variety" of soil cover.**

UDC 621.371

Bibliography - 32 references *Received 27.08.2018*

RENSIT, 2018, 10(2):193-208 **DOI: 10.17725/rensit.2018.10.193**

Content

1. INTRODUCTION

In a number of countries have developed aircraft synthetic aperture radar (*SAR*) operating in wide range of wavelengths, including decimeter (*P*) and meter (*VHF*) bands [1-5]. Comparison of radar images of the same area in different wavelengths shows the qualitative differences that are connected with the features of the surface reflection and the influence of reflection and absorption of electromagnetic radiation from subsurface layers. Electromagnetic radiation of different wavelengths penetrates into the land cover at different depths, so the question of the development of methods of using radar location images (RLI) obtained in different wavelength ranges for deep layered sensing of earth covers raises. This method of layered subsurface sensing qualitatively different from the classical method based on the sensing of short pulses.

In Russia the complex SAR "IMARC" [1] operating simultaneously in four wavelength ranges *X* (4 cm), *L* (23 cm), *P* (68 cm) and *VHF* (254 cm) at various polarizations *HH*, *VV*, *VH* and *HV* is

developed. This complex gave the possibility to obtain multi-frequency polarization matrix of radar images. Analysis of radar images of the complex allowed us to offer one of the possible methods for constructing depth profiles of the "effective" soil moisture of agricultural lands in winter time in the European part of Russia. Ground-based experiments for mapping of soil moisture at different depths in limited areas and the results of determination of parameters of inhomogeneities in the upper subsurface layers with GPR was dictated by the need to justify the proposed algorithm for joint interpretation of radar images of the same area obtained in different wavelength ranges.

Until recently the real practice of subsurface sensing was related to the time of separation of signals coming from subsurface layers and objects located below the surface. A subsurface remote sensing from the airplane (helicopter) or the surface of layered earth cover by radio impulse [6, 7] is considered to be generally accepted. The effective duration of these impulses is nanoseconds and less at the normal direction of propagation of electromagnetic radiation to the surface.

Reflection occurs at the junction of layers or objects having different dielectric properties. The interpretation is based on the separation of signals over time from the surface of various layers or objects located under the soil layers. The method of probing the Earth's surface using vertical sensing at different frequencies is much less frequently used [8, 16]. Despite the complex subsurface structure of the Earth cover, great success has been achieved in the application of GPR for solving a number of scientific and applied problems [7].

At present, aviation complexes of SAR operating in a wide range of wavelengths, including decimeter (*P*) and meter (*VHF*) ranges [1-5] have been developed in a number of countries. Comparison of radar images (*RI*) of the same terrain in different wave bands shows qualitative differences that are related both to the features of surface reflection and to the effect of reflection and absorption of electromagnetic radiation from subsurface layers. Electromagnetic radiation (EM) of different wavelengths penetrates into cover at different depths, so the question of the development of methods for the use of *RLI* in different wavelength ranges for deep layer-by-layer sensing of earth cover. This method of layer-by-layer subsurface sounding is qualitatively different from the classical method based on sensing the earth's surface with short pulses.

In normal sensing with the help of GPR the analysis uses mirror or quasi-mirror reflection components in combination with the laws of reflection and refraction. Diffuse components are a side effect that makes interpretation difficult. Radar images correspond to the diffuse scattering component, which is related to the roughness, inhomogeneities of the upper layer of the earth's surface. Simulation of the back reflection for different EM wavelengths from the unknown structure of the inhomogeneities of the subsurface layer is impossible in general. In the simplest cases, the role of reflection from the subsurface layers is attempted to be taken into account by their influence on the reflective properties of the surface layer. For example, the physical basis for the study (detection) of groundwater is the change in the back reflection on the roughness of the soil cover caused by additional moistening of the upper layers of the soil due to capillary phenomena - by changing the moisture of the overlying soil layers (capillary rim) and, consequently, reflectivity. Despite the attractiveness of the idea of using multi-frequency SAR for constructing a deep profile of the upper layer of the Earth cover, there is no noticeable breakthrough in this direction. Therefore, consideration of any attempts to jointly use multi-frequency radar images to determine the depth profile of the upper layer of the earth's surface is of great interest.

In this paper, we consider the possibility of constructing a deep profile of a homogeneous part of the earth's surface based on the results obtained with the help of the SAR that was developed by the Concern "Vega" [1]. The complex simultaneously operated in four wavelengths 4 cm, 23 cm, 68 cm and 254 cm in different polarizations *HH, VV, VH* and *HV*. The analysis of the *RLI* of this complex made it possible to propose one of the possible methods for constructing a depth profile of the "effective" (see below) soil moisture of agricultural lands in the winter period in the European part of Russia.

Ground experiments on soil moisture mapping at different depths in some parts of the terrain, as well as to determine the parameters of inhomogeneities in the upper subsurface layers with the help of GPR

were dictated by the necessity to substantiate the proposed algorithm for the joint interpretation of the same radar plot obtained in different wavelength ranges.

When considering the problem, two principal questions arose:

1. How can we perform the modeling of the upper layer of the underlying surface with an unknown structure to build a deep profile?
2. We must develop an algorithm for calculating the depth profile based on the results of radar survey in different wavelength ranges.

2. SUBSTANTIATION OF THE APPROACH FOR DETERMINATION OF THE DEEP SURFACE

The first step in solving the problems of subsurface sensing of soil cover with the help of multi-frequency SAR was the calculation of the estimates of the backscattering signal from different subsurface objects at wavelengths 4, 23, 68 and 254 cm which are used in the SAR complex [1]. The calculations were performed under the assumption that there is no surface roughness and volume scattering but only taking into account the attenuation in the medium. The results of model calculations of scattering from a spherical object, a dielectric disk, a metal plate in a soil are given in [9-13, 15]. In this case, the problem of finding reflection from a dielectric object was solved in a rigorous electro-dynamic formulation. The dependence of the effective scattering area (ESA) on the frequency of the signal, on the size of the object, on the parameters of the soil, on the direction of incidence of the plane wave, and on the polarization was investigated. For calculating the absorption in wet sandy and clayey soils wet sandy the model presented in [9, 14] was used. As a result of calculations in [12, 13] the following conclusions were made.

1. For a dielectric object or a cavity in the ground, when the size of the object is comparable to the wavelength, oscillations of the reflected signal are observed depending on the wavelength in consequence of the resonance effects. For large wavelengths, the signal decreases monotonically with increasing wavelength.
2. For extended objects at high frequencies, oscillations of the reflected signal are observed as a function of the angle of incidence which is due to the rupture of the backscattering diagram.
3. The amplitude of the reflected signal can serve as one of the signs on the basis of which, when using a set of frequencies, it is possible to make assumptions about the nature of the object found in the ground.
4. The dependence of the amplitude of the reflected signal on the wavelength and the angle of incidence, in principle, can be used to estimate the dimensions of subsurface objects. However the absence of a priori information on the depth of the location of the object and the properties of the soil, the strong dependence of the attenuation on the wavelength, are a serious obstacle in the recognition of objects.
5. The recognition problem can be posed for objects located in sandy ground or sandy-clay soil with a low clay content and low moisture.
6. Losses are very large in the clayey soil, so that sensing is possible only to very small depths - less than 0.5 m when long waves are used.

In accordance with conclusions 4-6, you can "outline" the range of tasks that can be addressed:

a) subsurface remote sensing with a relatively simple geological structure and with a special dryness of rocks in the absence of vegetation cover;

b) subsurface remote sensing of frozen soils;

c) solving problems such as mapping the hydrological regime when the groundwater depth is located at a shallow depth (mapping of flood zones).

Similar calculations and estimates of scattering of objects can be found in other works.

In the solution of the reflection problem even in a rigorous electro-dynamic formulation the surface layer above the object is assumed to be homogeneous with known dielectric properties, scattering from the soil layer is not taken into account (only attenuation is taken into account), the reflection from the object and the soil layer are not compared.

In addition, based on calculations for reflection from various objects in homogeneous soils, carried out in these studies, the following conclusions were drawn.

The dependence of the amplitude of the reflected signal on the wavelength, in principle, can be used for the purpose of identifying subsurface objects. The amplitude of the reflected signal can serve as one of the indications on the basis of which, when using a

set of frequencies, it is possible to make assumptions about the nature of objects in the ground.

Apparently, the recognition problem can be posed for objects located in sandy ground or sandy-argillaceous ground with low clay content or low moisture. Losses are very high in clay so that remote sensing is possible only to very shallow depths - less than 0.5 m or in the case of relatively low losses (low temperature, low moisture) up to 1-1.5 m. The losses are especially high at high frequencies. Therefore, the longest waves 254 cm, and in some cases 68 cm can practically be used from the existing set of having wavelengths. The insufficient number of frequencies at which a signal can be received and analyzed is an obstacle in the task of identifying objects.

In addition, in the absence of a priori information on the depth of the location of the object and the strong dependence of the attenuation on the wavelength, the effects associated with the influence of the shape and type of the object on the amplitude of the reflected signal will be greatly distorted by the effect of attenuation in the ground.

Oscillations of the reflected signal are observed depending on the wavelength due to resonance effects when we investigate a dielectric object or cavity in the ground at sufficiently high frequencies and when the size of the object is comparable with the wavelength. For big wavelengths the signal decreases monotonically with increasing wave length.

For extended metal objects at high frequencies oscillations of the reflected signal are observed depending on the angle of incidence. The oscillations are due to the rupture of the scattering diagram. The ruggedness of the scattering diagram can serve to estimate the size of a metal object. However, this requires a larger set of wavelengths with a smaller difference in neighboring wavelengths than in the considered wavelength set. The largest signal in the case of high frequencies is expected within the narrow lobes of the scattering diagram. At low frequencies, the reflected signal is much larger at large angles of incidence far from the normal to the surface of the object. In the case of extended dielectric objects, the discontinuity of the scattering diagram can be less pronounced.

The amplitude of the reflected signal decreases strongly when the sensing direction approaches to the horizon. Therefore it is necessary to choose the sensing angles the closest to the normal.

As a consequence of these conclusions the *X* and *C* bands have limited possibilities for subsurface remote sensing. The key moment for the development of the technique and algorithm for layer-by-layer subsurface remote sensing will be the representation of the volume inverse reflection mechanism.

However the main drawback of the performed computations is that the object is considered to be located in a homogeneous medium whose surface is flat.

The complexity of using multi-frequency polarization images for layered subsurface remote sensing of vegetation and soil cover is that it is necessary to use volumetric scattering information, which is practically nonexistent. Taking into account the fact that the composition, structure, mineralization and moisture of the subsurface layers can be very diverse and affect the reflection in different wavelength ranges is different, a detailed modeling of the backscattering from the subsurface layers and objects is very problematic even in each individual case.

Under studying reflection from the earth's surface with oblique sensing the focus is on reflection from the rough boundary of the surface, assuming that the surface has constant dielectric properties. The backscattering for oblique sensing is determined by the roughness of the section - the ratio of the root-mean-square deviation of the surface height (σ) and the wavelength of the radio emission (λ) σ/λ. In the case of a 4-frequency SAR, the ratios σ/λ_i can have a wide spread: $\sigma/\lambda >> 1$ for the short-wavelength range $\lambda = 4$ cm; $\sigma/\lambda << 1$ for P ($\lambda = 68$ cm) and VHF ($\lambda = 2.54$ m) ranges. The surface can be considered smooth if $\sigma < \lambda/2\cos\Theta$ (Rayleigh criterion). According to the above criterion for a long-wavelength SAR channels a number of surfaces are smooth.

In [20, 21], an approach (the method of small perturbations $\sigma/\lambda << 1$) is considered for solving scattering on slightly rough surfaces. As a result, the following conclusions are drawn:

1) The backscattering for VV and HH polarizations depends on the difference in the dielectric properties of the air and the surface $\sim|\Delta\varepsilon|^2$, and also on the spectral density of the surface roughness under the condition $2\pi/\Lambda = 2(2\pi/\lambda)\sin\Theta$, where λ is the wavelength of the electromagnetic radiation, Δ - the

roughness wavelength, and Θ - the observation angle (Bragg condition).

2)The cross-polarization components of the scattered field are equal to zero.

Radar images of the earth's surface at wavelengths of 4, 123, 68, 254 cm have shown that the cross-polarization components of the scattered field are always observed, even for the VHF range, when many slightly rough surfaces can be considered smooth.

It should be noted that in the presence of vegetation cover the problem of reverse reflection is greatly complicated. Because of the complexity of modeling surface irregularities, especially with vegetation and inhomogeneities in the upper soil layer. The upper layer of the Earth in modeling in a number of cases is represented by a planar layered structure whose layers have different dielectric properties. However, when considering the upper layer of the Earth's surface in the form of homogeneous dielectric layers having smooth boundaries, back reflection (according to the laws of geometric optics) should be absent, which does not correspond to the experiments.

In [22-24], the question of effect of soil moisture on back reflection was investigated (in some experiments, the surface was rolled up to reduce the roughness). It was shown that the inverse reflection at some angle to the surface is directly proportional to moisture (m): $\sigma_{0i} = L_{0i} + L_{1i}m$ and weakly depends on the surface roughness. From the obtained results, one can conclude that the inverse reflection is determined not only by the surface roughness, but also depends on the dielectric spatial inhomogeneity of the surface. In this case, the characteristics of these inhomogeneities depend on the average value of soil moisture. By analogy with the reflection from a rough surface, in order to explain the results obtained in [22, 24], it can be assumed that the inverse reflection depends on the value of the spectral density of the dielectric spatial inhomogeneity of the surface, i.e. from the spectral density of the spatial spectrum of the dielectric inhomogeneities of the surface under the condition $2\pi/\Lambda = 2(2\pi/\lambda)\sin\Theta$ where λ is the wavelength of the electromagnetic radiation, Λ - the wavelength of the spatial dielectric inhomogeneity, and Θ - the observation angle (the Bragg condition). With such an examination, if the spatial physical properties of the surface change, then an inverse reflection of electromagnetic radiation (EMR) should also be observed from an even flat surface.

Thus, the reverse reflection for oblique sensing should depend not only on the spatial spectrum of the surface roughness, but also on fluctuations in the dielectric properties of the surface - the inverse reflection will be proportional to the Bragg spectral component of the fluctuations as the roughness of the dielectric permittivity of the surface.

The heterogeneity of the soil cover is a widely known phenomenon. In soil science there is the concept of "variety" and the individuality of the soil cover [25]. The term "variety" of the soil cover is understood to mean the heterogeneity of the properties of the soil cover along the horizontal plane, and also in depth. A review of the literature on this question can be found in [25]. Despite the extensive research on this issue, it was impossible to use the results obtained by soil scientists to develop a mechanism for the back reflection of EM waves due to the lack of specific values for both the magnitude of the fluctuations and the spatial spectral functions of these inhomogeneities. This explains the need for ground-based research on the physical characteristics of the upper surface layer.

3. EXPERIMENTAL INVESTIGATIONS OF THE SOIL COVER OF THE SOIL COVER

3.1. Prerequisites for conducting experimental studies

It is known that moisture first of all determines the dielectric properties of the soil (sand, loam, clay, etc.) [9, 14]. With the increase in soil moisture, the filling of micro pores with water increases, the uneven filling of micro pores leads to an increase in the spatial inhomogeneity of the dielectric constant. Confirmation of this can be observed by analyzing the results of experimental works [25]: when drilling a borehole over a water lens in the desert, it turned out that with increasing mean moisture content of the soil its fluctuations in depth increase (**Fig. 1**).

The authors do not relate the fluctuations in moisture to the presence of a layered soil structure. Under modeling of back reflection, when the upper layer of the Earth's surface is represented in the form of flat layers, only the spectral density of the "variety" of the permittivity must be taken into account.

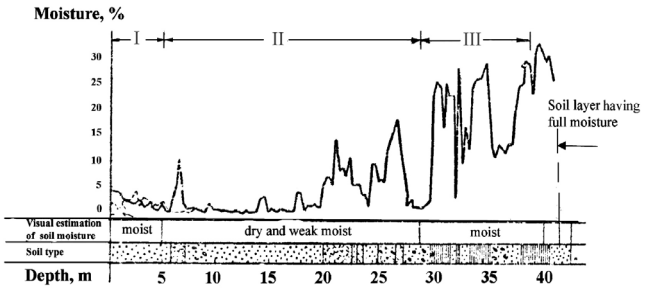

Fig. 1. *Diagrams of moisture in the zone of fixed sand in the Kara-Kum Desert.*

Extensive studies [14] of the influence of sand moisture on the absorbing properties for different wavelengths were made (the moisture value allows us to calculate the attenuation for the layer).

In our work, all the changes in the permittivity in a flat sub-layer are correlated to the "variety" of the moisture content of the sand. This is one of the assumptions of our model for the subsequent construction of a deep profile of the upper soil (changes in soil heterogeneity, roughness, salinity, etc., we correlate to the moisture content of sand). In this case, at first glance, unexpectedly very large and small (unreal) moisture values may appear, which we referred to as "effective" moisture).

This is due to the fact that we do not know anything about the structure of the subsurface layer. This is the main postulate of our work, which can be disputed. As a result, as will be shown below, the resulting deep profile of "effective" moisture requires additional physical interpretation, i.e. it is necessary to relate this or that layer of "effective" moisture to a tangible physical value, for example, snow cover, soil roughness under snow cover, frozen soil, etc. This stage of work is performed from purely a priori information, which must correspond to the physical meaning.

Fig. 2 shows a diagram of the layers of the Earth's surface involved in the formation of the back reflection.

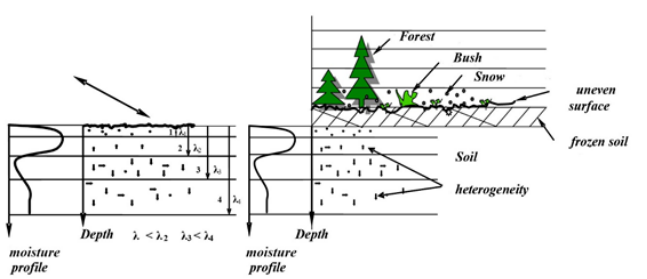

Fig. 2. *Scheme of distribution of soil layers participating in the reverse reflection of the radar signal of different wavelength ranges.*

In the absence of vegetation the RLI in the 4 cm range is formed by the layer 1, which may include roughness, in the 23 cm range - by the soil layer 2, also including the surface roughness, and so on.

3.2. Experiment to measure the "variety" of the moisture content at different depths of the upper soil layer

Experimental research was carried out in the autumn, when the green grass cover was absent. Along three parallel lines, located at a distance of 50 cm from each other and 7 meters long on a flat horizontal surface every 50 cm, boreholes were drilled to a depth of 2 m. From the depths of 30 cm, 83 cm, 136 cm, 189 cm soil samples were taken to further determine the moisture content. Analysis of the samples showed that the upper layer of the soil is clay silt, to the depth of 83 cm - the average loam, at depths of 136 cm and 189 cm - moraine moss, i.e. the soil composition was relatively homogeneous. **Fig. 3** shows the dependence of soil moisture on the distance along one of the straight lines corresponding to different depths. The length of the plot of 7 meters showed variations in soil moisture. Measurements of moisture in soil layers located at different depths from the surface showed that the soil moisture fluctuates for each depth relative to the average value at least 50 cm apart and for different depths and practically independently of each other (correlation coefficient $R << 1.7$). Since in the layers located at different depths, the average humidity turned out to be different, and the soil composition was relatively homogeneous, a comparison of the dispersion value with the average moisture value showed that for a given humidity range and a particular soil section the magnitude of humidity fluctuations increases with increasing soil

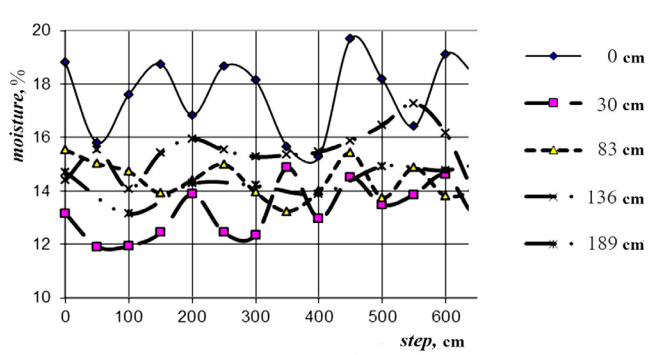

Fig. 3. *An example is the spatial variation of soil moisture at different depths.*

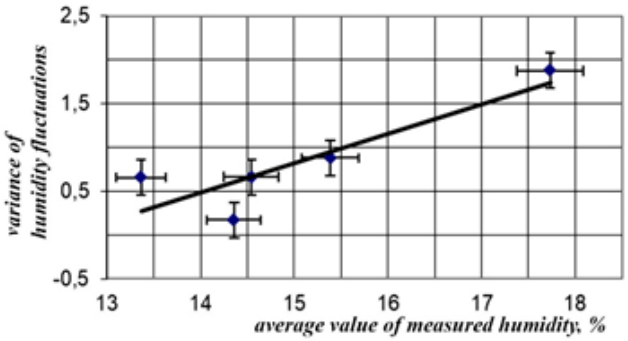

Fig. 4. *Dependence of dispersion of humidity fluctuations on average values of measured soil moisture.*

moisture $\delta m_l = C_1 m_l$ (m_l is the average moisture value in layer l in Fig. 3).

From this experiment the following conclusions were drawn:

1) indeed, at least at a distance of 50 cm both in depth and in space, the humidity changes,

2) the mean square value of humidity fluctuations is directly proportional to the value of humidity (at least for the given experiment at the indicated values of humidity) **Fig. 4**,

3) analysis of the dependence of humidity fluctuations along a straight line at different depths showed that humidity fluctuations at different depths are slightly correlated (mean value of correlation coefficient of moisture fluctuations between layers located at a distance of 30 cm was 0.17).

The second experiment was carried out in the following way: on the area of 1 m^2 every 10 cm from the upper layer soil samples were taken for moisture measurement.

Based on the results of these two experiments, the spatial spectra of humidity fluctuations were calculated, 1/cm. The experimental data are shown in **Fig. 5**.

Characteristic was the fact that the spatial moisture spectra are broad, the spectral densities for wavelengths of 23, 68 and 254 cm are approximately the same, although experiments were conducted at different times in different suburban areas.

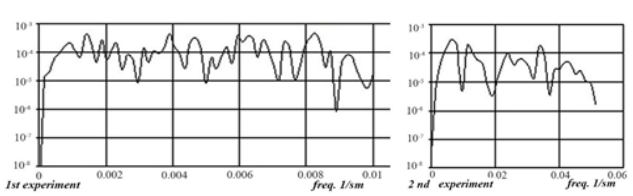

Fig. 5. *Spatial moisture spectrum.*

3.3. "Variety" of the subsurface layer of the earth's surface

The heterogeneity of the soil cover is determined not only by moisture, but also by soil type, salinity, roughness, the presence of the root system of plants, etc. However, drilling studies do not allow the study of such inhomogeneities.

It is known that to study layered soil systems, the detection of objects in the upper soil layers, etc. GPR are used. At the same time, there are doubts whether it is possible to use GPR to study the inhomogeneities of the medium. The attempt was made to use two types of GERAD-type GPR systems [26, 27] to assess the nature of heterogeneities in the permittivity of the upper soil layer in two sections of an even surface which had different values of the backscattering in the VHF band. The experiment was carried out in the following conditions: in a free section at a distance of 20 meters from each other, boreholes were drilled to a depth of 2.5-3.0 m and a deep moisture profile was measured (**Fig.** 6).

In both regions the soil is sandy and to a depth of about 2.5 meters sand moisture ~7÷10% (the real part of the complex dielectric permittivity $\varepsilon \approx 8$), the thickness of the capillary rim is about 1 meter.

To isolate the reflected signals, determine their time shifts, etc. A wide arsenal of established methods is used [27, 28]. In this paper we used methods for processing the results of georadar surveys [27]. The optimal sequence of processing steps of GPR survey of the upper layer of the soil in the forest was worked out according to the results of measuring the reflection from a metal object buried in the earth to a depth of 70 cm from the surface.

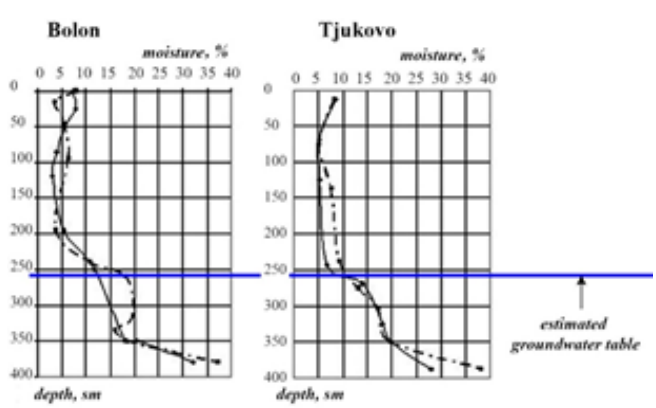

Fig. 6. *Depth moisture profiles in two study areas.*

The main processing steps and their influence are shown in **Fig. 7**.

The image in Fig.7, No. 1 corresponds to the original image, the first stage of processing corresponds to the Hilbert transform - obtaining an image in a unipolar form and emphasizing the transition from white to black. The type of the georadar image after such processing is shown in the figure (Fig. 7, No. 2). The next stage is connected with finding the impulse response of the medium. It is known [6] that the signal reflected $u(t)$ from the surface can be represented as convolution of a radiated signal $s(t)$ with an impulse response of the medium $g(t)$: $u(t) = s(t)*g(t)$. Since convolution in the time domain corresponds to the product of the spectra of the corresponding functions in the spectral region [28], then: to obtain the impulse response, we need to perform the operation:

$$G(f) = U(f)/S(f) \quad (1)$$

and calculate the inverse Fourier transform of $G(f)$. Here $U(f) = ft(u(t))$, $S(f) = ft(s(t))$, $G(f) = ft(g(t))$, where ft is the Fourier transform. The problem is that the modulus of the spectrum of the original signal vanishes in some regions of the selected frequency range, as a result, the uncertainty of the type of division by zero can arise in the calculation using formula (1). To solve this problem, the authors of [28] proposed the following solution: when calculating equation (1) in the denominator, one introduces a deliberately positive additive much smaller than the maximum amplitude: $S(f)$: $G(f) = U(f)/S(f) + 0.01\max S(f)$. In this case, the impulse response of the medium will be: $g(t) = ifft(U(f)/S(f) + 0.01\max S(f))$, here $ifft$ is the fast inverse Fourier transform. This algorithm is implemented in the inverse filtering procedure in this paper. After this processing step, the GPR image of the metal object looks as shown in Fig. 7 (No. 3).

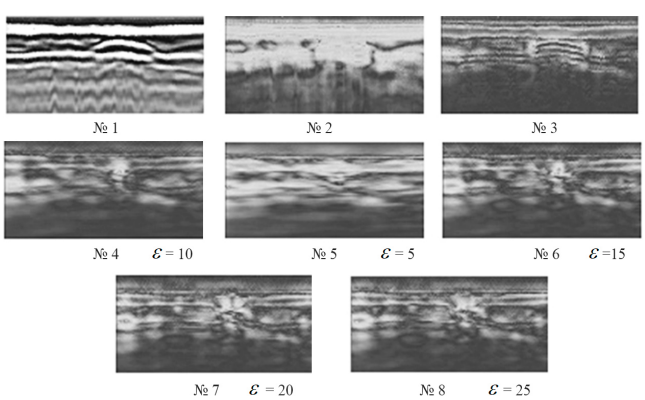

Fig. 7. *Elaboration of a technique for processing GPR survey on a metal object located in the upper layer of sand for different values of the permittivity.*

It should be emphasized that all restrictions related to spectral processing (distortion of the pulse due to dispersion and the frequency dependence of the absorption) are no less, and may even be more relevant to inverse filtering. That is, reliable results using inverse filtering can be expected in non-absorbing media, or in weakly absorbing media at relatively shallow depths. Note: in [29], inverse filtering is seriously criticized. However, this method turned out to be one of the main stages of processing in this paper.

The final stage of processing corresponded to the performance of synthesizing the aperture in the direction of movement of the antenna block for various values of the dielectric constant. The synthesis of the image can be carried out at different values of the permittivity, which characterizes the propagation velocity of EM waves in the medium. Fig. 7 (№ 4÷8) presents processed GPR images with different values ε. The analysis of the obtained images showed that the optimum image is obtained at ε = 10. As one was noted earlier, when drilling wells and measuring moisture profiles, the real part of the dielectric constant of the upper soil layer turned out to be equal ε ≈ 8. Values ε obtained in different ways are consistent. Later, when processing the measurements, we used ε = 10.

The GPR survey was carried out along the line between the drilling points and along lines parallel to it at distances of 0.5 and 1 meter. To account for the fluctuations in motion, a pair of GPR surveys were conducted along each line. To compare the results of different "passes" (as far as the images of the two passes differ, coincide with each other), a physico-mathematical value was introduced [30] - the average value of the coefficient of autocorrelations between different layers. Its meaning is presented below. In **Fig. 8** the results of GPR survey are shown in two sections of the surface located one from another at a distance of about 5 km. The drilling points *A, B, C, D* and the effect of drilling on the nearby soil are shown in the Fig. 8.

On GPR images, the upper soil layer (up to 2.5 m) was split into a number of sublevels (the quantization step ~ corresponded to the range resolution element). For each sublevel of the received GPR images, the

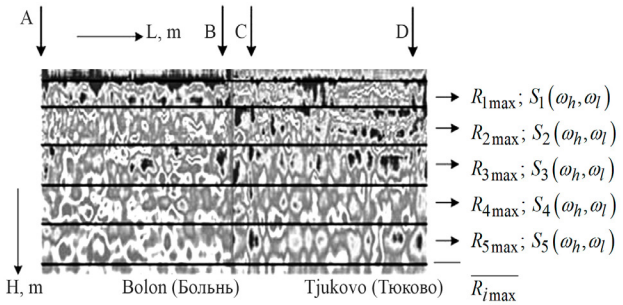

Fig. 8. *Results of GPR survey in two parts of the surface between the drilling points.*

mutual autocorrelation function and its maximum value R_{1m} were calculated. The average value of the maximum values of the correlation coefficients $\overline{R}_{1\max}$ was used as a quantitative measure of the coincidence of the survey results. The processing of GPR results by this method for the same site allowed us to estimate by the values $\overline{R}_{1\max}$ the repeatability of the results of each "pass", and also at what offset aside from the central line of the "passage" the correlation disappears. As an example, **Table 1** gives the values of the maximum correlation coefficients for two passes along a single line

The results of the processing of graphic files showed that the correlation analysis is very sensitive to the accuracy of "setting" the initial parameters - it is necessary to set very carefully the beginning of scanning horizontally and vertically. In addition, there is a strong dependence on the contrast of images. Hence it follows that during processing it would be desirable to introduce one more step - preliminary filtration of secondary images, especially in terms of increasing contrast and reducing noise.

The secondary images obtained after the treatment considered above also made it possible to calculate the spatial spectrum of inhomogeneities at different depths. In **Fig. 9** shows the spatial spectrum of inhomogeneities at different depths of two surface sections.

Table 1.

Correlation values for repeated passes.

Plot of land	Correlation coefficient
R1	0.4061
R2	0.5839
R3	0.3058
R4	0.5183
R5	0.5111
$R_{сред.}$	0.4650

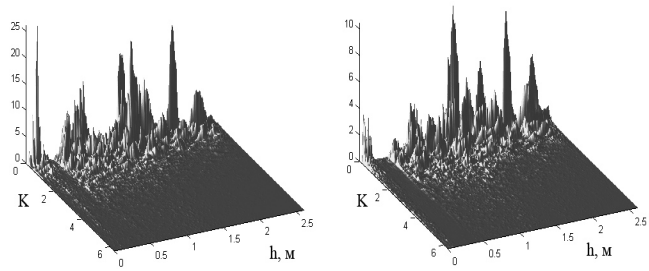

Fig. 9. *Spectrum of spatial fluctuations of inhomogeneities for two sections.*

In Fig. 9 the x axis represents the spatial wave number K, the y axis the depth, and z the intensity of the spectrum in relative units. It can be seen that the spatial fluctuations of the inhomogeneities, measured with the help of GPR, are concentrated at depths of up to one meter (up to the penetration depths of the EMR) and have a very rugged appearance. In addition, spatial spectra along parallel lines spaced 0.5 m apart are independent (the mutual correlation coefficient was about 0.1). When averaging over three lines parallel to spaced apart distances of 0.5 and 1 meter, the spatial spectra are smoothed out.

4. CONSTRUCTION OF THE DEPTH PROFILE OF "EFFECTIVE" HUMIDITY BY RESULTS OF MULTIFREQUENCY RADAR LOCATION

The task of remote sensing of terrestrial coverings by means of radio signals in different wavelength ranges is related to the determination of the distribution profile of the complex permittivity of the investigated surface $\varepsilon(z)$, where z is the coordinate associated with the depth.

Interpretation of radar images of terrestrial coverings at different frequencies represents an incorrect inverse problem [8, 19, 31]. An approximate solution of the inverse problem in the general case is found by constructing a smoothing functional representing the discrepancy functional between the results of measurements of the scattered field and the model direct problem [31]. This task in the general case consists in the determination of the required parameters by the informative characteristic $P(\varepsilon)$ obtained from the reflected signal. One of the most universal informative parameters of the investigated object is the frequency dependence of the complex reflection coefficient. As indicated in [30], a popular approach to solving similar problems is the method of parametric optimization, which

consists in constructing a mathematical model of the investigated medium and minimizing the functional (objective function) $\rho(\varepsilon)$ characterizing the distance between the informative parameter measured experimentally $P_e(f,\varepsilon)$ and theoretically calculated $P_t(f, \varepsilon)$. The objective function is defined as follows

$$\rho(\varepsilon) = \sum_{i=1}^{L} \left| \frac{P_e(f_i,\varepsilon) - P_t(f_i,\varepsilon)}{P_t(f_i,\varepsilon)} \right|^2, \quad (2)$$

where $f_i (i = 1, 2, ..., L)$ is the set of frequencies at which the informative parameters are measured and calculated.

According to [31], the inverse problem has a unique and stable solution only if the initial experimental and calculated theoretical data are determined on an infinite frequency interval, which in practice is unattainable. An experimentally informative parameter is measured with some error. These circumstances cause incorrectness of the inverse problem being solved, which is expressed in the existence of a large number of side minima of the functional (2). In addition, in order to calculate the model information sign $P_t(f, \varepsilon)$, a direct electrodynamic problem must be solved, which is also a problem. To improve the solution of such an ill-posed problem, various algorithms are used: the neural method [32], the use of additional a priori information in constructing a smoothing functional [8].

In the case of using the SAR IMARK complex for the purpose of subsurface sounding, the problem is complicated by the fact that only 4 wavelengths are used, as well as the impossibility of creating even an approximate model of the inverse reflection of the subsurface volume. Under such conditions, the main attention should be paid to a priori information. In general, the search for solutions will be limited to curves (the moisture profile in depth), which can be approximated by polynomials of the third degree.

To develop an algorithm for layer-by-layer sounding of terrestrial surfaces, a direct electrodynamic problem must be solved. To implement the method of constructing a depth profile, as a first assumption, the surface is represented in the form of flat thin parallel sub-layers, regardless of the type (plant, snow cover, frozen soil, etc.). Each sub-layer is characterized by a coefficient of attenuation and reflection. Let's imagine that there is a surface area with a homogeneous reflectivity σ_{0i} (the effective scattering area for four wavelengths λ_i is different). In this case σ_{0i} - the effective coefficient of back reflection of a thin layer at the depth of occurrence h when sounding at an angle θ. Then the EPR σ_{0i} value is represented as:

$$\sigma_{0i}(\theta) = A\int_0^\infty \sigma_i(h) e^{-2\int_0^{\cos\theta_i} \alpha_i(x)dx} dh, \quad (3)$$

where $\alpha_i(h)$ is the dependence of the attenuation coefficient of electromagnetic waves for the wavelength λ_i on the depth, θ is the angle of propagation of electromagnetic waves (at this stage it is assumed that it is constant in the medium). It is seen that it is necessary to simulate two dependencies $\alpha_i(h)$ and $\sigma_i(h)$. The back reflection of a thin layer from the depth of occurrence h and its possible connection with the attention coefficient $\alpha_i(h)$ are unknown. The reverse reflection in the case of a planar sub-layer will be observed only in the presence of spatial dielectric inhomogeneities in the su-layer itself within the radar resolution element. Thus, it is necessary to relate the attenuation coefficient to the reflection coefficient. Initially, we will perform this procedure for a moist, homogenous soil, having a dependence $\alpha_i(h)$ - the attenuation coefficient on depth with the dependence $\sigma_i(h)$ - the reflection coefficient for different wavelengths.

Numerous experimental data have shown that the inverse reflection at some angle to the surface is directly proportional to moisture: and depends little on the surface roughness (see **Fig. 10**).

The increase in humidity leads both to an increase in the attenuation coefficient, and to an increase in the reverse reflection. For a homogeneous layer of soil with a constant moisture content in depth, following expression (3), the reflection coefficient must have the form. Suppose that there is a relationship between the attenuation and reflection coefficients of a thin layer of the type.

$$\sigma_i(h) = \beta_{0i}\alpha_i(h) + \beta_{1i}\alpha_i^2(h). \quad (4)$$

Since $\alpha \sim m$ then following Eq. (3), the EPR will indeed have the form $\sigma_{0i} = A_{0i} + A_{1i}m$. Thus, in order to explain the inverse reflection from a smooth surface and its subsurface layers, it is natural to assume that in each sub-layer there

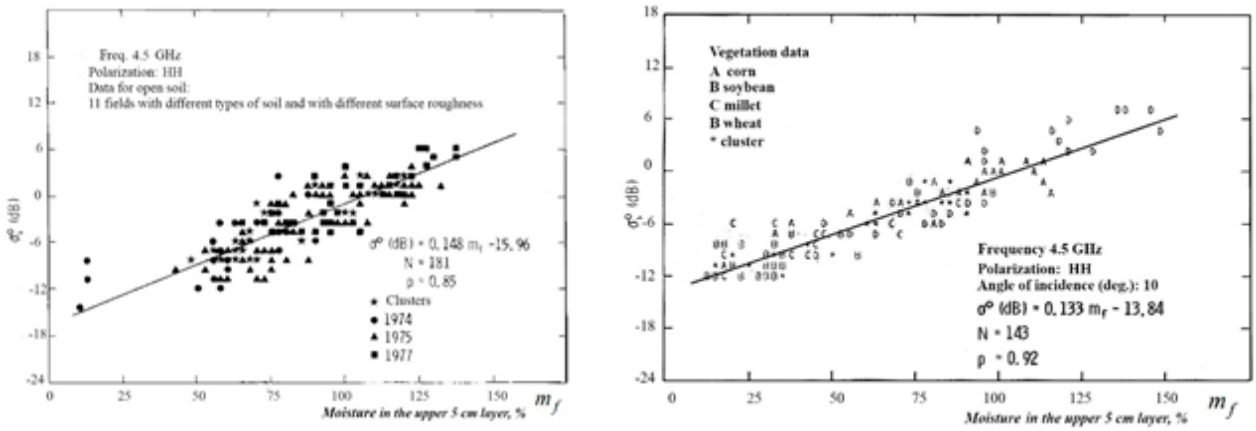

Fig. 10. *The coefficient of reverse reflection of the open soil as a function of humidity (field humidity) for various conditions of surface roughness and various textural soil compositions* [22-24].

are spatial dielectric inhomogeneities within the resolution element. An increase in humidity leads to an increase in the attenuation coefficient $\alpha \sim m$ and simultaneously to a stronger spatial dielectric heterogeneity of the soil, which enhances the inverse reflection.

In formula (1) it is assumed that the reflection coefficients from adjacent layers are independent, i.e. fluctuations in humidity are independent. Calculations of the correlation coefficient between the dependence of humidity on the distance for different layers in our experiment showed that the average value of the moisture coefficient between the layers 0-30 cm, 30-83 cm, 83-136 cm, 136-189 cm is 0.17-0.15. Prior to this stage, we only operated on inhomogeneities related to humidity. We extend this representation, generalizing it to all inhomogeneities in general, i.e. we introduce the concept of "effective" humidity. For definiteness, i.e. the construction of a theoretical model, as the investigated soil, we will consider sand with some "effective" moisture.

Thus, the construction of a theoretical model of back reflection will be based on the profiles of "effective" humidity:

1) We represent the soil (of various types, roughness, frozen soil, etc.) in the form of sand, which has some "effective" moisture.

2) We are given an arbitrary depth profile of the "effective" humidity in Fig. 10*a*.

3) Based on the results of [14, 15], we determine the dependence of the absorption coefficient of the sub-layers for four wavelength ranges $X = 4$ cm, $L =$ 23 cm, $P = 68$ cm and $VHF = 254$ cm;

4) According to the expressions (3)-(4), we calculate the EPR values for 4 wavelengths;

5) From the ESR values measured as a result of radar survey at the same frequencies with the help of the SAR IMARK complex, we find the integral value of the discrepancy between theoretical (p.4) values and experimental data.

The procedures for clauses 2-5 are repeated until the discrepancies are minimal in Fig. 10*b*.

5. EXPERIMENTAL RESULTS

Multi-frequency radar survey was carried out in the winter, which was characterized by heavy snowfalls and strong (up to -30 degrees) frosts. As a priori information was taken - the depth of the snow cover on the fields of 50 cm, the depth of freezing is of the order of 50 cm. **Fig. 11** represents the frequency-polarimetric matrix of the radar images of the site (size of a section of 3x3 km^2) of the selected landfill.

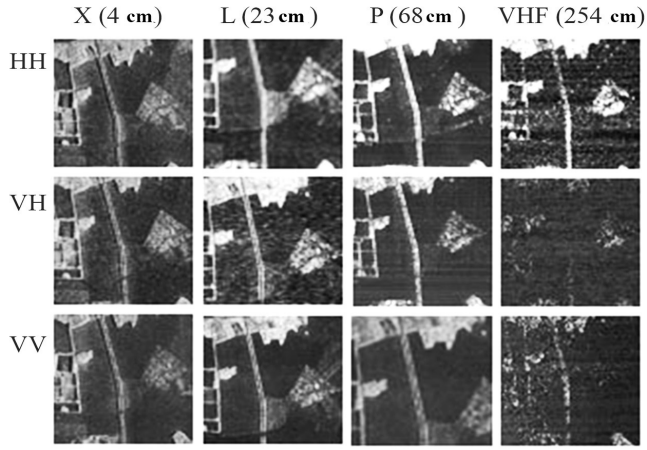

Fig. 11. *Multi-frequency Polarimetric Radar Matrix test polygon.*

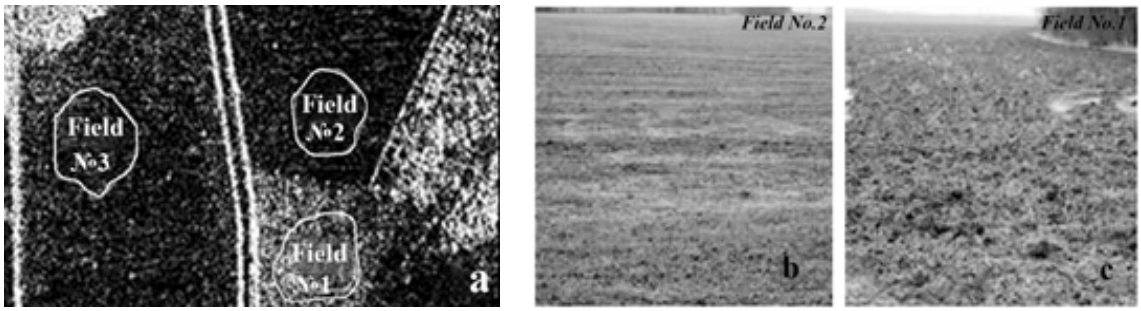

Fig. 12. *Areas of the Earth's surface used to interpret the results of RL survey.*

Fig. 12 indicates the agricultural fields No. 1, 2, 3, whose RLIs were used to interpret subsurface sensing. Inspection of the fields after the fall of the snow showed: field number No. 2 (Fig. 12*b*) is a flat area with a shallow roughness and winter wheat shoots; field No.1 (Fig. 12*c*) is a plowed field with a roughness of about 20-30 cm; field No. 3 is an flat area of terrain with low stubble, in the radar images of which a qualitative difference is observed in the meter range on *VV* and *HH* polarizations.

The average intensity and dispersion of the RL signal for field No. 2 are minimal over the entire wavelength range and on all polarizations, so it is chosen as a "support" for relative calibration. Preliminarily, the RLIs of each field was subjected to spatial averaging (spatial filtering) of 2000 pixels to reduce the influence of the spectroscopic structure. After that, three or four identical sections were selected on each field, and there was an average and standard deviation. The values thus obtained were used to plot the contrasts of the wavelengths (**Fig. 13**). Under performing the work, the radar images in the *X, L* and *P* bands were calibrated with corner reflectors, in *VHF*, using reflection from the transmission line supports [18]. Reflection from angle reflectors and power line supports were used to obtain relative contrast values.

From Fig. 13 that the contrasts for different fields and polarizations are different. Therefore, it can be assumed that the effective moisture profile on different polarizations will be different.

5.1. Building an effective moisture profile from depth

The success of constructing a profile of "effective" humidity depends on the use of available a priori information about the underlying surface [8]. As a priori information was taken:

- The thickness of the snow cover on the selected fields is the same and is ~40-60 cm.
- Between the snow and the soil there is a rough surface layer, which is due to the processing of the land and the presence of vegetation.
- The thickness of the frozen soil in all fields is the same and is ~80 cm.

Fields No. 1 and No. 2 are located in close proximity to each other and therefore it can be assumed that the structure and moisture of the soil at a depth of more than 1.4 m are the same. The moisture content of the soil (sandy soil), measured at a depth of ~1.5 m in the vicinity of this field, was ~40%.

In **Fig. 14***a* two proposed moisture profiles on *HH* polarization are presented as an example, in Fig. 14*b* a profile in which the theoretical and experimental contrasts coincide.

The results show that the effective moisture profile depends on the polarization, i.e. different soil layers contribute to the formation of the reverse reflection.

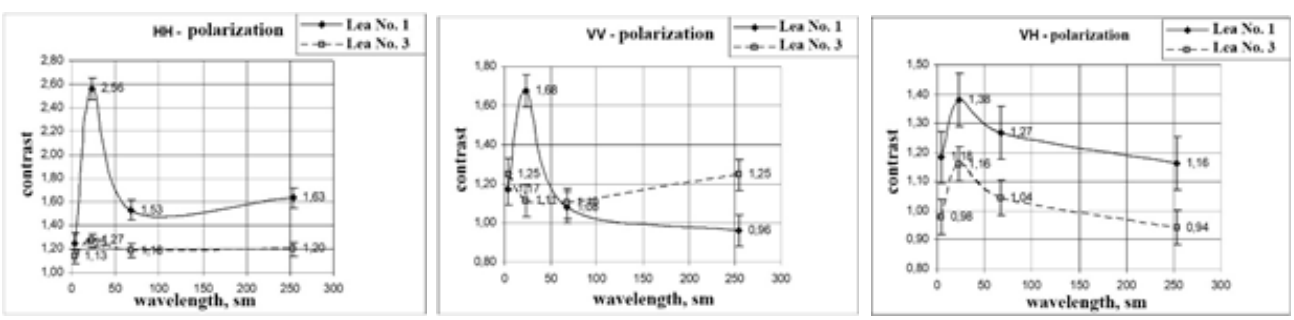

Fig. 13. *Relative contrast values for Fields 1 and 3 on different polarizations.*

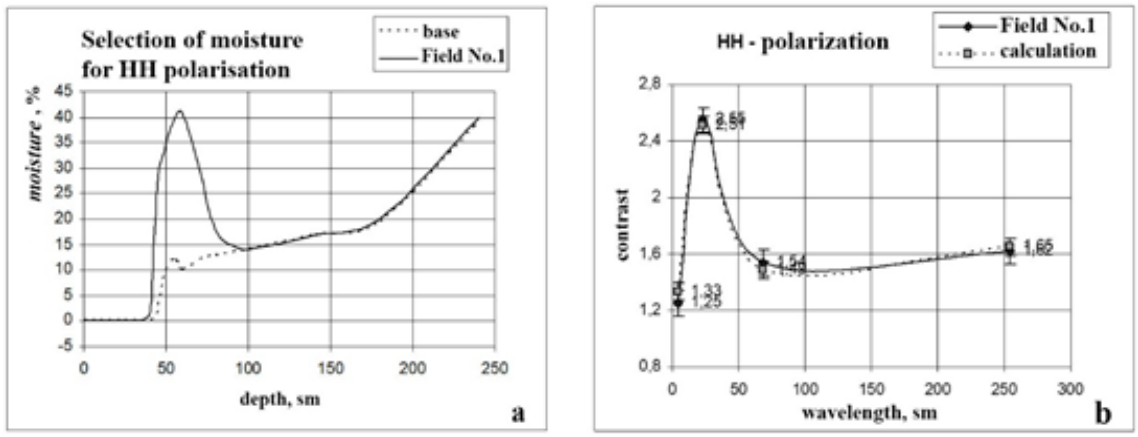

Fig. 14. *Profiles of "effective" humidity on the reference field and field No. 1.*

The complexity of the simulation was that there is no information about attenuation in different wavelength ranges, data on the presence of spatial inhomogeneities in snow and in frozen soil on an element of ~15x15 m^2. When interpreting it was assumed that the state of the surface (snow, roughness, frozen soil, distribution of humidity along the depth, etc.) corresponds to some effective value of moisture in accordance with the proposed procedure (see paragraphs 4, 5), the moisture profile was selected, so that the theoretical and experimental contrasts coincide.

5.2. Analysis of the obtained interpretation results

When examining *RL* images, fields No. 1, No. 2, No. 3 were selected (Fig. 12). The analysis shows that for radar fields No. 1 and No. 2 in the *X, P* and *VHF* ranges there is no contrast, in the *L* range the contrast is significant. The conclusion is that, in the λ = 4 cm range, the RLIs are formed by the snow cover, the damping in the snow cover is such that the rough layer of the soil does not affect the reflection in the *X* range. In the *L* range, the attenuation in the snow is weakened and the snow-frozen ground affects the character of the image. The heterogeneity of the snow-frozen soil layer for the *P* and *VHF* ranges is small and this layer is flat for these ranges. Reflections in the *P* and *VHF* bands define deeper layers. The results of the treatment confirm this. At depths of 40-60 cm, a dramatic increase in the effective moisture content is observed, which is determined by the roughness. For *VH* polarization, this layer turned out to be somewhat deeper. The deep layers affect all polarizations in the same way.

The peculiarity of the obtained results on the determination of the effective moisture profile in field No. 3 is that the transition layer snow-frozen ground has little effect on the inverse reflection in the wavelength bands *L, P* and *VHF*. Since the upper soil layer is a stubble, the effect is explainable. For the reverse reflection, the depths are influenced by the depths h > 150 cm. For *VV* polarization, the effective humidity is greater than the *HH* polarization, which is manifested in the *RLI* images (see the element *VHF-VV* and *VHF-HH* of the matrix in Fig. 2). A comparison of the photographs

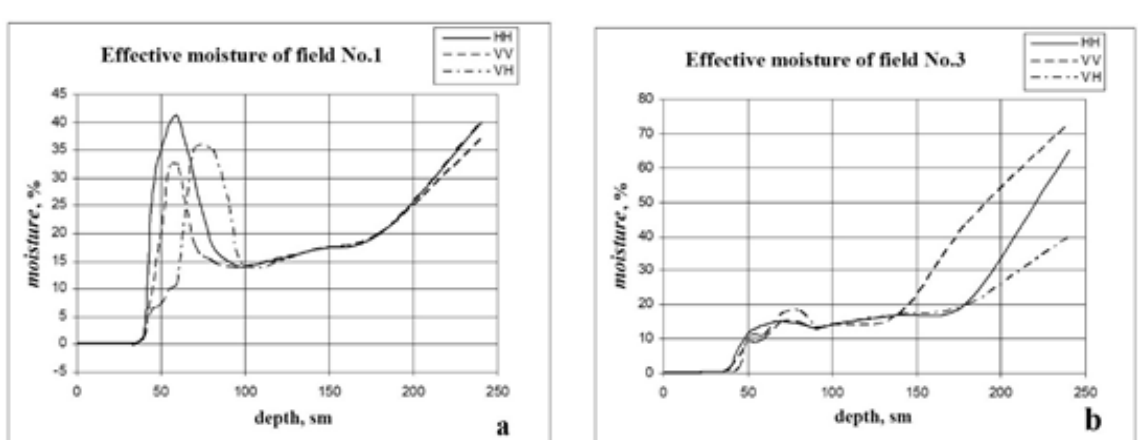

Рис. 15. *Profiles of "effective" humidity in field No. 1a and field No. 3b calculated on radar sounding on different polarizations.*

of this area for 2003 and 1987 shows that the area of field No. 3 increases due to the destruction of the forest massif, and the feature in the image is probably explained by the presence of vertical roots under the upper soil layer. Thus, it can be concluded that the proposed method allows analyzing the nature of subsurface soil layers in the winter period of time.

6. CONCLUSION

The use of multi-frequency side-view radar with a synthetic aperture for layered subsurface sounding of the earth's surface is of great interest. However, the reconstruction of the deep profile of the upper layer of the Earth's surface by multi-frequency (with a limited number of wavelength ranges) radar images represents an incorrect inverse problem. An approximate solution of the inverse problem in the general case is found by constructing a smoothing functional representing the discrepancy functional between the results of measurements of the scattered field and the model direct problem. For the calculation of a model informative characteristic, a solution of the direct electro-dynamic problem is necessary. However, the physicochemical structure of the upper cover of the earth is so complex that it does not allow to adequately simulate the reverse reflection from subsurface soil layers for different wave bands. The representation of the top cover of the soil in the form of a series of uniform layers with even or rough surfaces is possible only in individual cases. The spatial spectra of the "variegation" of the soil cover both in space and in depth are broad and related both to moisture fluctuations and soil composition. It makes sense to talk only about the averaged layer structure of the soil in a limited area, i.e. to represent the upper layer of soil in a limited area in the form of flat even sub-layers, the reflection of which is due to the "variegated" physicochemical characteristics of this layer and is determined by the Bragg component of the spectrum of "variegation" of this sub-layer.

In order to somehow approach the solution of the problem of layer-by-layer surface sounding of the upper surface cover, unusual postulates have been made in the work, within the framework of which this problem is solved. The upper layer of the soil is supposed to consist of sand, the sub-layers of which have flat surfaces, and all changes in the dielectric constant are related to the "variegation" of the moisture content of the sand, i.e. changes in the type of soil heterogeneity, roughness, salinity, etc., we correlate to the "effective" moisture of sand, which is the main postulate of this work. Given different profiles of "effective" humidity, it is possible to solve a direct problem and construct a smoothing functional that represents the residual functional between the results of measurements of the scattered field and the model direct problem. However, the resulting deep profile of "effective" moisture requires additional physical interpretation, i.e. it is necessary to relate this or that layer of "effective" moisture to a tangible physical value, for example, snow cover, soil roughness under snow cover, frozen soil, etc. This stage of work is performed from purely a priori information, which must correspond to the physical meaning.

The work was carried out with the financial support of the ISTC, project No. 2806.

REFERENCES

1. "IMARK – Multi-Frequency Airborne Polarimetric Radar System Operating on Board of TU-134A Flying Laboratory for Remote Observations of the Earth's Surface". Moscow Scientific Research Institute for Instrument Engineering, MNIIP/VEGA-M Corporation, Russia, 1998, 8 pp.
2. Freeman A, Durden SL, Zimmerman R. Mapping Subtropical Vegetation using Multi-frequency, Multipolarization SAR Data. *Proc.Int. Geoscience and Remote Sensing Symp.* 1992:1686-1689.
3. Kutuza B, Shutko A, Plushev V, Ramsey E, Logan B, DeLoach S, Haldin A, Novichikhin E, Sidorov L, Manakov V, Nelson G. Advantages of synchronous multi-spectral SAR and Microwave Radiometric observations of land covers from aircraft platforms. *Proc. EUSAR 2000, 3-rd European Conference on SAR* (23-25 May 2000), Munich, Germany, 2000:663-666.
4. Ulander L, Pierson W, Lundberg M, Follo P, Frolind P, Gustavsson A. CARABAS-II SAR change detection performance on ground targets concealed in foliage. *Proc. of EUSAR 2004, 5th European Conference on Synthetic Aperture Radar*, Ulm, GE, 2004:297-300.
5. Gustavsson A, Ulander L. Combining various ISR assets to create a common and complete ground picture. *Proc. of EUSAR 2004, 5th*

European Conference on Synthetic Aperture Radar, Ulm, GE, 2004:301-304.

6. Finkelstein M, Karpukhin V, Kutev V, Metelkin V. *Podpoverkhnostnaya radiolokatsiya* [Subsurface Radiolocation]. Moscow, Radio i svyaz' Publ, 1999, 266 p.
7. Grinev AYu. *Voprosy podpoverkhnostnoy radiolokatsi.* Moscow, Radiotekhnika Publ, 2006, 416 p.
8. Mirtova E. Resheniye obratnykh zadach podpoverkhnostnoy radiolokatsii optimizatsionnymi metodami [Solution of inverse problems of subsurface radar by optimization methods]. *Thesis for the degree of PhD*, Riga, 1988, 193 p.
9. Druchinin SV. Models for calculation of dielectric constant of moist sandy-clayey soils in wavelengths from centimeters to tens of meters. *Proc. GPR 2000, 8-th Intern. Conference on Ground Penetr. Radar*, Gold Coast, Australia, 2000, 26-31.
10. Druchinin SV. Models for calculation of dielectric permittivity of moist sandy-clayey soils in wide range of frequencies. *Proc. SSTA 2000, Intern. Conf. on Subsurface Sensing Technologies and Applications*, San Diego, (30 July-4 Aug.), California, USA, 2000.
11. Druchinin S, Izyumov S. Measured and calculated dielectric permittivity of moist clayey soils. *Proc. 6-th Meeting of Environmental and Engineering Geophysics,* Bochum, (Sept. 3-7), Germany, 2000:P-GR09.
12. Kutuza B, Kalinkevich A, Pliushchev V, Druchinin S. Multi-frequency SAR for Object Detection in Upper Subsurface Layers of the Earth. In: *Complementary of Ladar and Radar, RTO-MP-092,* RTO/NATO, France, 2003.
13. Kalinkevich A, Kutuza B, Pliushchev V. Druchinin S. *Zarubezhnaya radioelektronika, Uspekhi sovremennoy radioelektroniki*, 2001, 31-39.
14. Leschanskiy J. Lebedeva G. Shumilin V. Elektricheskiye parametry peschanogo i glinistogo gruntov v diapazone santimetrovykh, detsimetrovykh i metrovykh voln. *Izv. VUZov. Radiofizika*, 1971, 4(14):563-569.
15. Druchinin S. Models for calculation of dielectric constant of moist sandy-clayey soils in wavelengths from centimeters to tens of meters. *Proc. 8th Intern. Conf. on Ground Penetrating Radar*, (27 April 2000), doi: 10.1117/12.383576.
16. Mirtova EV, Karpukhin VI. Issledovaniye primeneniya optimal'nykh metodov k resheniyu obratnykh zadach zondirovaniya ledovykh pokrovov. *Teoriya i tekhnika radiolokatsii, navigatsii i radiosvyazi v GA*, Riga, 1986:38-44.
17. Druchinin S, Izyumov S. Measured and calculated dielectric permittivity of moist clayey soils. *Proc. 6-th Meeting of Environmental and Engineering Geophysics,* Bochum, (Sept. 3-7), Germany, 2000:P-GR09.
18. Kalinkevich AA, Krilova MS, Manakov VYu. K voprosu ob ispol'zovanii opor LEP v kachestve repernykh ob'yektov pri interpretatsii RLI RSA UKV diapazona. *Trudy 4 Vseross. nauchn. konf. "Radiofizicheskiye metody distantsionnogo zondirovanii sred"*, Murom, 30.06.-3.07.2009, 186-190.
19. Grinev AYu, *Chislennyye metody resheniya prikladnykh zadach elektrodinamiki* [Numerical methods for solving applied problems of electrodynamics], Moscow, Radiotekhnika Publ, 2012, 336 p.
20. Yakovlev O, Yakubov V, Uryadov V. Pavel'yev A. *Rasprostraneniye radiovoln* [Propagation of radio waves]. Moscow, Lenand Publ., 2009, 496 p.
21. Bass F, Fuks I. *Rasseyaniye voln na statisticheski nerovnoy poverkhnosti* [Scattering of waves on a statistically irregular surface], Moscow, Nauka Publ, 1972, 424 p.
22. Ulaby FT, Moore RK, Fung AK. *Microwave remote sensing.* London, Addison-Wes1ey Public. Comp., 1981.
23. Ulaby FT, Batlivala PP. Optimum Radar Parameters for Mapping Soil Moisture. *IEEE Transaction and Geoscience Electronics,* 1976, 2(GE-14):81-93.
24. Ulaby FT, Cihlar J. Moore RK. Active Microwave Measurement of Soil Water content. *Remote Sensing of Environment*, 1974, 3:185-203.
25. Chubarov V. *Pitaniye gruntovykh vod peschanoy pustyni cherez zonu aeratsii* [Groundwater supply of sandy desert through aeration zone]. Moscow, Nedra Publ., 1972, 135 p.
26. Marchuk V, Smirnov V. *Trudy Vseross. nauchn. konf. "Sverkhshirokopolosnyye signaly v radiolokatsii, svyazi i akustike"*, Murom, 2003:455-459.
27. Marchuk V. Metodiki provedeniya eksperimentov po radiolokatsionnomu podpoverkhnostnomu zondirovaniyu Zemli i planet zemnoy gruppy [Methods of conducting experiments on radar subsurface probing of the Earth and the

terrestrial planets]. *Thesis for the degree of PhD.* Fryazino, 2008, 163 p.

28. Marple SL. *Digital Spectral Analysis with Applications*. Prentice-Hall, Englewood Cliffs, NJ, 1987.
29. Armand N, Lukin D, Chubinskiy N. Nauchnyy sovet Rossiyskoy Akademii nauk po kompleksnoy probleme "Rasprostraneniye radiovoln", Muromskiy institut Vlad.GU.
30. Kalinkevich A, Krylova M, Masyuk V, Marchuk V. Using georadars to study heterogeneities of the top layer of coniferous forest soil. *Radiotekhnika,* 2009, 3:98-103.
31. Tikhonov A, Arsenin V. *Metody resheniya nekorrektnykh zadach* [Methods for solving ill-posed problems]. Moscow, Nauka Publ., 1979, 285 p.
32. Khilkevich V. Opredelenie parametrov zemnykh pokrovov s pomoshchyu neyronnogo metoda. *Trudy Vseros nauchn. konf. "Distantsionnoye zondirovaniye zemnykh pokrovov i atmosfery aerokosmicheskimi sredstvami"*, (June 20-22) Murom, 2001:147-151.

ULTRA WIDEBAND SOUNDING SIGNALS IN HYDROACOUSTIC SYSTEMS

Anatoly V. Sknarya, Anatoly A. Razin, Sergey A. Toshchov, Aleksey I. Demidov
V.V. Tikhomirov Scientific Research Institute of Instrument Design, https://niip.ru
Zhukovsky 140180, Moscow Region, Russian Federation
sknarya.a@otd301.niip.ru, razin.a@nio3.niip.ru, toshovserdey@mail.ru, aleksii-ad@yandex.ru

Abstract. **Results of comparison of full-scale tests of active sonar systems - sonars with narrowband and ultra wideband (UWB) sounding signals with linear frequency modulation of pulses are presented. It is shown that the use of UWB signals with a large base allows to resolve multiple echo-signals from the target in the time domain, and a wide operating frequency band allows for an efficient spectral analysis of the received signal. The principal difference between the mutual-correlation functions of the echo signals for the cases of narrowband and UWB sounding is shown. Spectral portraits of targets, various in form and material, obtained with the use of UWB signals are presented. Sounding the targets with a UWB signal showed a higher degree of contrast and clarity of the acoustic images in comparison with the use of the narrowband signal. Thus, it is shown that UWB signals can be used to solve problems of recognition and classification of underwater objects in difficult conditions**

Keywords: **ultra-wideband signals, sonar, targets classification**

UDC 621.396.96

Bibliography - 9 references *Received - 24.08.2018*
RENSIT, 2018, 10(2):209-212 **DOI: 10.17725/rensit.2018.10.209**

Content

1. INTRODUCTION

Modern requirements to the technical characteristics of hydroacoustic systems, which solve the problem of classification of various underwater objects, force the developers to search for new methods and signals for solving this problem.

The first sonars used as a probing signal a short tone. At the turn of the 1970s and 1980s, when the question of improving the sonar parameters was particularly acute, there was a revolutionary transition to the use of complex narrow-band signals as probing signals, for example, chirp signals. It should be noted that such a transition in radar occurred much earlier - in the late 50-ies of the twentieth century. The use of complex narrow-band probing signals in active hydroacoustic systems (HAS) contributed to the development of sonar with high technical characteristics, which allowed solving most problems for several decades.

However, at the present time there is a need for further improvement of active HAS. The use of narrow-band sounding signals allowed, with the preservation of high resolution in range, to increase the range of action of the sonar by 2-3 times [1]. However, in this case, further increase in the range of the SAS operation due to the use of narrowband complex signals to ensure high resolution in range is not possible because of the large attenuation of acoustic oscillations at high frequencies [2]. In addition, the bulk of the work is currently carried out in the coastal zone in shallow water. Under these conditions, such parameters of sonar as noise immunity and the possibility of working under multipath conditions are put on the first place.

2. MATERIALS AND METHODS

At the present stage of the development of sonar, effective detection of objects in the water column is possible only with the use of active sonars.

The emergence of new technologies that have significantly reduced their own target noise and their sizes make it very difficult to detect targets in the passive location mode. An example is the emergence of autonomous uninhabited underwater vehicles.

The problem is not only the detection of targets at the required range in difficult conditions, but also their classification. When narrow-band probing signals are used, classification of targets is performed either from an acoustic image (for example, targets lying on the bottom surface) or from trajectory measurements for moving targets. In the first case, it is necessary to obtain a high-quality contrast acoustic image with a high resolution on the background of the underlying surface, which is quite difficult and not always solvable, especially for forward-looking systems.

One of the ways to solve the above-mentioned problems is to use ultra-wideband signals (UWBS) as probing signals in active HAS [3]. Similar works have been actively conducted abroad in recent years [4, 5].

The use of a low-frequency range of operating frequencies with a significantly wider bandwidth relative to narrowband complex signals makes it possible to solve the "distance-resolution" problem more effectively [6]. At the same time, the use of a wider frequency band of the probing signal increases the noise immunity of active SAS and allows operation under multipath conditions.

3. RESULTS

In the V.V. Tikhomirov NIIP for several years, systematic work has been carried out to investigate the use of UWBS in sonar. Theoretical research refers to the development of algorithms for the formation of UWB, their processing and the influence on their properties of the propagation medium. At the level of engineering solutions, the development of reception, radiation and the whole sonar in general is being developed. In recent years, several sonar models with UWB sounding signals have been developed and their full-scale tests were carried out. The results thus obtained confirmed not only the possibility, but also the prospects of using these signals in active sonars, including for the solution of the "distance-resolution" problem [7, 8].

As an example, in **Fig. 1** and **Fig. 2** shows the acoustic images of the same bottom section

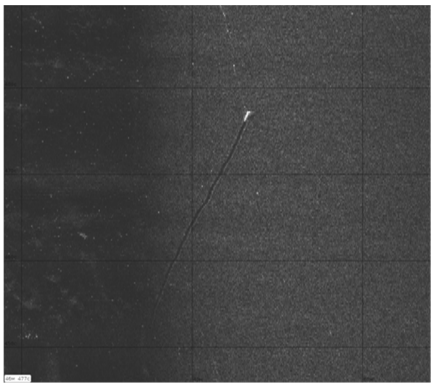

Fig. 1. *Acoustic image of a cylindrical object lying on the surface of the bottom, obtained with the help of Nesan SSVE-250.*

obtained during joint tests at the Ladoga of sonar side view (SSV) of the Neman series - SSVE-250 and the SSV model with the UWB sounding signal. In sonars, the LFM (linear frequency modulation) signal was used as the probing signal with the following parameters: Neman SSV - 6 ms signal duration, 24 kHz frequency deviation, lower frequency - 236 kHz; a SSV layout with a UWBS - a signal duration of 2 ms, a deviation of the frequency of 78 kHz, a lower frequency of 78 kHz. During the experiment, the receiving and transmitting antennas of the sonars were located on one bar that was attached to the ship's side. The sonar operation was carried out simultaneously. In this case, the carrier vessel moved from the left from the bottom to the top (see Fig. 1, and Fig. 2). A metal cylinder was used as the target, to which was attached a metal cable 11 mm in diameter, which ended in a buoy.

An essential advantage of the UWB sounding signal is the possibility of using a high information value of the echo signal when solving the task of classification of targets. When processing UWB signals, the formation of temporal and spectral

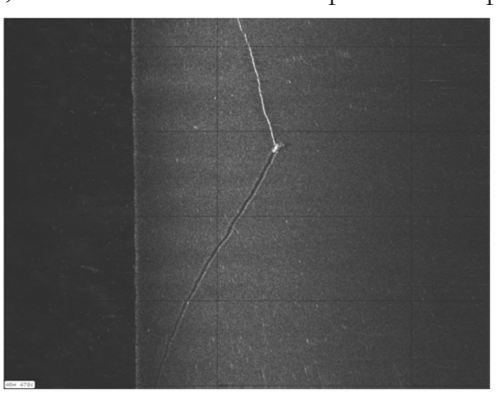

Fig. 2. *Acoustic image of a cylindrical object lying on the surface of the bottom, obtained with the help of a SSV layout with a UWB.*

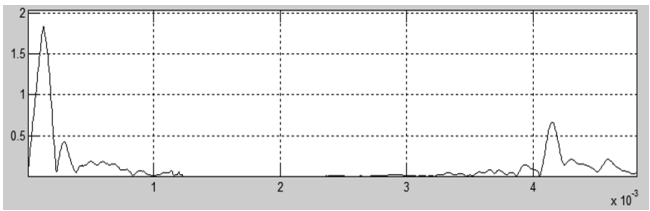

Fig. 3. *CCF echo signal reflected from a solid steel sphere with a diameter of 100 mm for the case of a narrow-band chirp signal.*

portraits of the target is possible. The use of UWB signals with a large base allows to resolve multiple echoes from the target in the time domain, and a wide operating frequency band allows for an efficient spectral analysis of the received signal.

In **Fig. 3** and **Fig. 4** shows the cross-correlation functions (CCF) of the echo signal reflected from a solid steel sphere with a diameter of 100 mm for the case of a narrow-band chirp signal (115-125 kHz) and a CCF of echo signal also reflected from the same sphere for a LFM UWB signal (78 -142 kHz). The abscissa is the time in ms. The scale along the abscissa axis for all graphs is the same. At the beginning of the abscissa axis, the CCF of the radiated signals is shown.

Fig. 3 and 4 show the fundamental difference between the CCF of the narrowband echo signal and the UWB of the UWB echo signal: in Fig. 4 CCF of echo signal from the target has a characteristic extended structure of several maxima, in Fig. 3 - CCF of narrowband signal is an envelope of a smooth contour with one maximum.

Table 1 presents the characteristics of some targets used during one of the field experiments.

In **Table 2**, photographs of targets, their spectral portraits (A) and CCF (B) are presented. The *X* axis in the graphs A is the frequency (in counts) and the *Y* axis is the normalized spectral density. On the *X*-axis, the time (in *s*) is plotted on the graphs of B, and the amplitude of the CCF (in the samples) along the *Y* axis. The data were obtained using the LFM UWB signal with the parameters indicated above.

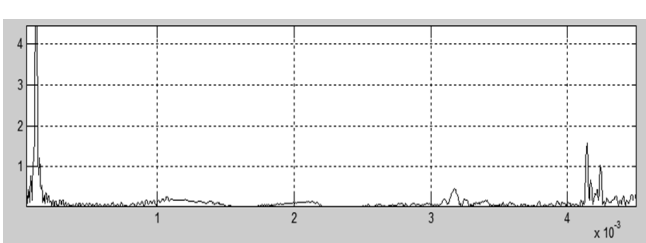

Fig. 4. *CCF echo signal reflected from a solid steel sphere with a diameter of 100 mm for the case of a LFM UWB signal.*

Table 1.

Set of targets and their main characteristics

№	Form	Overall dimensions, mm	Material	Type
1	sphere	Ø 105	steel	solid
2	sphere	Ø 100	foam plastic	solid
3	cylinder	Ø 57, ℓ=255	steel	solid
4	tube	Ø 110, ℓ=500	PVC	hollow

4. DISCUSSION

From the comparison of the acoustic images shown in Figs 1 and 2, it follows that the acoustic image obtained with the help of the SSV model with the UWB probe signal differs significantly better contrast and clarity. Especially it should be noted that in Fig. 2 clearly seen the cable, and in Fig. 1 cable was not found.

The graphs given in Table 2 show the difference between CCF and spectral portraits for different purposes in form and made from different materials, which can be used to classify targets, including in automatic mode without operator involvement. As for the nature of the formation of a temporary portrait, it can be quite complicated. The temporal portrait can be formed both due to the spatial extent of the target, and, for example, by excitation of various types of waves in the target, which leads to

Table 2

Portraits of targets

Таблица 1 – Портреты целей

№	Фотография	Портреты
1		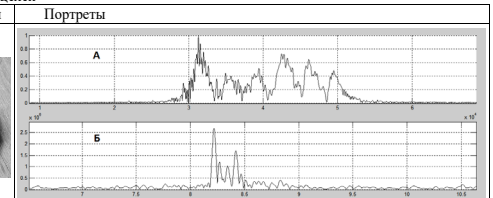
2		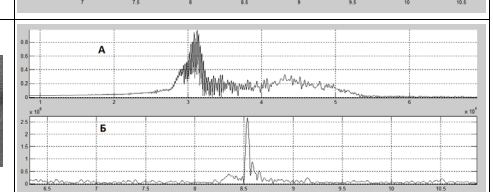
3		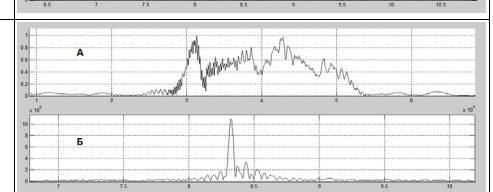
4		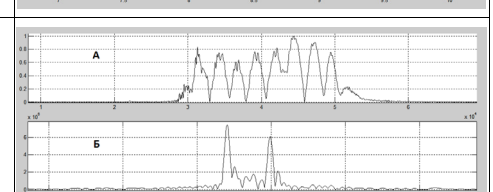

the formation of secondary echoes with differing time delays [9].

All this indicates the effectiveness of using ultra-wideband probing signals in active SSV as compared to narrowband signals.

CONCLUSION

Thus, the results show the possibility of obtaining high resolution at low frequencies and additional classification features when using UWB signals in active sonar systems. These properties of UWB signals can be used to solve the problem of recognition and classification of underwater objects.

REFERENCES

1. Demidov AI, Komochkov RS, Mosolov SS, Sknarya AV, Tutynin EV. Otechestvennye gidrolokatory so slozhnymi signalami proizvodstva OAO «NIIP». *Trudy 10th Vseross. konf. "Prikladnye tekhnologii gidroakustiki i gidrofiziki"*, St. Petersburg, 2010, p. 152-154.
2. Evtyutov AP, Lyalikov AP, Kolesnikov AE, Korepin EA. *Spravochnik po gidroakustike.* Leningrad, Sudostroenie Publ., 1988, 552 c.
3. Астанин ЛЮ, Kostylev AA. *Osnovy sverhshirokopolosnyh radiolokacionnyh izmereniy* [Fundamentals of ultra-wideband radar measurements]. Moscow, Radio i svyaz Publ., 1989, 192 p.
4. Lew H. Broadband Active Sonar: Implications and Constraints. *Technical Report No. DSTO-TR-0435,* Melbourne, Australia, 1996.
5. Capus C, Pailhas Y, Brown K, Evans J. Underwater detection, classification and tracking using wideband sonar. *Proc. 3rd Intern. Conf. and Exhibition on Underwater Acoustic Measurements*, Nafplio, Greece, 2009.
6. Zalogin NN, Sknarya AB. Selection of sounding signal for sonar. *Proc. 13th Intern. Conf. "Radiolocation, navigation, communication*", Voronezh, 2007, p. 2722-2730.
7. Demidov AI, Komochkov RS, Sknarya AV, Toshchov SA. O perspektivah ispol'zovaniya v gidrolokacii sverhshirokopolosnyh zondiruyushchih signalov [On the prospects of using ultra-wideband probing signals in sonar]. *Izvestiya YUFU*, 2013, 9:90-96.
8. Sknarya AB, Toshchov SA. K voprosu o preimushchestve ispol'zovaniya sverhshirokopolosnyh signalov pri reshenii zadachi raspoznavaniya celej v gidrolokacii [On the issue of the advantage of using ultra-wideband signals when solving the problem of target recognition in sonar]. *Trudy 4th vseross. nauchn. konf. "Sverhshirokopolosnye signaly v radiolokacii, svyazi i akustike*", Murom, 2013, p. 66-69.
9. Shenderov EL. *Izluchenie i rasseyanie zvuka* [Radiation and scattering of sound]. Leningrad, Sudostroenie Publ., 1989, 304 p.

MULTI-BASELINE INTERFEROMETRIC SIDE SCAN SONAR FOR THE CONSTRUCTION OF HIGH-PRECISION BATHYMETRY

Roman O. Boldinov, Anatoly V. Sknarya

V.V. Tikhomirov Scientific Research Institute of Instrument Design, https://niip.ru

Zhukovsky 140180, Moscow Region, Russian Federation

boldinov@mail.ru, sknarya.a@otd301.niip.ru

Abstract. **Some results of processing data obtained with the help of multi-base interferometric sonar during its full-scale tests are presented. The possibility of reconstructing depths with the help of a multi-base interferometric sonar sonar with an accuracy not worse than 2% of the depth at the subterranean point is shown, which meets the requirements of the 5th edition of the International Hydrographic Organization Standard S-44.**

Keywords: **sonar, single-baseline and multi-baseline interferometry, bathymetry**

UDC 621.396.96

Bibliography - 9 references *Received 24.08.2018*

*RENSIT, 2*018, 10(2):213-216 **DOI: 10.17725/rensit.2018.10.213**

Content

1. INTRODUCTION

Recently, the development of technical capabilities to build modern side-scan sonar (HBS) has made it possible to obtain acoustic images of the bottom surface of high quality. But a further increase in the informativeness of the acoustic study of the bottom surface is associated with the development of technology and techniques for obtaining a detailed relief and the formation of a three-dimensional image of the bottom surface. Therefore, to date, the task of creating technologies and hydroacoustic complexes capable of forming, in addition to acoustic images, also high-resolution and high resolution images, is also topical. This task is able to solve, in particular, interferometric side scan sonar (ISSS) [1].

The history of ISSS development has been on for several decades and all this time the system has been constantly developing and improving.

And here it should be specially noted that very many successes in the field of achievements in modern sonar were laid back in the twentieth century and were based on the achievements in the field of interplanetary radiolocation, a vivid representative of which was Academician V.A. Kotelnikov. It is the use of many achievements in the field of interplanetary radar that made it possible, even then, and now to successfully solve many problems. And the development of domestic ISSS refers to such tasks.

Improvement of ISSS was carried out due to constant competition with multibeam echosounder in solving the problem of constructing the bottom relief. Both data systems have both positive and negative qualities.

The shortcomings of the "standard" ISSS should first of all be attributed to the low accuracy of depth measurements in areas with a special form of the bottom relief, namely, for sharp jumps and depth differences. The relief with such geometry is mainly manifested in the survey of shelf zones of marine areas with underwater mountain relief, as well as in monitoring the state of underwater structures. The accuracy of the restoration of depths in such areas of the bottom surface, in most cases, is unsuitable for hydrographic use.

A few publications on this topic do not answer the above problem of improving the accuracy of depth measurements.

The purpose of this work is to develop a system that allows not only to make an area survey and three-dimensional mapping of the bottom surface, but also to improve the accuracy of depth measurements using methods based on the statistical theory of radio engineering systems, probability theory and random

processes, optimal filtering theory, and laboratory studies and full-scale tests.

2. MATERIALS AND METHODS

The geometry of the sight of the classical one-way interferometer sonar of the lateral view is shown in **Fig. 1**.

The interferometer consists of one transceiver (A2) and one receiver (A1) antennas, the angle of deviation of the interferometer base B from the vertical is β, and the viewing angle to the object on the bottom surface is α. The required depth at the point z is $G = H - z$.

The principle of the ISSS operation is based on finding the phase difference between two signals reflected from the same resolution element on the bottom surface and received by two spaced-apart receive antennas. The phase difference found is the basis for constructing the relief of the investigated bottom section [2, 3].

If the ray path difference is denoted by $\Delta R = R_1 - R_2$, where $R_1 = c_s \cdot \tau_1/2$ и $R_2 = c_s \cdot \tau_2/2$ (c_s is the sound velocity in the water medium), then the expression for the interferometric phase difference (IPD) of the two signals view:

$$\Delta\varphi = 2\pi(R_1 - R_2)/\lambda = 2\pi\Delta R/\lambda, \quad (1)$$

where λ is the wavelength.

Omitting a number of mathematical transformations, we obtain the final depth to the point P [2]:

$$G_0 = R_1\left[\sqrt{1-\frac{R_1^2+B^2-\left(R_1-\frac{\lambda\Delta\varphi}{2\pi}\right)^2}{2BR_1}}-\cos(\beta)\frac{R_1^2+B^2-\left(R_1-\frac{\lambda\Delta\varphi}{2\pi}\right)^2}{2BR_1}\right]. \quad (2)$$

Expression (2) defines a unique relationship between the depth to the resolution element on the bottom surface, the IPD, the base B and the oblique range R_1.

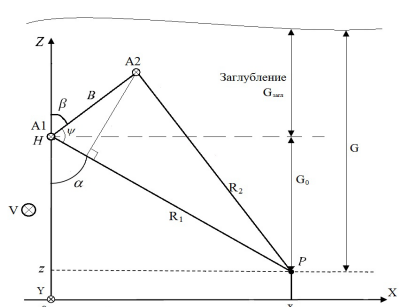

Fig. 1. *Geometry of the bottom surface survey.*

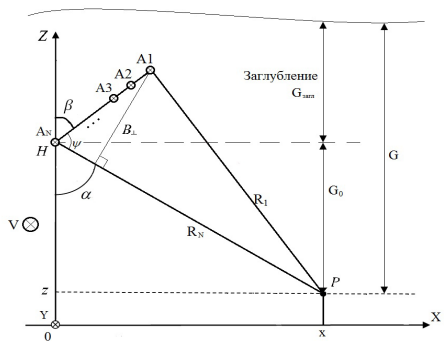

Fig. 2. *Geometry of the bottom surface survey of multi-base* ISSS.

It was the "standard" ISS that became the prototype in the development of its new modification, the multi-base ISS.

The features of the geometry of the bottom surface survey with a multi-base interferometric side scan sonar (MISSS) consisting of one transceiver (A1) and *N-1* receiving (A2-AN) antennas are shown in **Fig. 2**. The angle of deviation of the base plane In the interferometer from the vertical is β, the angle of sight to the object on the surface of the bottom (resolution element) is α.

The process of processing echoes in a multi-base ISS can be represented in the form of a block diagram, shown in **Fig. 3**.

In the block diagram of Fig. 3: AS - the aerial switch; TM - transmitter; RX1 is the receiving path of the first receiving channel; Rx N is the receiving path of the N-th receiving channel; IPD is the interferometric phase difference.

3. RESULTS

Let us consider some processing steps, shown in Fig. 2, in more detail on the example of data obtained during testing of the multi-base ISS mock-up at the V.V. Tikhomirov NIIP poligon.

The model of the multi-base ISS has the following characteristics: central frequency - 250

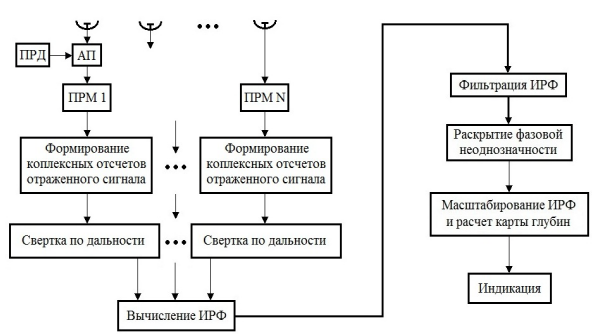

Fig. 3. *Block diagram of the stages of echo-signals processing in a multi-base ISSS.*

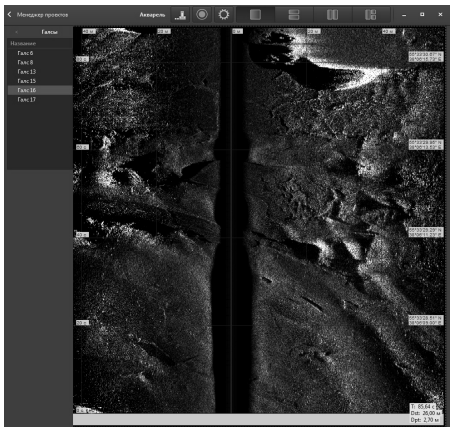

Fig. 4. *Acoustic image from the 1st channel of the multi-base ISS.*

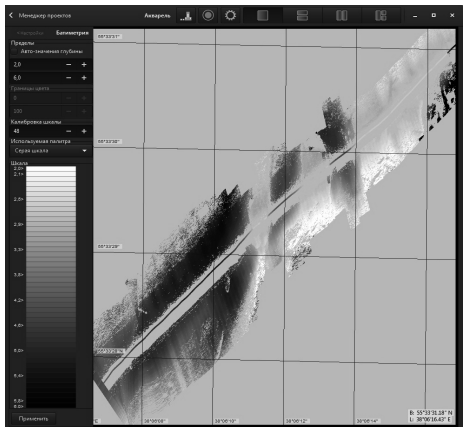

Fig. 6. *Bright image of the depth map in geographical coordinates.*

kHz; the width of the spectrum of the probe signal is 30 kHz; type of probing signal - chirp pulse; the duration of the probe pulse is from 3 ms; the number of receiving antennas is 6; the maximum size of the antenna base is 2.5 cm; angle of deviation of the base plane from the vertical - 30°; the width of the beam pattern of the radiating antenna along the azimuth is 1°.

In **Fig. 4**, by way of example, an acoustic image of the bottom surface obtained in real time after processing from the first channel of the multi-base ISS model is presented.

Antenna system of multi-base ISSS allows to form five interferograms corresponding to different antenna bases.

The most time-consuming stage of interferometric processing is the discovery of phase ambiguity (or "reversal" of the interferogram). The onset of phase ambiguity is due to the fact that the difference-phase values of the complex signal are calculated in the range [-π, π], and the phase difference itself can vary by several such intervals. Therefore, to obtain information on relative depths, it is necessary to eliminate the phase ambiguity. There are already several dozen methods for solving this problem [7]. Conventionally, they can be divided into two classes: local methods and global (integral) methods. For each class, there are solutions.

During the processing of data from the multi-base ISSS, a multi-base ambiguity disclosure method [8] was used, using information from different interferograms. The use of this method makes it possible to increase the accuracy of calculating the "unfolded" difference-phase values, and consequently, the calculation of depths, and also to avoid the errors inherent in the typical single-base methods of uncovering ambiguity.

Below are some of the features of the software developed by the multi-base ISSS.

In **Fig. 5** shows the brightness image of the depth map in real time of the bottom section from Fig. 4 in the coordinates of the range - the time of sounding.

In **Fig. 6** shows the calculation of the depth map in real time of the bottom section of Fig. 4 in geographical coordinates.

In **Fig. 7** shows a mosaic consisting of two intersecting depth maps, in geographic coordinates.

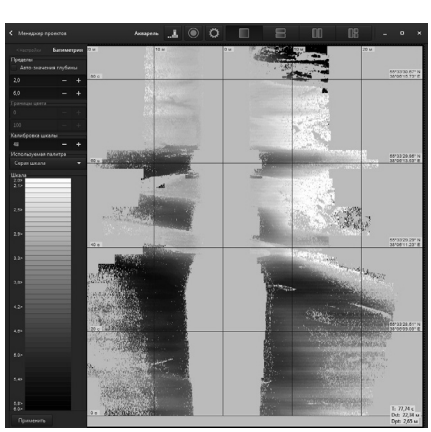

Fig. 5. *Brightness image of the depth map.*

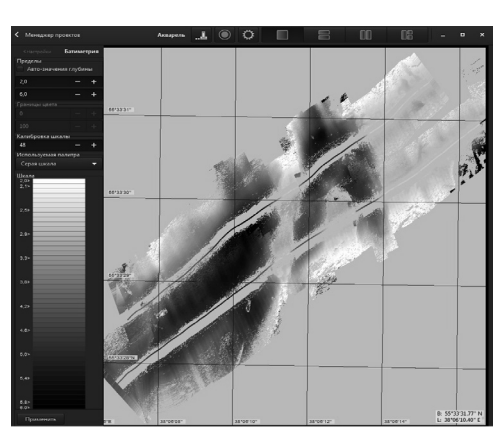

Fig. 7. *Mosaics of 2 lines in geographical coordinates*

4. DISCUSSION

From Fig. 6, a significant correlation of depths with intersecting lines is visible. Also, within the study area, a depth measurement was made at the bottom by a single-beam echo sounder at the reference points. Further, a comparison was made of the depths obtained as a result of processing in a multibase ISSS and the depths obtained with the echosounder at the reference points. As a result, the accuracy of measuring depths in the zone of view not exceeding 3 depths was calculated, which turned out to be no worse than 2% (~ 10 cm) from the depth at the sub-point.

The received accuracy meets the requirements of the 5th edition of the International Hydrographic Organization's S-44 standard [9].

5. CONCLUSION

In the present paper the following results were obtained:

1. The review, analysis and justification of the requirements for modern and prospective sonar complexes designed to produce detailed three-dimensional images and high-precision formation of bathymetric depth maps are reviewed.
2. Algorithms for processing interferometric data in a multi-base interferometric lateral sonar are developed.
3. A model of a multi-base interferometric SSS has been developed.
4. The working capacity of the multi-base ISSS model was confirmed on the basis of actual data obtained during its full-scale tests. The possibility of reconstructing the depths during sharp changes in the relief with the help of a multi-base interferometric SSS with an accuracy of at least 2% of the depth at the subterranean point is shown, which meets the requirements of the 5th edition of the International Hydrographic Organization Standard S-44.
5. A patent for the useful model "Interferometric sonar of lateral survey" was received (RF, 167401.2017.01.10) in January 2017.

REFERENCES

1. Richards MA. A beginners Guide to Interferometric SAR Concepts and Signal Processing. *IEEE A&E SYSTEMS MAGAZINE*, 21(6)5-29.
2. Boldinov RO, Baskakov AI, Sknarya AV. Potentsial'naya tochnost' interferometricheskogo gidrolokatora bokovogo obzora. *Vestnik MEI,* 2016, 3:66-71.
3. Boldinov RO, Sknarya AV. K voprosu o primenenii algoritmov postroeniya rel'yefa dna v interferometricheskom gidrolokatore bokovogo obzora "NEMAN ISSS-500. *Zhurnal Radioelektroniki*, 2017, 2.
4. Rodriguez E, Martin JM. Theory and design of interferometric synthetic aperture radars. *IEE Proceedings–F,* 1992, 139(2):147-159.
5. Sintes C, Llort-Pujol G, Gueriot D. Coherent probabilistic error model for interferometricsidescan sonars. *IEEE Journal of oceanic engineering*, 2010, 35(2):412-423.
6. Kendall WB. Unambiguous accuracy of an interferometer angle-measuring system. *IEEE Trans.*, 1965, SET-11(2):62-70.
7. Ghiglia DC, Pritt MD. *Two-dimensional phase unwrapping*. New York, Wilei, 1998.
8. You YN, Xu HP, Li JL, et al. Multi-baseline phase unwrapping via maximum likelihood phase gradient estimation. *Proc. IGARSS*, Quebec, Canada, 2014, pp. 374-377.
9. Strandart S-44 "Standarty MGO dlya s"emki rel'yefa morskogo dna" Mezhdunarodnoy gidrograficheskoy organizatsii (MGO), 5-ya redaktsiya. Monako, 2008, c. 17-18.

DYNAMIC CHAOS IN IRE: THE EMERGENCE AND DEVELOPMENT

Nikolay N. Zalogin

Kotelnikov Institute of Radioengineering and Electronics of RAS, http://www.cplire.ru
Moscow 125009, Russian Federation
zal.dunin@mail.ru

Abstract. **A review of the work on microwave electronics in the** Institute of Radioengineering and Electronics **over the past 60 years is presented. The discovery in 1962 of the generation in a 3-cm autogenerator (a plasma-electron beam in a pulsed magnetic field) of broadband noise oscillations is described. The work on increasing the generated noise power and efficient matching of the generator with the external path, which led to the creation of a noise generator - a solid-state oscillator of chaotic oscillations with a large number of degrees of freedom, as well as work on creating a generator of masking noise of computers. The work on noise radar, on the creation of interference stations for various types of radar stations - counteraction to air defense and anti-missile systems, was noted. The work on information aspects of the theory of dynamic chaos, on the creation of algorithms for generating pseudo-random sequences for digital communication and navigation up to pixel-by-pixel image encryption was touched upon. The characteristic feature of the works is the introduction of the results obtained into technical developments.**

Keywords: **microwave electronics, noise generators, noise location, noise stations**

UDC 519.6

Bibliography - 8 references *Received 15.08.2018*

RENSIT, 2018, 10(2):217-234 **DOI: 10.17725/rensit.2018.10.217**

Content

1. INTRODUCTION

Having a relatively small experience in writing memoirs, the author wants in advance to apologize to the readers in some subjectivity of the presentation of this material. Events that occurred 50 years ago, it is very difficult to describe without distortions caused by age-related changes in memory. Moreover, many participants in these events are no longer alive, while others with memory are even worse than the author. Most of the work carried out in those days had this or that classification of secrecy. Reports and other documents on them either lie in some archives, or simply destroyed. Therefore, in the absence of documentary materials, the reader can only trust the author. The author still hopes that most of the facts in this material are presented more or less reliably. The author also hopes that the following work will not cause any resentment to the witnesses of those events and the relatives of the Institute's employees who have already passed out of life. Since the author is in the singular (without co-authors), the presentation of the material will go from the first person.

The possibility of generating chaotic oscillations in self-sustained oscillating systems by a small number of degrees of freedom was discovered in the Department of Microwave Electronics of the Institute of Nuclear Physics of the Academy of Sciences of the USSR in the fall of 1962, as is usually the case, by accident. Therefore, it is expedient to begin the exposition from earlier moments. Let's start with 1957, when the author, after completing the third year of the Moscow Institute of Physics and

Technology, was sent to practice at the Institute of Nuclear Physics of the USSR Academy of Sciences.

2. BEGINNING

Actually, I got to IRE in June 1957 after finishing the third course of MIPT for practice. This practice lasted several days a week until the defense of the thesis. Therefore, becoming a junior researcher, I could already imagine what the department of ultrahigh-frequency electronics is headed by (on a voluntary basis), Nikolai Dmitrievich Devyatkov.

In those years it was believed that the development of microwave electronics had to proceed along an evolutionary path. All attention was paid to mastering the millimeter range. Before the jump, the optical range remained several years. In those years, difficulties in the development of amplifiers and generators of the millimeter range with the help of traditional microwave electronics such as TWT, BWO, magnetrons, etc. became apparent. Dimensions of the slowing structures with decreasing wavelength sharply decreased. The "sagging" of the longitudinal component of the electric field with which the electron beam interacted also increased. It became obvious that traditional methods are incapable of generating and amplifying powerful electromagnetic oscillations at frequencies of the order of 100 GHz. Therefore, an intensive search for new methods of generation and amplification in the millimeter range was carried out.

In IRE these works developed in two main directions. First, a powerful experimental setup was created, based on a linear electron accelerator to energies of the order of 3 MeV. It was assumed with the help of this accelerator to form and accelerate to near-light speed compact bunches of electrons and "flare" them in the so-called Motz undulator - a periodic system of transverse magnetic fields. We also considered the possibility of emission of electron bunches due to the Cherenkov effect in waveguides partially filled with a dielectric. This work, conducted on the instructions of the legislative organs, ended with a negative result. The grouping of the electron beam at the accelerator output was clearly insufficient. In addition, the magnetron frequency of 10 cm-range, providing electromagnetic oscillations for electron acceleration, was very unstable. As a result, instead of the expected kilowatts of radiated power in the millimeter range, milliwatts of noise oscillations were measured in this range. The project was clearly ahead of its time.

Secondly, the department began work on the feasibility of an electron-ion plasma pierced by a fast electron beam to amplify and generate electromagnetic waves. At that time, plasma was in special esteem in connection with the report of Academician I.V. Kurchatov in England during the visit there NS. Khrushchev. The investigation of plasma properties was mainly concerned with controlled thermonuclear reactions. However, the more we learned about the properties of the plasma, the more it was used for other uses. In particular, the rocket launchers started talking about plasma engines and simulating the entry of bodies into the atmosphere at hypersonic speeds, and electronics engineers about amplification and generation of electromagnetic oscillations using a plasma-electron beam system. The well-known theoretical physicist from the Kharkov Institute of Physics and Technology, Yakov Borisovich Feinberg, showed the possibility of increasing the degree of electron clustering in a fast electron beam penetrating an electron-ion plasma. In Kharkov and in IRE conducted experiments that confirm the possibility of amplification of microwave oscillations in this way.

My thesis work consisted in an experimental study of the possibilities of amplifying with a plasma-beam system signals in the 8 mm-range. The initial grouping of electrons was carried out using a resonator cut from a reflective klystron. Then the beam passed through the gas discharge region and in the second resonator provided excitation of electromagnetic oscillations. From the autobiographical book of Academician ND Devyatkov "Memoirs", published in 1998 by the publishing house of the journal "Radio Engineering", I learned that the results of the work were reported at one of the conferences in the US, of course, without my name among the authors.

In IRE in the mid-fifties in the laboratory Z.S. Chernova after graduating from Moscow State University appeared a young specialist V.Ya. Kislov. His father, Yakov Vasilievich Kislov, was one of Kurchatov's assistants during the creation of the atomic bomb, and many of his friends in the university were assigned to the IAE in the plasma units. Kislov conducted a number of theoretical

studies that showed that slow electromagnetic waves having a longitudinal component of the electric field can propagate in a certain frequency range from a plasma cylinder placed in a longitudinal magnetic field. In this case, unlike the spiral or other metal retardation structures, said component has a maximum on the axis of the cylinder. This means that the interaction of the plasma slowing structure with the electron beam must be much more efficient than in the case of traditional, vacuum TWT and BWT. The results obtained by V.Ya. Kislov, confirmed by the experiment, led to the fact that N.D. Devyatkov and Z.S. Chernov transferred a significant part of the department's staff to plasma topics.

In the fall of 1962, I enrolled in the correspondence IEP postgraduate course. The scientific adviser was Nikolay Dmitrievich himself, assuming complete independence in carrying out the work itself and discussing the results at the final stage. Theme of the work is the generation of electromagnetic oscillations in the millimeter range using a plasma-electron beam system.

According to theoretical conclusions V.Ya. Kislova, the generation of electromagnetic oscillations in the plasma counterpart of a backward-wave tube takes place in the range located between the plasma frequency determined by the plasma concentration or the electron cyclotron frequency determined by the magnitude of the longitudinal magnetic field and the so-called upper hybrid frequency (the square root of the sum of the squares of these frequencies). Calculations have shown that for experiments with millimeter waves, significant magnetic fields are required. Since there were no opportunities to purchase or manufacture solenoids providing the required fields, and especially power supplies of such solenoids at that time, the institute decided to create a device with pulsed magnetic fields. Such an installation was started. But in order not to lose time, work began on the installation with a solenoid that allows investigation of generation in a three-centimeter range of wavelengths.

3. BIRTH OF CHAOS

A glass vacuum system with continuous pumping was created. The device with which experiments were conducted consisted of a glass tube, on one side of which an electron injector with an oxide cathode was placed, and on the other a metal collector of electrons. The tube was placed on the axis of the solenoid. Plasma in the system was created by a fast (about one-one and a half kilovolts) electron beam in an atmosphere of mercury vapor. As it turned out in the course of the experiments, a high plasma concentration was obtained as a result of the microwave discharge that occurs when intense oscillations are generated in the plasma counterpart of a backward-wave tube.

By selecting the pressure of the residual gases, the current and voltage of the electron beam and the magnitude of the magnetic field, it was possible to quickly generate electromagnetic waves in the 3 cm band with the emission of these waves into space or into a waveguide. Measurements of the plasma concentration and the magnitude of the magnetic field confirmed the fact that a plasma BWO is operating. When the measurements of the spectrum of excited oscillations began, everything became incomprehensible. The screen of the spectrum analyzer IV-66 was clogged with intensive noises. We decided that we were aiming at an intermediate frequency amplifier and began to measure the spectrum with a tunable filter on the microwave cavity. And then the continuum. They remembered that plasma sources of noise work in microwave radiometers. But their spectral noise power density (SPMS) is defined as 65 kT. This corresponds to 2.6 10-13 W / MHz. At us SPMSH on 8 orders, i.e. in 100 million times more! Those. it's still generation.

All the surrounding staff could not say anything about this. At that time, the concept of the self-oscillator was for some reason associated with the Van der Pol generator and the corresponding second-order differential equation, which had only periodic solutions. All were in captivity of the phase plane, where the trajectories of motion could not in principle intersect. I think that the results of these experiments at that time could be appreciated and understood by a well-known expert in the theory of oscillations GS. Gorelik is the author of the famous book "Oscillations and Waves". He lectured us at MIPT and was the head of one of the laboratories at IRE. He told us that one can not fixate on the generator of Van der Pol, that self-oscillating systems can be much more complicated. But Gabriel Semyonovich a couple of years before he died under an electric train at Dolgoprudnaya station.

Detection of the generation of broadband noise oscillations and the impossibility of a clear explanation of this effect caused me the desire to tell this to all familiar people working in this field of technology.

The applied value of the detected effect was explained to me by two people. The first one is one of the employees of the Saratov Research Institute "Volna", trained at this time in the IRE. He popularly explained to me that many people in their institute are struggling to create broadband noise sources in the microwave range. The goal is to interfere with modern radar stations. These developments are mostly ineffective, because they are based on the modulation principle. He advised hastily to submit a closed application for the invention of a method for generating broadband noise oscillations and a device for its implementation.

The second person who showed great interest in the work was Captain Trofimovich (I do not remember his name and patronymic). At a seminar where I reported about a noise generator, he took me aside and advised me to stop open speeches on this topic. Trofimovich worked in the Central Research Institute of the Navy, located at that time in the Alexander Palace in Tsarskoye Selo.

The application for the invention (authors NN Zalogin and V. Ya. Kislov) was filed and registered in April 1963 [1]. It went pretty fast. Employees of the Committee for Discoveries and Inventions (then he was in the Greater Cherkassy Lane) recognized her as a pioneer and helped formulate everything according to the current standards. The authors received copyright certificates and 20 rubles of compensation. It should be noted that the material of the application was already formulated at a fairly modern level. In the application it was stated that chaotic oscillations arise due to the simultaneous excitation in the system of several frequencies that are not equidistant in frequency and the generation on the nonlinearity of the plasma of the set of combinational frequencies.

By the way, in the same 1963 (in March), a theoretical article by E. Lorenz "Deterministic non-periodic flow" was published in the American journal devoted to atmospheric physics [2]. In fact, in this paper we have presented differential equations corresponding to the simplest oscillator of chaotic oscillations. Nizhny Novgorod radiophysicists came across this work only in the second half of the 70s. The article was translated into Russian in 1981.

Thanks to the Central Research Institute of the Navy in the IRE, a research project "Sablja" was commissioned by the Legislative Bodies to increase the spectral power density of the generated noise signal and create a sealed mockup of the generator. The setting up of such work forced the management of the department to involve a fairly large team in its execution. It was also clear that the theme of my thesis should be changed.

4. NOISEOTRON

When performing the theme "Saber" there were problems associated with increasing the generated noise power and effectively matching the generator with an external path. It was decided to fill the plasma with the working space of a powerful TWT plasma in the hope that noisy oscillations would arise in the system, not on inverses, but on direct waves. To provide a positive feedback, necessary for self-excitation of the system, it was assumed that some of the power from the output of the powerful TWT would branch off and be directed to the input. Since the amplification factor of the powerful TWT was small, it was decided to turn on the feedback loop via the low-power TWT attenuator. Possible modes of generation instructed to check the young specialist - EA. Massine, a graduate of MEPhI, better known in those days as a master of sports in a handball. Yevgeny Anatolyevich took two standard 10 cm range lamps, an attenuator and started experiments. The scheme of switching on two UV-34 TWTs looked as shown in **Fig. 1**. The first TWT was a broadband amplifier and operated in a linear mode. Its output through a directional coupler was fed to a spectrum analyzer. The branched power part through the adjustable attenuator was fed to the second TWT. Its

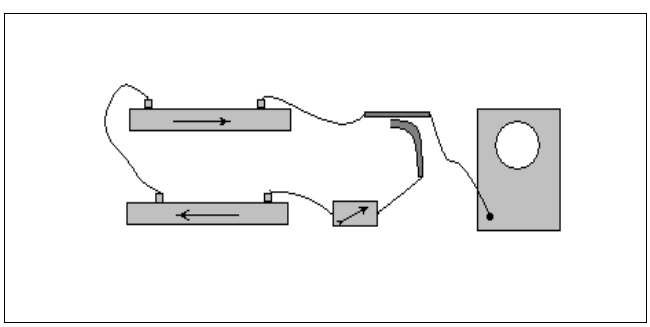

Fig. 1. *Scheme of the first noiseotron.*

output came to the input of the first TWT, closing the feedback loop.

There was a new shock for everyone. It turned out that such a system in some modes perfectly noises without any plasma.

Noises in such a system arose when the second TWT was overloaded by the microwave signal at the input and operated not as an amplifier, but as an attenuator with strong nonlinear distortions of the signal.

The experiment was carried out as follows. The attenuator was output to the largest attenuation - no feedback. Further, the power supply of the TWT was switched on, and the attenuation in the feedback loop gradually began to decrease. On the spectrum analyzer it was seen that there is a regenerative enhancement of the intrinsic noise of the TWT with spectral density maxima at the natural frequencies of the system. At a certain damping value, self-excitation conditions were fulfilled, and generation occurred at one of the natural frequencies. The amplitude of the oscillations with a further decrease in the damping grew, reached a maximum, and then its value began to fall. At some point, the amplitude self-modulation of the generated oscillations began. The auto-modulation period corresponded to the double bypass time of the feedback signal. It was visible on the spectrum analyzer. The modulation spectrum was then complicated by the appearance of harmonics and subharmonics of the modulation frequency. The complication occurred according to the law of 2-4-8 (rarely 16). For a finite number of doubling of self-modulation cycles, a continual component appears in the spectrum. Unexpectedly, with a further decrease in the decoupling in the feedback loop, the generated oscillations acquired the character of broadband noise with maxima of the SPMSH at the natural frequencies of the system. Sometimes there were additional maxima in the interval between own frequencies, indicating that the noise process is also covered by auto-modulation.

The observed effects caused a storm of discussions among the laboratory staff. Various versions of the interpretation of the results obtained were suggested. The idea that plasma is the main "culprit" of chaos of oscillations was finally rejected. A variant of the amplitude-dependent additional phase advance in the TWT is proposed. But then he did not cause much enthusiasm. It was clear only that the reason for the chaos is the behavior of the TWT - the nonlinear element. And everything turned out well with reduced electron beam currents, when the nonlinearity of the electron grouping is manifested more because of the small space charge.

The registration of the results obtained went according to the same scenario. Closed application for the invention and the possibility of publication in special periodicals. The application for the broadband noise generator-noiseotron, was submitted from three authors, employees of the department E.V. Bogdanova, V.Ya. Kislova and E.A. Massine in 1966 year. When considering the application, an American patent was discovered. It describes the source of noise on one TWT with external feedback. In VINITI, however, found significant differences in the structure of the generator and, especially, in the interpretation of its functioning. The author's certificate was received. In the open press it was published only in 1979 [3].

Among the developers of electronic devices, V.Ya. Kislov about the noise generator at a closed seminar in one of the Institute of the Ministry of Economic Development of the USSR caused a healthy recovery. I was told that two employees of the Saratov Research Institute "Volna" suddenly ran off with anxiety from the seminar. It turned out that they took a taxi to Bykovo airport and thence by plane to Saratov to urgently place and apply for some modification of the noise. Indeed, the possibility of obtaining high-level broadband noises without the development of special devices that require a significant change in the traditional technology of electrovacuum devices, was very attractive for both customers and electronic equipment developers.

It should be noted that it was at this time (the end of the sixties) that broad interest in the creation of broadband noise sources in the microwave band was of great interest from organizations responsible for countering the technical means of foreign intelligence. Thanks to this interest, decent funding was provided for research into the processes occurring in the noise generator and the development of samples of broadband noise generators.

The busyness with the noise-related themes led the laboratory to curtail research and development on plasma noise generators, which, due to

technological difficulties, did not promise a quick access to industrial designs. All work on plasma was transferred to the Fryazino part of the Institute, where Igor Fiodorovich Kharchenko from the Kharkov Institute of Physics and Technology appeared as the head of the laboratory №169. I managed to successfully defend my thesis on a plasma noise generator in early 1967. Nikolai Dmitrievich read the thesis before the binding and said that he had enjoyed reading the material and had no comments. After the defense, I immediately took up the noise drive theme.

Means of masking radiation, as always, were badly needed "yesterday". Since the OCD at the branch institute lasted more than three years, it came to the point that officers from the military units responsible for radio technical disguise were attached to the laboratory. Together, they created and established prototypes of noise drivers for temporary operation at facilities.

It is interesting that the creation and implementation of noise engines did not change the attitude of leading specialists of the Institute on the theory of oscillations to this topic. So, on the defense of the candidate's thesis EA. Myasin Academician Yu.B. Kobzarev said that he had many doubts about this work, but since the results are very useful for the defense industry, he will vote in favor. Professor A.E. Basharinov said that in generators with delayed feedback, on the contrary, fluctuations should have a higher degree of stability. Academician V.A. Kotelnikov wrote on one of the reports on the noise meter on the title page: "The work makes a strange impression." This remark could be translated as follows: "something is wrong here, because it can not be so." All open publications on noiseotron were banned not only because of the defensive significance of these works, but because they smell pseudoscience.

A great interest in the topic from the customers side and the associated concentration of human and instrumental resources of the laboratory made it possible to begin a systematic investigation of the processes leading to chaotization of oscillations in the noise generator. It is obvious that random processes are mathematically described only by parameters that are the result of averaging over time or a set of implementations. Simulation of direct generation is connected with a huge array of calculations. At that time, almost all academic electronic computers were located in the computer center of the USSR Academy of Sciences on Vavilov Street, access to it was carried out through a special laboratory, which was commanded by F.F. Dobryakova. At our disposal there were only electromechanical calculators "Mercedes" and "Rheinmetall", as well as a hand calculator "Felix". Therefore, it was decided to turn to experiment, since the meters of currents, voltages, power, spectrum analyzers were at hand. The construction of theoretical models was supposed to be carried out already on the basis of experimental data.

The experiments began with a detailed investigation of the characteristics of the TWT - a nonlinear element responsible for the chaotization of vibrations. The amplitude and phase characteristics of the lamp were studied for large input signals. Basically, of course, amplitude, as more accessible for measurements. In **Fig. 2** shows a typical amplitude characteristic of the UV-34 TWT in the low-current regime. The characteristic is normalized to the maximum output amplitude. In the same figure, we give variants of the approximation of the amplitude characteristic. As can be seen from the figure, the approximation using the function is very close to the real amplitude characteristic. However, it is hopeless to calculate the sequence of iterations on an arithmometer hopelessly long - you have to work with tables or resort to graphical mapping. The so-called logistic map differs from the experimental curve, but it must be calculated on an arithmometer without using tables.

It can be seen from the figure that with an increase in the amplitude of the input signal, the amplitude of the output signal first grows, then the saturation region follows, followed by a sharp drop in the output

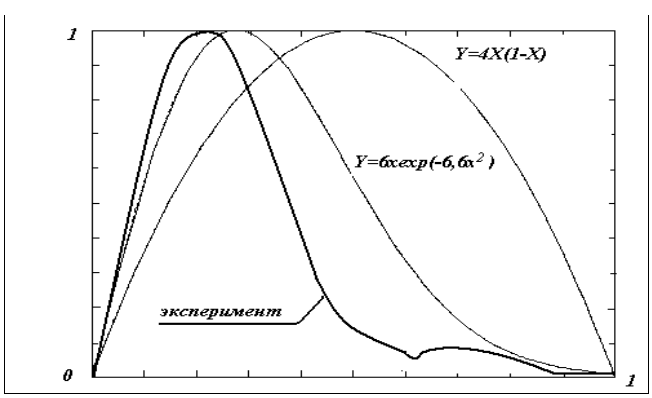

Fig. 2. *Amplitude characteristic of TWT and its approximations.*

amplitude with an increase in the input amplitude. Naturally, the assumption arose that for large values of the transmission coefficient of the feedback circuit, the generation with a constant amplitude loses its stability and the buildup of amplitude self-modulation begins. The experiment said the same thing. According to the measurements made, after the auto-modulation occurred in the two-cycle cycle, the auto-modulation period doubled. There were 3-4 acts of doubling, after which there was modulation chaos - a harmonic carrier, modulated in amplitude by noise. It required a computational confirmation that the development of automodulation could lead to chaos without any additional conditions, for example, fluctuations in the analog system. An alternative was a constant increase in the period of the cycle of amplitude changes.

The calculations were assigned to the chief theoretician of the laboratory, Vsevolod Nikolaevich Danilov. The whole room shook with the sounds produced by the electromechanical calculator. She was suffering not only from a laboratory assistant, who directly performed the calculations, but also the entire laboratory. This lasted for months. It turned out that calculations on an arithmometer inevitably led to cycles due to the finite digit capacity and the associated rounding of numbers. They began to look at the stability of cycles, introducing small perturbations. And here there were problems. It turned out that in some iterations the disturbance increases, while for others it decreases. The conversation was about an invariant measure, Lyapunov's indices, that mathematicians deal with similar questions. All this was done completely independently of Feigenbaum [4]. But the work was unexpectedly and tragically cut short. In early May 1977, Vsevolod Nikolayevich died during a hiking trip, before reaching the age of forty.

Nevertheless, it became clear both from experiments and from calculations that chaotic self-modulation occurs at a finite number of cycle doublings. In addition, it was finally clarified that the auto-modulation noise is only a precursor of the real broadband chaotization process, which develops in the noise core with even greater loads on the nonlinear element.

It was suggested that with a large steepness of the falling section of the amplitude characteristic of the TWT, the system lacks a nonlinear suppression of the small signal by a large one. There is the possibility of simultaneous excitation of oscillations at many natural frequencies of the system. Indeed, experiments on the two-frequency sounding of TWT conducted in Yu.V. Anisimova, showed that in a falling section with a large steepness, a strong signal passes through a lamp with attenuation, and an additional weak one amplifies. In this case, a combinational component appears with an amplitude that sometimes exceeds the amplitude of the weak signal. A very short moment of the appearance of oscillations was also detected at many natural frequencies of the system. A further decrease in the damping in the feedback loop already led to noise oscillations with a strong spectral rupture (maxima of the SPMS at its own frequencies).

At the end of 1972, revolutionary changes occurred in V.Ya. Kislov's laboratory. To ensure the Fryazino part of the Institute with qualified personnel, our director, Academician VA Kotelnikov, broke through the construction of a house near the metro station "Schelkovskaya". From the laboratory, subject to the transition to the Fryazino part of the apartment, Kislov himself, E.A. Measin, V.N. Danilov, Yu.V. Anisimova and E.V. Kalyanov, who moved to IRE from Saratov. As a result, the entire laboratory moved to Fryazino state at number 166. The wing of the IRE building (the former physics faculty of Moscow State University) facing the Kremlin turned out to be in an emergency condition due to a draft after a heat supply system failure. The equipment was transported to Fryazino and work on noise engine was continued there in the first building. I, who did not need to improve the housing conditions, nevertheless found myself in Fryazino, because I wanted to continue working on this topic.

Work on the oscillator of chaotic oscillations in FIDE was developed in three directions. First, the development was carried out to increase the power and efficiency of noise generators. Secondly, the physics of processes leading to noise generation continued. Finally, intensive searches for solid nonlinear elements began, which along with the TWT could provide chaos in the generators with delayed feedback.

Nikolai Dmitrievich Devyatkov is our head of department, at his time at the time was deputy director for scientific research at the Research Institute 160,

the head enterprise of the first department of the Ministry of Economic Development of the USSR, located in Fryazino. Despite the fact that the noise-related topics of the MEP were related to Saratov, Devyatkov organized work on noise generators in his institute. So in the department of E.A. Helvich was tested a 3-cm-3-kilowatt noise generator on standard TWT. Yuri Pavlovich Myakinkov developed a so-called single-balloon noise generator in which an amplifier and a nonlinear element were combined by one electron beam. At FIRE began to create a very powerful one-balloon decimeter of the decimeter range.

During this period, it was possible to make significant progress in studying the effect of phase shifts of the signal in TWT on the chaos of oscillations. Young (then) specialist VI. Kalinin, who came to the laboratory after graduating from the Gorky University, carefully and thoroughly studied the so-called nonlinear resonance in TWT with delayed feedback. It turned out that the natural frequencies of the system vary very much when the amplitude of the oscillations changes. It is interesting that on the defense of the thesis VI. Kalinin already no one spoke about the doubtfulness of the results. It seems that everyone understood how the noise generator works. Opponent - Doctor of Physical and Mathematical Sciences Mark Efremovich Jabotinsky said even that the thesis is drawn to the doctoral.

Interesting results, both experimental and calculated, were obtained by G.M. Vorontsov. He worked with a noise generator containing an amplifier on the VLBM, which is an effective amplitude limiter. Applying a bandpass filter at the input of the LBVO-nonlinear element, Vorontsov achieved the randomization of oscillations by means of an inverse transformation of phase modulation into amplitude modulation. It should be noted that in the Institute, although not in our laboratory, imported computers appeared. On one of them Georgy Mikhailovich acted both as a programmer and as an operator, having managed to create a decent digital model of such a noise generator.

My main interest in this period was the search for solid elements that could provide a randomization of oscillations in the noise generator instead of the TWT. It turned out, for example, that the inclusion of an electrically tunable iron-yttrium garnet filter (YIG filter) in the feedback circuit not only leads to a rearrangement of the band of generated noise, but also to stochastization of the oscillations. When a harmonic signal exceeding a certain threshold value is applied to such a filter, a signal modulated in amplitude and phase appears at the filter output. With a further increase in the amplitude of the input signal, the modulation acquired a chaotic character. The signal spectrum expanded beyond the working band of the filter. The possibility of adjusting the average frequency by an external magnetic field was preserved.

On this device NN. Zagolin, V.I. Kalinin, E.A. Miasin and V.V. Surin received an author's certificate for an invention with a priority of March 11, 1980 [5]. It became obvious that instead of the TWT, any solid-state amplifier can be combined in a noise-jet circuit with a ferrite device. In particular, a noise generator was created using a transistor amplifier developed by the employee of the research institute "Istok" G.V. Rovensky. A model of a two-circuit transistor noise generator with one of the contours made on a ferrite device was also created.

Since the mid-seventies, we have started a series of studies on the possibilities of using avalanche-passing diodes (LFDs) in noise generators. These works were carried out jointly with AI. Melnikov from "Istok". Anatoly I. Melnikov is an associate of A.S. Tager, laureate of the Lenin Prize for the creation of the LAP. He developed diode sources of microwave noise with an equivalent temperature of 5000 kT for radiometric equipment. LPD was surprisingly successful device in terms of implementation of devices that provide chaotic oscillations in the centimeter and millimeter ranges. Incorporated through the ferrite circulator into the TWT feedback, this diode worked perfectly as a non-linear element of the noise. Intensive noise was realized in the circuit with the LAP when sinusoidal oscillations were applied. The generator, assembled on a two-circuit scheme with two LAPs, was noisy. Finally, a diode intended for operation in radiometers could serve as a guiding source of noise in amplifying chains. As a result of his work with the LAP, he defended his thesis for a candidate's degree Belyaev.

In the second half of the 70's it became clear that there was a whole class of devices creating chaotic oscillations. The delay and non-linear resistance in

the feedback circuit used in the primary models of the functioning of the noise generator must be supplemented by coupled circuits with nonlinear inductances and capacitances. Those. The operation of such devices should be described in the general case by means of systems of nonlinear differential equations. The closeness to the truly chaotic behavior of the system increases with increasing degrees of freedom and the nature of nonlinearity.

The decisive work on classical noise was the doctoral thesis V.Ya. Kislov, in which he examined various methods of theoretical description of this device. At this time, one after another, work began on dynamic chaos. In the articles of Feigenbaum (1978-80), the universality of the behavior of iterative transformations was shown-the doubling of the periods and the transition to chaos for a finite number of doubling bifurcations. In the works of Ruelle and Takens on the theory of turbulence in the mid-seventies, the concept of a strange attractor was introduced, indicating the possibility of chaotic oscillatory motion in systems with finite dimensionality. In this connection, the work of Lorentz (1963) surfaced. Great contribution to the popularization and development of this direction was made by Nizhny Novgorod and Saratov radiophysics and mathematicians.

Truly "there is no prophet in his own country." Now the leadership of the Institute has become clear that the laboratory V.Ya. Kislov was not engaged in pseudoscience, but was at the level, and sometimes ahead of the new scientific direction. It was given permission to declassify the author's certificate, to publish the main scientific achievements on noiseotron, to participate in open seminars and conferences on this topic. The acquaintance with the results of the work of other scientists and the discussion of their results in a wide range of interested persons, as well as the electronic computers that appeared in the laboratory helped to complete the theoretical part of the noiseotron research and begin active work with noise generators on a solid element base.

The technical achievements of the laboratory remained mainly in the volumes of closed reports. And the work was done a lot. The possibility of obtaining intense noise in the range from hundreds of MHz to 10 GHz and above was demonstrated. The frequency band of simultaneous generation exceeded at times two octaves. So-called one-ball noise wheels were created. In them, the amplifier and the nonlinear element were in the same vacuum volume and the same electron beam was used. It was possible to provide electronic control of the band of generated noise within wide limits, both with the help of frequency-selective systems, and with tunable filters on iron-yttrium garnet and varactor diodes. On the contrary, the noise oscillations were eliminated in a given region of the spectrum. Some of the developments were implemented in special-purpose radio systems.

For a series of works on broadband, electronic noise generators in the microwave range, a group of IRE staff and industry institutes was awarded the USSR State Prize for 1980. In the laboratory laureat medals were given to V.Ya. Kislov, N.N. Zalogin and E.A. Massine. Laureate also became an employee of the Applied Problems Section (SPP) at the Presidium of the USSR Academy of Sciences Evgeny Chigin. Laureate medals were awarded in the Kremlin in a round hall under the dome, which is visible behind the mausoleum. The monetary prize went to a banquet in the restaurant "Prague".

5. TENTS

At present, there is much talk about the need to implement the latest achievements of science as quickly as possible in order to obtain a significant economic effect. I want to talk about how the so-called innovation policy was implemented 30 years ago.

In the summer of 1980, in connection with the preparation of materials for the State Prize, we were not at all until the Olympic Games. Vladimir Alexandrovich Kotelnikov, who nominated us for this award, very often brought to our laboratory various venerable scientists. Among them Academician Gury Ivanovich Marchuk was especially remembered. He was appointed Chairman of the State Committee for Science and Technology (SCST), which was then on Tverskaya between the Central Telegraph and the Moscow Soviet. The conversation turned out to be very lively. It turned out that Gurii Ivanovich worked a lot of time with nonlinear differential equations with a retarded argument. Therefore, he quickly understood everything and made an exceptionally interesting proposal for the development of the laboratory. He

offered us to understand the informative radiation of modern computer technology and, if necessary, to create devices for active radio engineering masking of these emissions. According to him, there is a great danger of interception of classified information processed in closed computing centers with the help of reception and decoding of spurious emissions. Marchuk then said a very interesting phrase: "If you solve this problem, I will give you a thousand people and a plant." This statement made a great impression not only on us, but also on VA. Kotelnikov, who was then not the last person in the Presidium of the USSR Academy of Sciences. As an experiment, a temporary scientific and technical laboratory (VNTL) was organized at the Academy of Sciences with increased financing and operational supply of materials and measuring instruments, capable of conducting not only scientific research but also experimental development.

The temporary laboratory included not only employees of the laboratory of electronic generators, but also leading experts of IRE on the theory of optimal signal reception, antenna devices, propagation of electromagnetic waves, etc. Officers of the military unit attached to the State Customs Committee of the USSR, as well as employees of the 8th Directorate KGB of the USSR. The laboratory really worked with full efficiency, often in the evening and at night, when extraneous radio emissions were minimal. In a short time it was found out that the most dangerous from the point of view of information leakage are the emissions of the display on the cathode-ray tube. The pulses of the brightness modulation of the electron beam had at that time steep fronts, and the high-frequency component of these fronts was effectively emitted into space by means of random antennas. The radiation efficiency increased with frequency according to the laws of electrodynamics, and the level of high-frequency spectral components, on the contrary, decreased with frequency. As a result of direct measurements, the range of the highest emission intensity was determined. It turned out that the reception of emissions with the restoration of textual information displayed on the screen of the early eighties displays is possible in the range from 100 MHz to about 500 MHz. On the basis of the usual portable TVs "Electronics-100" and "Youth", devices for intercepting emissions were created that allow reading the text on the display screen while in the car's cabin a hundred meters from the display. Naturally, directional antennas and low-noise input amplifiers were used for this. Using the features of horizontal display generators of even one type, it was possible to adjust one by one to the displays of different computers in the same room. It turned out that they practically do not create mutual interference. The level of these emissions was so small that it was necessary to use high-efficiency directional antennas located in the shadow of the radiation of the television center, and sometimes also the rejection filters of television channels.

The demonstration of interception and restoration of information on the screen of a standard TV, however, led to the indescribable horror of the responsible security personnel of defense and government agencies. We conducted these demonstrations together with the officers of the military unit attached to the State Committee of the USSR (SCC of the USSR), near the task of the information center of the USSR Academy of Sciences in Neskuchny Garden, near the IRE on Mokhovaya Street and even in the Kremlin near the Spassky Tower. The equipment for the interception of emissions was located in the UAZ truck - a "loaf" belonging to the State Customs Committee. On the screen of the display, whose radiation was to be intercepted, simple phrases like "Glory to Soviet Science!" Were printed in large print. or "IRE - Hurray!". I did not see it myself, but the operators claimed that one of the viewers really felt bad about the heart.

Informative spurious emissions also had magnetic disk drives at the time of writing and reading information in a sequential code. However, the probability of interception of such parcels and their identification by virtue of one-time and non-repeatability is extremely low.

To mask the described radiation in the laboratory, a special transistor noise generator was developed, which generates and emits broadband noise of relatively low level, responding to the norms for industrial radio interference and medical requirements. It was powered by a 12-volt DC source, it could also run on a battery. To ensure chaotic polarization of the masking radiation, three independently operating oscillators with loop

antennas in orthogonal planes were simultaneously used.

The masking noise generator, named by the authors of the "Tent", was protected by a number of author's certificates and was issued by the forces of the temporary laboratory for several years (**Fig. 3**). The "Shatras" were installed on many computer centers of government and defense institutions, each of which was contracted for research and development in relation to this facility. In this large-scale work the leading employees of the laboratory A.S. Dmitriev, V.P. Ivanov and many others. Until now, modified devices of this kind are produced by SKB IRE. As a result of the work of VNTL, the financial state of the IRE has significantly improved - there is an opportunity to update the instrument park. Employees of the laboratory, taking into account the bonus, received about twice the salary. Deductions to the trade union committee were so great that we went on a monthly basis to free excursions to Yerevan, Baku, Tbilisi, Sevastopol and other cities of the USSR.

At that time, individual computers and computer centers were not yet united by local and regional networks. The concept of "hacker" did not exist yet. In the period when market relations were created, large networks and removable storage devices on magnetic and optical disks, the problems of radio technical disguise of spurious emissions went to the background. The leakage of information went mainly through other channels. The necessary information was much easier to get on a flash drive, paying for a certain amount to some technical employee allowed to service computers, or "download" from the network using hacking techniques. One must assume that the

Fig. 3. *The generator of masking noises "Tent".*

systematic approach pursued by many organizations and firms to ensure the preservation of confidential information in computer networks will again revive a certain interest in spurious emissions, to minimize and mask them.

Marchuk, of course, did not give a factory after the completion of works on the protection of computer information. However, the work was put forward for the Prize of the Council of Ministers of the USSR. In 1984, we received medals from the hands of Guriy Ivanovich, and his diplomas were adorned with his signature.

6. NOISE LOCATION

In the second half of the 70s, when exactly, I do not remember, the staff of the Central Research Institute-3 of the Defense Ministry came to us in Fryazino. They very emotionally told about the discovery in the US patent literature of the method of analog obtaining of the function of mutual correlation of two broadband noise signals. From the theory of radar, it is known that the optimal probing signal is a broadband chaotic signal with a normal (Gaussian) probability distribution of instantaneous values. The trouble is that the acquisition of data on target parameters in this case is possible only by calculating the mutual correlation function between the emitted and received signals. Computer methods because of very high frequencies and a wide band of a signal do not work. Digitization of such signals is impossible. The essence of the analog method of obtaining the cross-correlation function consists in a double spectral analysis of the sum of the signals emitted and reflected from the target. The first spectrum of the sum acquires periodic ruggedness. Depending on the time shift between the realizations, some spectral components are summed in phase, others in antiphase. The secondary spectrum just characterizes this time delay, i.e. double the range to the target. From the point of view of mathematical statistics, this corresponds to the well-known Wiener-Khinchin theorem.

Having understood the essence of the method, we immediately decided to test its effectiveness experimentally. One of the premises of the laboratory was turned by windows to the SKB building. We are V.I. Kalinin switched on the noise generator, sending his signal through the horn antenna P6-23 to the SKB building. Another antenna

was connected to the ASH-2 spectrum analyzer. The noise signal came on the receiving antenna in two ways: as reflected from the wall of the SKB and as the transmitted on the side lobes of the directivity pattern of the transmitting and receiving antennas. On the spectrum analyzer, we saw a clear periodic ruggedness and calculated the distance to the CBS by the period of ruggedness. It turned out to be approximately 40 meters. Immediately they walked down to the courtyard with a tape measure and measured the distance manually. The data were docked with great accuracy.

With the "troika" was put a joint work, which was later transferred to an enterprise engaged in the near location in Tula. Parallel to the proposal of NA. Armanda went to work with the laboratory BP. Kutuzy. It was a question of remote measurement of the height of sea waves with reference to the so-called "Caspian monster". We are with RV. Belyaev went to the southern coast of the Crimea in the place Katsiveli, where, together with AA. Kalinkevich took measurements on the platform of the Black Sea Department of the Marine Hydrophysical Institute (CHOMGI). The possibility of measuring the height of waves from low-flying aircraft or helicopters was shown. Further work in this direction revealed the possibility of selecting moving targets, up to determining the respiration rate of a person in the ray of such a locator.

It should be noted that the double spectral processing method in radar works well only for very small ranges to targets. Everything is good only at distances of a few tens of meters. At long distances, the period of the rupture of the primary spectrum becomes so small that it requires a very narrow-band filtering and consequently an inadmissibly long time for estimating the primary spectrum in a sequential spectral analysis. The advantage of near-field radar with dual spectral processing is mainly in the extremely high resolution of the method in terms of range, but with the use of spaced reception antennas and angular coordinates. The work in this direction was interrupted due to the new responsible task of the IRE Directorate.

7. AWACS

I do not know if I can write about this now. But I'll write. This will be the last serious work done by the laboratory under the Soviet government. I think that after the collapse of the USSR, much more serious developments made in those times were declassified. In addition, there has been a long talk about the sale of systems based on the development of our laboratory to other countries.

In the spring of 1984 our director Vladimir Alexandrovich Kotelnikov came to our laboratory somehow without any accompaniment. He told us that he was at an important meeting in the Ministry of Defense yesterday about the opposition to the US AWACS system. I think that our reader knows exactly what it is (**Fig. 4**).

The meeting discussed the possibility of suppressing the flying radar along the side lobes of the radiation pattern of its receiving and transmitting antenna. Estimates of the required radiation power have shown values of the order of MW in a practically continuous regime. Given the low efficiency of the transmitter interference to power this device requires a power plant that can, in principle, provide electricity to a small city. If you suppress the main beam, then this will require power of the order of tens of watts and then at the moment of "smearing" the beam at the interference station. Since the radar operates with a beam of the order of 10, and the suppression should be carried out from the earth's surface from distances of the order of 150-250 km, several dozens of automatic, unattended stations will suffice to mask the aircraft and unmanned objects over the monitored territory.

Kotelnikov's proposal was considered by the laboratory staff in conjunction with specialists from the Voronezh Center of the Ministry of Defense, responsible for the problems of electronic warfare, and the Rostov Institute of the Ministry of Radio

Fig. 4. *AWACS aircraft.*

Industry. The idea is recognized as very promising. We made applications for the invention and started working. For this work, the lifetime of the VNTL was extended.

A computer simulation of various situations involving the use of AWACS was carried out. The detailed model of the station and the features of its use, obtained by us at the Ministry of Defense, made it possible to develop a model of a small interference station consisting of a receiving device that identifies the radar emissions and the transmitter of broadband interference in the entire range of radar operation

Together with the Rostov Institute, about 20 mockups of interference stations were developed and manufactured. Broadband noise generators and antenna systems related to IRE (for powerful transistor noise generators, NA Maksimov answered, for antennas AS Dmitriev). Receiving devices and automation were developed by Rostov. The stations were debugged at the Rostov Institute training ground near Matveyev Kurgan settlement. Each of the stations for certainty was called a female name. The whole set was called "girls" (**Fig. 6**).

The dimensions of the "girls" were determined by the size of the antennas and the battery, the electronics occupied a negligible place.

СОЮЗ СОВЕТСКИХ СОЦИАЛИСТИЧЕСКИХ РЕСПУБЛИК

ГОСУДАРСТВЕННЫЙ КОМИТЕТ СССР
ПО ДЕЛАМ ИЗОБРЕТЕНИЙ И ОТКРЫТИЙ

АВТОРСКОЕ СВИДЕТЕЛЬСТВО

№ 290590

На основании полномочий, предоставленных Правительством СССР, Государственный комитет СССР по делам изобретений и открытий выдал настоящее авторское свидетельство на изобретение:

Автор (авторы): Котельников Владимир Александрович
Ерухимович Николай Александрович Палатов Константин Иванович
Гуляев Юрий Васильевич Иванов Василий Петрович
Максимов Николай Андреевич Калинин Валерий Иванович
Перунов Юрий Митрофанович Киселев Владимир Яковлевич
Залогин Николай Николаевич Дмитриев Александр Сергеевич

Заявитель:

Заявка № 4507478/27836 Приоритет изобретения зарегистрировано в Государственном реестре изобретений СССР 22декабря1986г.

1 марта 1989г.

Действие авторского свидетельства распространяется на всю территорию Союза ССР.

Председатель Комитета

Начальник отдела

Fig. 5. *Author's certificate on the method of counteraction to DRLOU systems and the device for its implementation.*

The set of stations was transported to the test site near Orenburg for testing. An analog of AWACS, a Soviet A-50 aircraft with a "Shmel" radar station based in the Akhtubinsk area, barracks at a distance of about 200-250 km from the test site, and Tu-16 and Mig-21 flew from Orenburg to it. The tests showed that the targets on the radar station's line of interference were successfully masked, even at a distance of about 50 km from the radar. In the autumn of that year, a couple of "girls" were exported to the GDR, where they were already working on real AWACS, but in a passive mode (without turning on the transmitter of interference). The measurements showed that the interference stations "see" the real AWACS and are ready to reject interference. OCT "Tuman", conducted on the basis of this work in Rostov, led to the formulation of appropriate funds for armament. The performers mentioned in the author's certificate, as well as employees of the Voronezh Center and Rostov developers were awarded the USSR Council of Ministers Prize in 1989. There was no banquet about this - they were fighting with drunkenness.

8. SCIENTIFIC AND TECHNICAL TOURISM

The work carried out by the laboratory on the creation of radioelectronic countermeasures to long-range radar detection systems aroused keen

Fig. 6. *Employee of VNTL V.P. Ivanov with one of the "girls."*

interest among many specialists dealing with electronic warfare at that time. In particular, we talked about jamming various types of side-view radar with synthesized aperture, on countering air defense and missile defense systems of the Patriot type, on countering the radar "Cobra Yudy", etc. For the experiments, trips to Baikonur, Kamchatka, on Pacific Ocean. There was no great science in this matter, but it was so desirable to travel for public expense that it was impossible to refuse. Moreover, for a combination of two reasons - a serious form of admission to secret works and a stubborn refusal to join the ranks of the ruling party, I was absolutely out of the question. I do not regret that I neglected the end of my almost written doctoral dissertation and went on these trips. Impressions remained for the rest of my life. It should be noted that in the seventies we had already traveled to various ranges to find out the effectiveness of the noise signal on the radar and the radio reconnaissance station. Worked, in particular, in Smolino, Nizhny Novgorod region and at the air defense ground "Kapustin yar".

The first trip took place at Baikonur. At that time in the orbit was a military version of the space station "Salyut", designated as "Almaz". On it flew an experimental sample of the lateral view radar "Sword". By the way, in a slightly modified version of the "Sword" flew and on our institute aircraft IL-18, with reference to the peaceful program of remote sensing of the earth's surface.

It turned out that there is really no Baikonur. The airport where we arrived, had the name either "Far", or "Ultra". The town in which they lived was called Leninsk. North of Leninsk there was a Kazakh settlement with the railway station Tyrat. Further north, the highway and the railway along which the landfill sites were located ran parallel.

On Baikonur, every day we were taken to the Gagarin launch area (about 35 km from Leninsk). There we used our noise to attach to the radar "Kama". Kama accompanied the rockets on take-off. Therefore, its beam could be controlled within wide limits, both in azimuth and in elevation. Due to the peculiarities of the "Diamond" orbit, it took only two or three days to work. In our spare time we were taken to the "Energia-Buran" site. We looked at these cars in the hangar. Then already (much later) they found out that the roof of the hangar was covered with snow and the products were badly damaged. One night they drove to launch the Proton rocket - an impressive sight. The infrasound from the operation of the first-stage engines causes a shiver in the chest, even five kilometers from the start. Very beautifully in the night sky are separated "bokovushki".

The next work in the interests of missile men took place in the area of the Kura field in Kamchatka. We lived in a military town near the village of Klyuchi. Another group (VA Burykin, SO Starkov, BA Hadzhi) was on a ship that drifted northeast of Ust-Kamchatsk alongside the carrier of the Cobra Judy radar, Observation Island, . At that time, in accordance with the agreement with the United States, the destruction of medium-range missiles Pioneer (SS-20) was carried out. The rockets were destroyed by launching from the Chita area to the Kura test site. As far as I understand, our task was to test the effectiveness of masking the missile's head parts before entering their atmosphere, and also to look at the reaction of Americans to these actions. We worked on two launches, flying from the airfield "Klyuchi" on an AN-26 airplane. Confirmation of the effectiveness of camouflage was the calibration of the radar over the released balloon and a note with the statement that the counteraction to the radar facilities of ships in neutral waters is a violation of the accepted international norms.

We shone a hindrance to the Cobra through the airplane window, and in return received the strongest radar of the air defense radar of the ship. As a result, we suppressed the Cobra Judy, but our aircraft was

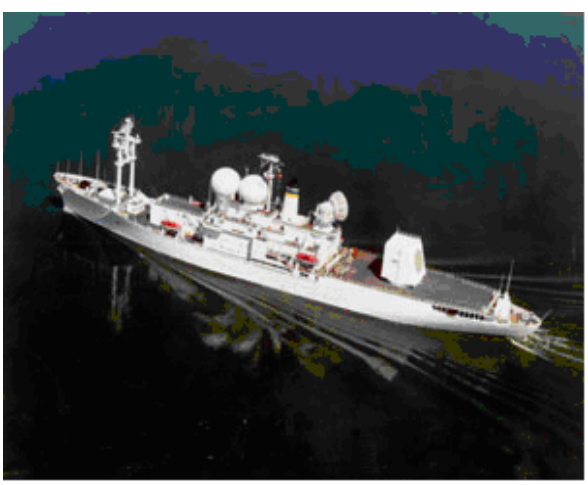

Fig. 7. *The ship "Observation Island." The radar with the Cobra Judy FAR in the stern.*

burned almost all on-board radio equipment. The pilots were very unhappy.

When we just arrived in Yelizovo (Petropavlovsk airport in Kamchatka), a nose in the nose with employees of the laboratory, BG, suddenly collided. Kutuzy, who flew to Kamchatka on their IL-18. Immediately agreed that they somehow fly past us with their "Sword", and we will light up on them a hindrance. IL-18 flew past us twice. The first time we did not work, and the second one made a noise at him. Unfortunately, the processing of the results was not made in real time, but in a special center near Moscow, where we were not allowed. The fact that we crushed the "Sword" reliably, we learned only after many years. But still nice.

In days off from work, and we spent almost a month in Klyuchi, there was a real rest. One of the first nights was watched behind the entrance to the atmosphere of the head parts of a rocket. They glowed like electric bulbs. They walked along the spurs of Klyuchevskaya hill, examined the so-called craters-parasites, collected mushrooms. We were riding a self-propelled barge along the Kamchatka River. Especially remember the flight by helicopter to the middle ridge, where the host army unit had a recreation center. There, hot springs, underdeveloped geysers with a water temperature of about 900 ° and a non-periodic outburst to a height of less than a meter, were adjacent to cold keys with a temperature of about 40 °. This allowed you to make outdoor pools, with a temperature controlled and swim in them at any time of the year.

There were so many spawning fish in the Kamchatka River that Andrey Ivanovich Panas, the future director of the Fryazino unit of the IRE, managed to kick a huge sockeye on the shore, meat and caviar which all the expedition participants ate for two days.

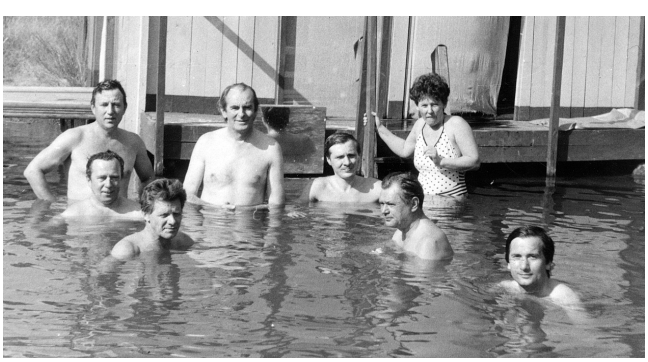

Fig. 8. *RV Belyaev, NN Zalogin and AI Panas in Kamchatka.*

9. PACIFIC OCEAN

It turned out that our visit to Kamchatka was considered a rehearsal for a more important event. The Dnepropetrovsk CBU prepared a test of a railway-based missile. It was planned to launch rocket launches from the Plesetsk landfill to the Pacific Ocean region to the southwest of the Hawaiian Islands. As the two areas for the destruction of the warheads were planned, we were divided into two groups. V.A. Burykin, A.I. Panas and S.O. Starkov left Viluchinsk on the Chukotka parachodka to a point south of the equator. I'm with NA. Maximov and A. Lyashchuk on the same parachodka, but with the name "Sakhalin", from Korsakov went to the area a little to the north of the equator. I do not mean to say the parachod, since the ship built in Poland, although it was fueled, but it heated the steam boiler, which, in turn, set in motion the steam engine. I got the cabin just above the steam boiler, and it was very noticeable in the tropics.

The path to the point of the alleged splashdown of the head parts took several days. Got into a pretty strong storm. Unpleasant, but bearable. On-board pitching during the drift is more disgusting. And in the drift we lay almost all the time waiting for the starts. Three days of drift - one night return to the point. During the day, almost all the time spent on the deck in the back of the ship, where there was a helipad. Binoculars watched the huge ships passing by, carrying cars from Japan to South America. We saw whales, sharks and a lot of flying fish. Two times they saw a green ray during the setting of the sun. The sun in these latitudes and at this time of year falls almost horizontally horizontally. At the last second you can see a bright green ray.

We did not have to work during this trip. It turned out that Observation Island is being repaired in a dock somewhere in the San Francisco area and will not be able to come to the test at a given point in principle. At that time a huge ship "Chazhma" was returning

Fig. 9. *The steamer "Sakhalin". Chukotka is the same.*

from some southern seas. We were transported with the equipment by helicopter to Chazhma, where we met with S.O. Starkov. A few days later we were already in Vilyuchinsk. V.A. Burykin and AI Panas arrived in Vilyuchinsk later on the flagship of the space flotilla "Academician Komarov."

The money received for participating in the expedition was spent on the purchase of personal computers. This turned out to be very useful, since with the collapse of the Union, the financing of all works practically ceased and the only opportunity to somehow engage in science was mathematical modeling.

10. DASHING 90's

As a result of the collapse of the USSR, the economic crisis and other factors, the financing of the Academy of Sciences almost completely ceased. In fact, the occupation of science has turned into a kind of social activity. Especially it affected the collectives dealing with mostly defense topics.

V.Ya. Kislov at this time completely reoriented to medical electronics. Employees who continued to deal with issues related to dynamic chaos, most of them united with A.S. Dmitriev. I, frankly, assumed that Alexander Sergeyevich, after reaching Kislov's critical age, would become the head of the department of microwave electronics. The fact is that unlike most of the laboratory's employees involved in applied experimental development, he actively studied the theory of dynamic chaos and soon after V.Ya. Kislov in 1988 defended on this subject a doctoral dissertation. But then something happened that resembles the events in North Korea. The head of the department was handed over to the youngest son of Vladimir Yakovlevich. Dmitrieva and her colleagues were transferred to the department, which was formerly headed by Academician Yury Borisovich Kobzarev. In the department of AS Dmitriev, active work continued on information aspects of the theory of dynamic chaos. More information about the research and development of this team can be found by referring to the Information and Communication Technologies on the basis of dynamic chaos (InformChaosLab) of the institute site http://www.cplire.ru/[6]. I will only say that three doctoral dissertations were defended in this department. A lot of work on dynamic chaos was also conducted in the Saratov branch of the IRE under the leadership of the brothers AP. and S.P. Kuznetsovs (see the section "Dynamic chaos" of the same site) [7].

In the Fryazino part of the IRE, in a laboratory headed by V.I. Kalinin also continued work on oscillators of chaotic oscillations and their applications in various fields of radio electronics.

I, and a few other employees who were out of work, at first engaged in issues related to algorithms for generating pseudo-random digital sequences. The fact is that the development of electronic computers, digital communications, navigation, etc. required the development of such algorithms, since there was practically no data on this direction in the open technical literature. It was desirable to create algorithms that ensure the generation of pseudo-random sequences of numbers of a possibly longer period with good statistical characteristics. It was desirable to provide a combination of relative simplicity of algorithms with the difficulties of its identification in the analysis of the sequence. In order to better understand the essence of the matter, it was decided to work with sequences of a finite set of positive integers. The question of the possible magnitude of the period stands in this case most acutely.

In this paper, it was natural to assume the use of the methods used to create models of analog oscillators of chaotic oscillations, in combination with some logical operations that are impossible when simulating such generators. The basic idea of obtaining large periods is to increase the geometric dimension of the system in which the generation occurs. Two main groups of algorithms were considered. This is a system that transforms at each step a certain vector, with dimension n, an analog of a system of n differential equations. Another option is analogous to a system with delayed feedback, where each successive sequence value is a function of several previous values. To ensure work with a limited number of positive integers, the algorithms used a logical operation - taking the remainder of the result of division, resulting from the next step of the number to the maximum of the numbers used.

As a result of the research, dependencies of the guaranteed period of generated sequences on the system dimension were obtained. It turned out that working with vector equations provides a longer

period than working with systems with a lagging argument.

On the basis of our research, V.V. Kolesov offered a method of pixel-by-pixel image encryption. This to some extent resembles the widely known method of double-permutation in cryptography. However, unlike signs and spaces, work occurs with individual pixels of the image. The resulting chaotic numerical sequences allow this to be done. It turned out that with this method it is possible to restore the whole image even with the loss of fragments of the coded matrix. More on this and much more can be found in the book "Broadband chaotic signals in radio engineering and information systems", published by the publishing house "Radiotekhnika" in 2006 [8].

In recent years, we have been able to resume work on the use of broadband chaotic signals in the active location. This time in sonar. The fact is that the velocity of propagation of longitudinal acoustic waves in an aqueous medium is about 20 thousand times less than the speed of propagation of electromagnetic waves in the atmosphere. This means that the wavelengths of the sounding signal characteristic of the radar are realized in sonar at frequencies of tens to hundreds of kHz. Modern computer technology easily copes with generation, digital-analog and analog-digital signal conversions, as well as with the correlation processing of such signals. The specific feature of sonar is also that longitudinal waves in water experience strong damping, the greater, the smaller the wavelength. As a result, there are serious problems in the development of sonar with increased range. The series of short pulses with high-frequency filling that are habitual for sonarization with increasing distance to the target require an increase in the time interval between pulses. This is necessary to ensure unambiguity in measuring the range to the target. As a result, the power of such signals is sharply reduced. An increase in the duration of pulses reduces the resolution of the location. The way out of the crisis is associated with the use of complex signals, combining a significant duration and thus power with a short autocorrelation function - a good resolution in range. The use of complex signals in sonar began according to traditional paths for radar detection. In particular, in the Fryazino part of the IRE, a sonar was developed using a signal with linear frequency modulation. However, the broadband chaotic signal is considered optimal for the active location of the signal. The duration of such a signal can be increased almost indefinitely, providing good power engineering while maintaining high resolution in range.

In recent years, we have started active work on mathematical modeling of various versions of sonars using broadband chaotic signals, and together with NIIP im. V. Tikhomirov, that in Zhukovsky, and the development of such sonar.

11. CONCLUSION

In the mid-fifties, it seems soon after the twentieth congress, Pyotr Leonidovich Kapitsa suddenly appeared at MFTI. He was one of the founders of the Institute, and after the so-called Nikologorsky exile and the return to the chair of the Director of the Institute of Theoretical Physics of the Academy of Sciences of the USSR, I decided to visit Dolgoprudny and talk with students. In the assembly hall of the Institute he spent about an hour talking with us. I especially remember the call of Petr Leonidovich never to study in science what you are not interested in doing. This was so contrary to the official instructions on the production discipline - "do what the boss orders", which I remember for a lifetime. It should be noted that for the last fifty-five years of my life I have tried to follow Pyotr Leonidovich's advice. I will also add that many of the employees with whom he worked or communicated all these years completely spontaneously followed Kapitza's precepts.

The second commandment, which we tried to follow, belonged to Nikolai Dmitrievich Devyatkov. He claimed that radio electronics is a technical science, and even in the Academy of Sciences, when dealing with radio electronics, it is necessary to strive for the introduction of the results obtained into technical developments. It should be noted that the point of view of Devyatkov was actively supported by Vladimir Yakovlevich Kislov. Being the head of the laboratory, the temporary scientific and technical laboratory, and then the department, he skilfully combined scientific research in the field of dynamic chaos with the implementation of developments aimed at creating unique means of electronic warfare and radar. The receipt of the USSR State Prize and two CM prizes of the USSR

was due precisely to the combination of scientific research in a new direction in radiophysics with technical developments that enabled the results of these studies to be implemented.

REFERENCES

1. Zalogin NN, Kislov VY. AS 28547 USSR. Application 961182 with priority from 15.04.1963.
2. Lorenz EN. Deterministic Nonperiodic Flow. J*ournal of the Atmospheric Sciences,* 1963, 20 (2): 130-141.
3. Myasin EA, Kislov VY, Bogdanov EV. AS 1053711 USSR. Application 0984513 from 8.07.1983 with priority from 22.06.1967.
4. Feigenbaum MJ. Quantitative universality for a class of nonlinear transformations. *J. Statist. Phys.*, 1978, 19: 25-52.
5. Zalogin NN, Kalinin VI, Myasin EA, Surin VV. Microwave noise generator. AS 936373 with a priority of 11/03/1980.
6. InformChaosLab. Information and communication technologies based on dynamic chaos. http://cplire.ru/eng/InformChaosLab/index.htm.
7. Theoretical nonlinear dynamics, Saratov.http: // www.sgtnd.narod.ru/rus/index.htm
8. Zalogin NN, Kislov VV. *Broadband chaotic signals in radio engineering and information systems.* Moscow, Radio Engineering, 2006, 208 p.

NOISE RADAR OF MILLIMETER RANGE

Vladimir V. Kolesov, Evgeny A. Myasin

Kotelnikov Institute of Radioengineering and Electronics of Russian Academy of Sciences, http://cplire.ru
Moscow 125009, Russian Federation

kvv@cplire.ru, eam168@ms.ire.rssi.ru

Abstract. **Practically all modern users of radar systems require an increase in the number and quality of information obtained from the observed space. Multifunctionality and efficiency of modern radar systems can be provided by the development and application of effective broadband technologies, unconventional digital algorithms and new adaptive applied solutions for the problem of processing signals and images in order to identify and recognize various classes of low-contrast objects. In the work on the basis of the IMPATT noise generator, a noise radar model working in the 8-mm range and having a frequency spectrum of the noise signal frequency up to 1 GHz was developed and investigated. The layout of the model includes an IMPATT noise generator module based on a one-diode circuit operating in an 8-millimeter wavelength range with an integrated output power of 40 mW and a non-uniform spectral characteristic of about 6 dB. Receiving and transmitting modules include antennas, waveguide elements: matching elements, impedance matcher, directional couplers, detector heads and attenuators. The computerized control unit provided program-algorithmic support of operating modes and double spectral processing of the signal. An experimental study of the noise radar model in the laboratory demonstrated a high resolution over a range of 15 cm (with an effective bandwidth of 800-900 MHz). The noise immunity of a radio engineering channel model based on a spread-spectrum signal was experimentally investigated. The maximum noise immunity for a radio channel with spreading was determined by the signal-to-noise ratio at the receiver input, at which signal restoration becomes impossible for a given averaging time. In the noise immunity experiment, two types of interference were used: sinusoidal interference, close in frequency to the transmitted signal, and broadband interference matched to the transmitted signal by the spectrum. The results of experiments showed that for both types of interference, the maximum noise immunity is ~25 dB. Thus, ultra-wideband radar technologies based on noise signals are characterized by good electromagnetic compatibility, can be effectively used in the compilation of a radar portrait of an object, as well as in monitoring, positioning and control systems operating under conditions of intense interference.**

Keywords: **ultra-wideband technologies, complex signals, noise signals, radar, noise generator, millimeter range, dual spectral processing, noise immunity, resolution, electromagnetic compatibility**

UDC 621.391

Bibliography - 27 references
RENSIT, 2018, 10(2):235-256

*Received - 31.08.20***18**
DOI: 10.17725/rensit.2018.10.235

Content

1. INTRODUCTION

At present, a promising direction is actively developing in radar, representing broadband and ultra-wideband technologies. In the framework of this direction it is possible to move to a qualitatively new level of solving radar problems for remote detection of objects. In addition to the energy criterion (at the "yes" level "no") of detecting an object against the background of noise and the underlying surface, it is possible to proceed to the formation of a radar portrait of the object and to develop systems for automatic recognition of an object by its portrait, which qualitatively increases the information capabilities of radar systems (radar systems) . Radar with signals with a wide range of frequencies makes it possible to perform highly accurate, informative measurements of the parameters of reflecting objects under difficult electromagnetic conditions under the influence of active and passive interference [1, 2].

The main modern technologies that can ensure the realization of these opportunities are:

- technology of generation, emission and reception of broadband signals based on dynamic chaos [3],
- technologies for processing broadband signals based on fractal analysis and revealing the structural features of the target's radar portrait, which allows detecting and recognizing low-contrast targets in real time in automatic mode when comparing the signal with a reference radar portrait [4].

One of the promising areas that significantly increase the information content of the radar is the use of short-pulse ultra-wideband signals with a spectrum width of 1 GHz or more. In radar with UWB, the increase in informativeness is due to the reduction in the pulse volume of the radar by range. Thus, with a change in the duration of the probe pulse from 1 μs to 1 ns, the depth of the pulsed volume decreases from 300 m to 30 cm. Ultra-wideband radars with pulsed radiation of less than one nanosecond duration have a high spatial resolution of the order of several centimeters when measuring range. When objects are detected at a significant distance from the radar, the necessary signal-to-interference ratio at the receiver input is achieved due to the giant peak power for single ultrashort pulses [5, 6].

In radars with continuous in time radiation of ultrabroadband sounding signals, for example, noise signals, it is possible to obtain the same signal-to-noise ratio at the input of the receiver when the average power of continuous radiation is reduced many-fold. The noise signals in the radar receiver are compressed in the time domain due to the correlation convolution, or in the frequency domain during the double spectral processing [7].

Noise UWB radars continuously emit random electromagnetic signals with a low spectral power density into the surrounding space. Along with the high informativeness and resolution of the measurements, noise radars are characterized by the secrecy, low probability of interception (Low Probability of Intercept) of their own noise emissions and electromagnetic compatibility with other operating means, including narrow-band systems [8].

A certain disadvantage for all radars with continuous radiation is the penetration into the receiving path of the signal from the transmitter, therefore the problem of forming a narrow radiation pattern and efficient shielding of the antennas seems to be quite important [9].

The increase in the accuracy and resolution of radar measurements is due to the complication of the structure and the expansion of the frequency band of the sounding signal. The main requirements for noise radars are high information content and resolution of measurement, stealth, low probability of interception of intrinsic noise emissions and electromagnetic compatibility with other operating facilities, including narrowband systems [10].

The use of complex broadband and ultrabroadband probing signals is one of the promising directions in radiolocation. The use of signals generated on the basis of chaotic algorithms allows to achieve practically the highest noise immunity of the radar to the effect of various interference [11]. The development of the technology of discrete systems and digital processing practically at the frequencies of sounding signals significantly expands the boundaries of the use of

modern radar systems based on phased arrays with adaptive control of their modes and joint processing of signals.

The use of UWB signals in the radar allows:

- to improve the accuracy of measuring the distance to the object and the resolution of the range and angular coordinates, the effectiveness, stability of the radar to the effects of external and narrowband electromagnetic radiation, and interference;
- recognize classes and types of objects;
- simplify the protection equipment against all kinds of passive interference; to eliminate interference dips in the radiation pattern when observing the object at low angles.

A promising application of broadband signals in radar is the use of phase-manipulated signals of continuous radiation with a large base (up to 106) and a minimum peak power [12]. Such SH signals are called noise-like probing signals. Radar systems with a SH signal of detection of ground objects have increased noise immunity and stealth operation [13].

The most complete requirements for simultaneous resolution in range and speed are the noise signals. The main advantages of noise signals in comparison with other complex signals are the following:

- the noise sounding signal is similar to the internal noise of the receiver of the radio technical reconnaissance station, which provides a significant increase in the stealth operation of the radar, which makes it difficult, first, to register the fact of the radar operation and, secondly, to determine the parameters of its probing signal;
- taking into account the prospects of translating the short-range radar into a millimeter range of radio waves, it should be borne in mind that a radar with a noise-like signal can be simply coupled with passive location systems;
- from the general provisions of information theory it follows that the complication of the waveform and the increase in its duration makes it possible to increase its informativeness [14].

2. METHODS FOR PROCESSING RADAR SIGNALS

Signal processing methods are an integral part of radar information acquisition (RLI), the mathematical description of which is rather complicated. The processing procedure for radar signals is one of the most important processes of highlighting useful information. A special place is also given to equipment that can be successfully used to solve problems of constructing radio images from the data of reflected signals from detected objects [15].

In radars with continuous in time radiation of ultrabroadband sounding signals, for example noise signals, it is possible to obtain the same signal-to-noise ratio at the receiver input when the average power of continuous emissions is reduced many-fold. Compression of noise signals in the radar receiver is performed in the time domain due to correlation convolution, or in the frequency domain in the process of double spectral processing. Radar with dual spectral processing is based on the interference of completely incoherent reference and received noise signals [16, 17]. The application of methods for spectral processing of the noise signal makes it possible to improve the accuracy of radar measurements, since frequency measurements currently have the highest possible accuracy.

Double spectral processing, sometimes referred to as cepstrum processing, is an alternative method to the correlation processing of signals in noise radar. As a result of double spectral processing, it is possible to obtain the response component at the output of the receiver as a function of the mutual correlation of the emitted signal and noise reflections from the detected object. The effect of interference with the distributed spectrum on the receiver leads to a decrease in the correlation peak in the secondary spectrum relative to the noise level [19].

3. STRUCTURE OF NOISE RADAR

The radar noise signal n (t) with frequency band Δf is assumed to be stationary and ergodic, which allows us to find the statistical characteristics of random processes, averaging in time individual implementations. This circumstance is important

in noise radar in the case of correlation or double spectral processing of continuous noise signals in real time. The procedure of averaging over an ensemble of a set of statistically independent realizations of random processes is a convenient method of theoretical investigation in noise radar, however, it is rarely used in practice when measuring the mutually correlated function of the emitted and received noise signals due to the complexity or impossibility of realizing the averaging procedure in real time.

At the output of the noise generator, part of the radiated signal branches into the receiver channel of the receiver. The level of the reference signal can be smoothly controlled by means of a controlled attenuator. The reference signal is fed to the input of the linear adder in the radar receiver circuit. On the other input of the linear adder comes an additive mixture of signals from the receiving antenna. The fundamental difference between radar based on interference and double spectral processing of broadband signals is the operation of linear summation of the received sounding and reference noise signals in the linear part of the receiver.

Dual spectral processing of radar signals is performed in the frequency domain, in contrast to the correlation convolution of signals, which occurs in the time domain. Alternative methods of radar with correlation and double spectral processing of signals have fundamental differences in receiver design schemes, however, lead to close results in the implementation of radar measurements [20].

A typical form of the model spectrum of the total noise signal is shown in **Fig. 1** fragment of the spectrogram at the mean frequency f_0 = 3050 MHz. The spectrum fragment in the 100 MHz band is an interference pattern of 10 alternating

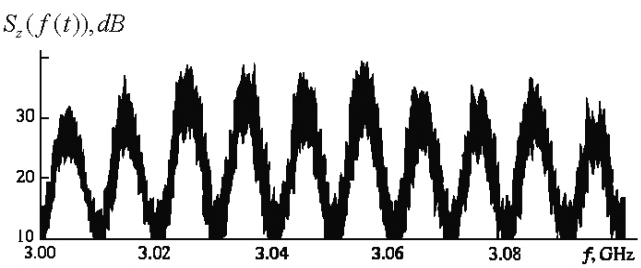

Fig. 1. *Fragment of the spectrum of the ultra-wideband total noise signal.*

bands for the power spectral density, depending on the current frequency *f*.

The initial spectrum of the total noise signal extends over a wide frequency band $\Delta f \approx 2000$ MHz with a lower frequency $f_l \approx 2000$ MHz and an upper frequency $f_h \approx 4000$ MHz. The fragment of the spectrum in Fig. 1 is measured by probing a point object remote from the locator at a distance $L = 15$ meters. The signal reflected from the object is delayed for a time $T = 2L/c = 10^{-7}$ seconds. The number of interference fringes or maxima in the initial spectrum of the total signal will amount to a large value $N = \Delta fT = 200$.

When the frequency band Δf of the sounding noise signal decreases, the number of interference maxima and minima in the spectrum of the total signal decreases. When the frequency band is $\Delta f = 10$ MHz, only one interference maximum $N = \Delta fT = 1$ is observed in the spectrum. The interference of partially coherent noise signals with a narrow frequency band $\Delta f < 10$ MHz occurs under the condition $T \le \tau_c$ when the relative delay $T = 10^{-7}s$ becomes less than the coherence time $\tau_c \approx 1/\Delta f$.

4. MEASUREMENT OF RANGE IN NOISE RADAR

When adding incoherent delayed signals, a periodic interference pattern is observed in the spectral range of the measurements. The spectrum of the total signal is modulated by a function with a period $F_m = 1/T$ inversely proportional to the relative delay of the signals.

The period of modulation of the F_m spectrum in the frequency domain is inversely proportional to the relative delay T of the probing signals:

$$F_m = \frac{1}{T} = \frac{1}{|T_1 - T_0|}. \quad (1)$$

Taking into account the relation $T_1 = 2L_1/c$, it follows from expression (1) that the required range to the target is uniquely calculated as:

$$L_1 = \frac{c}{2}\left[T_0 + \frac{1}{F_m}\right]. \quad (2)$$

Here, T_0 is a known path delay in the reference channel.

The incoherence condition for the delayed signals is written in the form

$\Delta f/F_m >> 1.$ (3)

It follows from (3) that when interference of completely incoherent noise signals is interfered, many F_m scales of periodic modulation of the spectrum (9) in the frequency band Δf of the radar signal are stacked.

In the spectrum band Δf of the total signal, there are many interference fringes (Fig. 1) and many F_m scales of periodic modulation are stacked so that $\Delta f/F_m >> 1$. The period $F_m = 1/T$ of the spectral modulation contains useful information about the relative delay $T = T_1 - T_0$ of the radar signals. If we measure the period F_m of spectral modulation, we can uniquely determine the required range by formula (2).

The secondary spectrum $G_s(F)$ contains a useful spectral peak at the middle frequency F_1 and low-frequency components of the signal and interference concentrated mainly near the zero frequency (**Fig. 2**).

The appearance of an information peak in the secondary spectrum $G_s(F)$ as a function of cross-correlation between the reflected and reference signals leads to the detection of a remote object by a radar with double spectral processing of the ultra-wideband noise signal.

During the calculation of the secondary spectrum $G_s(\mathbf{F})$, an information spectral peak is extracted and a remote object is detected. To determine the parameters of the object, the average frequency F_1 is measured, as well as the information peak level. The required range to the object is uniquely determined by the formula

$$L_1 = \frac{c}{2}\left[T_0 + \frac{F_1}{V_s}\right]. \quad (4)$$

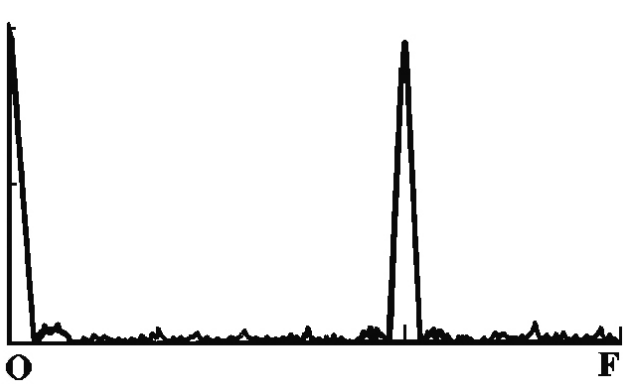

Fig. 2. *Secondary spectrum of the total noise signal.*

Thus, the unambiguous determination of the target range L_1 and the transmission coefficient h in the propagation channel is realized as a result of the second Fourier transform for the spectrum of the sum signal.

The level of low-frequency components can exceed the information peak under the influence of strong interference. To avoid distortion of the information peak, it is possible to compensate for interfering low-frequency components in the secondary spectrum. For this purpose, a double spectral analysis of the received radiation is performed in the absence of useful reflections, when there is no information peak in the secondary spectrum. As a result of the mathematical operation of subtraction of secondary spectra in the presence and absence of a useful signal, only the information peak remains in the form of the envelope of the cross-correlation function. The average frequency F_1 of the information peak uniquely determines the required range to the object.

A radar receiver with dual spectral analysis performs a measurement of the cross-correlation function for the reflected and emitted signals. Such a receiver can be considered as an optimal receiver of the correlation type in the first approximation for a long averaging time, when the variance of the random estimate for the measured cross-correlation function is small [21].

5. RESOLUTION AND ACCURACY OF SPECTRAL MEASUREMENTS

The resolving power of radar measurements is determined by the possibility of distinguishing two closely located objects. The marks from two objects with delays T and $(T + \Delta T)$ can be resolved by measuring the secondary spectrum if the corresponding informative spectral peaks $G_a(F - FT)$ and $G_a(F - FT + \Delta T)$ are frequency-separated by the width of the spectral peak (**рис. 3**).

Each spectral peak in the secondary spectrum is described by a cross-correlation function for signals with a corresponding relative delay. The width of each spectral peak is $\Delta F_c = V_S \cdot \tau_c$, and is determined by the coherence time τc of the radar signal to within a constant V_S.

Thus, two spectral peaks in the secondary spectrum are resolved if they are shifted by the frequency $\Delta F = FT + \Delta T - FT = V_S \Delta T$, which exceeds the width of the spectral peak $\Delta F_c = V_S \tau_c$

$$\Delta F \geq \Delta F_c \text{ or } \Delta T \geq \tau_c. \quad (5)$$

The range resolution for the location of two point reflectors located at a distance L and $L + \Delta L$ amounts to

$$\Delta L = \frac{c}{2\Delta f}. \quad (6)$$

Each informative peak $G_a(F - FT)$ and $G_a(F - FT + \Delta T)$ in the secondary spectrum is a cross-correlation function for the reference signal reflected from the given target. When probing targets with noise signals with a uniform spectrum in the frequency band Δf, a cross-correlation function is measured, the width of the main lobe at the level of the first minimum is $\tau = 1/\Delta f$ and inversely proportional to the band of the probing signal. In the case of double spectral processing, two reflected signals differ if they are separated in time by an interval that exceeds the correlation time.

An estimate of the accuracy of measuring the range to the object L is found by differentiating expression (6)

$$\delta L = \frac{c}{2}\left[\delta T_0 + \frac{F}{V_s}\frac{\delta F}{F} - \frac{F}{V_s}\frac{\delta V_s}{V_s}\right]. \quad (7)$$

The differential (7) reduces to the form

$$\delta L = \left[L - \frac{cT_0}{2}\right]\left[\frac{\delta F}{F} - \frac{\delta V_s}{V_s}\right] + \frac{c\delta T_0}{2}. \quad (8)$$

Here $\delta F/F$ is the relative error of the measurement of the mean frequency F for the information peak in the secondary spectrum $G_S(F)$. The differential (8) also depends on the relative error $(\delta V_S)/V_S$ of determining the V_S frequency for the first spectrum analyzer and on the error in determining the constant delay δT_0 in the receiver reference channel. In turn, the secondary spectrum of $G_S(F)$ is calculated by Fourier transform from the primary spectrum. The relative error $\delta F/F$ of the measurement of the mean frequency F for the information peak in the secondary spectrum $G_S(F)$ is determined by the relative error $\delta f/\Delta f$ of the measurement of the primary spectrum with the frequency band Δf. Then the expression for the square of the error in measuring the range L is reduced to the final form.

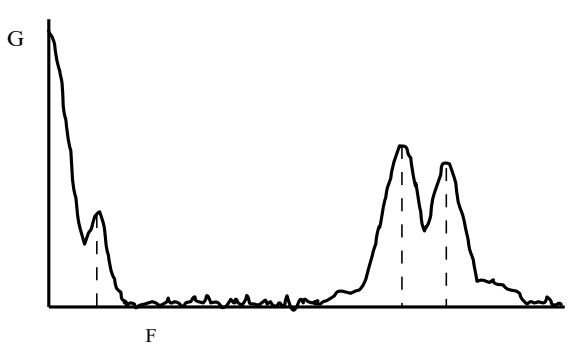

Fig. 3. *Spectral resolution of two point reflectors.*

Here $\delta F/F$ is the relative error of the measurement of the mean frequency F for the information peak in the secondary spectrum $G_S(F)$. The differential (8) also depends on the relative error $(\delta V_S)/V_S$ of determining the V_S frequency for the first spectrum analyzer and on the error in determining the constant delay $\delta \mathbf{T}_0$ in the receiver reference channel. In turn, the secondary spectrum of $G_S(F)$ is calculated by Fourier transform from the primary spectrum. The relative error $\delta \mathbf{F/F}$ of the measurement of the mean frequency F for the information peak in the secondary spectrum $G_S(F)$ is determined by the relative error $\delta f/\Delta f$ of the measurement of the primary spectrum with the frequency band Δf. Then the expression for the square of the error in measuring the range L is reduced to the final form

$$(\delta L)^2 = \left(L - \frac{cT_0}{2}\right)^2\left[\left(\frac{\delta f}{\Delta f}\right)^2 + \left(\frac{\delta V_s}{V_s}\right)^2\right] + \left(\frac{c\delta T_0}{2}\right)^2. \quad (9)$$

The error in measuring the range becomes smaller with decreasing errors $(\delta V_S)/V_S$ and δT_0. If there is no error when setting the frequency scan rate $\delta V_S = 0$ and the constant delay in the reference channel is known to be $\delta T_0 = 0$, then the error in measuring the range to target L is in the form

$$\delta L = \left[L - \frac{cT_0}{2}\right]\frac{\delta f}{\Delta f}. \quad (10)$$

Those. the distance measurement error decreases with increasing the frequency band of the probing signal Δf and with the improvement of the resolving power δf of the first spectrum analyzer [22].

Thus, the main results of applying double spectral processing of the signal are as follows.

When the fully incoherent reflected from the object and the reference signal are added, a periodic

interference pattern is observed in the spectral range of the measurements. The spectrum of the total signal is modulated by a function with a period inversely proportional to the relative delay of the signals. In the spectrum of the total signal, there are many interference fringes and many scales of periodic modulation are laid down, when the relative delay of the signals is many times greater than the coherence time.

Measurement of the period of spectral modulation is due to the Fourier transform of the spectral density of the total signal as a periodic function of frequency. The secondary spectrum of the total signal contains a useful spectral peak at the middle frequency and low-frequency components near the zero frequency. A useful spectral peak corresponds to a mutually correlated function for the delayed and reference radar signals. The average frequency of the information peak is determined by the relative delay of the signals, and the magnitude of the peak depends on the attenuation of the signals in the propagation channels. Measuring the frequency and level of the spectral information peak, uniquely determine the distance to the object and the transmission coefficient in the propagation channel.

The resolving power and accuracy of radar measurements by the method of double spectral analysis are determined by the frequency band of the sounding signal. The accuracy of the range measurement is enhanced by improving the resolving power of the first spectrum analyzer and by introducing a known delay in the radar reference channel.

Dual spectral analysis is a quasi-optimal signal processing in the sense that the secondary spectrum of the sum signal contains informative peaks as a cross-correlation function for useful reflections and a reference signal.

In addition to informative peaks at the main frequencies, the secondary spectrum contains combinational components at the difference frequencies. Each combination component at the difference frequency is a cross-correlation function for a pair of signals received from the respective partial reflectors. The appearance of combinational components at the difference frequencies in the secondary spectrum indicates the detection of a complex object from partial point reflectors. The largest frequency in the spectrum of the combination components determines the radial size of the complex object.

The appearance of combinational components at the difference frequencies may cause difficulties in identifying the main spectral peaks in the secondary spectrum. To avoid ambiguity of the range measurements, it is necessary to introduce additional delay into the receiving channel and to carry out the frequency separation of the spectral peaks in the secondary spectrum. Then the main spectral peaks are shifted to the high-frequency part of the secondary spectrum, and the combination peaks remain in the low-frequency region. The boundary frequency separating the main and combination peaks in the secondary spectrum is determined by the largest radial dimensions of the complex object.

The detection zone for a radar with spectral analysis can extend directly from the transceiver antennas if an additional delay is set in the receiving path for the required value and the condition for interference of completely incoherent signals is satisfied. The greatest detection range is determined by the resolution of spectral analysis by frequency. The increase in the maximum detection range is achieved by a constant delay in the radar reference channel.

The spectral method of radar makes it possible to obtain the same information about the range as in the case of a mutually correlated method, but it has no practical limitations when using ultra-wideband noise signals. With the increase in the frequency band of the probing signals to units of gigahertz, the implementation of noise correlators with controlled or multi-lead delay lines for a priori unknown time is a technically difficult task.

Information about the range to the object is continuously distributed over the entire spectrum of the ultra-wideband total signal. The true range can be determined from fragments of the general spectrum, when other parts of the spectrum are lost or struck, for example, by strong active interference. In this case, the resolving power decreases, and the informativeness of spectral interferometry. A similar effect of restoring information on the part of the

interference pattern is observed in coherent optics and holography.

6. WIDEBAND MILLIMETER WAVE DIODE NOISE GENERATORS

The principles of stochastization of oscillations in electron-wave systems with delay were used as the basis for constructing experimental models of diode GSh. A comparative analysis of the characteristics of the noise signal of solid-state semiconductor generators using Gunn diodes and avalanche-passing diodes (PDDs) in the centimeter wavelength range determined the choice of the active element for the noise generator in favor of the latter. LDPs were also used in noise generators (GSLPDs) of the millimeter wave band [23].

Low-power generators (with a power of up to 100 mW) can be developed in a solid-state version using a single-diode circuit using an LAP. The analysis of the domestic element base showed that domestic industrial single-pass diodes 2A717A-G, 33GHz-37.5GHz range, or KA717-V, G range 37.5 GHz-53.5 GHz can be used as the LAP, which provided in the single-mode generators of harmonic oscillations the output power up to 100 mW and overlapped the range from 8 mm to 6 mm. In this case, the range of operating currents of these diodes ranged from 100 mA to 150 mA, and the breakdown voltage was 20 ... 22 V. For working with diodes of the KA-717-A-G series, a special power source was created, which ensures the operation of the LAP at high breakdown voltages and large operating currents.

The waveguide design of a single-mode harmonic oscillator on the LPD (GLPD) with an open-cavity open-cavity resonator was taken as the basis of the generator design. Schematically, the design of the resonator chamber of the GLDD is shown in **Fig. 4**.

In Fig. 4 that the autogenerator includes the following elements: an open-wave open resonator formed by a disk terminating the current lead and a heat sink of the LAP, a resonance frequency tuning device (movable plunger) and a decoupling filter in the power circuit and an additional tunable resonator (in Fig. 4, not shown). The adjustment of the communication with the load was carried out with a coupling screw located at the center of the wide wall of the waveguide between the diode and the load. The diode was placed in a standard waveguide 7.2x3.4 mm. No other filtering devices such as resonant windows or resonance gaps have been used

In this design, by regulating the current through the diode and tuning elements, it is possible to obtain in stellar oscillation mode a stochastic oscillation mode with a bandwidth of ~ 400 MHz-000 MHz and an output power of ~ 50 mW ... 30 mW, respectively, in the 8 mm wavelength range.

The phenomenon of stochastization of oscillations is a fundamental property of a nonlinear autooscillatory dynamical system, and the state of generation of stochastic (noise) oscillations is as natural as generation of regular oscillations. The oscillatory system GSLPD does not have an external feedback line, the change in the transmission coefficient of which can change the degree of nonlinearity in the system. It is a complex multimode resonator, and therefore it is impossible to single out one control parameter, the variation of which could change the operating modes of the generator without changing the nonlinear characteristic of its active element or the property of the oscillatory system [24]. This circumstance substantially complicates the search and adjustment of stochastic regimes, both in the experimental investigation of such a generator, and in the mathematical modeling of processes occurring in it [25]. Therefore, for the experimental

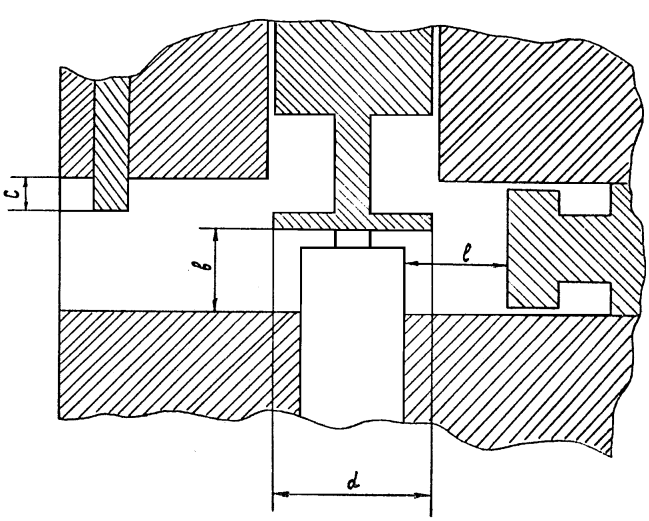

Fig. 4. *Construction of a resonator chamber of a GLPD.*

investigation of the signal generated by the GLDD, depending on the variation of various control elements of the structure and current through the diode, a special stand was created, which allows measuring not only the output power, but also the spectral characteristic of the generated signal. It should be noted that for some applications it is necessary to have an idea of the distribution of the probabilities of the signal or of the distribution of the probabilities of its envelope, on the basis of which one can judge the degree of their proximity to the Gaussian or Rayleigh distribution, respectively. This fact has sufficiently served as a basis for choosing an LAP as an active element for a noise generator [26].

7. MODEL OF THE RECEIVING AND TRANSMITTING UNIT SSR

A block diagram of the layout of the receiving and transmitting block SSR is shown in **Fig. 5.** The measuring part of the noise radar provides a double spectral processing of the total signal to determine the range to the object and contains two spectrum analyzers (AS) in its composition. The first one is high-frequency, with the help of which the spectrum of the total signal (the signal reflected from the object + reference signal) is analyzed at the carrier frequency in the millimeter wavelength

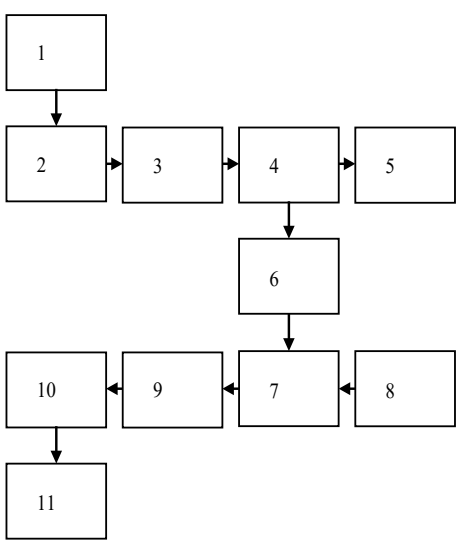

Fig. 5. *Block diagram of the receiving and transmitting unit SSR: 1- power supply, 2 - noise generator 8 mm of the wave band, 3 - gate-isolation, 4 - directional coupler of the reference signal, 5 - radiating antenna, 6 - attenuator, 7 - adder received and reference signals, 8 - receiving antenna, 9 - spectrum analyzer, 10 - ADC, 11 - computer.*

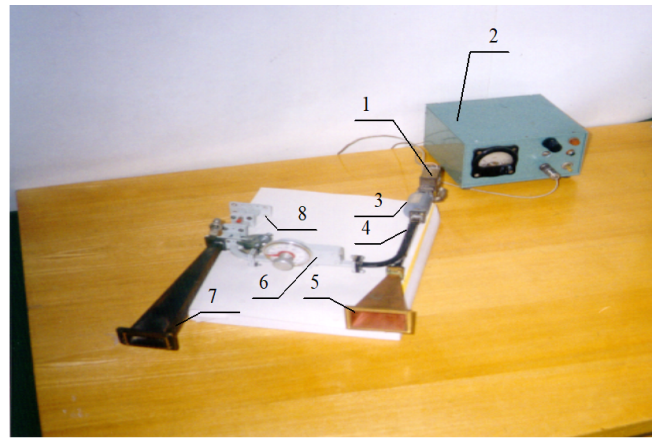

Fig. 6. *Model of the receiving and transmitting unit SSR: 1 - LDP-noise generator of 8 mm wave band, 2 - power supply, 3 - ferrite isolation valve, 4 - directional coupler of the reference signal, 5 - emitting horn, 6 - attenuator, 7 - receiving horn, 8 - adder of the received and reference signals.*

range. The second spectral transformation is carried out using a standard ADC connected to a personal computer.

The hardware part of the noise radar is shown in **Fig. 6**.

The width of the GS spectrum can be adjusted by means of the operating current through the diode. For example, at a diode current of I = 93 mA, the spectral width is 700 MHz, and at a current I = 100 mA, the width of the GS spectrum is 800 MHz. The output power is 3.6 mW and 4.4 mW, respectively.

8. RADAR MEASUREMENT OF DISTANCE

To test the calculated theoretical relationships made in the analysis of the double spectral signal processing method, when measuring distances using the developed transceiver unit under laboratory conditions, test measurements were made at distances L_1 = 3.5 m and L_2 = 10 m to the signal reflector. Calibration of the SIR layout consists in determining the hardware constants that depend on the relative position of the reflecting antennae of the reflector required for metrological radar measurements. The mobile stand with the SCHL layout is shown in **Fig. 7.**

For the two measured distances, the corresponding coefficients α and L_0 were found, which are constant for a given SSR configuration, as a result of solving the system of equations:

Fig. 7. *Mobile stand with SCHL layout.*

$$L_1 = \alpha\Omega_1 + L_0,$$
$$L_2 = \alpha\Omega_2 + L_0, \quad (11)$$

where Ω_1 = 99.4 Hz, Ω_2 = 293.3 Hz are the measured frequencies in the secondary signal spectrum after double spectral processing.

As a result of solving the system of equations (11), the following values of these constants were obtained: α = 0.0335, L_0 = 0.174 m.

To check the coefficients obtained, measurements were taken at intermediate distances of 6.37 m and 7.1 m from the measured values of modulation frequencies Ω_3 = 185 Hz and Ω_4 = 207 Hz, obtained by double spectral processing of the signal from the spectrum analyzer C4-60. The control measurements of the distance by the laser range finder yielded an almost exact coincidence (up to 10 cm) with radar measurements obtained by the double spectral signal processing method.

The modulation frequencies corresponding to different distances to the reflector in the primary spectrum were determined on the basis of a secondary spectral transformation of the primary total spectrum of the reflected signal with the reference signal. A photograph of the total spectrum of the reflected signal with a reference signal on the screen C4-60 is shown in Fig. 8.

Fig. 8. *The total spectrum of the reflected signal with the reference signal on the screen C4-60 (scanning scales -50 MHz / div).*

9. STUDY OF THE RESOLVING POWER OF THE SIR MODEL FOR THE RANGE

To realize the maximum range resolution it was necessary to extend the band to the maximum possible in the given design of the transmitting module. For this purpose, a high-frequency diode KA717B was used in the GSh. In **Fig. 9** shows the types of broadband spectra of the noise signal of the spectrum at different operating currents of the GSH. It should be noted that the expansion of the band reduces the integrated power of the noise signal to units of milliwatts.

As can be seen in Fig. 9, the maximum spectral width is ≈1000 MHz, while the high-frequency part of the spectrum (above 700 MHz) has a significant unevenness and a lower value of the noise power density.

To obtain the maximum amplitude in the modulation signal of the total frequency spectrum, it is necessary to vary the power level of the reference signal.

Adjustment of the tap-off power from the emitted noise signal was carried out using a calibrated precision attenuator. The calibration schedule of the attenuator is shown in **Fig. 10**.

In **Fig. 11** is a photograph of the total spectrum of the reflected signal with a reference signal on the screen C4-60 at a distance to the reflector of 2.4 m. Fig. 11 it can be seen that only the central part of the primary signal spectrum, shown in Fig. 8. Thus, the expected resolving power will be ≈0.14 m.

In **Figs. 12, 13** and **14** show the results of double spectral processing of the signal from the spectrum analyzer C4-60 at a distance of 2.4, 2.55 and 2.7 m from the reflector.

As seen in Fig.12, the mark from the reflector in the secondary spectrum is determined by the frequency Ω = 143.3Hz.

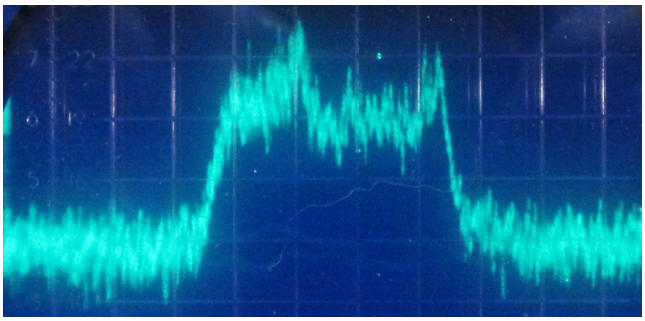

a) spectral characteristic of the GS in noise mode at a current of 136 mA. The scale is 200 MHz / div. P = 4.3 mW. The spectral width is ~ 800 MHz, the spectral unevenness is ~ 3 dB.

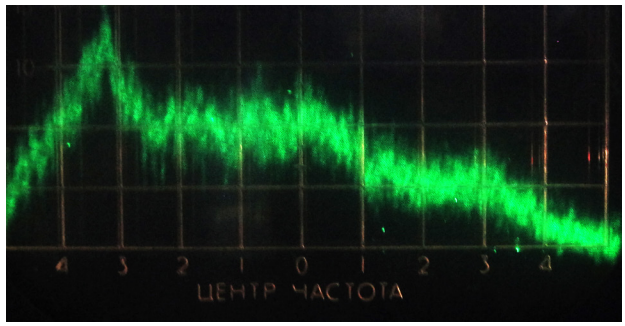

b-spectral characteristic of the GS in noise mode at a current of 145 mA. Scale 100 MHz / div. P = 3.5 mW. The spectrum width is ~ 1000 MHz, the spectral unevenness is ~ 5 dB.

Fig. 9. *Types of spectra of the noise signal GSh.*

As can be seen in Fig. 13, the mark from the reflector in the secondary spectrum is determined by the frequency Ω = 150 Hz.

From Fig. 14 that the mark from the reflector in the secondary spectrum is determined by the frequency Ω = 156.55 Hz.

Thus, the real resolving power of the SIR layout in determining the range is determined by the achieved characteristics of the noise signal and in this case is 15 cm.

Obtaining the necessary radar characteristics by distance is provided by the use of existing transmit-receive modules of the appropriate power with the necessary input and output parameters. The values of all the basic parameters for the SSR can be obtained from the basic radar equation:

$$R_{\max} = \sqrt[4]{\frac{P_{tr} G_{tr} G_{rc} S_{eff} \lambda^2}{(4\pi)^3 P_{rc-\min}}}, \qquad (12)$$

where R_{max} is the maximum working range of the SSR, P_{tr} is the radiation power of the radio transmitter, P_{rc-min} is the minimum signal power at the receiver input, G_{tr} and G_{rc} are the transmission and receive antenna gain factors, S is the effective scattering area of the reflector, and λ is the wavelength of the emitted signal.

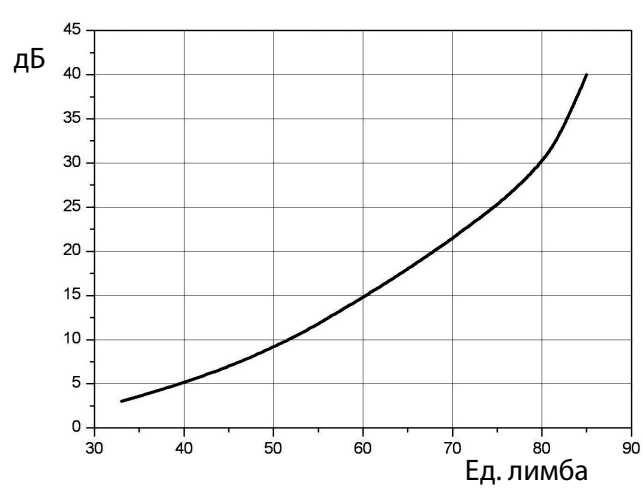

Fig. 10. *The calibration schedule of the attenuator.*

It follows from relation (12) that to increase the range it is necessary to increase the transmitter power, increase the sensitivity of the receiver, and use antennas with maximum amplification factors. Parabolic antennas in the MM-range of wavelengths have significant gain factors of 10^4-10^5 depending on the dimensions of the paraboloid. Agilent Technologies is using exclusive technologies such as a low noise signal path and a special Noise Floor Extention technology to eliminate noise due to distortion, further expand the dynamic range and provide an average level of the receiver's own noise of -140 dBm at a frequency of 50 GHz

Thus, in order to provide an operational range of SHRL of the order of 500 m with an effective area of scattering of the object of 1 m^2 with a potential resolution in the range of about 10 cm (1 GHz probing noise band), using 1 m parabolic antennas and a mixer sensitivity at the receiver input

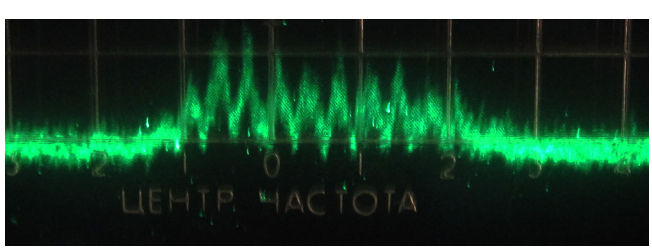

Fig. 11. *The total spectrum of the reflected signal with the reference signal on the screen C4-60, scale -200 MHz / div (distance to the reflector 2.4 m).*

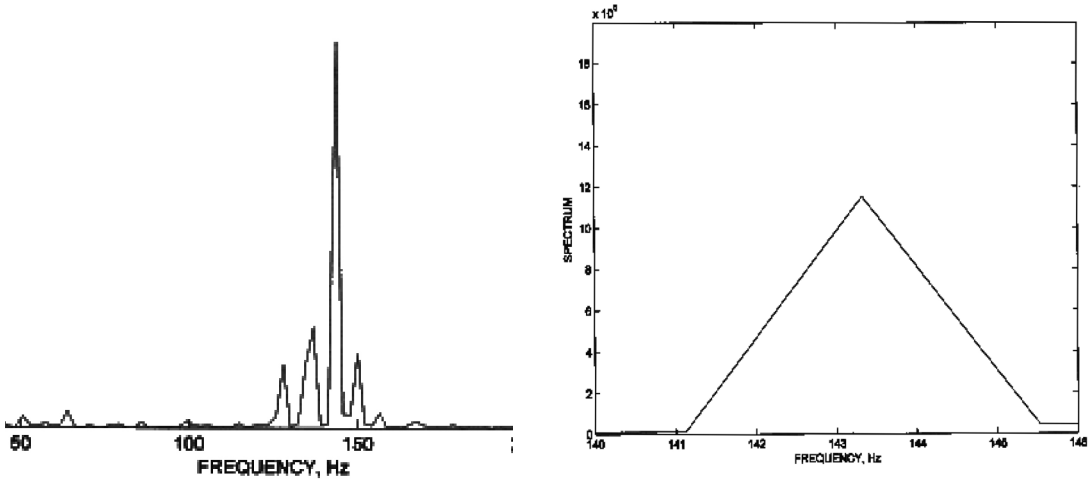

Fig. 12. *The results of double spectral processing of the signal from the spectrum analyzer C4-60 at a distance to the reflector of 2.4 m.*

-140 dBm, it is necessary to use a transmitter with an integrated radiation power of the order of 200 W.

10. ESTIMATION OF NOISE IMMUNITY OF SHRL UNDER THE EFFECT OF NARROWBAND AND BROADBAND INTERFERENCE

An important quality of noise radars with continuous emission is energy concealment from electronic reconnaissance means. The radiated signals of the SRLS at the input to the receivers are under noises and therefore are indistinguishable from them in terms of their correlation properties.

The extension of the signal bandwidth is usually achieved by such carrier wave modulation that forms a modulated signal with a bandwidth wider than the modulating function. An effective way of expanding the signal spectrum is its phase modulation [27]. It is implemented on the basis of a discrete phase manipulator. In order to provide a wide frequency band, the use of a π-modulator is most effective, in which two states correspond to the absence of a phase shift (zero shift) and a phase shift by π. Such modulators are effectively implemented in bridge circuits with switching p-i-n diodes.

The noise immunity of a radio engineering channel model based on a noise-like carrier was experimentally investigated (**Fig. 15**). Coders implemented one of the developed algorithms for generating a class of chaotic signals.

The spread of the transmitted signal from the microwave generator (1) was extended by means of the microwave phase manipulator FM1 (3). The microwave signal at the middle frequency Fcp entered the FM1 input, whose control was carried out by a chaotic binary pulse train from the encoder (6). As a

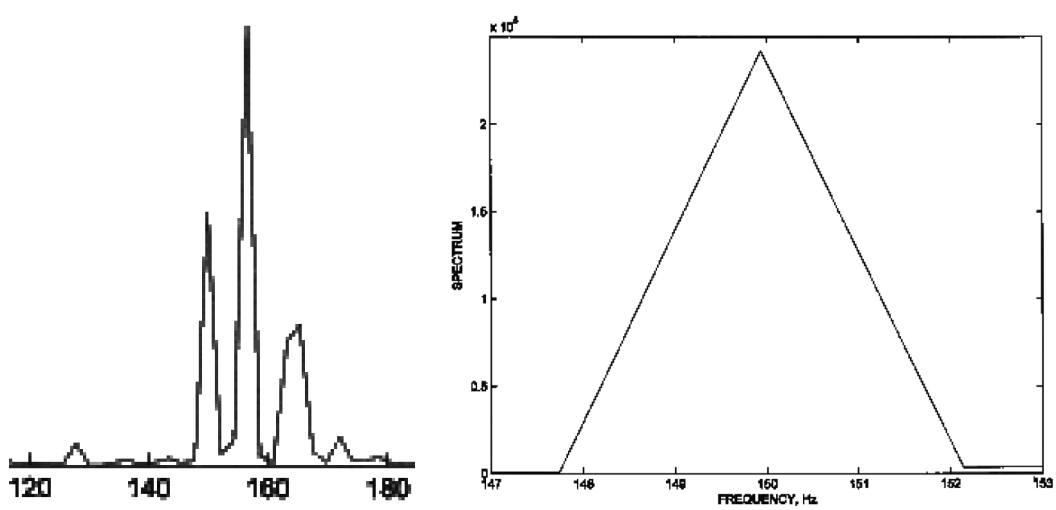

Fig. 13. *Results of double spectral processing of the signal from the spectrum analyzer C4-60 at a distance to the reflector of 2.55 m.*

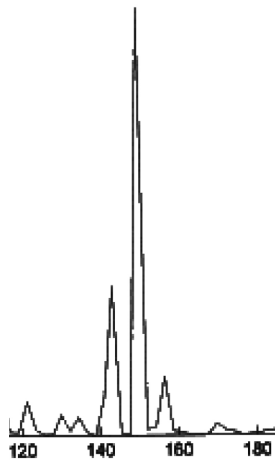

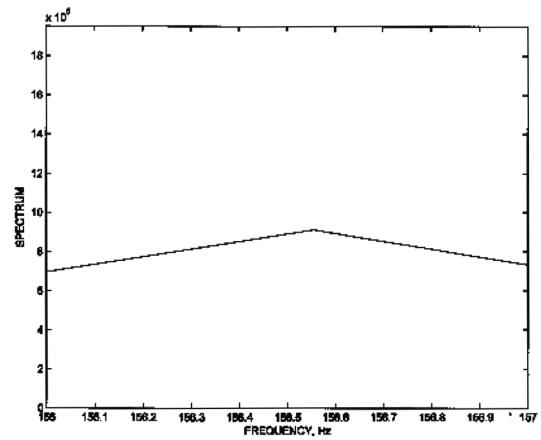

Fig. 14. *The results of double spectral processing of the signal from the spectrum analyzer C4-60 at a distance to the reflector of 2.7 m.*

result, a noise signal with a continuous spectrum was observed at the output of FM1 (3).

The signal with the frequency Fm entered the input of a phase modulator controlled by a chaotic binary pulse train from the digital encoder. At the output, the signal had a continuous noise-like spectrum. To this signal the interference signal was mixed, the total signal was radiated by the transmitting signal and received by the receiving antenna. In the receiving module the convolution of the received signal was made, for this purpose it was fed to an identical modulator, to which an identical chaotic binary sequence was fed.

In an experiment to determine noise immunity, two types of interference were used: sinusoidal interference, close in frequency to the transmitted microwave signal, and broadband interference matched by the spectrum with the transmitted signal (Fig. 15). Broadband interference was formed using the microwave phase manipulator FM2 (4). Control of FM2 (4) was carried out by a separate encoder (7) with the same clock frequency as the encoder (6) of the transmitter. The coding sequences of the two encoders (6) and (7) are different and uncorrelated in time. The experiment was performed with the synchronization of the coding sequences for the modems of the transmitter and receiver, which was provided by the use of an adjustable delay (9). The reverse coherent compression with respect to the frequency of the received signal was made by the modem (5) in the receiver circuit.

As a criterion for noise immunity, the coiled signal was exceeded at the output of the receiver (12) above the noise background, depending on the signal-to-noise ratio at the receiver input.

In **Fig. 16** shows the results of measuring the signal-to-noise ratio (S_c/S_n) at the output of the receiver depending on the ratio of interference

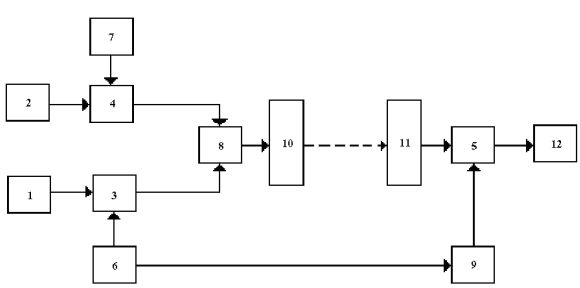

Fig. 15. *Block diagram of an experiment to study noise immunity of a channel with a noise-like carrier. Microwave signal generators and interferers -1 and 2, respectively; phase modulators ΦM1, ΦM2 and ΦM3 - 3, 4 and 5; encoders 6 and 7; Microwave totalizer - 8; adjustable delay line - 9; transmitting and receiving microwave antennas - 10, 11, spectrum analyzer -12.*

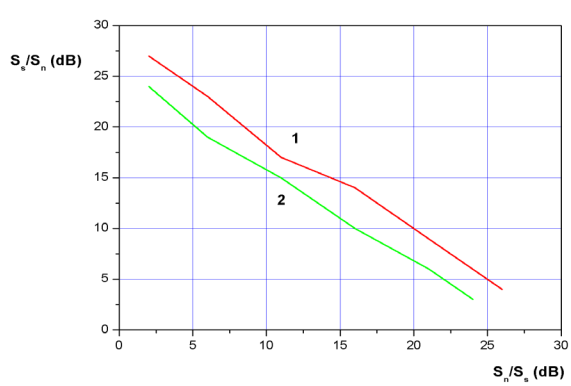

Fig. 16. *The signal-to-interference ratio (Sc / Sш) at the output of the receiver depending on the ratio of the interference levels and the signal at the receiver input (Sш / Sc) for two kinds of interference: narrowband (1) and broadband (2).*

levels and the signal at the receiver input (S_n/S_c) for two kinds of interference: narrowband (1) and broadband (2). The maximum interference immunity for a radio channel with spreading is determined by the signal-to-noise ratio at the receiver input, at which signal restoration becomes impossible for a given averaging time.

Thus, the experimental results show that for both types of interference, the maximum noise immunity is ~ 25 dB. Under the influence of narrow-band interference, the spectrum of the total signal and interference at the receiver's input has the form of continuous in the band broadband noise corresponding to the received signal with spreading, above which the sinusoidal noise rises. The decoder in the receiver ensures convolution and extraction of a useful signal. Simultaneously there is a "blurring" of the power of narrow-band noise across the spectrum in the entire band, turning the noise into a noise pedestal over which the convoluted signal rises.

1. CONCLUSION

Practically all modern users of radar systems require an increase in the number and quality of information obtained from the observed space. Multifunctionality and efficiency of modern radar systems can be provided by the development and application of effective broadband technologies, unconventional digital algorithms and new adaptive applied solutions for the problem of processing signals and images in order to identify and recognize various classes of low-contrast objects.

In the present work, a noise radar model operating in the 8-mm band and having a frequency spectrum of the noise signal frequency up to 1 GHz is developed, developed and studied on the basis of the noise generator. The layout of the model includes an LPD noise generator module based on a one-diode circuit operating in an 8 millimeter wavelength range with an integrated output power of 40 mW and a non-uniform spectral response of about 6 dB. Receiving and transmitting modules include antennas, waveguide path elements: matching elements, decoupling, directional couplers, detector heads, attenuators. The computerized control unit provided program-algorithmic support of operating modes and double spectral processing of the signal.

An experimental study of the noise radar model in the laboratory demonstrated a sufficiently high accuracy of the radar range measurements in the entire measurement range for dual spectral processing of the signal, as well as a high resolving power over a range of 15 cm (with an effective bandwidth of 800-900 MHz).

The noise immunity of a radio engineering channel model based on a noise-like carrier was experimentally investigated. The maximum noise immunity for a radio channel with spreading was determined by the signal-to-noise ratio at the receiver input, at which signal restoration becomes impossible for a given averaging time. In the noise immunity experiment, two types of interference were used: sinusoidal interference, close in frequency to the transmitted signal, and broadband interference matched to the transmitted signal by the spectrum. The results of the experiments showed that for both types of interference, the maximum noise immunity is ~ 25 dB.

Thus, ultra-wideband radar technologies based on noise signals are characterized by good electromagnetic compatibility, can be effectively used in the compilation of a radar portrait of an object, as well as in monitoring, positioning and control systems operating under conditions of intense interferenc

REFERENCES

1. Immoreyev IYA. Ultra-wideband radars: new opportunities, unusual problems, system features. *Bulletin of MSTU. Ser. Instrument making,* 1998, 4: 25-56.
2. Bunkin BV, Reutov AP. Directions of development of radar systems. *High technology,* 2002, 4:8-12.
3. Kolesov VV, Potapov AA. The Information Technologies on Dynamic Chaos for Telecommunication, Radar and Navigation Systems. *Electromagnetic Phenomena*, 2005, 5(2(15)):89-104.
4. Potapov AA. The Textures, Fractal, Scaling Effects and Fractional Operators as a Basis of New Methods of Information Processing and Fractal Radio Systems Designing. *Proc. SPIE,*

2009, 7374:73740E-1-73740E-14 (http://spie.org/x648.html?product_id=829032).
5. Verba BC, Dod VK, Trofimov AA, Chernyshev MI. Application of ultrashort pulses in radar systems of airborne patrol complexes. *Materials I Int. Conf. "Ultra-wideband signals and ultrashort impulses of the radar, communications and acoustics"*. Suzdal, 2005. Moscow, *Proceedings of the RNTORES them. A.S. Popov,* 2005, no. 1.
6. Skosyrev VK, Osipov ML. Features and properties of short-pulse radar. *Bulletin of Bauman MSTU, Specialist no. "Radioelectronics*", 1999, №4.
7. Chapursky VV. Uncertainty functions of UWB multifrequency signals. *Tr. Conf. "Ultra-wideband signals and ultrashort pulses in radar, communications and acoustics.*" Suzdal, 27-29 Sept. 2005, p. 21-25.
8. Bystrov RP, Dmitriev VT, Potapov AA, Sokolov AV. *Questions of perspective radiolocation*. Ed. A.V. Sokolov. Moscow, Radiotekhnika Publ., 2003, p. 20-48.
9. Kolesov VV, Fionov AS, Gorshenev VN. The modeling of the radioabsorbing medium on the basis of composite materials from the polyvinylchloride plastisols. *RENSIT*, 2014, 2(2):138-161.
10. Varakin LE. *Communication systems with noise-like signals*. Moscow, Radio i svyaz Publ., 1985.
11. Belyaev RV, Kalinin VI, Kolesov VV. Interference immunity of a spread spectrum communication system based on chaotic binary codes. *J. of Communications Technology and Electronics,* 2003, 48(10):1157-1185.
12. Belyaev RV, Kalinin VI, Kolesov VV. Formation of a noise-like carrier in spread spectrum communication systems. *J. of Communications Technology and Electronics,* 2001, 46(2):214-223.
13. Belyaev RV, Vorontsov GM, Kislov VYa, Kolesov VV, Krupenin SV, Popov AM, Ryabenkov VI. Complex Chaotic Discrete Signals in Telecommunications, Radar and Navigation Systems. *J. of Communications Technology and Electronics,* 2006, 51(9):1116-1128.
14. Grinev AY. (ed.) *Broadband and ultra-wideband signals and systems*. Moscow, Radiotekhnika Publ., 2009.
15. Solovyev NA, Slukin GP, Chapursky VV. Model of radio image of objects in the holographic radar systems of the planned analysis. *J. of Communications Technology and Electronics,* 2018, 63(6):619-624. DOI: 10.7868/S0033849418060153.
16. Kalinin VI. Ultra-wideband radar with double spectral processing of noise signals. *Radiotekhnika*, 2005, 3:25-35.
17. Astanin LYu, Kostylev AA. *Fundamentals of ultra-wideband radar measurements*. Moscow, Radio i svyaz Publ., 1989.
18. Radzievsky AT, Trifonov PA. *Processing ultra-wideband signals and interference*. Moscow, Radio i svyaz Publ, 2009.
19. Chapursky VV, Sablin VN, Kalinin VI, Vasilyev IA. Wideband Random Noise Short Range Radar with Correlation Processing for Detection of Slow moving objects behind the Obstacles. *Proc. of the 10th Intern. Conf. on Ground Penetrating Radar*. Delft, Netherlands, 2004, p. 199-202.
20. Kalinin VI, Chapursky VV. The effectiveness of the dual spectral analysis. *J. of Communications Technology and Electronics*, 2006, 51(3):303-313.
21. Zalogin NN, Kalinkevich AA, Kirillin KA. Calculation of the signal-to-noise ratio for a radar station. *J. of Communications Technology and Electronics*, 1993, 38(2):278.
22. Kalinin VI, Chapursky VV, Cherepenin VA. Ultra-wideband noise radar with high spatial resolution. *Tr. 3rd All-Russia. scientific and technical. Conf. "Radiolocation and radio communication"*. Moscow, 2009, p. 194-196.
23. Kislov VYa, Myasin EA, Zalogin NN. On nonlinear stochastization of self-oscillations in an electron-wave generator with delayed feedback. *J. of Communications Technology and Electronics*, 1980, 25(10):2160.
24. Kalyanov EV, Kalinin VI, V.Ya. Kislov VYa. Parametric excitation of complex and chaotic oscillations in a dynamical system with a resonator in a chain of delayed feedback. *Journal of Communications Technology and Electronics*, 2002, 47(8):984-997.
25. Kalyanov EV, Kalinin VI. Autostochastic system with parametric excitation. *Technical Physics Letters*, 2002, 28(13):46-50.
26. Myasin EA, Kotov VD. Broadband diode generators of millimeter wave noise. *Radiotekhnika*, 2005, 3:46-50.
27. Kalinin V, Panas A, Kolesov V, Lyubchenko V. Ultra wideband wireless communication on the base of noise technology. *Proc. 16th Intern. conf. on microwaves, radar and wireless communications,* 2006, Krakow, Poland, 2:615-618.

APPENDIX

NOISEOTRON OR MY LIFE IN THE 16th DEPARTMENT OF IRE RAS

Myasin E. A.

Kotelnikov Institute of Radioengineering and Electronics of RAS, Fryazino Branch, http://www.cplire.ru
Fryazino 141190, Moscow Region, Russian Federation

eam168@ms.ire.rssi.ru

Content

1. DOFRYAZINSKY PERIOD IN THE LAB. 162

I read not without interest this narrative on the theme "My Life in Science" by my colleague Mr. N.N. Zalogina. Of course, it seems to him that everything was exactly as he remembers or wants to remember. Will have to continue in the same spirit.

I will not correct the author's memories of events related to my person in terms of obtaining a broadband noise signal in the ring system of two TWTs, but I will still make some observations about some events in my being of development and the formation of "chaotic" subjects in the laboratory V.Ya. Kislova. Especially since I was his deputy from 1968 to 1980. Yes, indeed, I, Myasin EA, moved to work at IRE from the company PO Box 1598 in Sredmash a year after the end of MEPhI in order to become and have the opportunity to participate in international competitions abroad. It happened on October 2, 1962. I was not yet a master of sports, but I really wanted to be from childhood. The working atmosphere in the laboratory was so creative and interesting, and most importantly, it concerned completely unfamiliar technical fields (microwave electronics, technical electrodynamics, plasma theory, etc.) that I spent about a year mastering these new fields of knowledge. I have learned something from literature in MEPhI. Well, I did not forget the university course of mathematics and physics. He studied with pleasure and even with frenzy, because he did not want to be lagging behind. In the process of this "acclimatization" head. lab. I was attached to the work of various experimental groups so that I could learn with a new experimental technique for me. My young teacher, Erdeni Vladimirovich Bogdanov, was my mentor and teacher, a model of attitudes toward obtaining experimental results, over the next few years. Under his leadership, I, after all, remained on the installation of the first pulsed ruby laser in IRE, received from Z.S. Chernova, "underground" nickname "caretaker laser beacon," and became a co-author of my first publication in a private press on the heterodyning of laser radiation using photo TWT ten-centimeter range.

Despite the lack of mutual understanding, which happened later with years of teamwork, I am grateful to V.Ya. Kislov, and because he took me to his laboratory and gave me an opportunity to comprehend the wisdom of a new science and technology for a year, and I will remember this for the rest of my life.

Probably, the laboratory staff first looked at me with suspicion, still "stranger", but I did not notice, they were all pretty intelligent people: both scientists and laboratory assistants.

At that time, the staff of the laboratory 162 was remarkably friendly: they celebrated the significant dates of the employees, celebrated holidays, went to demonstrations, and later even ate my hunting trophies-a wonderful wood-grouse noodles and two five and a half kilogram wood grouses.

I think that V.Ya. Kislov did not regret that he took me to work, like many other employees, whom I once was a "stranger" and who, thanks to the discovery of the noise, were able to defend their Ph.D. theses and not only them. Today, unfortunately, I can not ask V.Ya. Kislov this question, since he died after the tragic events that happened to him in the 90s. And if it were not for these events, he probably still had a lot to do, because he was truly devoted to science, he was talented in everything: in understanding the physics of phenomena, in

developing theoretical models, in organizing work and in recruiting personnel. I was his first graduate student. He did not teach me anything, but I learned a lot from him!

It is appropriate to recall here the mentioned topic "Saber", which characterizes in many ways the character of V.Ya. Kislov, his style of work and decision-making. This was the first contractual work, in which the "severe" parameters of the broadband noise signal, necessary for the presentation of the commission for acceptance of work, were recorded. On this TK in the IRE before this, apparently, no one dared. In the Institute wall newspaper, who apparently knows about this TK anonymous wrote under the photograph of V.Ya.: "The Saber is hanging over you sharp, it's quite easy to cut yourself off!"

The co-executor of the work was the Kharkiv Physicotechnical Institute, in which a model of a noise generator was created on the basis of a self-made electrodynamic spiral-plasma system. I (according to the memoirs of NN Zalogin, a young specialist) went to Kharkov and meticulously carried out the acceptance of this part of the work. For which he paid, because he was late for the return train Kharkiv-Moscow due to a joyful feast in connection with the recognition that I had completed the work on time and in full. I had to get to Moscow in the trolley of a freight train, where I was allowed to load after meeting my "untried" with the station's head.

In our laboratory, such a generator was a Vesnianka TWT, 10 kW of the UHF of the decimeter range, which operated under continuous pumping. This TWT, in which instead of the usual Pierce gun was built a magnetron gun (as noisy), V.Ya. got it in "Titan", or, as they said then, in the Southwest. TWT worked under continuous pumping, and I was responsible for working on this high-voltage stand. We have generated broadband noise in the entire TWT band, varying the pressure of the residual gases in its volume, but in the form of noise bands with a very poor degree of overlap. Here N.N. Zalogin is right, there was not enough reinforcement. The output power of the generator was, of course, not 10 kW, but of the order of 5 kW exactly, and in continuous mode. It happened a little before my business trip to Kharkov, so I used to pick on them.

The work was successfully commissioned by the State Commission, in the "peak" to ill-wishers, but not without an emergency. While explaining the principles of Vesnyanka's work to members of the commission, I, as I had never done before, put my elbow in a metallized dressing gown on a metal frame that served as a fence and an electrical safety margin when working at the stand. The result was not slow to show itself. From the negative electrode of the rectifier connected to the electron gun of the TWT (the lama collector was at the floor), there was a breakdown of the air gap of 20-30 centimeters on the fingers of my hand. There was a spark and a characteristic crackle. I rested my hand, but the members of the commission were frightened. It happened in 1964.

This passion for work did not pass for me in vain. In the same 1964 my team SK "Kuntsevo" became a bronze medalist of the USSR Championship on a hand ball, and me and a number of other team players were awarded the title of Master of the USSR sort of handball. During the presentation of the certificate, the coach invited me to become a professional athlete.

The conversation was like this. "How much do you get?" - "120 rubles." - "You will receive 150 rubles, be listed at the plant as an engineer and train four times a week. Have agreed? ". And I answered without hesitation: "No!", Thus signing the end of my sports career, not immediately, but, as it turned out, in the foreseeable future.

Nevertheless, training and competition continued in 1965, and in 1966, and so until 1974, although, in 1970, already in the team of the second division "Locomotive". I was away from work for training and competitions, taking leave at my own expense. At first these were absences within the Union, but in 1966 my team became the USSR Champion and got the right to play for the European Champions Cup, and it was necessary to go abroad. I needed a description from the Party Committee and the Trade Union Committee, and I received it, and traveled to many countries of Europe, thanks to the fact that Zarem Sergeevich Chernov supported me signing my positive characteristic for me, I do not know why I trusted. Of course, I could not fail him and never failed. In addition, I owe him and the fact that he became the head of the laboratory 168. And, of course, I always remember this. Unfortunately, he has not been with us for a long time.

But between the fees and competitions I still worked. And, after the break with a special pleasure. Be that as it may, it was in 1966 that I was fortunate enough to deal with the TWT modes in the noise circuit, about which N.N. Zalogin.

2. THE FRYAZINO PERIOD

In 1970, I, like most employees of the lab. 162, went to work in the lab. 166 of the Fryazino part of the IRE, as mentioned above, and continued to work on the properties of various variants of noise noise and its possible introduction into various systems. At the same time, we had to interact with the staff of the lab. 168, engaged in the implementation of research results lab. 166 and the lab. 169, which will be discussed in more detail later.

After the award in 1980 of our work of the USSR State Prize, the leadership of the department in the person of Z.S. Chernova (through the parliamentarian NN Zalogin) invited me to participate in the competition for the post of head of the laboratory 168, which was temporarily performed by V.V. Evdokimov.

Unlike the choice of the professional sportsman's activity, not only money was put on the scales (400 rubles head of the lab, instead of 300 rubles), but, in general, my subject. I had to jump off the train that I had borne, which was gaining momentum. There was something to think about! But then I remembered (in general, I never forgot) that in the laboratory of 166 I worked in the position of the doctor of medical sciences. until 1977 (after defending his Ph.D. thesis in 1970). I did not address my boss with a request to transfer me to the position of senior researcher, moonlighting as an expert in the Supervisory Board of the VPTB, sometimes going to throw everything to ... .mater. And the decision was made: I agreed and on February 4, 1980 I became the head of the laboratory 168. And today I do not regret this at all! V.V. Evdokimov became my deputy. In tandem with him, we continue to work today.

So, formally, I left, but still stayed in this "noise" and, as I understand today, could not help but stay. But now I myself determined what to do when and to whom. The first four years were given to the reorganization of work in the laboratory, although in VNTL V.Ya. Kislov, I was doing something inessential. The situation was not simple, the topic was diametrically opposed to what was in the laboratory 166.

Before continuing on this narrative, it is necessary to make a small digression and note the contribution of the lab. 168 in the development of the direction associated with the generation of stochastic signals. About this, for some reason, I forgot to mention in my story NN. Zalogin.

Laboratory 168 was organized in the Fryazino part of the IRE Academy of Sciences of the USSR in January 1966 at the initiative of Academician ND. Devyatkov. The purpose of its creation was the development on the basis of ideas generated in the 16th Division, semi-industrial experimental samples of new electrovacuum microwave devices to accelerate the process of their introduction into industry. For this purpose, with the help of the Istok enterprise, the laboratory was equipped for two years with technological equipment that, in principle, allows the creation of sealed-off electrovacuum UHF devices in both metal-glass and metal-ceramic designs and conducts their experimental research. Highly qualified specialists of technologists were involved along with young specialists. The head of the laboratory was at this time I.M. The wretched.

The first step of laboratory 168 (1966-1968) was the creation on the basis of theoretical and experimental results obtained in the lab. 169 (head of the Laboratory of Physics and Mathematics, IF Kharchenko), sealed metal-glass samples of plasma noise generators of the decimeter range with an output power of the order of 1 W in continuous mode and a power spectral density (2-5) x10-3 W / MHz in the band 600-1400 MHz.

The next direction of the laboratory (1969-1974 gg.) Was the development and creation of a series of powerful sealed metal-ceramic samples of the noise generator together with employees of the lab. 166 (head of the laboratory Dr. V.V. Kislov). For the first time in the USSR, a one-cylinder continuous-mode noise generator with an output power of 2.4 kW in the 100-1400 MHz band and a noise generator with an output power of 600-700 W in the 300-3500 MHz band was created (Fig. 1). However, due to the lack at the time of effective small-size magnetic focusing systems, these developments were not introduced into the industry.

Nevertheless, already in 198? year, one copy of a one-balloon decimeter of the decimeter range was

supplied for the research of the operation of the equipment in one of the enterprises of Moscow.

At the moment of my arrival in the lab. 168 in 1980 she led (since 1974) the study of physical processes in an orotron-generator with an open resonant electrodynamic system and longitudinal electron-wave interaction. Temporary Acting Head. the laboratory was Valery Vyacheslavovich Evdokimov. Actually, the management was carried out from the Moscow part of the IRE directly to Z.S. Chernov and Grigory Alexandrovich Bernashevsky. The experiments were conducted in a 3 cm wave band. Again had to learn! But about the orotron a separate conversation, and now about the return to "native penates".

3. NOISE RADAR AND BROADBAND DIODE NOISE GENERATORS

In 1984, a card for the development of a noise radar of 8 mm range came into 1 department. I do not remember why I was introduced to her. Probably, according to old memory. I went to V.Ya. To Kislov. I ask: "Will you do this work?" He answers: "No. I have so much to do about it! ". "Then I undertake, and you will also be the leader, but at first your employees will help in the 3 cm range, because no element base 8 mm range, not to mention the noise generators that need to be created, not available. Do you agree? "-" Yes. " Thus began my penetration into the millimeter wavelength range and a return to the generation of stochastic oscillations already in generators on avalanche-passing diodes. Thus, the beginning of the mastering of the millimeter wave band (MMDV) by broadband diode noise generators in the IREE of the Academy of Sciences of the USSR belongs to 1984 and is associated with the formulation of works on noise radar in the 8 mm wave band [1], and the "man from the Troika" about which NN mentioned. Zagolin, was Yu. Yakimchuk.

To begin such studies (without having any element base of the 8 mm range), a large amount of experience accumulated by this time in the IRE of the USSR Academy of Sciences on the phenomenon of the transition of oscillators of harmonic oscillations to the mode of generating broadband noise has allowed. These studies were carried out not only in electron-wave systems with delayed feedback (AOS) [2-5], but also in semiconductor diode generators of the centimeter wave band made by N.N. Zalogin and R.V. Belyaev [6]. This phenomenon, later called the "nonlinear stochastization of oscillations in dynamical systems," was discovered in the Institute of Physics and Engineering of the USSR Academy of Sciences in 1966, for the first time both in our country and abroad, and then studied in detail in electron-wave systems with (ZOS) [2]. Unfortunately, as N.N. Zagolin, because of the important applied importance of these studies in the microwave range, their main results were published much later [2-5], when in the scientific literature a real boom began to study this fundamental property of nonlinear dynamical systems of various nature. Investigations carried out at the Institute of Physics and Technology of the Academy of Sciences of the USSR [2-5] led to the creation of a special class of generators of stochastic (noise) oscillations - "noise wheels", the features of which were considered in [7].

The basis for the construction of experimental models of diode GS was put the necessary signs of stochastization of oscillations in electron-wave systems with a delay, which made it possible to begin the development of the 8 mm range from the experiment and only after some time to consider the theoretical model of such a generator [8]. A comparative analysis of the characteristics of the noise signal of generators using Gunn diodes and avalanche-passing diodes (PDD) in the centimeter wavelength range, performed by the authors of Ref. 6, determined the choice of the active element for the noise generator in favor of the latter. LAPs were also used in noise generators (GSLPDs) of the millimeter wave band.

Great contribution to the development of this direction in the lab. 168 was brought in by the engineer of the laboratory, and now by the doctor of science, Viktor Dmitrievich Kotov, whom I managed to persuade to switch from "orotron" subjects to "solid".

Of course, the agreement on the creation of the 8 mm wide SHRLS layout was successfully implemented. GSLPD was created. Experiments were conducted to investigate the work of this locator, in which a large share of participation was Valery Ivanovich Kalinin. But the most important thing is that at the expense of this contract 168 first-time instruments and a 8-mm HF path appeared in laboratory 168. Further for a number of years

work was carried out to improve the design of this GSLPD, its characteristics, the process of transition to noise generation mode and the possibility of creating SHRLS based on it for various applications were studied. It was shown the possibility of overlapping only 8 mm of the range 4 - 5 GSLLPD with a spectrum width of 800 MHz ... 1000 MHz. All this was done according to the contracts with the Customers, the financial means from which provided the possibility to continue equipping the laboratory with equipment of this range, which was very useful for moving the orotron in the 8 mm range. Although the work under the Agreements was conducted according to a closed plan, after all, with the permission of the Customer, it was possible to publish something in the open press, for the first time in 1990 [9]. Then, the need for noise generators of 3 mm range appeared in the Customers. This range was also mastered in the pre-perestroika period. GGLPDs were created with a 3 mm range with a spectrum width of up to 8 GHz, operating at the 2nd harmonic generation of the 8 mm range LDP produced in Nalchik. The theory of this GSLPD was considered in [10]. A young specialist, and later a graduate student, Yury Veniaminovich Andreev, made a big contribution to the theoretical description of the process of transition of the GSLPD to the mode of noise generation. And in this case, the money earned made it possible to equip the laboratory with equipment and a waveguide channel of 3 mm range. So 3 mm panoramic meter VSWR, which m.ns. lab. 168 Boris Andreevich Belyavsky brought after the alteration of a lower-frequency device from Vilnius, and works today.

4. DASHING 90's

In the dashing 1990s, reformist liberals (and, in fact, the second echelon of the party nomenclature) seized power in the USSR, disrupted the Great Soviet Empire, and overnight liberated the verbiage of the liberal media that muddied the Soviet Union and brought down the financing of science, military industry, education, medicine and ... Millions of Soviet people were actually unemployed and did not receive wages for months. So employees of the cathode department - one of the main departments of the FGU NPP "Istok" - in the morning before the work went to put the tents on the market, and in the evening to clean them. Speculators, bandits and thieves, who accumulated millions on trading bases, in stores, in state bodies of material values management during Gorbachev's perestroika period, were able to only partially legalize them. They welcomed the new power, becoming masters of real estate, factories, steamships, etc. Millions of ordinary people, in order to survive, became "shuttle traders", and the whole country turned into a consumer goods market. To feed their families, some of the qualified specialists left the country, and a part that did not want to leave their homeland was forced either to become street vendors and quit their favorite work or to survive in beggarly conditions, trying to save a business that has invested more than one year of life, adapting to existing conditions. Of course, there were some who followed the veiled advice of the devil: "Enrich yourself!" By Mr. Yeltsin. Or they were expected to be corrected in accordance with the question of Mr. Berezovsky, incidentally, corresponding member of the Academy of Sciences of the USSR: "If smart, why poor?". This public imposed on the citizens of the country, in the recent past, Soviet people, instead of the 10 Christian commandments (the code of honor of the builders of communism) their mentality of the leadership of the loan interest and successfully continues to do this through their media today.

In these troubled years I had to find ways to save the business, to find at least some kind of financial assistance to my employees and myself. Saved the noise theme. It was necessary, along with

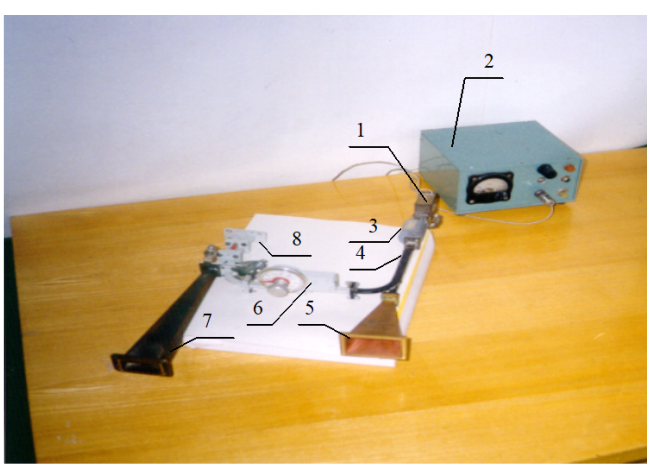

Fig. 1. *Receiving-transmitting block of SHRLS.*
1 - noise generator (GSH) of 8 mm wave band, 2 - power supply, 3 - ferrite isolation valve, 4 - directional reference signal coupler, 5 - emitting horn, 6 - attenuator, 7 - receiving horn, 8 - adder of received and reference signals.

academic themes, to deal with EHF-therapy (thanks to ND Devyatkov and the successor of his case to Oleg Vladimirovich Betsky). It was decided to use relatively narrow-band GGLPAs that generate a noise signal near the known wavelengths of 7.1 mm, 5.6 mm, 4.9 mm as sources of radiation in devices for EHF therapy [11, 12]. It was organized by LLC "SHLEM" (founders EA Maisin and VD Kotov), which produced and successfully sold devices with the same name. In this work, most of the technical staff of the laboratory were involved. Naturally, the results of clinical trials of these devices were published, not only in our country, but also abroad [13]. In the end, in 2002 LLC ordered "a long life", as I realized that it's already hard to sit alone on several chairs and you need to make a choice.

CONCLUSION

To the noise theme already within the framework of academic programs of the lab. 168 has addressed in the future [14]. In 2002, a new method for analog-to-digital signal processing in SHRLS was proposed [15], implemented experimentally on a laboratory model of SHRLS [16, 17]. At the same time, the results of our experimental studies on GSLP were published [18]. Currently, these GSLPDs are used in experimental radio-vision systems at FIDE named after. V.A. Kotel'nikov Academy of Sciences [19].

REFERENCES

1. Volzhin VN, Yakimchuk SE, Kislov VY, Kalinin VI, Measin EA, etc. The method of radar. AS No. 792183, BL. №48, December 1980
2. Measin EA, Kislov VY, Bogdanov EV. Method for generation of electromagnetic noise oscillations: A.C. N1125735, published on 23.11.84. BL N43 with priority from June 22, 677
3. Kislov VY, Zalogin NN, Myasin EA. Investigation of stochastic autooscillatory processes in self-excited oscillators with delay. Radio Engineering and Electronics, 1979, 24 (6): 1118.
4. Kislov VY, Myasin EA, Zalogin NN. On nonlinear stochastization of auto-oscillations in an electron-wave generator with delayed feedback. Radio Engineering and Electronics, 1980, 25 (10): 2160.
5. Kislov VY. Theoretical analysis of noise-like oscillations in electron-wave systems and self-excited oscillators with delay and strong nonlinearity. Radio Engineering and Electronics, 1980, 25 (8): 1683.
6. Belyaev RV, Zhernovenkov AS, Zalogin NN, Melnikov AI. Experimental study of the excitation of noise oscillations in the GLDD. Radio engineering and electronics, 1996, 41 (12): 1484-1489.
7. Anisimova SE, Vorontsov GM, Zalogin NN, Kislov VY, Myasin EA. Chromotron. Radio Engineering, 2000, 2: 19-25.
8. Andreev SE, Myasin EA. Investigation of the dynamics of the model of an odd-diode generator on the LPD. Radio Engineering and Electronics, 1989, 33 (11): 2358.
9. Myasin YeA, Kotov VD, AndreevYuV. Ka-Band Lardge Bandwidth Noise Signal Source. Proc. 15th Intern. Conf. on Infrared and Millimeter Waves. Dec. 10-14, 1990, Orlando, Florida, USA Conf.Digest, pp. 631-633.
10. Andreev SE, Myasin EA, Kotov VD. On the problem of generation of the second harmonic in the model of an autostochastic oscillator on an avalanche-spill diode. Radio engineering and electronics, 1991, 36 (2): 426-428.
11. Myasin EA, Kotov VD, Andreev SE. A generator with a nondeterministic signal of the MM range for biomedical research. Thesis VII. Vses. sem. "Application of low-intensity EHF radiation in biology and medicine". 13-15 Nov. 1989, Moscow, p. 134.
12. The meat of EA, Kotov VD. The device for EHF therapy "Helmet-1." Proceedings of Int. simp. "Millimeter waves of nonthermal intensity in medicine". Part 3. Moscow, 1991, p.739-734.
13. The meat of EA, Kotov VD. Application of EHF-therapy for hypertensive crises. Tr. Int. Conf. on hypertension, Tokyo, 1999, p. 108.
14. Myasin EA, Black LF. etc. Project 2.4, Study of the propagation of millimeter wave broadband signals in the surface layer of the atmosphere and determination on this basis of the limitations imposed on the extremely achievable characteristics of locating systems with noise and broadband signals. Sat. reports on the scientific projects of the Russian Ministry of Science and Technology "Physics of Microwaves". N. Novgorod, 2001, p.77-81.

15. The meat of EA, Kotov VD. The noise radar. Certificate of utility model number 25797. Priority from 22.04.2002.
16. Massine EA, Ilyin AYU, Kotov VD, Chmil AI. Noise 8 mm radar wave band with spectral and digital signal processing. Tr. 4-th Intl. Conf. "Digital signal processing and its applications". Moscow, 2002, p. 210-213.
17. Massine EA, Kotov VD, Ilin AI, Chmil AI. Noise radar with analog and digital signal spectral processing. Radio Engineering, 2005, 3: 36-40.
18. The meat of EA, Kotov VD. Broadband diode generators of millimeter wave noise. Radio Engineering, 2005, 3: 46-50.
19. Materials of the reports of the FIDE RAS. Report lab. 176.

DIAGNOSTICS AND CORRECTION OF THE FUNCTIONAL STATE OF THE HUMAN ORGANISM WITH THE "CHARM"-DIAGNOSTIC COMPLEX

Nikolay D. Devyatkov, Vladimir Ya. Kislov, Vladimir V. Kolesov, Vladimir I. Grachev

Kotelnikov Institute of Radioengineering and Electronics of Russian Academy of Sciences, http://cplire.ru
Moscow 125009, Russian Federation

info@cplire.ru, kvv@cplire.ru, grachev@cplire.ru

Absrtact. **The therapeutic-diagnostic complex (TDC) is intended for electropuncture diagnostics and correction of the functional state of the organism with the help of puncture extremely high frequencies (EHF)-therapy. TDC allows to conduct studies of the electrophysical parameters of the skin as a function of time, to search for acupuncture points on the human body, diagnostics using the methods of Nakatani and Voll, and puncture EHF correction of a person's functional state. TDC is applicable for assessing the effectiveness of any type of treatment in the clinic, in express diagnostics in the course of medical examinations, medical examinations, medical care in medical institutions, in assessing the health status of people in everyday life.**

Keywords: **functional state of the human body, electropuncture, EHF-therapy, acupuncture points, electrophysical parameters of the skin, express diagnostics**

UDC 538.573.61

Bibliography - 25 references *Received - 26.08.2018*

RENSIT, 2018, 10(2):257-268 **DOI: 10.17725/rensit.2018.10.257**

Content

1. INTRODUCTION

At the present time, in connection with the development of methods of the system approach in medical diagnostics, reflexology, preventive medicine, valeology, methods of non-medicamentous influence, on the one hand, and with the development of methods of radio electronics, control theory and telecommunication and information computer technologies, on the other hand, it becomes possible task of monitoring, diagnosis, evaluation and correction of the functional state of the human body in real time.

Among the ranges of electromagnetic waves used in medicine as diagnostic and therapeutic tools, the range of extremely high frequencies has recently been widely used. The development of the physical foundations for the creation of equipment in the millimeter range was conducted under the guidance of Academician ND Devyatkov, starting with the 60-ies of the last century. Along with powerful sources for technical purposes, low-intensity solid-state sources of MM radiation based on avalanche transfer diodes (HDLs) and Gunn diodes were created, on the basis of which industrial samples of sources for medical use were developed [1].

The effectiveness of the biological effect of low-intensity electromagnetic radiation in the millimeter range as a physical factor for the construction of new medical equipment is justified by the fact that all terrestrial biological objects are protected by the atmosphere from exposure to solar radiation of the millimeter wavelength range. Therefore, biological objects, including humans, have increased sensitivity in

this wavelength range. In laboratory studies for the first time it was experimentally found that low-intensity MM-radiation has a pronounced biological effect [2].

As a result of developments based on the results of numerous clinical trials, a whole gamut of therapeutic EHF-devices was created, for which licenses were issued by the Ministry of Health of the Russian Federation. The basis of all these devices, mass-produced at a number of industrial enterprises of the Russian Federation, are priority developments of the basic EHF-type device "Yav" based on LPD generators.

Long-term clinical experience of successful application of EHF-therapy has shown its effectiveness in affecting certain areas of the body, including. reflexogenic zones and acupuncture points. Electrophysical parameters of the skin in such zones and points are used in electropuncture techniques to diagnose the functional state of various systems and organs. Monitoring of the results of EHF-correction of the functional state of the human body was carried out with the help of a computerized electropunctural diagnostic complex.

In the Kotelnikov Institute of Radioengineering and Electronics of RAS team of developers under the leadership of Academician N.D. Devyatkov and Professor V.Ya. Kislov was established the therapeutic and diagnostic complex "CHARM" (TDC "CHARM"), intended for electropuncture diagnostics and correction of the functional state of the human body with the help of created EHF-equipment [3]. The combination of electropuncture express diagnostics with puncture EHF-therapy made it possible to develop a method for assessing the effectiveness of treatment, control and correction of the functional state of the human body [4].

Based on modern methods of radioelectronics, the TDC "Charm" allows to perform an objective electropunctural express diagnostics of the functional state of the main internal organs of the human body using the method of riodorak (based on the measurement of skin electrical conductivity in 24 representative points), and puncture EHF correction of the imbalance of the functional state of the meridian system and bringing it to normal. (Hereinafter, the terminology adopted in eastern reflexotherapy is used.)

At the heart of the worldview of ancient Chinese philosophy is the doctrine of "yin" and "yang." According to this teaching, all things and phenomena have two opposing sides, complementing each other, these are two complementary parts of the whole. Different relationships between yin and yang determine the different states of the surrounding world, including the state of the human body. According to Chinese medicine, the human body is also divided into two opposite functional parts. The concept of yang in the body include: the upper body, its surface, back, six "hollow" organs (stomach, large intestine, small intestine, gall bladder, bladder and so-called "triple heater" -functional system corresponding to the endocrine system). To the concept of yin are: the inner part of the body, the stomach, six "dense" organs, the so-called. organs of energy storage (heart, lungs, spleen, kidneys, liver, pericardium), blood.

For traditional Chinese medicine, the "organ" is not so much an organic structure, but mainly a functional system that is related to the physiological and psychological state of the organism. All organs of the yang interact with the yin organs and with each other according to cyclic laws (a large circle of circulation). This interaction takes place over a certain time cycle and along certain meridian lines. Interaction of meridians with each other individually and in the system as a whole ensures dynamic maintenance of homeostasis. Thanks to these interrelations, it is possible to conduct disease diagnostics, treatment and prevention of diseases. The disease in this model is considered as a violation of the harmonic balance between yang and yin, and the doctor's task is to diagnose and correct the state of the meridian system.

The behavior of the meridian system can be modeled by methods of nonlinear dynamics [5]. Numerical analysis of such a self-oscillating system makes it possible to obtain information on various states of the meridian system corresponding to normal and pathological states.

Puncture correction is based on the principles of oriental reflexology medicine, which has ancient

roots and millennial traditions, covers the study of the physiology of the human body, its pathology (the origin of diseases and their causes), methods of medical research, diagnosis, therapy and disease prevention. One of the main diagnostic methods in oriental medicine is pulsodiagnostics, and the therapeutic method is acupuncture. In this case, in comparison with western medicine, not a disease is treated, but a patient, i.e. improve the functional state of all systems of the body, its organs and defense mechanisms. The basis of the method of treatment is to adjust the condition of 12 main functional organs (meridians) - internal and external, by means of acupuncture, providing a stable dynamic homeostasis of the organism on the basis of a correct diagnosis.

According to traditional oriental medicine, the state of the biologically active point (acupuncture point) reflects the functional state of the corresponding organ, the active point is, as it were, the organ window into the external world. Deviations in the work of internal organs lead to changes (reflexes) of certain points on the surface of the body. Thus, there are many points with increased conductivity on the human skin, the location and degree of excitation of which clearly depends on the disease [6].

At present, low-intensity radiation of millimeter wavelength range (4.9 mm, 5.6 mm, 7.1 mm) is used in EHF-therapy when exposed to reflexogenic zones. Low-intensity millimeter radiation refers to non-ionizing radiation. It in principle can not have a destructive effect on the cells of the body and therefore is safe. For more than 20 years of millimeter wave application in clinical practice it has been shown that a positive therapeutic effect is achieved in the treatment of a number of diseases, and there are practically no obvious contraindications. To date, we can name a significant number of various diseases in which the effectiveness of EHF-therapy has been proved: peptic ulcer and duodenal ulcer, pain syndromes, dermatology, hypertension, diseases associated with circulatory disorders in the brain and extremities, a number of oncological diseases, hematology, neurological diseases, gynecological diseases, postoperative conditions, ischemic heart disease, and others.

Stressing the effectiveness of EHF-therapy, it is possible to distinguish the following features of it: non-invasiveness of the method, use of EHF-therapy as monotherapy (ie, drugless therapy with a polytherapeutic effect, when treatment of a single disease treats secondary diseases), lack of allergy to EHF- radiation, the presence of positive emotions in patients with treatment (pain sensations disappear when exposed) [7].

2. THE EQUIPMENT OF THE MEDICAL-DIAGNOSTIC COMPLEX "CHARM"

The main goal of developing a therapeutic-diagnostic complex (TDC "Charm") is the creation of new medical equipment that can replace the traditional technique of diagnostics and acupuncture, simplify acupuncture recipes, thereby ensuring its mass, including domestic, use.

TDC "Charm" is a new computerized complex with diagnostic software, therapeutic recipes for equalizing pathological abnormalities and an extensive database, while three systems are connected together in a single complex: rapid diagnostics of human body systems, puncture EHF exposure and a technique for correction of functional states of the main organs (EHF-puncture recipes).

The complex includes:

- portable personal computer of "Notebook" type, remote electronic unit with measuring electrodes.
- a software package that provides the user with a user-friendly interface that allows you to display all current information on the monitor, maintain a database, search, display information in the form of graphs and tables on the monitor and printer;
- therapeutic device for EHF therapy with an EHF-radiation indicator operating at fixed wavelengths of 5.6 and 7.1 mm and having a low power flux density (10 mW/cm^2);
- technical description and methodical manual.

The measuring part of the electronic board has a galvanic isolation from the patient's body along the power circuits through the information channels from the computer and is therefore absolutely safe. This design allows you to work in the absence of mains supply (in the field, with seriously ill patients,

Therapeutic-diagnostic complex "Charm" for electropuncture express diagnostics and EHF-therapy (option with autonomous power supply).

Apparatus "Yav-D" with a remote irradiation head for puncture EHF-therapy.

Apparatus "KVCH-ND2" of the new generation with autonomous power for puncture EHF-therapy (wearable version).

The device "KVCH-ND" for three frequency ranges 7.1: 5.6 and 4.9 mm for puncture EHF-therapy.

Fig. 1. *Equipment for diagnosis and EHF-therapy.*

etc.). In this case, complete information is stored in the database.

The complex allows searching for acupuncture points on the human body;

- conduct electropuncture diagnostics by the method of riiodorak;
- conduct research on the electrophysical parameters of the skin as a function of time;
- EHF-correction of the functional state of the internal organs of man.
- In this case, the time of examination of one patient does not exceed 5 minutes.
- As an example, the following areas of application of the complex can be named:
- express diagnostics for the professional examination of work collectives, employees of firms, for the prophylactic examination of population groups, for the care of patients from polyclinics, hospitals, hospitals, medical posts, in assessing the health status of family members, etc.,
- for therapeutic purposes to regulate bioenergetic and physicochemical processes in the tissues and systems of the human body,
- to evaluate the effectiveness of treatment (drug, surgical, radiation, etc.)

Simplicity in handling and management of the complex makes it possible to apply it not only in medical institutions, but also in the home. The complex allows rapid diagnosis and correction of

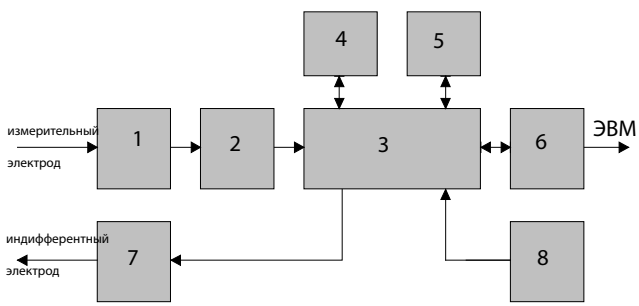

Fig. 2. *Block diagram of the measuring unit TDC Charm: 1-input converter, 2 - analog-digital converter, 3 - microprocessor, 4 - random access memory, 5 - read-only memory, 6-optocoupler block, 7 - reference voltage block , 8 - rechargeable battery.*

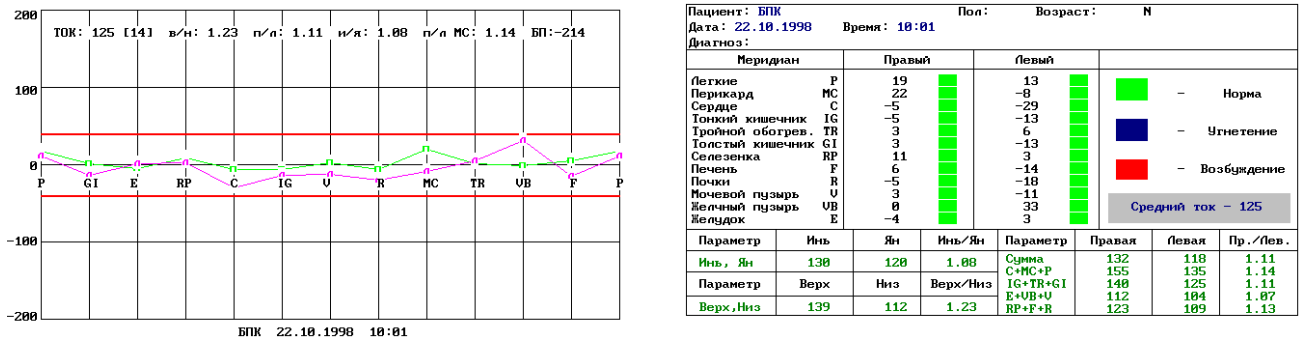

Fig. 3. *Diagram and table of the functional state of a practically healthy person. In the red lines (± 40), the corridor of normal values is limited.*

12 major functional systems of the body-lungs (P), vascular system (MC), heart (C), small intestine (IG), endocrine system (TR), spleen / pancreas (RP), liver (F), kidney (R), bladder (V), gallbladder (VB), large intestine (GI) and stomach (E) - according to the electropuncture conductivity condition of meridians in 24 representative points (ryodoraku method) [8], as well as assess the condition of individual human organs (or parts thereof) according to the Foll method [10], in which Parameters transient process after applying acupressure points dosed low power signal. The most optimal combination is the method of ryodoraku and elements of the Voll method.

In **Fig. 1** shows the developed equipment for diagnosis and EHF-therapy. In Fig. 2 shows the block diagram of the measuring unit TDC "Charm". In **Figs. 3-7** shows the diagnostic maps of a healthy person, an example of EHF correction of a functional state and various pathological conditions.

TDC "Charm" was approved in the institutions of the Ministry of Health of the Russian Federation and medical institutions of the Ministry of Defense of the Russian Federation. Clinical trials were conducted according to the decision of the Committee for New Medical Technology of the Ministry of Health of the Russian Federation. The conducted tests showed the effectiveness of the TDC "Charm" in the treatment of various groups of diseases.

At the same time, positive recommendations were given on the application of TDC "Sharm" for the treatment of stroke, diabetes, trigeminal neuralgia, osteochondrosis, hypertension, etc., as well as a more general method for those cases where conventional medical treatment is used. For example, EHF puncture therapy, performed with the help of TDC "Charm" as part of complex treatment in patients with complicated osteochondrosis of the spine, allows, in comparison with the control group in a shorter time and completely to stop pain syndromes, to restore the volume of active movements in the joints and sensitivity of the skin in the corresponding zones of innervation.

In the treatment of type 2 diabetes mellitus, there was a significant reduction in the glucose level in the blood of patients with fasting. In patients with cerebral circulation and hemiparesis, a decrease in spasticity on the side of hemiparesis and a normalization of blood pressure were observed. In patients with hypertensive disease of the first stage

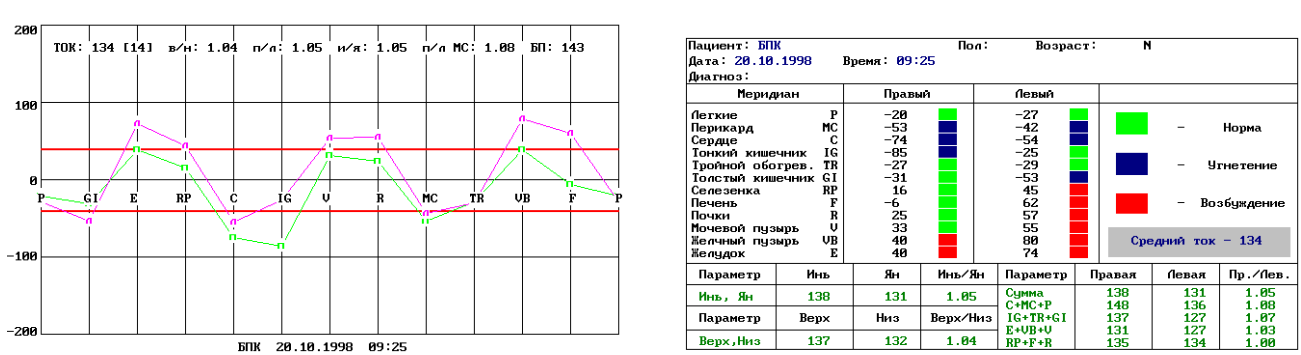

Fig. 4. *Diagram and table of a patient's functional state before EHF-correction. In the red lines (± 40), the corridor of normal values is limited.*

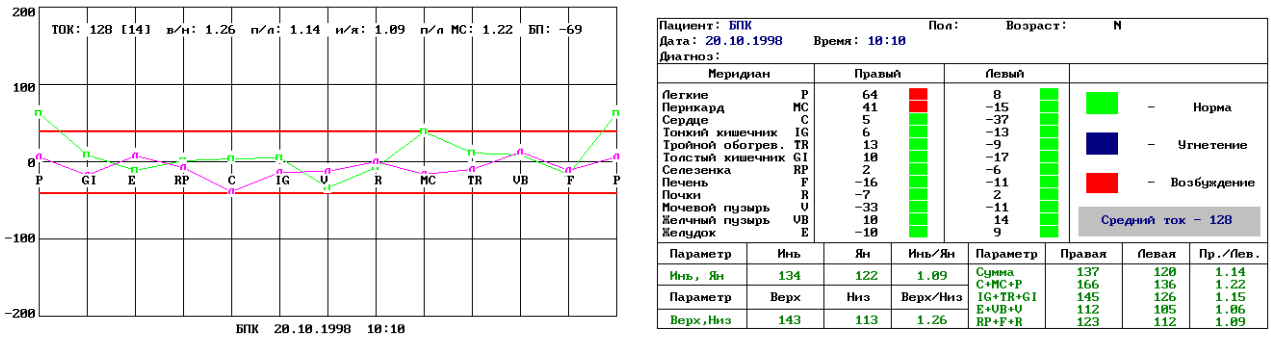

Fig. 5. Diagram and table of a patient's functional state after EHF-correction. In the red lines (± 40), the corridor of normal values is limited.

after the application of EHF punctures in a complex of therapeutic measures, the clinical recovery came quite quickly and effectively. During the clinical trials of side effects and complications of EHF-puncture therapy, applied in accordance with the above method, was not observed.

3. METHODOLOGICAL BASIS OF ELECTROPUNCTURE DIAGNOSTICS

Virtually all processes in the body are accompanied by a change in the electromagnetic characteristics, which can be fixed by various contact and non-contact physical methods. One such method is electropuncture diagnostics, based on the measurement of electrocutaneous characteristics [10].

The most common and currently promising electropuncture techniques (Nakatani, Voll, auricular, etc.) measure the skin-galvanic reaction by means of contact metal electrodes with a probing voltage of a certain sign (in the Nakatani technique negative, Voll-positive). This ensures the stability of the contact resistance in the contact area of the skin with the measuring electrode [11, 12]. Electropuncture techniques are based on empirically selected parameters of the electrical measuring circuit.

In all electropuncture diagnostic measurements, the skin is a transitional element for the external measuring circuit. As is known, the skin has sensitivity in a wide range of the electromagnetic wave spectrum [13], carrying out active energy and information interaction of the organism with the external environment. As an organ, the skin is one of the oldest biosystems of the body, from the simplest to the mammals and man. Apparently, the system of autoregulation of various biochemical processes occurring in the skin is laid still at the embryonic stage of the development of the human body, and at the initial stage has a rather simple structure, which in turn is organically linked with nearby rudiments of various organs and parts of the body, and then, developing with the body, takes a complex, ramified character [14]. Thus, it is possible to explain the appearance of reflexogenic reactions in certain places on the skin when exposed to various internal organs.

The skin has its own system of autoregulation, which, apparently, is neurohumoral in nature. The epidermis of the skin and the epithelium of the digestive tract are two tissues most prone to direct influences from the outside world. In both tissues, mature differentiated cells are found in

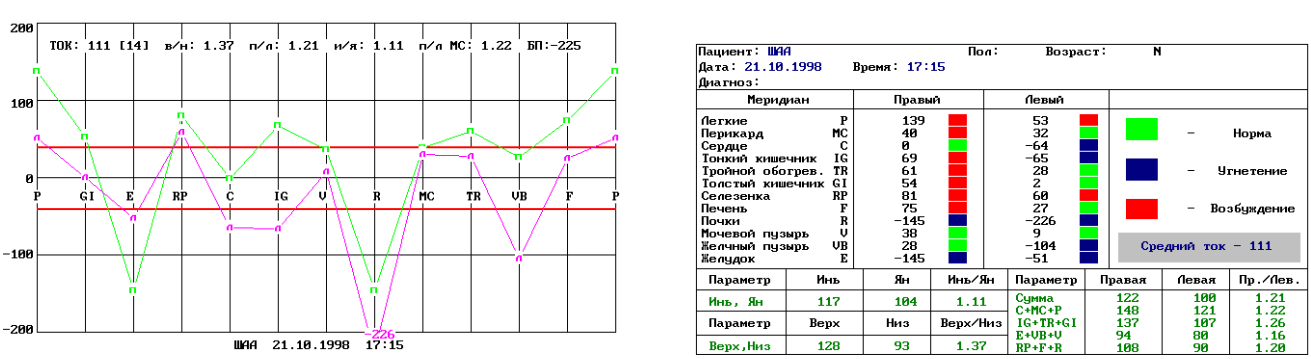

Fig. 6. *Diagram and table of the functional state of a patient with chronic diseases of the stomach, kidneys and gallbladder.*

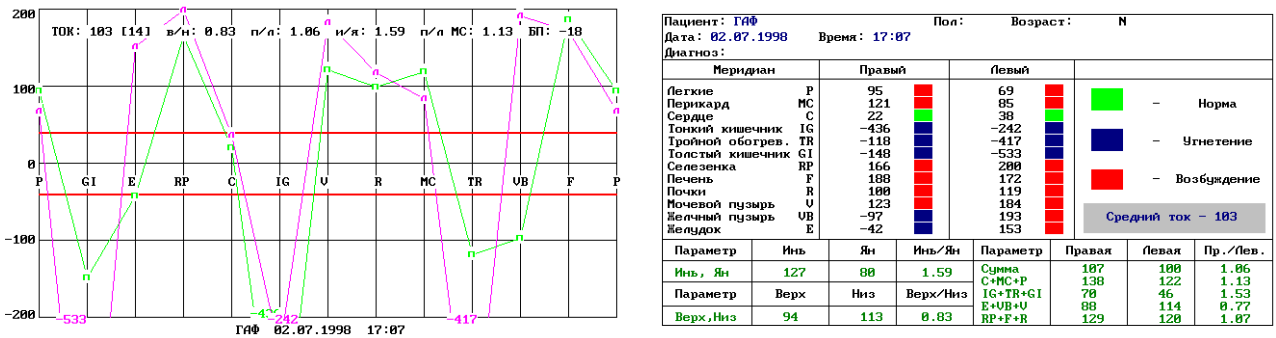

Fig. 7. *Diagram and table of the functional state of a seriously ill patient.*

the most vulnerable areas, are quickly worn out and are also quickly replaced as a result of the proliferation of less differentiated cells in more protected areas.

Liquid media are in their enclosing volumes, bounded by surfaces with different properties. The permeability of these surfaces for different components of liquid media is different and variable, provides a state of dynamic equilibrium. At the same time, the water and electrolyte balance are functionally inseparable [15].

The primary condition of normal vital activity of the body cells (and skin cells in particular) is the constancy of the ionic composition and pH of biological fluids. Preservation of the constancy (homeostasis) of differences in the electrolyte composition of blood plasma and extracellular fluid, on the one hand, and intracellular fluid, on the other, is one of the defining properties of the body's regulatory systems.

Thus, the diagnosis of the functioning of metabolic processes in the skin can serve as the basis for biomedical diagnostic techniques.

4. BIOPHYSICAL FUNDAMENTALS OF ELECTROPUNCTURE DIAGNOSTIC METHODS

If the monitoring of metabolic processes in the skin is taken as the basis of the method of functional diagnostics, then the problem is in the first approximation reduced to measuring the electrophysical characteristics of that electrolyte medium that directly participates in metabolic processes at the cellular level through cell membranes in the active layers of the epidermis and dermis.

The upper layers of the epidermis are densely lying keratinized cells with a low water content and have a relatively high electrical resistance. In direct contact with a metal measuring electrode, almost all the probe voltage is applied to a relatively small area between the electrode metal and the lower layers of the epidermis, which are saturated with an intercellular fluid, which is a strong electrolyte of a complex chemical composition.

Thus, the measured conductivity of the transition region consists of conductivity with respect to the high-resistance upper layers of the epidermis and the intrinsic conductivity of the cells of the intermediate layers of the epidermis. In this case, it is necessary to take into account not only the layered structure of the epidermis and the dermis, but also the porosity of the various skin areas, which determines its excretory and mechanoreceptor properties. It is also known that in the field of biologically active points of BAP, the skin has increased looseness and saturation with the intercellular fluid [16].

Thus, in order to increase the information, and therefore the diagnostic value of the method, it is necessary to isolate from the integral conductivity of the entire measured circuit the electrophysical characteristics of the biologically active layers of the epidermis and dermis.

The model representation of the measuring electrical circuit in the first approximation should include the electrophysical characteristics of the layers of the skin cells themselves, and also take into account the shunting action of the porous cellular structure, which, when filled with electrolyte, can make significant changes in the quantitative relationships.

5. SOME RESULTS OF CLINICAL TRIALS OF TDC "CHARM"

The examination and treatment was carried out in three groups of patients:

1. diabetes mellitus type 2 (insulin-independent),
2. hypertensive disease of the 1st stage and neurocirculatory dystonia according to the hypertonic type,
3. osteochondrosis of the spine with radicular syndrome.

The examination of patients with the help of TDC "Sharm" followed by EHF-puncture therapy of revealed abnormalities was carried out, usually in the morning hours on an empty stomach, or 2 hours after eating or carrying out any other procedures. Points of influence were chosen according to the rules of traditional oriental acupuncture. The initial information for the choice of impact points was tabulated and graphical data obtained as a result of conducting electropuncture diagnostics with the help of TDC "Charm". The method of tonification of the "oppressed" meridians was used as the main method of influence. In those cases quite often encountered, when there was a friendly change of several meridians (two, three) at the same time, the so-called group lo-points were used for the therapeutic effect.

The results of the impact were taken into account by repeated electropuncture diagnostics after 1-1.5 hours and after 1 day; For one exposure session, two to five points were used, the selection of which was carried out individually, depending on the diagnostic results.

The clinical picture of diabetes was first described almost 2,000 years ago by the Roman philosopher and physician Celsus, but the problem of cure for him has not been resolved to this day. From the moment of detection of the disease, the patient, as a rule, is attached to the sugar-reducing drugs for the rest of his days and is exposed to their side effects. An important actual problem is the reduction, with other equal conditions, of the dose of the drugs used due to physical methods of treatment and, in particular, EHF-therapy.

12 patients (9 men and 3 women aged 39-56 years) with type 2 diabetes mellitus were examined and treated with the help of the "Charm".

Eight patients had complications of the disease in the form of diabetic polyneuropathy, angiopathy of the vessels of the kidneys, retina of the eyes, lower limbs. All patients had concomitant diseases: peptic ulcer disease of the duodenum (4 persons); chronic ischemic heart disease (5 people); urolithiasis (2 people); consequences of transferred serum hepatitis (1 person). The duration of the disease, confirmed by medical documents, ranged from 1 year to 15 years. All patients were on treatment in a specialized department and received complex therapy: mannil, vascular, antisclerotic, trophic drugs, antihypoxants, vitamins, symptomatic agents, treatment with hyperbaric oxygenation.

All patients had a significant deviation of the diagnosed parameters from the norm, which, as a rule, were multidirectional in different meridians. At the same time, it should be noted that the manual meridians (IG, TR and GI were in a state of "oppression." Weakened patients with low mean current for the first treatment session used point RP21-symmetrically, for 5-6 minutes on each side. In subsequent sessions MS5, TRS, V65, RP6, E36, and less frequently GI11, VB34, etc. were used more frequently. The time of exposure to the point depended on the degree of "depression" of the meridians and was 3-4 minutes at the exponent (1-1.5) N up to 8 min at the exponents greater than 2 N. The total exposure time for one session was in Pr affaires to 30 minutes.

When comparing the changes in blood glucose in the blood of fasting patients in the group receiving EHF-therapy and in the control group, it is evident that in the first there is a distinct decrease in blood glucose from 14.0 ± 8.2 mmol/l to 6.6 ± 1.8 mmol/l on average group for two weeks, while in the control group there were only fluctuations of this averaged index in the range of 7-11 mmol/l with a weak tendency to decrease in the first two weeks of stay in the hospital.

This is clearly seen in **Fig. 8**, which shows the dynamics of fasting blood sugar, depending on the duration. However, the differences between the compared groups at the end of the treatment course were statistically significant ($p < 0.05$ by the Wilcoxon test), which proves the effectiveness of the EHF-therapy.

Thus, it was shown that EHF-puncture therapy can be recommended in the complex treatment of type 2 diabetes mellitus, since, without exerting side effects on a person in this way of administration, at

the same time contributes to a faster and more stable decrease and normalization of glucose in blood of patients [18].

The importance of the problem of treating patients with essential hypertension is still not reduced, which is due to the wide spread of the disease all over the world, and the severe consequences to which it leads. The constant intake of drugs is often accompanied by serious complications, in connection with which the possibility of applying EHF-puncture therapy is very relevant.

A clinical examination of 18 patients with stage I hypertensive disease and neurocirculatory dystonia was carried out according to the hypertonic type, accompanied by cephalgia, cardialgia and other asthenoneurovalic symptoms (6 women and 12 men aged 20 to 46 years).

In addition to blood pressure indicators, all the patients studied central hemodynamics: minute volume of blood circulation (MO, ml / min), stroke volume (VO, ml), heart rate (heart rate, min).

The control group consisted of 20 hypertensive patients of the 1st stage and neurocirculatory dystonia according to the hypertonic type, who received drug therapy according to indications.

EHF-therapy was carried out by the apparatus "Yav". Time and conditions of the procedure are the same as in the previous group on diabetes. Electro-puncture diagnostics in all patients revealed suppression of the upper meridians (IG, TR, GI) and a slightly higher average current in some degree than in the groups of patients with other diseases. The course of treatment consisted of ten procedures. Points for exposure were chosen solely from the results of a diagnostic study in an amount of two to four points per session with a total duration of 12 to 30 minutes. The most frequently used points were TR8, MS, on both sides, as well as points GI4, E36.

In all patients, as a result of the treatment, there was a decrease in arterial pressure-systolic and diastolic to normal indications; decrease in heart rate. The minute volume decreased on average from 4.21 ± 0.37 to 3.8 ± 0.51. The dynamics of arterial pressure in the compared groups is clearly shown in **Fig. 9.**

Thus, after the application of EHF punctures in a complex of therapeutic measures for this nosology, clinical recovery has come quite quickly and effectively. TDC "Charm" provides the possibility of objectifying and visualizing the process of treatment and especially dispensary observation of the patient in dynamics [18].

The next group consisted of patients with complicated cervical and lumbosacral osteochondrosis: 4 women and 6 men aged 32 to 46 years with a disease duration from 3 to 15 years. In seven cases, the pain syndrome was caused by the inflammatory process (radiculitis, ganglionovrit), and in three cases it was discogenic. In both ancient and European medicine, this pain syndrome indicates the appearance of painful palpation points that have diagnostic or therapeutic significance. Based on this, the points of general action E36, GI4, MC6, RP6, TR8, V60 and the point of meridian of the spleen / pancreas and the posterior-median meridian were used in the treatment of this category of patients. Each patient received ten sessions of EHF-therapy with a total duration of the session from 16 to 30 minutes. In addition, patients received

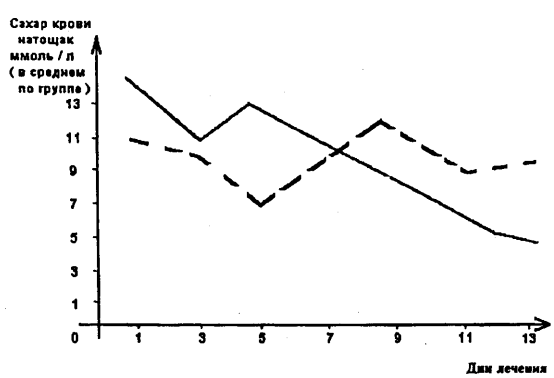

Fig. 8. *Dynamics of fasting blood sugar in a group of patients with diabetes mellitus (solid curve-group receiving EHF-therapy, dashed-control group).*

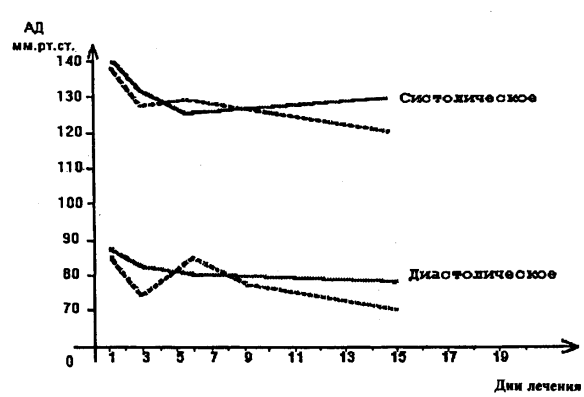

Fig. 9. *Dynamics of arterial pressure in patients with NDC and hypertensive disease (dashed curve-group receiving EHF-therapy, continuous-control group, 1-systolic pressure, 2-diastolic pressure).*

physiotherapeutic and medicamental treatment. In the control group, EHF-therapy was not performed. Criteria for the effectiveness of treatment were: the dynamics of reducing the intensity of pain and the timing of their elimination, restoration of skin sensitivity and the volume of movement of the joints. The intensity of pain was determined subjectively by a 4-point system: severe pain - 3 points, moderate - 2, weak - 1, no pain - 0 points.

In the group of patients who received EHF-therapy, the pain syndrome was completely eliminated in all the treated patients by the 11th day. In parallel, they recovered the volume of active movements in the joints and restored the sensitivity of the skin in the corresponding zones of innervation. The average dynamics of treatment of this group of patients and the control group is shown in **Fig. 10**. For diagnostic signs, EHF correction leads to statistically reliable normalization of the balance of meridians, corresponding to the time for clinical recovery.

As a typical example, one can consider the case of a patient P. (36 years old), hospitalized for emergency indications with the diagnosis of "ganglionovritis with severe pain syndrome." Cervical osteochondrosis. After two sessions of EHF-therapy (the points of the collar zone, as well as V43, V60, IG9, IG10, TR8, E36, GI4, GI11) were used, pain in the neck, right shoulder, and active movements in the cervical spine increased. After the seventh session, only minor pains remained in the area of the right shoulder, which completely stopped after the tenth session. The sensitivity of the skin and the volume of active movements in the cervical spine and shoulder joint were completely restored.

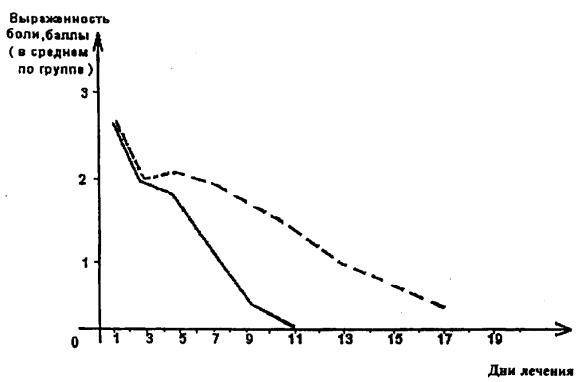

Fig. 10. *Dynamics of pain syndrome changes in patients with osteochondrosis (solid curve-group receiving EHF-therapy, dashed-control group).*

With electropuncture diagnostics after the conducted course of EHF-therapy, the normalization of diagnostic indices attracts attention. Normalization was characterized by a high degree of reliability for the entire group of patients. On average, in the group of patients who received EHF-therapy, the pain syndrome was completely eliminated and the volume of active movements was restored to 11 days. In the control group, similar indicators were achieved by day 17 and only partially. Thus, we can conclude that TDC "Sharm" is highly effective in diagnosing and treating patients with complicated osteochondrosis of the spine with severe pain syndrome and can be successfully used both in hospitals and in polyclinics [18].

6. CONCLUSION

Thus, it is shown that the therapeutic-diagnostic complex "Charm" has wide reflex-therapeutic possibilities:

- Express diagnostics by the method of riiodorak;
- measurement of the characteristics of transient processes by the Foll method;
- exposure to low-intensity EHF-radiation for the purpose of correcting the functional state of individual organs, systems and the entire human body.

With the help of the "Charm" apparatus direct electrophysical measurements demonstrated the existence on the cutaneous surface of the human body of well conducting lines that coincide with the classical meridians [18]. On the basis of the reflexotherapy complex, it is also possible to study the phenomena associated with electropunctural manifestations of homeostasis, to study the complex system of points of acupuncture and meridians [19]

Clinical trials of TDC "Charm" have shown its effectiveness in the treatment of a wide range of diseases and, in particular, diabetes, cerebral circulation disorders [20], neurocirculatory dystonia, hypertension, osteochondrosis [17], inflammation of the trigeminal nerve [20], as well as many other diseases. TDC "Charm" has proved effective in diagnosing surgical pathologies and the process of rehabilitation in the postoperative period [223], in the diagnosis of psychophysiological [23] and stress conditions [24].

With the introduction of the "Charm" TDC and new technologies on its basis, a significant social and

economic effect can be obtained in mass medicine [25].

REFERENCES

1. Golant MB, Vilensky RL, Zyulina EA, etc. A series of wide-range low-power generators of millimeter and submillimeter wavelengths. *PTE,* 1965, 4:136-139.
2. Devyatkov ND, Golant MB, Betsky OB. *Millimeter waves and their role in life processes.* Moscow, Radio i svyaz Publ., 1991, p. 169.
3. Devyatkov ND, Kislov VY. Computerized electrophysical diagnostics and EHF correction of the functional state of internal organs of a person. *Radiotekhnika i elektronika*, 1994, 39(12):2059.
4. Devyatkov ND, Kislov VY, Kolesov VV, Smirnov VF, Otchertsov AV. Medical-diagnostic complex "Sharm". *Coll. reports "Millimeter waves in medicine and biology*". Moscow, IRE RAS, 1995, p. 178-179.
5. Belyaev RV, Kislov VY. Multi-loop auto-oscillation system with delay as a model of the system of acupuncture points of the human body. *Radiotekhnika i elektronika,* 1999, 44(11):123.
6. Luvsan Gavaa. *Methods of oriental reflexotherapy.* Novosibirsk, Science, 1991.
7. Belyi YuN, Kislov VY, Kolesov VV, Smirnov VF, Teodorovich SL. Some applications of computerized diagnostics and EHF correction of the functional state of internal organs of a person. *Col. reports "Millimeter waves in medicine and biology*". Moscow, IRE RAS, 1995, p. 74-76.
8. Hyodo MD. *Ryodoraku treatment and operator approach to acupuncture.* Osaka, Japan, 1975.
9. Voll R. *Topographic Positions of the Measurement Points in Electroacupuncture According to Voll. Vol. 1-4*. Uelzen, ML-Verlags, 1977.
10. Niboyet JEH. *Le traitement des algies par l'acupuncture*. Paris, Maisonneuve, 1979.
11. Nakatani Y, Yamashyta K. *Ryodoraku Akupunkture.* Tokyo, 1977.
12. Voll R. *Kopfherde, Diagnostik und Therapie mittels Elektroakupunktur und Medikamententestung***.** Uelzen, Med.-Lit. Verlag, 1974.
13. Berezovsky VA, Kolotilov NN. *Biophysical characteristics of human tissues.* Kiev, Naukova Dumka, 1990.
14. Falin LEE. *Atlas on normal histology and embryology*. Moscow, 1957.
15. Semenov NV. *Biochemical components and constants of liquid media and human tissues*. Moscow, Medicine, 1971.
16. Fiore MSH. *Atlas of human histology*. Philadelphia, 1957.
17. Devyatkov ND, Gulyaev SE, Belyi UN, Kislov VY, Kislov VV, Teodorovich SL, Vasin IY, Polyanskaya LN, Kolesov VV, Smirnov VF, Chigin EP. Electrophysical fundamentals and clinical applications of diagnostics and EHF correction of human functional states. *Radiotekhnika i elektronika* 1995, 40(12):1887-1899.
18. Aksenov AV, Grachev VI, Kolesov VV, Smirnov VF. Study of the electrical conductivity and potential of the skin for medical diagnosis. *Abstracts of the II Congress of Biophysicists of Russia-1999*, Moscow, 1999, p. 639-640.
19. Devyatkov ND, Grachev VI, Kislov VV, Kislov VY, Kolesov VV. Monitoring and maintenance of body homeostasis using electrophysical methods. *Theses of the 55th session of the RNTUES named after. A.S. Popova "Radioelectronics and Communication at the Turn of the Millennium"*. Moscow, 2000, p. 228-229.
20. Devyatkov ND, Belyi UN, Vasilenko AM, Kislov VY, Kislov VV, Kolesov VV, Smirnov VF, Chigin EP. The use of new reflexotherapeutic methods on the basis of the "Sharm" therapeutic-diagnostic complex in the treatment of patients with cerebral circulation disorders. *Millimeter waves in biology and medicine,* 1996, 8:5-16.
21. Megdyatov RS, Arkhipov VV, Kislov VY, Kolesov VV, Smirnov VF. The use of the therapeutic and diagnostic complex "Sharm" in the complex therapy of neuralgia of the ternary nerve. *Millimeter waves in biology and medicine,* 1995, 5:20-24.
22. Barannikov AS, Belyi UN, Grachev VI, Kislov VYa, Kolesov VV, Panchenko IP, Smirnov VF. Electropuncture diagnostics of surgical pathologies and EHF-therapy of the rehabilitation process in the postoperative period. *Millimeter waves in biology and medicine,* 1999, 2:37-44.
23. Barannikov AS, Belyi UN, Grachev VI, Kislov VYa, Kolesov VV, Panchenko IP, Smirnov VF. Restoration of psychophysiological functions in the postoperative period with the help of

radiation from the EHF-range. *Biomedical radio electronics*, 1999, 2:49-55.

24. Belyi YuN, Grachev VI, Kislov VV, Kislov VYa, Kolesov VV. Electrophysical monitoring of the states and their correction by low intensity millimetric radiation. *Proc. 12th Int. Crimean Conf. "Microwave & Telecommunication technology"* (Crimico'2002), Sevastopol, Crimea, Ukraine, 2002, p. 67.
25. Belyi YuN, Kolesov VV, Chigin EP. EHF-technology - as an element of telemedicine. *Transactions 14 Ross. simp. with Int. participation "Millimeter waves in medicine and biology"*. Moscow, 2007, p. 75-78.

.

INTELLIGENT VIDEO MONITORING OF THE BEHAVIOR OF RATS IN THE SOCIAL RECOGNITION TEST OF COGNITIVE CAPACITY ON THE WORKING MEMORY

Alexei A. Morozov, Olga S. Sushkova, Yuri V. Obukhov
Kotelnikov Institute of Radioengineering and Electronics of RAS, http://www.cplire.ru
Moscow 125009, Russian Federation
Ilia G. Komoltsev, Margarita R. Novikova, Natalia V. Gulyaeva
Institute of Higher Nervous Activity and Neurophysiology of RAS, http://www.ihna.ru
Moscow 117485, Russian Federation
morozov@cplire.ru, o.sushkova@mail.ru, outaudiofillin@gmail.com, mrnovikova.ihna@mail.ru, nata_gul@mail.ru, yuvobukhov@mail.ru

Abstract: **The aim of this work is automation of neurophysiological experiments, namely, intelligent video monitoring of the behaviour of laboratory rats during the social recognition cognitive test on the working memory. The test is conducted in the box with a sawdust background, simultaneously with EEG recording. Automatic video processing supplies objectivity of the interpretation of the results of the testing and provides new possibilities for the standardizing of the neurophysiological experiments. In the paper, methods and means for the logical description and analysis of the behaviour of experimental animals are considered. Recommendations for improving the experimental technique of the social recognition test are elaborated on the base of the results of the experiments with the automatical video processing.**

Keywords: **intelligent video monitoring; behaviour analysis; rats; social recognition; object-oriented logic programming**

UDC 538.573.61

Bibliography - 15 references *Received - 13.09.2018*
RENSIT, 2018, 10(2):269-278 **DOI: 10.17725/rensit.2018.10.269**

Content

1. INTRODUCTION

The test "social recognition" is one of the types of tests for working memory used in neurophysiological studies. The purpose of the test is to test the cognitive capabilities of the experimental animal, namely, its ability to memorize other animals.

During the test, another rat B is placed in the cage (box) with the experimental animal (rat) A (see **Fig. 1**). Experimental animal A for some time gets acquainted with animal B. This is expressed in the fact that animal A approaches B and sniffs it. These actions can be repeated several times. In the course of the test, the experimenter determines the total time spent by the animal A to get acquainted with the

Fig. 1. *During the test for social identification in a cage with an experimental animal, a young male is placed.*

animal B. After a few days, the test is repeated again with the same animals and the time spent by the rat A for acquaintance with the rat B is determined. If during the re- spent by the rat on acquaintance, is much less than in the first experiment, it is concluded that rat A remembers rats B, and therefore her cognitive abilities are not violated.

To ensure the correctness of the results of the "social recognition" test, the following test rules are applied:

1. As experimental animals in neurophysiological tests, as a rule, only males are used. Female rats are not used to ensure that the test results are not affected by the menstrual cycles of experimental animals.
2. The animal B is used by young rats (young males). Adult rats are not used so that the test results are not affected by the possible aggression of one animal in relation to another. In addition, due to the fact that animals A and B of the same sex, the possibility of sexual behavior of animals is prevented.

Neurophysiological tests considered in this work are characterized by the following features:

1. Tests were carried out in a plastic box, on the bottom of which sawdust was poured. The litter of sawdust is traditionally used as a hygienic means for the content of experimental animals, including, and for conducting neurophysiological tests. There is an opinion that the sawdust litter is a habitual habitat for the animal, and therefore the absence of sawdust could affect the results of the experiments. Unfortunately, when using automatic methods of analyzing the behavior of an animal, the presence of litter from sawdust becomes a factor seriously complicating the recognition of the animal. The problem is that the animal's hair is about the same color as the sawdust. In addition, the bottom of the cell is unevenly illuminated (usually in the center of the illumination is slightly stronger than at the edges). At the level of image processing algorithms, this leads to the fact that the image of the trunk of the rat and the background image do not have a clear separation in the color spaces "red-green-blue" (RGB) and "hue-saturation-brightness" (HSB), and for analyzing video images it is necessary to use more sophisticated (for example, textural) recognition methods.
2. Cognitive tests, considered in the work, are an integral part of the experimental study of the reaction of rats to craniocerebral trauma. During the experiment, an electroencephalogram (EEG) of the animal is recorded, so a cable is connected to the head of the rat, transmitting the EEG signals to the amplifier (see Figure 2). The cable is attached to the head of the rat with a special EEG-cap of a dark brown or bright brown color. The amplifier is a rectangular box suspended above the cage. The movements of the rat on the bottom of the cell lead to a chaotic movement of the EEG cable in the field of view of the video camera. In addition, in the field of view of the camera sometimes falls the case of the amplifier EEG signals. The color of the amplifier's enclosure at certain lighting angles is similar to the color of the coat of experimental animals. Sometimes the body of the amplifier overlaps the image of the rat. All this complicates the analysis of video images of rats and can lead to loss of video capture (see **Fig. 2**).

Note that the commercial video monitoring systems for neurophysiological experiments (such as Noldus EthoVision XT [1] and Clever Sys SocialScan [2], see review [3]) are not intended for processing video images obtained on the background of sawdust coinciding in color with animal hair. Manufacturers of such systems, as a rule, recommend using special aviaries with a contrasting background (for

Fig. 2. *The EEG cable connecting the head of the rat with the EEG signal amplifier, randomly moves in the field of view of the video camera. The case of the amplifier closed the image of the young male, which resulted in loss of video capture.*

example, a black background for white rats or a white background for black rats) for carrying out experiments. It is also recommended to color the experimental animals in colors that are easily discernible against the background of the enclosure. In the course of the work, experiments were performed on the coloration of rats with the help of potassium permanganate (see **Fig. 3**), but it turned out that this method of coloring makes even more difficult to recognize the shape of the animal against the background of sawdust, since the color of the trunk becomes uneven.

In this paper, the problem of intelligent video monitoring (automatic analysis of video images) of the behavior of rats during the "social recognition" test, conducted in conjunction with the recording of EEG in boxes with litter of sawdust, is solved. Next, methods and means for the logical description and analysis of the behavior of experimental animals during the test will be examined. In addition, recommendations will be developed to improve the methodology for conducting the "social recognition" test, taking into account bottlenecks and contradictions in the test rules found in the automatic analysis of animal behavior.

Fig. 3. *The contour of the body of the experimental animal is poorly visible against the background of the litter of sawdust.*

2. COLLECTION OF EXPERIMENTAL DATA

To carry out the experiments at the Institute of Higher Nervous Activity and Neurophysiology of the Russian Academy of Sciences (IHND and NF RAS), a laboratory stand was installed (see **Fig. 4**) equipped with high-resolution color cameras DBK 33GX174 (The Imaging Source Europe GmbH, Germany). The video was recorded with a resolution of 640 x 480 pixels and a frame rate of 30 Hz (bitrate 28.79 Mbps, AVI video file format) in order to ensure sufficient detail of video images and at the same time, if possible, reduce the size of video files.

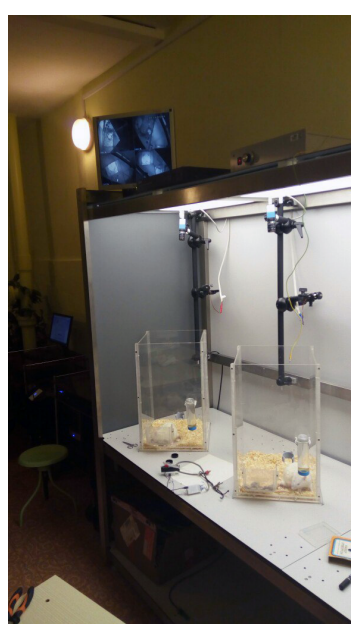

Fig. 4. *Laboratory stand in IHND and NF RAS, equipped with color cameras of high resolution.*

In accordance with the rules of the "social recognition" test, the following stages of the video image analysis can be distinguished:

1. Recognize the images of two rats A and B, where rat A is the animal on which the experiment is performed, and rat B is the young male planted in the cage during the test.
2. Measure the distance between rats A and B.
3. Calculate the total time TS, during which rats A and B were adjacent to each other, namely, closer to a given threshold of distance SD.

Of course, TS time is only a rough estimate of the time spent by rat A on sniffing of rat B. It will be further shown how adequate this assessment is and what factors are unrecorded.

Let's consider in detail the various stages of analyzing the video image.

3. SPLIT THE FOREGROUND AND BACKGROUND

To recognize images of rats, one can use one of the standard algorithms for isolating blobs on a video image, however, the recognition of rats is not limited to the task of selecting blobs, because there is no one-to-one relationship between the analyzed objects (animals) and video image blocks. The exact meaning of the term "blob" depends on which algorithm is used to allocate blobs, so the problem of the relationship between video objects and blobs will be discussed below, after discussing the algorithm for selecting blobs.

Due to the fact that video shooting of rats is carried out against the background of litter from sawdust, it is impossible to apply standard background subtraction algorithms to isolate blobs. When the rat moves along the bottom of the cell, the sawdust is shifted, and the background subtraction algorithms allocate large foreground images, including litter areas, affected in one way or another by the rat as a foreground. In such a situation, a video surveillance system (for example, [1]) can use a background subtraction to study the trail of the rat movement or an approximate evaluation of the rat movement area, but not to recognize the rat body in the image.

The isolation of blobs on the basis of color information and image brightness of the rat also does not allow stable recognition of the rat against the sawdust, as experiments with video processing have shown that images of rats and litter do not have a clear separation in RGB and HSB color spaces [4, 5]. For this reason, texture recognition methods were used to isolate blobs.

Texture method of blob selection uses for the recognition of images of rats the fact that the animal's fur has a smoother surface than sawdust. The main difference of the texture method is that it analyzes the image in a sliding window and therefore, in particular, does not allow to determine the exact coordinates of the recognized elements of the image.

Blobs were allocated by means of the built-in class VideoProcessingMachine [5, 6] of the object-oriented logical language Actor Prolog [7-15]. To improve the quality of recognition, a combination of texture and color methods for selecting blobs was used, namely, the following operations were used to isolate blobs:

1. In the HSB color space, a subspace is distinguished with a saturation from 0 to 100 conventional units (on a scale of 0-255) and brightness from 55 to 255 conventional units (on a scale of 0-255).
2. The modulus of the gradients of the channel "brightness" is calculated as the smoothness of the surface. The calculated values of the modules are normalized; while values in the range 1-10 are reduced to a scale of 0-255. Then the values are averaged in a sliding window of 27x27 pixels. After these transformations, pixels with smoothness from 60 to 200 conventional units (on a scale of 0-255) are selected.
3. The selected areas of the image are processed using the "erode" operations by 5 pixels and, then, "dilate" by 5 pixels.

4. The formed compact fragments of the image are allocated as blobs with the help of the algorithm for quick allocation of blobs TWO_PASS_BLOB_EXTRACTION, implemented in the class VideoProcessingMachine. The following parameters of the algorithm were set: the borders of the blob (horizontal_blob_border and vertical_blob_border) - 7 pixels, the minimum admissible area of the blob is 1000 pixels.
5. Of all the blobs detected in the video frame, three blobs with the largest area are selected. Three blobs must be isolated because, in addition to the two rats, a foreign object (the experimenter's hand, the body of the EEG signal amplifier, etc.) can get into the field of view of the video camera, and at this stage of analysis it is impossible to determine which blobs correspond to rats, and which foreign object.
6. Blanks inside blobs are painted over (fill operation).
7. In accordance with the principle of the virtual video processing machine implemented in the VideoProcessingMachine class, the above operations are automatically repeated for each frame of the video image.
8. Based on the information gathered during the processing of the sequence of frames, the trajectories of moving the blobs (the command blb_track_blobs) are computed. The following parameters of the blob trace algorithm were set: the minimum track length (minimal_track_duration) is 25 frames, the maximal allowed invisibility time of the blob (maximal_blob_invisibility_interval) is 5 frames.
9. Choose three blobs with the longest trajectories of displacements. In general, the trajectories in the video frame can be more than three, because new blobs can appear during the analysis of the sequence of frames, and old blobs can be deleted.

Here is the fragment of the program on Actor Prolog that loads the above commands into the virtual machine for video processing:

```
-- Pause video processing:
vpm ? suspend_processing,
-- Delete all the commands specified previously:
vpm ? retract_all_instructions,
-- Reduce the frame size
-- (proportionally, up to a width of 360 pixels):
vpm ? img_resize_image (360, -1),
-- Create a new foreground mask:
vpm ? msk_push_foreground,
-- Select pixels with low color saturation:
vpm ? msk_select_foreground ('SATURATION', 0, 100),
-- Select pixels with high brightness:
vpm ? msk_select_foreground ('BRIGHTNESS', 55,255),
-- Calculate the smoothness estimate of the texture:
vpm ? pxl_select_image_channel ('BRIGHTNESS'),
vpm ? pxl_compute_gradient ('MODULUS'),
vpm ? pxl_normalize_pixels (0,10),
vpm ? pxl_smooth_image (13),
-- Select pixels with the specified smoothness:
vpm ? msk_select_foreground (60,200),
-- Round off the resulting spots:
vpm ? msk_erode_foreground (5),
vpm ? msk_dilate_foreground (5),
-- Select blobs:
vpm ? blb_extract_blobs (
      'Rats', 'TWO_PASS_BLOB_EXTRACTION'),
-- Choose the three largest blobs:
vpm ? blb_select_front_blobs (3,
        'FOREGROUND_AREA'),
-- Fill voids in blobs:
vpm ? blb_fill_blobs,
-- Trace blobs:
```

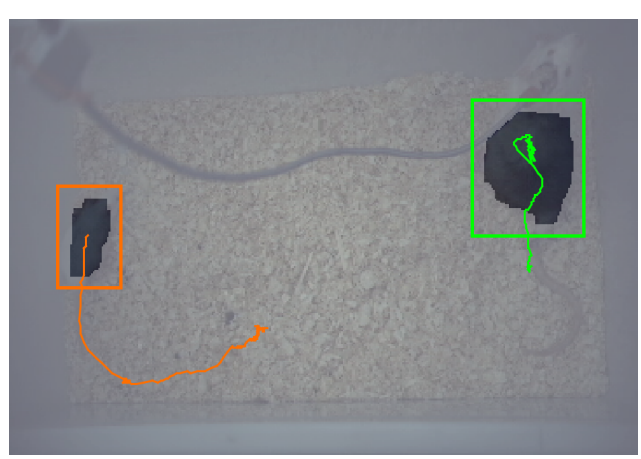

Fig. 5. *Blobs selected using the texture method.*

```
vpm ? blb_track_blobs,
-- Select the three longest tracks:
vpm ? trk_select_front_tracks (
        3, 'NUMBER_OF_FRAMES',
        'DESCENDING_ORDER'),
-- Select all image channels:
vpm ? pxl_select_image_channel ('ALL'),
-- Resume processing frames:
vpm ? process_now.
```

In **Fig. 5** gives an example of the results of video processing. Pixels selected as the foreground image are highlighted in dark gray. Blobs are indicated by green and orange rectangles. In addition, the lines of the corresponding colors show the trajectories of the displacement of the mass centers of the blobs.

The sequence of the video frame processing instructions considered realizes the stage of low-level analysis of the video image [8, 10, 11]. The result of this stage are the graphs describing the trajectories of blob movements in the video frame. At the next stage, the stage of high-level analysis, a logical analysis of these graphs is performed, and conclusions are drawn about the behavior of rats during the test.

4. DETECTION OF RATS

In accordance with the rules for carrying out a neurophysiological test, one or two rats may be in a separate video frame. These rats may have several blobs:

1. One blob, if, for example, one rat was selected as a foreground fragment, and the second, for some reason, no, or if the rats are close to each other and merged into one blob.
2. Two blobs, for example, if each rat corresponds to a separate blob.
3. More than two blobs, for example, if the image of the rat was separated by an EEG cable.

In addition, additional blobs corresponding to the EEG-amplifier body, fragments of the EEG-cable, the experimenter's hand, reflections of light from the box walls, and other random factors may appear on the video image. At the level of the low-level analysis of the video image, three blobs of the largest size, with the largest track length, are selected.

The following model of the video scene is used. It is assumed that there are from 0 to 2 rats in the video frame. At first, there are no rats in the video frame, then new rats may appear, but the total number of rats can not exceed two. Each rat has current coordinates in the video frame. If two rats A and B are detected in the video frame, a distance DPAB between the centers of mass of the blobs (in pixels) is used as a rough estimate of the distance between them, and as a more accurate estimate - the distance DMAB between the nearest points on the rectangular borders of the blobs in meters (Actor Prologue allows you to convert the coordinates in pixels to the coordinates in meters in accordance with the specified matrix of projective transformations).

In the course of the experiment, the tracks of the blobs may break off and reappear, and in general it is impossible to determine whether the newly appeared track is the continuation of the trajectory of the rat lost some time ago, or a new object appeared in the frame. In the model, the DP threshold of the DPAB distance is entered, to which the rat can move for the time that its video capture has been lost. It is assumed that the threshold DT is 75 pixels.

The blobs observed in the video frame are put in correspondence with the alleged images of the rats. The following logical rules apply:

1. When analyzing the next video frame, the logic program tries to place the observed blob tracks in correspondence with the rats detected during the processing of the previous frames. In accordance with each BV block, the rat is located closest, however, no further than the preset threshold DT.
2. If no rat is located near the DT to the BV block and the number of recognized rats is less than two, it is considered that the BV blob corresponds to the new object. In this case, a new rat is added to the model, and coordinates of the BV blob are taken as its coordinates.

3. If there are rat RIs in the model that do not have any blobs in the current frame and in the previous frames there were BI blobs whose tracks disappeared in the current frame, the program assumes that some rats turned out to be invisible in the current frame (for example, their image was blocked by an extraneous object). In this case, each rat RI is matched with the nearest BI blob if the distance between them does not exceed the threshold DT.
4. If there was an RI rat in the model, in accordance with which no blobs were delivered, but in the previous frame, the DMAB distance between the two rats did not exceed the SD threshold (taken equal to 0.02 meters), it is considered that the rats came close to each other , and their images merged. The coordinates of the rat RI are taken equal to the coordinates of the rat currently visible.

The experiments showed that the above set of rules allows to adequately interpret the video image of rats, including in situations where rats are approaching and moving away from each other. In this situation, the model of the video scene used does not distinguish rat A from rat B, and this is its drawback. However, this is unimportant from the point of view of the test results, since the experimenter is only interested in the distance between the rats. Conditionally it is considered that the rat A corresponds to blobs, the size of which was the largest compared to other blobs at the time of its appearance. Rat A is marked green, and rat B is orange (see **Fig. 6**).

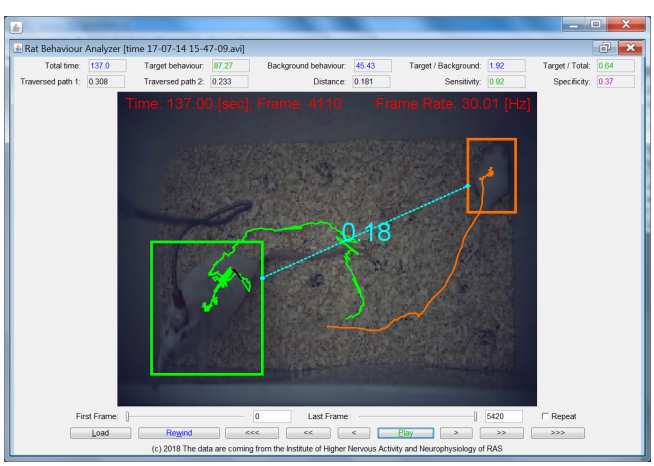

Fig. 6. *The logic program analyzes the behavior of rats. The blue line indicates the distance between the rats. The remaining notations are the same as in Fig. 5.*

5. ANALYSIS OF THE BEHAVIOR OF RATS

Based on the rules of the analysis of the video scene, formulated in the previous section, a logical program was developed that analyzes the behavior of rats during a neurophysiological test. 9 experimental video recordings were analyzed (see **Table 1**). In the algorithm for analyzing the behavior of rats, it was assumed that rat A sniffed rat B when the observed distance between DMAB rats was ≤ 0.02 meters.

To assess the quality of recognition, all 9 videos were analyzed manually. Time intervals have been identified in which rat A sniffs rat B. **Table 2** gives estimates of the sensitivity and

Table 1.
Results of the analysis of the behavior of rats.

№	Test time (s)	Share of social activity (sec)	Social activity (%)
1	181	15	8
2	181	112	62
3	181	120	67
4	181	133	74
5	181	127	70
6	181	140	77
7	181	109	60
8	181	126	69
9	185	180	97

Table 2.
Estimates of the sensitivity and specificity of the recognition algorithm.

№	Sensitivity	Specificity
1	0.88	1.0
2	1.0	0.63
3	0.93	0.35
4	0.95	0.38
5	0.95	0.43
6	0.98	0.4
7	0.93	0.37
8	0.96	0.56
9	1.0	0.08

specificity of the algorithm for recognizing the desired behavior of a rat, calculated by comparing the results of manual marking of video recordings with the results of automatic analysis.

The estimates in Table 2 show that the logical method of recognition has a sufficiently high sensitivity (in most cases, above 90%), but the specificity of the method is rather low (in most cases, less than 50%). A detailed analysis of video records showed that the recognition algorithm is mistaken in the following cases:

Rats can be near, but do not sniff each other. For example, in **Fig. 7**b, the rats practically touch each other, but their attention is directed to an object from above.

Rat B can also sniff Rat A, and the algorithm will erroneously detect the social activity of rat A (see the example in Fig. 7c).

There were reported cases of abnormal behavior of rat A when it captured rat B with forelegs and for a long time sniffed the genitalia of rat B (see the example in Fig. 7d). Most likely, these actions were not a manifestation of the sexual behavior of rat A, because she did not attempt to perform coitus. Perhaps these actions are a manifestation of the deto-oriented behavior of an adult in relation to a young rat. These actions are also erroneously interpreted by the algorithm as recognition by rat A of rat B.

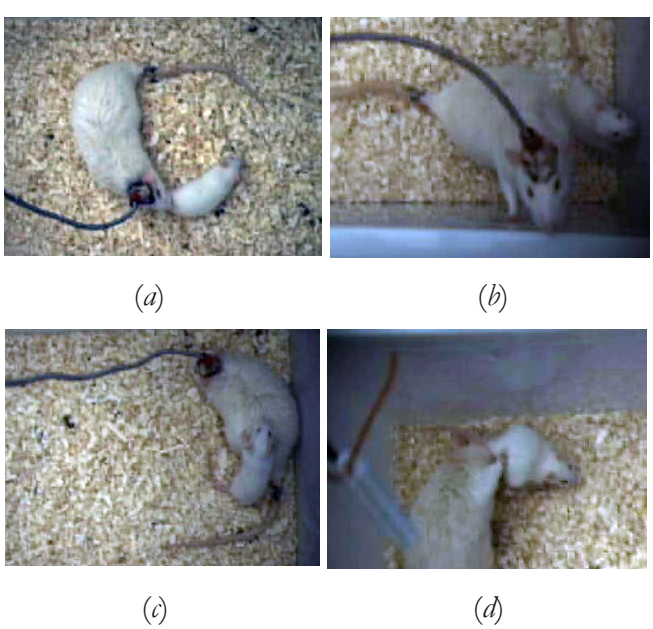

(*a*) (*b*)

(*c*) (*d*)

Fig. 7. *Examples of behavior of rats: (a) Rat A sniffs rat B, (b) Rats just sit next to, (c) Rat B sniffs rat A, (d) Quasi-sexual behavior of rat A.*

With the manual analysis of the results of the "social recognition" test, the above examples of the behavior of rats can be interpreted in different ways, depending on the experimenter's opinion, which, of course, casts doubt on the objectivity of the conducted study of the behavior of rats. Low estimates of the specificity of automatic recognition of the desired behavior of rats indicate that to ensure the correctness of test results, it is necessary to make changes in the methodology for conducting it. Based on the experiments performed, the following additional test rules can be recommended:

The test must be carried out in a large enough enclosure to reduce the chance of the rats being accidentally located next to each other (without communication between the rats).

At the beginning of the test, the young male B must be inserted sufficiently far from the rat A so that the automatic recognition algorithm has time to carry out the video capture of both rats separately.

It is advisable to investigate the possibility of decreasing the probability of the deto-oriented behavior of the rat A during the test.

It is advisable in some way to restrict the freedom of movement of rat B in an aviary to reduce the likelihood of an erroneous recognition of the situation of "rat B sniffing rat A" as a manifestation of social activity on the part of rat A.

6. CONCLUSION

The method and software for intelligent video monitoring of laboratory rats on the basis of the object-oriented logical language Actor Prolog [15] was developed. The method allows to analyze video images of experimental rats in non-standard conditions when it is impossible to apply existing systems of animal behavior analysis. In particular, it allows analyzing the

social behavior of rats in a box with a bed of sawdust under conditions of low contrast of images and uneven illumination. A logical description and analysis of the behavior of rats with a cognitive test on the working memory of "social identification" was carried out. Based on the results of the experiments, recommendations were developed for improving the test procedure.

AKNOLEJMENT

The authors are grateful to Anna Olegovna Manolova and Irina Pavlovna Levshina (IHND and NF RAS) for their help in conducting the experiments.

The study was carried out at the expense of a grant from the Russian Science Foundation (project No. 16-11-10258).

REFERENCES

1. Noldus LP, Spink AJ, Tegelenbosch RA. EthoVision: a versatile video tracking system for automation of behavioral experiments. *Behavior Research Methods*, 2001, 33(3):398-414.
2. Clever Sys Inc; 2018. Available from: http://cleversysinc.com.
3. Tscharke M, Banhazi TM. A brief review of the application of the machine in livestock behaviour analysis. Agrárinformatika. *Journal of Agricultural Informatics*, 2016, 7(1):23-42.
4. Morozov AA, Sushkova OS. On the development of methods and algorithms based on object-oriented logical programming for video monitoring of laboratory rats. In: *Sat. Works of the IV International Conference and the Youth School "Information Technologies and Nanotechnologies"* (ITNT-2018), April 24-27, 2018, Samara, Samara National Research University, 2018, p. 1182-1192.
5. Morozov AA, Sushkova OS, Vaniya SM. Development of Methods and Algorithms Based on Object-Oriented Logic Programming for Video Monitoring of Laboratory Rodents. In: *Signal-Image Technology & Internet-Based Systems (SITIS-2017), 13th International Conference IEEE,* 2017, p. 311-318.
6. Morozov AA, Sushkova OS. Virtual machine for low-level processing of video images in Actor Prolog. In: *Sat. Works of the IV International Conference and the Youth School "Information Technologies and Nanotechnologies"* (ITNT-2018), April 24-27, 2018, Samara, Samara National Research University; 2018, p. 1275-1285.
7. Morozov AA, Sushkova OS, Polupanov AF. Object-Oriented Logic Programming of Intelligent Visual Surveillance for Human Anomalous Behavior Detection. In: Rivas-Lopez M, Sergiyenko O, Flores-Fuentes W, Rodriguez-Quinonez JC (eds.). *Optoelectronics in Machine Vision-Based Theories and Applications*. Hershey, IGI Global Publications, 2019, p. 134-187.
8. Morozov AA, Sushkova OS. Real-time analysis of video by means of the Actor Prolog language. *Computer Optics*, 2016, 40(6):947-957.
9. Morozov AA, Sushkova OS, Polupanov AF. Towards the Distributed Logic Programming of Intelligent Visual Surveillance Applications. In: Pichardo-Lagunas O, Miranda-Jimenez S (eds.). *Advances in Soft Computing, Part II*. Cham: Springer International Publishing, 2017, p. 42-53.
10. Morozov AA. Development of a Method for Intelligent Video Monitoring of Abnormal Behavior of People Based on Parallel Object-Oriented Logic Programming. *Pattern Recognition and Image Analysis*, 2015, 25(3):481-492.
11. Morozov AA, Vaish A, Polupanov AF, Antciperov VE, Lychkov II, Alfimtsev AN, et al. Development of the concurrent object-oriented logic programming platform for the intelligent monitoring of anomalous human activities. In: Plantier G, Schultz T, Fred A, Gamboa H (eds.). *BIOSTEC 2014, vol. 511 of CCIS*. Heidelberg, Springer, 2015, p. 82-97.

12. Morozov AA. Logic Object-Oriented Model of Asynchronous Concurrent Computations. *Pattern Recognition and Image Analysis,* 2003, 13(4):640-649.
13. Morozov AA. Actor Prolog: an Object-Oriented Language with the Classical Declarative Semantics. In: Sagonas K, Tarau P (eds.). *IDL 1999*. Paris, France, 1999, p. 39-53.
14. Morozov AA. The Prolog with Actors. *Programmirovanie*, 1994, (5):66-78 (in Russ.).
15. Morozov AA, Sushkova OS. The Intelligent Visual Surveillance Logic Programming Web Site, 2018. Available from: http://www.fullvision.ru.

DYNAMIC-CHAOS INFORMATION TECHNOLOGIES FOR DATA TRANSMISSION, STORAGE, AND PROTECTION

Yuri V. Gulyaev, Rostislav V. Belyaev, Georgy M. Vorontsov, Nikolay N. Zalogin, Valerii I. Kalinin, Erast V. Kal'yanov, Vladimir V. Kislov, Vladimir Ya. Kislov, Vladimir V. Kolesov, Evgeny A. Myasin, Evgeny P. Chigin

Kotelnikov Institute of Radioengineering and Electronics of RAS, http://www.cplire.ru
Moscow 125009, Russian Federation

gulyaev@cplire.ru, belyaev@cplire.ru, info@cplire.ru, zal.dunin@mail.ru, val.kalinin@mail.ru, kalianov@ms.ire.rssi.ru, info@cplire.ru, kvv@cplire.ru, eam168@ms.ire.rssi.ru, chigin@cplire.ru

Abstract. **Information technologies based on dynamic chaos are considered. Their promising applications in data transmission, processing, storage, and protection are reviewed. Wideband data transmission channels that use complex signals with a large processing gain produced by dynamic chaotic systems are described. Finitedimensional mathematical algorithms are proposed for calculation of chaotic signals by reconstructing nonlinear dynamics in dissipative systems with delay. It is shown that a digital data transmission system with spread spectrum and dynamic code escape exhibits high noise immunity and security, is electromagnetically compatible with other devices, and guarantees reliable and confidential data transmission in a complex electromagnetic environment. Schemes of data masking, protection, processing, and transmission are implemented in original chaotic algorithms.**

Keywords: **information technologies, dynamic chaos, broadband systems, algorithms for computing chaotic signals, dissipative systems with delay, noise immunity, security**

UDC 004.93, 621.391

Bibliography - 45 references *Received 16.06.2003* [1]

RENSIT, 2018, 10(2):279-312 **DOI: 10.17725/rensit.2018.10.279**

Content

1. INTRODUCTION

In classical radiophysics, the occurrence of noise has always been associated with fluctuations in the thermal and shot nature. The enrichment of the frequency spectrum of oscillations of generators of electromagnetic oscillations was expressed in the presence of harmonics or subharmonics of the fundamental frequency, and the finite width of the spectral line of the generators was explained by the influence of fluctuations. Therefore, the discovery in the IRE of the RAS in the mid-sixties of the generation of noise oscillations was, to some extent, an unexpected event for specialists in the field of radiophysics [2]. The intensity and frequency band of the noise obtained on plasma and electronic devices such as a traveling wave tube (TWT) could not be explained by the influence of fluctuations. The nature of the generation of such intense chaotic oscillations could be explained on the basis of the methods of nonlinear dynamics in self-oscillating systems with delayed feedback. Around the same time, Lorentz in a numerical experiment on an essentially simplified model of convective instability of the earth's atmosphere, reduced to three ordinary nonlinear differential equations of the first order, showed the possibility of the appearance of chaotic oscillations [3].

The development of mathematical concepts of the possibility of the appearance of complex non-periodic motions in dynamical systems goes back to Poincaré, which introduced the notion of homoclinic trajectories with respect to the problem of motion of a system of three interacting bodies [4]. Further studies showed that for dynamical systems of a very wide class, complex irregular motions are no less characteristic than classical regular processes. The fact was amazing that such motions are possible in dynamical systems with a small number of degrees of freedom. Prior to this, it was intuitively assumed that a complex chaotic motion is possible in systems with an infinite or very large number of degrees of freedom. This assertion was contained in the model of turbulent motion of the hydrodynamic system developed by Landau in 1944 [5]. The establishment of a complicated chaotic character of the motion of a dynamical system with a small dimension is rather nontrivial.

Since the beginning of the 1960s, IRE RAS has been working on the development of direct-microwave generators of the microwave range, mainly in the framework of solving the problems of electronic warfare. It was then that the original idea of a noise generator - a noise generator based on a ring auto-oscillation system consisting of an O-or M-type microwave amplifier and a special non-linear element providing stochastization of the generated oscillations was proposed. Generators of this type were implemented on TWT, in plasma, and later in semiconductor transistor and diode generators [6-13].

In the late 1970s, a large number of works appeared on the detection of chaotic motion in a variety of systems and environments. As a result, the classification of transition scenarios from monochromatic oscillations to chaos in various dynamic systems began. The widening of the research front allowed us to reach generalizations and reveal the patterns of the onset of chaotic motion. As a result, this led to the development of ideas about a strange attractor as an image of the motion of a dynamical system in its phase space. At present, the concept of dynamic chaos is identified with the notion of a "strange attractor" introduced by Ruelle and Taken [14]. A specific feature of the motion of a dynamical system on a strange attractor is that unstable trajectories in its phase space are attracted not to a limit cycle or torus having integer dimension, but to a stable Cantor set having a fractal dimension [15]. Previously, complex dynamics in conservative systems was discovered in the works of Chirikov and Zaslavsky [16].

Further studies were conducted on the way of establishing ever wider classes of dynamic systems (both natural, representing natural phenomena, and mathematical models and technical systems) in which the effects of dynamic chaos were observed. The patterns of scenarios for transitions to chaos are established and the basic necessary conditions for the existence of chaotic motion are elucidated [17].

The chaotic motion of dynamical systems has a number of specific features. The realizations of this motion have a power spectrum continuous in the frequency band, an exponentially decreasing autocorrelation function, a Gaussian probability distribution function of the values. At the same time, dynamical chaos systems are characterized by purely dynamic properties such as an extremely high sensitivity to the initial conditions and associated exponential dispersal of close trajectories.

Earlier, the study of mechanisms for the formation of chaotic movements of dynamic systems was carried out mainly on radiophysical and radio electronic systems. These results have shown that the chaotic properties of dynamical systems can find practical application. The current direction is the search for new technologies based on the use of specific properties of dynamic systems in a state of dynamic chaos. This served as a basis for the development of a number of new areas of research, including in such areas as informatics, biophysics, chemistry, medicine, dynamics of natural phenomena (for example, earthquakes) [17].

One of such promising areas is research in the field of creating new telecommunication systems based on the properties of chaotic dynamics. The chaotic dynamics of systems attracts the possibility of obtaining complex oscillations by simple devices in structure, the realization of a large number of different chaotic modes in one device, a large information capacity, a variety of methods for inputting an information signal into chaotic, the ability to synchronize the transmitter and receiver, and confidentiality in the transmission of messages. Such a variety of chaotic manifestations of dynamic systems has caused various approaches to the use of chaotic regimes of dynamical systems in the field of communication [18]. An important direction in this case is the development of new classes of algorithms for the formation of sequences with the properties of random processes based on chaotic dynamics [19-22]. This opens the possibility of developing new information technologies and creating new promising methods of using chaotic signals for the transmission, processing, storage and protection of information.

2. INFORMATION MEDIA ON CHAOTIC ALGORITHMS

The search for information carriers (processes and signals) with an increased information capacity and mathematical algorithms that generate such processes is the most urgent task in the development of new information technologies. The basic concept in the field of information technology is "information coding", usually interpreted as a synonym for "information representation". Such carriers of information can be graphics (pictures), texts, musical notations, numbers, sequences of electromagnetic, optical or other signals.

The term "information systems" includes all devices that provide the receipt, processing, transmission and storage of information. These are various sensors that transform external influences (sound, image in the form of a light field of various local intensity, pressure, temperature, chemical composition of the environment, etc.) into electrical signals, electronic systems for converting and processing signals based on computer technology and this means of radio communication and telecommunications . The information in these systems is recorded

either in the form of a continuous electrical signal - an analog form of information coding, or as a sequence of electrical pulses - a digital encoding form. With analog coding, the necessary information is transmitted by the corresponding amplitude or frequency of oscillations of the continuous electrical signal. In digital form, information is expressed in the form of a binary code specified by an electrical pulse, for which, for example, the logical state "0" corresponds to the absence of an electrical voltage (or current), and the state "1" is its presence. Digital codes due to good protection from errors and interference, high processing speeds in computer systems and high transmission density over communication channels are prevalent in modern information systems.

A. Discrete Generating Algorithms for Forming Chaotic Signals

From the theory of information, it is known that stochastic signals generated by random processes possess the greatest information capacity. The main problem in the development of information carriers in digital telecommunication channels is the difficulty of generating random binary sequences using a short master key. Mathematical algorithms that form pseudo-random sequences (PNRs) of numerical values based on the key must have a number of necessary properties:

1) arbitrarily large length of the nonperiodic segment of the obtained SRS,

2) the statistical similarity of the resulting sequence of numbers to the properties of a purely random sample,

3) the possibility of software and hardware implementation of a random number generator for application in a communication channel with an appropriate speed.

In spite of the fact that quite a lot of algorithms for generating pseudo-random sequences are known, in practice a recursive algorithm is used to generate binary memory bandwidths, when an infinite sequence is constructed based on a linear recurrence relation and some initial values, each successive term of which is determined from previous. Binary sequences based on recurrence relations are easily implemented on a computer in the form of programs and circuitry based on high-speed multi-bit binary shift registers.

Attempts to adapt for digital algorithms operations on real numbers ended in failure, since replacing the actual number with its approximate value greatly changes the statistics of the obtained sequence. The rounding operation introduces an unpredictable disturbance into the generating algorithm, and the resulting sequence ceases to be statistically independent, and therefore random.

The main method of obtaining the memory bandwidth at present is the formation of M-sequences (sequences of the maximum period) on the basis of shift registers, when the numerical value at a given moment is determined by linear relations with some weight (code) with respect to the previous terms of the sequence. In this case, the weight coefficients are selected in such a way as to ensure a rapid decrease in the correlation function up to order values, where N is the length of the M-sequence period. The biggest drawback of this method is the lack of a mathematical apparatus that makes it possible to obtain algebraic polynomials generating sequences of a maximal period of arbitrarily large degree, moreover, information on high-degree polynomials suitable for noise-immune encoding is exclusively secret.

The known classes of memory bandwidths, both linear (M-sequences, Hadamard, Gold, Kasami sequences, etc.), and non-linear (Legendre sequences, bent sequences, etc.), have certain drawbacks and do not satisfy some of the requirements listed above. A definite solution to the problem is the use of noise-like signals (SHPS), formed by nonlinear systems with dynamic chaos. Such SNS, having correlation properties no worse than M-sequences, have an almost unlimited set of lengths, can form ensembles of signals of large volumes and are

non-linear, which makes it difficult to recognize them for later playback.

All known dynamical systems with a small number of degrees of freedom that have dynamic chaos (the "strange attractor") - the attractor of Lorentz, Ressler, the Chua system, ring systems with delay and purely amplitude nonlinearity - also do not provide correlation functions with the necessary parameters.

Good statistical properties have dynamic systems in which both dissipative (amplitude) nonlinearity and reactive (phase) nonlinearity are present simultaneously. In self-oscillatory systems with phase nonlinearity and delay, phase balance conditions, mode synchronization conditions are violated as a result of phase nonlinearity, and in the process of chaotic oscillations, there is a weakening of intraspectral connections and a faster (in comparison with other autostochastic systems) splitting of correlations in the generated signal. Signals with good correlation properties can be obtained in a class of nonlinear ring systems with delay, in which both active (amplitude) and reactive (phase) nonlinearity are present simultaneously. The scheme of such a system can be represented as a ring of three blocks (**Fig. 1**).

The self-oscillation mechanism in such a system can be described by a complex integral equation, where the action of all functional blocks is taken into account:

$$\hat{x}(t) = \int_{-\infty}^{t} g(t-\tau)\hat{F}(\tau - T)d\tau, \quad (1)$$

which can be transformed to a discrete form:

$$\hat{x}_k = (1-\exp(-h))\hat{F}_{k-N_z} + \exp(-h)\hat{x}_{k-1}, \quad (2)$$

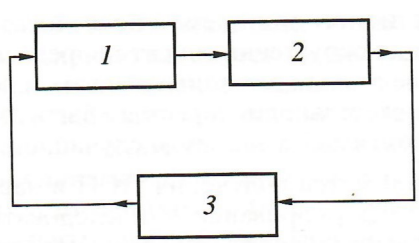

Fig. 1. *Model of a dynamic system with chaotic behavior: 1 - non-linear amplifier; 2 - delay line; 3 - filter*

if we introduce a rectangular filtering of the signal, represent the functions g and in the form of orthogonal Kotel'nikov series and carry out some transformations. Here = aexp (iφ), = F (ak) exp [φk + Φ (ak)], Nz is the retardation parameter, h is the sampling step chosen in accordance with the Kotel'nikov theorem [22]. The non-linear amplitude conversion functions F (x) and the phase of the signal Φ (x), which determine the process of stochastization of oscillations in a given dynamical system, depending on the choice of the type of the nonlinear amplifier, can be quite complicated. The determining factor for the signal to obtain the desired statistical properties is the presence of a steep slope of the phase characteristic with respect to the value of the signal at the input of the nonlinear element. By numerical computer analysis, the system parameters were selected in order to obtain a developed randomness of auto-oscillations and a rapid decrease in the autocorrelation function of the signal (ACF).

The calculation of the values of the mutual correlation function (ICF) has shown that the shape of the SCF is qualitatively similar to the ACF type, and its largest emissions tend to decrease with an increase in the duration of realizations in accordance with a similar law.

In the practical implementation of a new class of signals in digital communication technology, which is based mainly on the binary code, there are two possibilities for obtaining binary signals. The first method is associated with clipping of multi-level signals obtained as a result of calculations. As shown by the numerical experiment, the binary quantization of a multilevel signal practically does not worsen its correlation properties.

The second method is the direct construction of discrete self-oscillating systems. For example, the algorithm for obtaining a binary signal in a discrete autooscillatory system can have the form

$$x_k = \text{sign}[F(x_{k-N})] + x_{k-1}. \quad (3)$$

This relation was obtained directly from Eq. (2).

Based on the mathematical model of a ring auto-oscillating system with strong amplitude-phase nonlinearity, filtration and delay, a discrete generating algorithm of a chaotic signal is developed and investigated, which belongs to the class of algorithms of recurrent-parametric type with delay. The form of the algorithm of this class in general form has the form of a discrete functional transformation (mapping):

$$x_n = f(x_{n-1}, x_{n-2}, ..., x_{n-Nz}), \quad (4)$$

where x_n and x_{n-1} are the newly calculated member of the pseudo-random sequence being formed at the n-th step and the previous term of this sequence at the (n-1)-th step, N_z is the retardation parameter equal to the number of sequence members in the delay interval x_{n-1}, x_{n-2}, ..., x_{n-N}, which completely determine the new value of X_n and must be specified as the initial condition in the first step, and the function $f(x)$ reflects the amplitude and phase transformations in the generating circular self-oscillating system in chaotic mode. The algorithm is defined on the set M of integers of the natural series belonging to the closed numerical interval $[M_1, M_2]$, ($M_2 > M_1$, $M = M_2 - M_1 + 1$), and forms an almost uncorrelated pseudo-random sequence of integers by a probability distribution close to uniform, and correlation characteristics, corresponding to the requirements imposed on the coding signals.

A feature of delayed algorithms is that the mapping formula they specify can output a new value of xn beyond the domain of the algorithm $[M_1, M_2]$. Therefore, the formula of the algorithm (4) must be supplemented by a special operation that ensures the return to the given numerical interval of the value xn of each newly calculated member of the sequence in the event that it is outside its boundaries. Transformations of this kind with the mapping of a numerical set "into themselves" have long been known. An example is the well-known baker's transformation [15]. Other types of transformations are possible, but among them one should especially highlight those that do not make significant changes in the probability distribution of the generated numbers.

B. Reconstruction of nonlinear dynamics for a system with delay

Theorems on the reconstruction of nonlinear dynamics in the embedding space [24] state the existence of a one-to-one and finite-dimensional mapping for the original infinite-dimensional system with delay. However, theorems on the reconstruction of nonlinear dynamics do not give a general way of constructing finite-dimensional diffeomorphic mappings. By the method of reconstruction of nonlinear dynamics, it is possible to determine the smallest dimension of a new dynamical system, which more than twice can exceed the fractal dimension of the original chaotic attractor.

When developing discrete mathematical algorithms for the formation of broadband chaotic signals on the basis of self-sustained oscillating systems with delay, the problem of the finite-dimensional representation of highly nonequilibrium nonlinear dynamics arises. Let us consider dissipative dynamical systems for which the initial volume in the phase space is compressed. An important property of dissipative systems with delay is the convergence of bounded trajectories to finite-dimensional manifolds in the original phase space with a quadratic metric [25].

Chaotic attractors in infinite-dimensional dynamical systems with delay have finite fractal dimension [26]. A finite-dimensional description of bounded trajectories on the original chaotic attractor can be carried out by reconstruction of nonlinear dynamics [24].

The behavior of many dynamical systems with delay is determined by a first-order differential equation of the general form:

$$dx(t)/dt = \Phi[x(t); x(t-T); \mu], \quad (5)$$

where Φ is a nonlinear operator, T is the retardation time, and μ is the control parameter. Each state of the dynamical system (5) is given

by the continuous trajectory $x_k(\tau)$ on the kth time interval $t = kT + \tau$ ($0 < \tau \leq T$) by the duration T. The set of all chaotic trajectories x_k of length T forms an attracting set-attractor $M(T) = \{x_k\}$ in the infinite-dimensional phase space L_2 (T) of the original system (5).

Let us introduce in the space $L_2(T)$ of continuous functions the mean square metric and define the distance between arbitrary functions in the form

$$\rho(x_k, x_m) = \|x_k - x_m\|. \quad (6)$$

The norm of each function is assumed to be bounded.

An important property of dissipative systems with delay is the convergence of bounded trajectories to finite-dimensional manifolds in the original phase space $L_2(T)$ with quadratic metric.

Let the chaotic attractor $M(T) = \{x_k\}$ with fractal dimension D_c be contained in a compact manifold MD of integer dimension $D \geq D_c$. Then, according to the embedding theorem, the chaotic attractor $M(T) = \{x_k\}$ can be projected uniquely onto the subspace MN with the embedding dimension $N \geq 2D + 1$ [27].

A finite-dimensional description of motions on a chaotic attractor can be carried out in the reconstruction space M2D + 1 by using N = 2D + 1 new dynamical variables. To find these variables, we use the well-known procedure of orthogonal projection of continuous functions onto finite-dimensional subspaces [28].

If we choose the basis $\{\varphi_i(\tau)$ in L_2 (T); i = 1, 2, ..., N} from orthonormal functions, for example in the form of weight functions with displacement on a finite interval of time T, then the time displacement for neighboring basis functions is determined by the ratio of the delay time in the system to the dimension of the embedding:

$$\Delta\tau = T/(2D + 1) \quad (7)$$

We construct a linear, functional subspace M2D + 1 spanned by a system of basic functions $\{\varphi_i\}$. We perform the orthogonal projection of chaotic functions $\{x_k(\tau)\}$ from L_2 (T) onto the constructed space $M_2D + 1$:

$$\tilde{x}_k(\tau) = \sum_{i=1}^{2D+1} x_k(i)\varphi_i(\tau). \quad (8)$$

Here the numerical coordinates $x_k(i)$ of the expansion of the function with respect to the system of basis functions $\{\varphi_i(\tau); i = 1, 2, ..., N\}$ are in the form of a scalar product:

$$x_k(i) = (x_k, \varphi_i) = \int_0^T x_k(\tau)\varphi_i(\tau)d\tau. \quad (9)$$

A representative function. is a one-to-one projection in the space $M_2D + 1$ for the initial chaotic function $x_k(\tau)$, according to Takens' theorem on reconstruction of nonlinear dynamics [24].

The set of numerical coordinates $\{x_k(1), x_k(2), x_k(2D + 1)\}$ defines a (2D + 1) - dimensional vector X_k in the recovery space.

The coordinates of the vector Xk = {xk (i)} are determined by the scalar product (9) with the weight functions {φi}, and therefore in the general case they differ from the discrete samples of the chaotic trajectory. Finding the numerical coordinates (9) will require computational costs for the orthogonal decomposition procedure (8) in the system of basis functions {φi} defined on a finite time interval T. However, the dimension (2D + 1) of the reconstruction space constructed in this way is the smallest according to the reconstruction theorem Takens [24].

When calculating the coordinates of the vector Xk = {xk (i)}, the sampling step (7) is equal to the ratio of the delay time T in the dynamical system (5) to the embedding dimension (2D + 1). Expression (7) determines the largest discretization interval for a finite-dimensional representation of the original trajectories {xk (τ)}. Here D is the dimension of a compact set that contains the initial chaotic attractor for the dynamical system (5).

Thus, as a result of methods for reconstructing nonlinear dynamics for a delayed system (5), a lower bound for the dimension of the embedding N is obtained:

$$N = 2D + 1, \quad (10)$$

which more than twice exceeds the fractal dimension Dc of the chaotic attractor itself [30]. The dimension of the manifold D ≥ Dc is the closest integer complement for the fractal dimension Dc of the chaotic attractor. The largest step of sampling Δτ is determined by the lower boundary N = 2D + 1 for the embedding dimension by the formula (7). This result is important from a practical point of view for constructing discrete mathematical models. Finite-dimensional nonlinear algorithms unambiguously describe the chaotic behavior of the initial infinite-dimensional dynamical system with delay (5) under the condition that the dimension of non-linear algorithms is more than twice the fractal dimension of the original chaotic attractor.

C. Synthesis of a set of chaotic codes

Identification of transmitted messages by its own chaotic code of m initial conditions for a chaotic trajectory

$$X_0 = \{x_0(h), x_0(2h), \dots, x_0(mh)\}^T \quad (11)$$

allows code division and code addressing for all subscribers in the communication network.

The base of the chaotic signal is the number of discrete samples n used to transmit one bit of useful information. In the course of message transmission, the base n of the chaotic signal can be arbitrary with respect to the dimension of the embedding m. In practice, the chaotic signal base is set by the information transfer rate and the duration h of one elementary symbol for the chaotic code. The base n of the chaotic signal is an important parameter, determines the real volume of the system of chaotic signals and characterizes the noise immunity of the communication system with spreading spectrum.

Creation of a large ensemble of binary chaotic codes is carried out by a simple mathematical algorithm of the form

$$\begin{aligned} y_k &= sign[F(x_k)], \\ x_k &= (1-\exp(-h))sign[F(x_{k-m})] + \exp(-h)x_{k-1}, \end{aligned} \quad (12)$$

with the help of which chaotic processes are calculated in a strongly nonequilibrium dynamic system with delay [19]. Here the parameter h denotes the step of sampling by the Kotelnikov sample theorem, and the integer m determines the number of samples on the delay interval in the system (12), which is the embedding dimension for a set of chaotic codes by Takens' theorem on reconstruction of nonlinear dynamics [24].

Coding in the broadest sense is understood as representing messages in a form convenient for transmission over a communication channel. The encoding procedure consists in making a one-to-one representation of the transmitted messages by n-dimensional signals from the redundant set Mn of dimension n. The power of the set Mn or the number of different code sequences with duration n is determined by the value C = bn, where b is the code base.

Chaotic code sequences are formed by a mathematical nonlinear algorithm with a retarded argument (12). In the given domain of control parameters, the generating algorithm (12) has a strongly nonequilibrium chaotic dynamics. Each message is transmitted by a single and never repeating chaotic code combination of n binary symbols.

The distance between arbitrary binary codes Yk = (ylk, y2k, ..., ynk) and Y1 = (yll, y21, ..., ynl) in the original space Mn is given by the Hamming metric d (Yk, Yl), which indicates the number positions with non-matched symbols for the selected code pair. Synthesis of the system of optimal chaotic codes consists in choosing from a given criterion a subset Un from the whole set Mn of chaotic codes. The code distance of the selected subset Un is a number

$$D = \min d(Y_k, Y_l), \quad (13)$$

where the minimum is over all distances determined between the codes of the subset Un. The code distance of the subset Un is characterized by the remoteness of the two closest code sequences from each other.

The chaotic codes Yk = (ylk, y2k, ..., ynk) of large duration n are not repeated. An analysis

of a lot of chaotic codes shows that the code distance of the whole set increases with the length of the code and tends to a value equal to half the length of the code [30].

Chaotic codes of great duration are distributed in Hamming space in such a way that they become almost equidistant from each other by half the length of the code. The mutual scattering of chaotic codes is due to strong local instability and subsequent mixing of chaotic trajectories in the initial dynamical system with delay (5). The quasi-equidistant distribution of chaotic codes for a long duration indicates the approximation of the group properties of codes to the optimal ones in the sense of the Hamming metric [30].

The chaotic code yk is fully reproduced in the receiving device with an accurate specification of m initial samples for the generating algorithm (12). If the initial readings are not accurately specified, even a small error leads to an exponential discrepancy between the perturbed and specified trajectories and after a short time the perturbed code is completely different from the given code. In this case, the restoration of transmitted information based on the disturbed code becomes impossible. The exact set of m initial samples determines the identifier of the subscriber and is also the key when restoring a confidential message.

Thus, theoretical research and numerical modeling of mathematical models with chaotic dynamics will allow developing new information technologies for the protection of information resources. Based on the numerical simulation of chaotic algorithms, it is possible to build a large system of complex STS (signals with a large base) or chaotic key codes. Dynamically changing chaotic codes will make it impossible to uncover real-time information resources of open telecommunications systems. Development of discrete mathematical models based on systems with chaotic dynamics will also offer a fundamentally new technology for cryptographic closure of information resources.

3. APPLICATION OF DISCRETE CHAOTIC ALGORITHMS IN BROADBAND TELECOMMUNICATIONS

The development of new generation telecommunication systems is based on the use of broadband signals with a large information capacity and provides an increase in the speed of information transmission and an increase in the stability of the operation of systems in the presence of disturbing factors [31, 32]. Such signals are used to transmit information in multi-channel systems with code division, wireless spread spectrum communication systems, etc. The use of NTS allows receiving messages with a signal-to-interference ratio of much less than unity, and combating the influence of multipath propagation, mitigating the effects of many types of interference and providing high stealth in operation and electromagnetic compatibility with other radioelectronic facilities due to the emission of continuous in time SNS with very low spectral density.

When developing narrow-band digital communication channels, there are difficulties in finding a compromise between conflicting requirements. In multi-user communication systems, the mandatory requirement is to ensure the efficiency of spectrum utilization, measured in bits per second per hertz. High quality of information transfer requires the use of high-speed encoders, as well as a coding method that would detect and correct errors. All this is connected with the introduction of redundant information in the transmitted data and ultimately leads to an increase in the bandwidth of the channel.

As an alternative, broadband and ultra-wideband channels for personal radio communication are currently being developed. Expansion of the frequency spectrum (spread spectrum) occurs when non-sinusoidal signals

are used: noise-like carrier, ultrashort video pulses, etc.

In connection with the rapid development in recent years of multichannel autonomous communication systems and the transmission of information with code separation, the problem of constructing SHPS systems remains extremely topical. A signal system is a set of signals defined by a single construction rule (algorithm). The number of signals in the system L is called the volume of the system, which is usually taken to be compared with the base of the BTS B, equal to the product of the signal width Δf by its duration T: B = ΔfT. If L << B, then this is a small system of signals, L ≈ B is normal and for L >> B a large system. The problem of constructing large systems of phase-modulated (FM) SHPS with good correlation properties is rather complicated [31].

The main method of obtaining NTS at the present time is the formation of M-sequences on the basis of shift registers with a system of linear feedbacks.

It is known that for communication systems with NTS, not any noise signals, but signals possessing a number of certain properties, such as

1) the broadband B = ΔfT >> 1,

2) the uniformity of the noise spectral density in the communication channel band,

3) ACF signal should have one narrow peak and small lateral emissions,

4) the code sequences generated by the signal must satisfy the following randomness criteria:

a) the code must be balanced, i.e. the number "+1" should not be different from "-1",

b) the probability of the appearance of a block of k identical symbols should be close to 1/2k (for a binary code). This criterion is analogous to the requirement of the absence of kurtosis in relation to the Gaussian distribution in a multilevel signal,

5) the reproducibility of the signal at the receiving end of the communication system must be ensured;

6) in the signal system, a) equality of energy and the same band of all signals should be ensured.

b) a small level of cross-correlation of signals.

To the above, you can add a few more requirements. For example, the maximality of the so-called Hamming distance in the signal space, ensuring the simplicity of the algorithm to reduce the amount of computation.

This set of uneasy requirements, which for brevity can be called "good statistical and correlation properties," is traditional and partially implemented in already used systems with SNP.

A. Shapel-like carrier formation in spread spectrum communication systems

In recent years, interest in the so-called broadband and ultra-broadband methods of information transmission has increased noticeably. Broadband communication channels in their structure are designed for the transmission of discrete signals and are already digital. Broadband radio communication in its properties and methods of technical implementation is significantly different from conventional traditional methods of radio communication using for the transmission of signals with a bandwidth significantly wider than the band of the transmitted message and information reception methods based on the use of signals of various shapes consistent with the form of the transmitted signal. In such systems, all users operate in the same frequency range, wider than in the case of traditional narrowband frequency-time-division communication systems. Each subscriber channel uses its own identification code or its own code sequence to distinguish users. At the input of the receiving device of the individual user, simultaneously with the useful signal, not only ordinary natural disturbances come in a given frequency band, but also interfering signals from transmitters of other subscribers, as well as reflections due to multipath. The complex electromagnetic environment in the coverage area of telecommunications means imposes additional stringent requirements on the pseudorandom signal system, which is

used to encode and transmit information over communication channels. An ensemble of code sequences used by different systems or a single multichannel system must have good cross-correlation and group properties [32].

When creating systems with code division of subscriber channels (CDMA) it is important to choose the mathematical algorithms that generate a large ensemble of memory bandwidth. Formed pseudo-random sequences must have the necessary statistical and spectral properties, as well as good auto- and cross-correlation characteristics. Special requirements are imposed on the volume of the ensemble of orthogonal memory bandwidths, which is necessary for simultaneous and stable operation of many users in the common spatial zone. Mathematical algorithms must generate a set of statistically independent pseudo-random codes of great duration and high structural complexity to ensure confidentiality in the transmission of information.

The use of broadband signals in information transmission systems offers a number of important advantages:

1) the possibility of receiving signals with high reliability with the power of interference in the frequency band of the signal much greater than the signal power;

2) a significant increase in noise immunity against a number of deliberate interference, as well as impulse and narrowband;

3) increasing the resolving power of signals and, as a consequence, the possibility of a significant improvement in the operation of the communication system in conditions of multipath propagation of radio waves;

4) the possibility of constructing asynchronous multicast systems with code division of subscribers operating in the common frequency band;

5) the possibility of creating information transmission systems in which it is difficult to find and maintain radiation sources.

Broadband signals are formed, as a rule, by expanding the bandwidth of the information signal and / or by expanding the carrier spectrum. The extension of the signal bandwidth is usually achieved by such carrier wave modulation that forms a modulated signal with a bandwidth wider than the modulating function. A typical example of a signal with bandwidth expansion is frequency modulation with a large modulation indexıo

The extension of the band is also characteristic of digital signals with additional noise-immune encoding, since the introduction of redundant symbols, while maintaining the unchanged transmission rate of the message, necessitates a reduction in the duration of each symbol. This widens the bandwidth of the transmitted coded signal. It should be noted that simple binary redundant coding complicates the structure of the information signal (especially for powerful codes), but does not significantly expand the bandwidth of occupied frequencies.

A significant drawback of systems using simple bandwidth expansion due to analog carrier modulation by the information signal is that they are able to work satisfactorily only at large signal-to-interference ratios in the entire frequency band of the transmitted (and received) signal.

The situation is different with the signals formed due to the expansion of the frequency spectrum. Such signals are called complex signals. These signals are formed as a result of modulation of the carrier wave by a special function that extends the frequency spectrum and is independent of the transmitted message. As a rule, when expanding the spectrum, complex signals occupy a wider frequency range than when the band is expanded due to the information signal. To expand the frequency spectrum and obtain a complex signal, it is possible to modulate the amplitude, phase or carrier frequency. The spreading function must be identical for the transmitter and receiver, so that on the receiving side it is possible to perform

an inverse transformation - the "convolution" of the spectrum - at which the demodulation takes place and the signal is filtered in the message band.

An effective spreading function must satisfy certain requirements regarding bandwidth, receiver structure, and message transfer method. The broadening function must be deterministic, have a noise-like wide uniform spectrum (large base), and therefore, a relatively long duration and a narrow ACF with small lateral ejections, an ensemble of different spreading functions used by different systems or a single multichannel system must have good correlation properties.

Expanding function can be analog or discrete, but practically the most promising opportunities for creating NTS is the use of digital (discrete in time and in time) expansion functions. Such spreading functions are formed on the basis of digital code sequences. In some cases, simultaneous expansion of the spectrum and signal band is possible, when, for example, along with the application of the spreading function, digital noise-immune encoding of messages with restoring codes is used.

Signals with a spreading spectrum in turn are divided into coherent and incoherent. An example of an incoherent signal with spreading is a burst of radio pulses, modulated in amplitude. With such a signal, the information carries amplitude, and the pulse sequence expands the spectrum. Another characteristic example is signals with pseudo-random frequency tuning (random frequency jumps from one frequency channel to another). Incoherent complex signals are characterized by the ratio of the bandwidth of the signal spectrum to the information band (or the information transfer rate), this ratio serves as the equivalent of the base for non-coherent signals and determines the gain in noise immunity in the allocation of SNP against noise.

Coherent complex signals over most indicators exceed signals with incoherent spreading of the spectrum, but incoherent signals are simpler for the realization of both receivers and transmitters (modulators). In the process of receiving and processing of coherent SNSS in an optimal receiver, a signal with base $B >> 1$ is compressed into a simple signal with a base $B \approx 1$ containing information. There are two types of signal compression: time and frequency. As a rule, the limiting coefficient of compression in time and frequency is the same and equal to the signal base. Physically, compression is achieved by summing all the spectral components of the signal with compensation for the differences in their phase raids, i.e. due to the coherent summation of all the spectral components of the signal. As a result of compression, the complex signal becomes simple (with a base $B \approx 1$) having a spectrum width of the same order as the message carried by it. The limiting compression ratio is achieved only in the optimal receiver, ideally coordinated with the signal.

The basic properties of a complex signal with spreading are determined not by the modulation of the carrier, but by the properties of a modulating (expanding) oscillation. It is from the form of the ACF of this oscillation that the finite width of the spectrum of the complex signal and the uniformity of its spectral density within the frequency band depend.

Radio frequency loading, combined with the need to provide covert and noisy communication, led to the development of new communication systems with encoding broadband pseudorandom signals. In such systems, all users operate in the same frequency range, much broader than in the case of traditional frequency-division communication systems, but each of them uses its own identification code or its code sequence. At the same time, not only ordinary noise and fluctuations of the fluctuating nature come to the input of the receiving device of an individual user, but also signals from other subscribers and multipath signals. This imposes additional requirements on the signal systems used to encode and transmit information over such code-division-coupled communication channels.

It should be specially noted that it is preferable to use for the encoding of extremely long non-periodic memory bandwidths, which, as is known, increases the stealthiness of information transmitted over the channel and makes it difficult to decipher [31, 32]. When creating a system with code division of subscribers (CDMA), it is important to select the type of memory bandwidth that should have not only good statistical and correlation characteristics, but also a large range of lengths that allows the formation of large signal ensembles, as well as high structural complexity ensuring high confidentiality when transmitting information.

At present, chaotic algorithms that describe the behavior of nonlinear dynamical systems most completely satisfy all the above requirements. The characteristic features of these algorithms are the use of delay and nonlinearity in them. Advantages of such algorithms include the ease of software and hardware playback and the need to transmit for synchronization only a limited set of initial conditions that uniquely determine the launch of the algorithm. The use of noise-like chaotic signals (SHCS) in radio systems makes it possible to improve the noise immunity and reliability of information transmission in channels with a complex of interference and distortion, and also to approach the problem of electromagnetic compatibility of radio facilities of various purposes in a new way.

A special condition typical for code division systems is work against the background of interference created by other code groups in the same frequency range. Therefore, the creation of code-division-based communication systems requires the development of generation algorithms to create a system of high-volume coding signals and to study their statistical and correlation properties.

B. Shock-like carrier formation

To form a radio channel with a noise-like carrier, the modulation of the sinusoidal microwave signal should be provided at the transmitting terminal by the spreading chaotic pulse sequence generated by the chaotic algorithm, followed by its demodulation at the receiving terminal. The most effective way to extend the signal spectrum is phase modulation. It is realized by means of a phase modulator of the FM device, which changes the phase shift of the signal passing through it. According to the principle of operation FM can be divided into smooth (analog) and discrete (digital), by the method of inclusion to the external circuit - to reflective and passive, as well as passive (without amplification) and active (with amplification of the signal). For use in broadband communication systems, FMs must provide the required phase shift with minimum losses, high speed, low amplitude parasitic modulation, phase modulation at the permissible power level and in the required frequency band, good alignment with the microwave path, stable parameters when changing the level of input power, the characteristics of the microwave path, the voltage of the control signals, and have small dimensions and mass.

In digital communication channels, to ensure a wide frequency band, the use of a two-position FM is most effective, in which two states correspond to the absence of a phase shift (zero shift) and a phase shift by π (π-modulator). Usually phase modulators in the microwave range use a discrete change in the length of the transmission line between the input and output of the modulator under the action of control pulses. For example, if the line length has changed by $\lambda/2$ (where λ is the wavelength in the line) under the influence of the input pulse, then the phase of the output oscillations will change by π (the phase modulation index $\Phi = \pi/2$). For switching the line length discretely, switching elements are used, which are most often used as *p-i-p*-diodes. The advantage of such schemes is that there is no need to use the circulators and bridges that are difficult to manufacture and adjust.

It is known that the spectral composition of FM oscillations is much more complicated than amplitude-modulated oscillations.

When modulated with a sinusoidal signal, the expression for the phase-modulated oscillations has the form

$$X(t) = A\sum_{-\infty}^{+\infty} J_n(\varphi)\sin(\omega + n\Omega)t. \quad (14)$$

From this it can be seen that the spectrum of FM oscillations consists of a carrier frequency ω (n = 0) with amplitude AJ0 (φ) and an infinite number of lateral frequencies located symmetrically on both sides of the carrier (ω ± nΩ) with amplitudes AJn (φ). However, in practice only those frequencies whose amplitudes are not very small in comparison with AJ0 (φ) play a role. Since the values of the Bessel function decrease very rapidly with increasing n for a given argument φ, in many cases of practical importance we can confine ourselves to the first terms of the series. However, for signals with a large modulation index, the terms of the series play an important role up to n = 10, since the amplitude distribution does not allow them to be neglected.

The shape of the frequency spectrum is many times more complicated if the carrier frequency is modulated by a non-sinusoidal and non-periodic signal.

The FM signal with a sinusoidal carrier f0 during a step change in phase can be represented as:

$$X(t) = \sum_{k=1}^{N} A\sin 2\pi f_0[t + k\Delta T(-1)^{j_k}]; \quad (15)$$
$$0 \le t \le \Delta T,$$

where A is the amplitude, f0 is the carrier frequency, ΔT is the length of the manipulated sinusoidal segment, equal to the whole number of half-periods of the sinusoidal signal, the parameter jk takes the values 0 and 1 in accordance with the given code sequence determining the law of the jump (± π) phase change of the carrier.

The working frequency band at the same time significantly expands. The FM signal spectrum has in the region of the main maximum a shape close to the half-period of the sinusoid, with a maximum at the carrier frequency f0. The width of the spectrum is determined by the length of the manipulated segment of the sinusoid ΔT and is equal to f0 / n, where n is the number of carrier periods in the interval ΔT.

When modulated by periodic functions, the signal spectra have a line-like form. In the case of modulation with a noise-like discrete signal, the spectrum is continuous, and its dimensions are determined by the maximum frequency (the clock frequency).

The inverse transformation of the FM signal into a pulsed form is carried out by calculating the ICF of the recorded signal with X (t). In the absence of frequency and phase distortions of the recorded signal, the FM signal after the correlation transformation will have the form of an ACF signal.

C. Chaotic algorithms for creating extension functions

It is shown that for ShChS constructed on the basis of discrete chaotic algorithms all the requirements necessary for spreading the spectrum and forming a noise-like carrier are fulfilled: these signals are wideband with a large base, their spectral density in the transmission channel band is uniform, the ACF has one narrow peak and small lateral emissions, the signal is fully reproduced in the receiver, which is necessary for correlation processing. In addition, the SHS code sequences satisfy the randomness criteria. The characteristics of aperiodic ACF for both binary and converted binary signals are in good agreement with the correlation properties of random sequences.

The closeness of the statistical characteristics of the SHCS to the characteristics of the Gaussian process is also an important qualitative indicator that ensures the structural concealment of the useful signal against a background of noise interference, also in most cases having a normal distribution. This, in turn, provides high noise immunity. The structure of the M-sequence is usually restored by its difference from the normal random process.

The conducted estimates of the volume of the signal system show that on the basis of the ShChS, the prospects for solving the problem of constructing signal systems with large volume, providing increased energy and structural concealment, are opened. Dynamically changing chaotic codes will make it impossible to open in real time the information resources of open telecommunications systems, thus ensuring high confidentiality and noise immunity.

D. A SPREAD-SPECTRUM COMMUNICATION SYSTEM BASED ON CHAOTIC BINARY CODES

In the microwave region, a model of a radio terminal for a broadband communication system with spreading on the basis of a phase shifter bridge with a fixed phase shift $\varphi = \pi$ was developed and experimentally investigated. In investigating the properties of the communication channel, the simplest model of a two-terminal broadband communication channel with a noise-like carrier was used using a digital generator that forms a chaotic sequence of pulses, a phase microwave modulator-demodulator in microstrip and horn antennas. It was assumed that the communication channel consists of the transmitting part (the phase modulator providing the spreading of the spectrum) and the receiving part (the demodulator-the convolution device, through which the carrier was restored). Any special interference in the channel was not made and it was believed that the transfer of the microwave signal from the transmitter to the receiver occurs for a small time compared to the pulse duration.

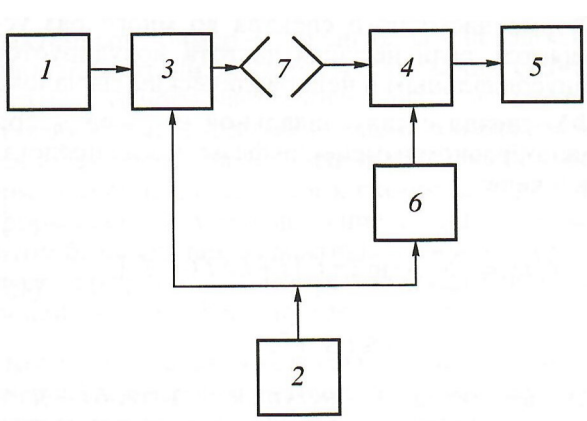

Fig. 2. *Block diagram of a communication channel model with a noise-like carrier: 1 - generator of a sinusoidal microwave signal; 2 - digital generator of chaotic coding signal; 3 - phase modulator of the transmitting terminal; 4 - phase demodulator of the receiving terminal; 5 - spectrum analyzer; 6 - discrete lag unit; 7 - horn antennas.*

The block diagram of the model (Fig. 2), realizing the communication channel with the noise-like carrier, contains the generator of the sinusoidal microwave signal 1; the digital generator is the source of the coding chaotic sequence 2, the phase modulator 3, the phase demodulator 4, the spectrum analyzer 5 connected to various points in the circuit, the discrete delay unit 6, and the horn antennas 7

When conducting experiments to demodulate the microwave signal, phase modulated by a chaotic code sequence generated by a digital oscillator, it was assumed that the modulator and the demodulator were completely synchronized, i. E. coherent mode of operation. In practice, this was provided by feeding the modulating signals simultaneously to the modulator and demodulator units.

The broadening of the spectrum of the communication channel was carried out using a broadband FM, which was created on the basis of a bridge circuit of a microwave phase shifter with a fixed phase shift to one of the possible states $\varphi = \pi/2, \pi/4, \pi/8, \pi/16$. Switching of the phase-shifting segments of the microstrip line is made by high-frequency *p-i-p*-diodes with a short relaxation time not exceeding 5 ns. The tuning range for the modem is greater than an octave. Control of *p-i-p*-diodes in the phase shifter circuit is carried out by chaotic binary codes, which are generated by a programmable digital processor according to the developed mathematical algorithm. For each subscriber, programmatically establishes its own chaotic code by selecting the N-dimensional vector of the initial samples. A multidimensional digital array specifying a vector of initial samples is the subscriber identification parameter. A programmable encoder for the formation of individual chaotic codes is based on high-speed FPGA technology.

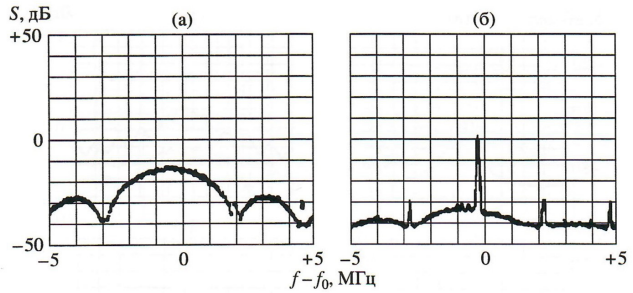

Fig. 3. *Code spreading of the signal spectrum in the transmitter (a) and coherent signal frequency compression at the receiver (b), f0 = 2600 MHz.*

The transmitted digital information can be entered into the communication channel either by frequency modulation (FM) of the microwave carrier frequency or by changing the phase of the coding signal. The code spreading operation for the FM signal carrying the information is performed by the phase modulator in the transmission modem circuit directly on the carrier signal frequency. The signal emitted by the transmitter with the information component has a continuous noise spectrum (Fig. 3a), whose main energy fraction is in the frequency band Δf = 2FT. The clock frequency FT of chaotic binary codes is set by the frequency synthesizer in the modem scheme and in the experiment FT = 1 MHz. The information message is a sequence of binary symbols in the form of current pulses with a clock frequency of 20 kHz.

The dimensionality N of the numerical identifier or the vector of initial samples is at least N> 1. This important condition for the generating algorithm ensures a stable mode of multimode chaos in the formation of codes with good correlation and statistical properties. The transmitted SNS with the information component has a continuous noise spectrum and in its structure is practically indistinguishable from a random process with the same frequency band.

The digital processor of the encoder can operate in cyclic and aperiodic modes. When cyclic formation, chaotic codes are repeated with a specified period. In aperiodic mode, the digital processor generates a continuous and non-repeating sequence of chaotic symbols. In this way, it is possible to dynamically change the codes during the entire transmission time of the data. The developed data transmission system with dynamic code change, according to the results of Shannon [31], practically excludes the possibility of cryptographic disclosure of messages.

At the receiver, information is allocated after the relative delay of the received and reference codes has been eliminated and the SNS frequency is compressed. In the experiment, data transmission is performed with dynamic code change due to the continuous generation of non-periodic sequences.

A copy of the chaotic binary code is generated in the receiver by a digital processor based on the generating algorithm when the N-dimensional numeric identifier or the initial

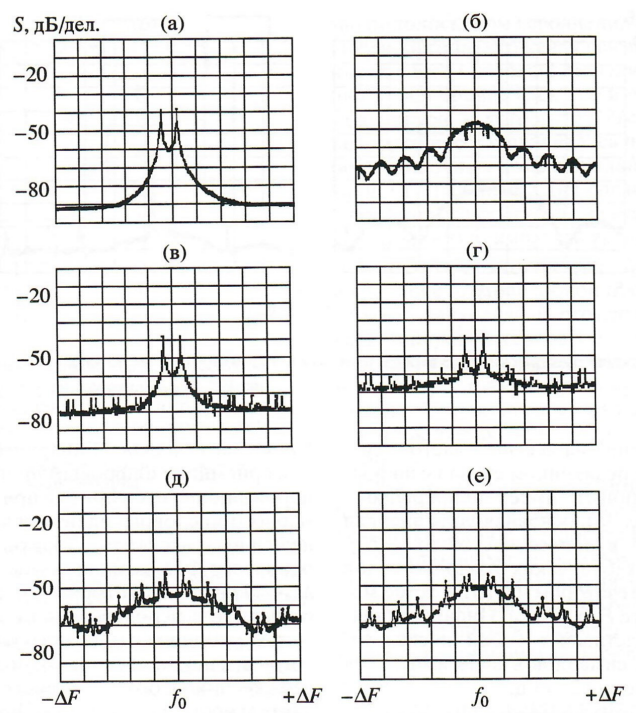

Fig. 4. *Transformation of the spectrum of the signal when passing through a communication channel: the spectrum of the information FM signal (a); spectrum of the transmitted signal with code spreading and information component (b); spectrum of the reconstructed signal after the demodulator with full synchronization (in); the spectra of the reconstructed signal from the information component when the reference chaotic code lags for a time τ = 0.1T (g), 0.3T (d), 0.5T (e); T is the pulse repetition period of the coding sequence.*

sample vector is specified exactly. The reverse conversion of the received FM signal is carried out by a phase demodulator, which restores the phase of the signal when using as a reference signal a copy of the chaotic code. Compression of the received signal by frequency is possible only if the received and reference codes are delayed within the duration of one clock cycle. The effectiveness of this is illustrated by the energy spectra for the decoded signal (Figs 4a, 4c-4e). In Fig. 4c shows the spectrum of the signal at the demodulator output during synchronization of the received and reference codes, when the delay of codes $\tau = 0$ is absent. The spectrum of the reconstructed signal contains an information component similar to the spectrum of the FM signal at the output of the information modulator in the transmitter (Fig. 46). In the absence of active interference, the level of information components exceeds by almost 40 dB the receiver's own noise and by 35 dB the parasitic components with a clock frequency of FT = 1 MHz.

With a single symbol $T = 1/FT = 1$ μs, the delay of the reference code by only $\tau = 0.1T$ leads to a 14 dB decrease in the information component in the spectrum to a level of 26 dB relative to the noise pedestal (Fig. 4d). When the reference code $\tau = 0.5T$ is delayed (Fig. 4e), the level of the information component practically disappears. Simultaneously with the increase in the delay τ, an increase in the level of both the noise pedestal and parasitic components at multiple FT frequencies in the spectrum is observed due to incomplete convolution of the received signal. When the delay of the reference code is increased over the duration of one clock cycle $\tau > T$, the information component in the spectrum is indistinguishable against noise and the restoration of transmitted information becomes impossible. The carried out experiment on data transfer with dynamic change of chaotic codes showed that effective recovery of useful information occurs only at a small delay $\tau < 0.5T$ of the reference code. The results of the

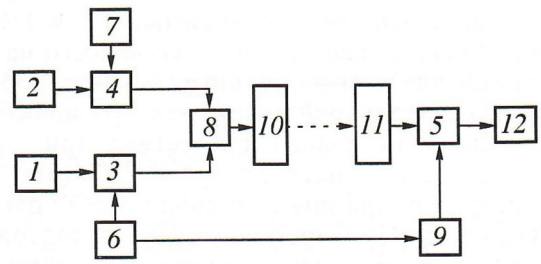

Fig. 5. *Scheme of investigation of noise immunity of the terminal model with a noise-like carrier: 1 and 2 - microwave signal and noise generators; 3, 4, 5 - phase modulators; 6, 7 - coders; 8 - microwave adder; 9 - adjustable delay line; 10, 11 - transmitting and receiving antennas, 12 - spectrum analyzer.*

experiment on the transmission of information in a communication system with spread spectrum and dynamic code change indicate the need for accurate synchronization of the reference code in the receiver.

We experimentally investigated the noise immunity of a radio-based model based on a noise-like carrier, in which binary chaotic signals were used to transfer information. The scheme of the experiment is shown in Fig. 5, where 1 and 2 are microwave signal and interference generators, respectively; 3, 4 and 5 - phase modulators FM1, FM2 and FM3; 6 and 7 - coders; 8 - microwave adder; 9 - adjustable delay line; 10 and 11 - transmitting and receiving microwave antennas; 12 - spectrum analyzer. The coders implemented one of the algorithms for generating a class of chaotic signals of the type given above.

The spread of the transmitted signal from the microwave generator 1 was carried out using a microwave modem FM1.3 The microwave signal at the forward frequency Fcp was applied to the input of the modem, whose control was performed by a chaotic binary pulse train from the encoder 6. As a result, a noise signal c continuous spectrum.

In the experiment to determine the noise immunity, two types of interference were used: sinusoidal interference, close in frequency to the transmitted microwave signal, and broadband interference matched to the transmitted signal by the spectrum. Broadband interference

was formed using a microwave modem FM2 4. Control of the modem 4 was performed by a separate encoder 7 with the same clock frequency as the encoder 6 of the transmitter. The coding sequences of both encoders 6 and 7 are uncorrelated in time. The experiment was performed with the synchronization of the coding sequences for the modems of the transmitter and the receiver. Synchronism was provided by the use of an adjustable delay 9. The reverse coherent compression with respect to the frequency of the received signal was performed by the modem 5 in the receiver circuit.

As the noise immunity criterion, the coiled signal was exceeded at the output of the receiver 12 above the noise background, depending on the signal-to-noise ratio at the receiver input. Under the influence of narrow-band interference, the spectrum of the total signal and interference at the receiver's input has the form of continuous in the band broadband noise corresponding to the received signal with spreading, above which the sinusoidal noise rises. The PM3 decoder ensures convolution and extraction of a useful signal. When decoding, narrow-band interference is blurred along the spectrum in the entire band and turns into a noise pedestal, above which a collapsed information signal appears.

Broadband interference is formed when the signal of generator 2 passes through FM2, and at the input of the receiver its spectrum has the form of broadband continuous noise, which is similar to the noise spectrum of the information signal at the output of FM1. The total spectrum of the signal and broadband interference at the input of the receiver has the form of continuous in the band of broadband noise and is shown in Fig. 6a. The spectrum at the output of the receiver as a result of convolution in FM3 for a ratio of interference powers / input signal equal to 10 dB is shown in Fig. 6b.

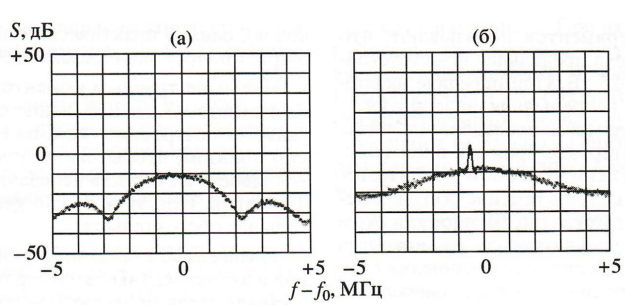

Fig. 6. *The total spectrum of the signal and broadband interference at the input of the receiver (a) and its output (b).*

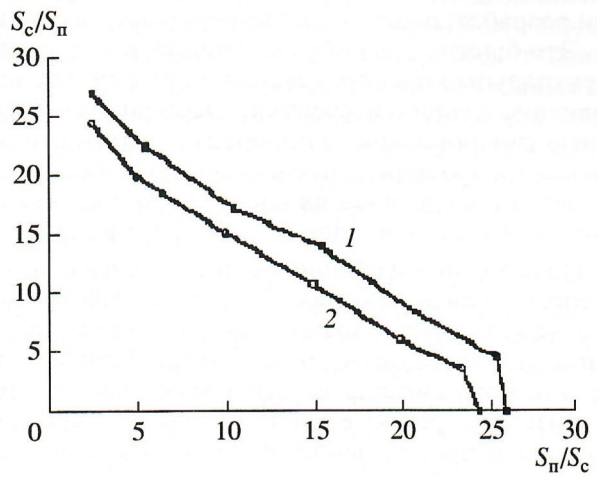

Fig. 7. *Dependence of the signal / interference ratio Sc / Sn at the output of the receiving device on the magnitude of Sn / Sc at the input of the receiver: 1 – narrowband interference; 2 - broadband interference.*

In Fig. 7 shows the results of the measurement of the signal-to-noise ratio (Sc/n) at the output of the receiver depending on the ratio of the interference levels and the information signal at the receiver input (S/Sc) for two types of interference: narrowband 1 and broadband 2. Maximum interference immunity for the communication system with spreading is determined by the signal-to-noise ratio at the receiver input, at which the restoration of the transmitted information becomes impossible for a given averaging time.

The results of experiments show that for both types of interference, the maximum noise immunity is ~ 25 dB. When transmitting information, a continuous non-periodic coding chaotic sequence is used, realized on an interval of time of arbitrary duration. In this way, a dynamic code change occurs during the entire time of data transfer. According to Shannon, in this case the possibility of cryptographic disclosure of the message is practically excluded [31]. This result indicates the potential application of the investigated system with spreading on the

basis of chaotic codes in multi-station mobile communication systems with a high degree of confidentiality.

The main problem with the use of complex signals in the transmission of information in the communication channel is the problem of searching for and time synchronization of complex signals. A search search method is known when the correlation integral is calculated with respect to the shifted reference signal and the time offset maximizing this correlation is selected as an estimate of the time position of the received signal. However, for a large area of a priori uncertainty of signal delays and a large signal base necessary to ensure high noise immunity, such a method in hardware implementation leads to a significant search time, and when parallel processing on several correlators - to an undesirable increase in the complexity of communication equipment. With a software implementation based on a computer, this method requires a large amount of RAM and high-speed processors.

To reduce the search and synchronization time, fast search algorithms are developed. These are fast Fourier transforms and other spectral transformations that simplify the execution of the convolution operation. The peculiarity of the synchronization algorithm is that the main purpose of signal transmission over the communication channel is to determine their temporal position, and the auxiliary transmission of information.

By complex are usually understood signals for which the product of their duration on the occupied frequency band is much greater than unity. It is known that the product of the duration of any impulse signal per its frequency band is approximately equal to unity. Therefore, in order for this product to be more than one, it is necessary to apply special algorithms that extend the spectrum of the signal.

It should be noted that simple binary redundant coding complicates the structure of the information signal (especially for powerful codes), but does not substantially extend the bandwidth of occupied frequencies.

The most difficult moment in designing a communication system based on complex signals is the construction of a synchronization system in such a way that it does not degrade the noise immunity and the transmission rate for basic information. In this case, it is necessary to take into account a number of additional circumstances:

1) the decrease in the stability of the reference oscillators and the equivalent frequency fluctuations in the communication channel make it necessary to significantly increase the transmission rate of the "synchronization information" and, consequently, to reduce the noise immunity,

2) signals for the transmission of synchronization information may differ in their structure from the signals for the transmission of basic information, i.e. may be suboptimal,

3) to synchronize complex composite signals, in order to perform simple clock synchronization, one has to use the entire complex form of the composite signal, and this is possible only when synchronizing over the period of the total signal.

When using direct convolution at the receiver input, the synchronization and information transfer problems can be solved in practically the same ways. In this case, the functional diagram of the radio terminal can consist of almost standard units.

When synchronizing, it is necessary to perform the following operations in sequence:

1) search, smooth scanning in phase either directly clock frequency or the code combination of this subscriber,

2) capture and synchronization of the clock frequency, subscriber identification, notification of synchronization with the subscriber, notification of the start of the information message, launch of the generator of the NTS,

3) periodic adjustment of the timing parameters.

Thus, to improve the noise immunity of the sync channel, information on it must go not only at the beginning of the communication session, but also during the whole cycle of information exchange between the receiver and the transmitter.

Using the principle of direct convolution of the signal at the input, the information and sync channel can be placed in the common frequency band, dividing them structurally in the receiver and the transmitter (the highest frequency of the clock is the clock frequency of the reference oscillator). In this case, the information about the phase of the clock frequency of the reference oscillator and the identification code of the subscriber will be circulated in the sync channel. The presence of a link via the sync channel is continuously monitored both on the receiving side and on the transmitting side.

With a stable sync channel, a noise-like signal generator is generated at both ends of the link path, generating a non-periodic random sequence, which serves to encode and decode the information bits.

The obtained results testify to the possibility of using pseudorandom signal systems formed by chaotic algorithms as coding sequences for broadband transmission systems with code division channels. A digital communication system with spread spectrum and dynamic chaotic code change has high noise immunity and increased confidentiality in data transmission under conditions of a complex electromagnetic environment, the effects of strong interference and multipath signal propagation. High-speed digital processors based on finite-dimensional algorithms with nonlinear dynamics create a large ensemble of chaotic binary codes, which makes it possible to practically implement the code division of a large number of subscribers. The transfer of data with the dynamic change of chaotic codes makes it difficult to cryptographically disclose confidential messages.

E. A digital chaotic code generator

In the process of encoding information, the coding sequence is imposed on the information sequence according to a certain law. It is known from information theory that the best coding function is a random process (white noise). The main problem in encoding information in digital communication channels is the difficulty of generating random binary sequences.

Analog noise generators, which have been intensively developed in previous decades, have a specific application, related mainly to the problem of creating artificial interference and calibration of various measuring devices and devices [33]. Physical simulation of randomness by means of physical phenomena such as radioactive radiation, shot noise at thermoemission of electrons or avalanche breakdown in a zener diode, does not give real random processes. Therefore, instead of physical processes, various mathematical algorithms are used to form random sequences. The development of methods of computational mathematics led to the development of special software methods for generating sequences of random numbers. In their use, special statistical methods of computation have been developed, for example the Monte Carlo method.33 Pseudo-random generators are used not only in cryptography but also in complexity theory in other areas of discrete mathematics.

Two basic methods are used to generate random numerical sequences: a method based on the use of digitization of analog physical processes and computational methods that allow generating streams of numbers with statistical properties of random numbers, but actually formed with the help of deterministic algorithms, as a result of which they were called pseudo-random .

Based on the developed generating algorithm for the formation of a discrete chaotic sequence, a digital channel for information transmission was developed.34 The central element of this scheme is a digital chaotic sequence generator that implements the operation of such an algorithm.

Discrete algorithms that form chaotic sequences like those described in [19] can be simply implemented with the help of high-speed digital technology.In principle, such a digital sequential computational algorithm can be implemented on the basis of a high-speed microprocessor package, for example DSP. [36] However, for work in real time in practice, the simpler and cheaper is the matrix method of generating a chaotic sequence, when in the address space the speed based on a pre-computed array of data, a data table is formed for each complete set of input values from this table, a sample of the current chaotic sequence values is sampled using standard digital buses of any bit length (8-, 16- , 32-bit ones).

After the emergence of open telecommunications networks, the methods of protecting information in the course of its transmission, processing and storage were actively developed. This direction is connected both with the needs of encryption of digital information, and with the advent of new telecommunication technologies using broadband communication channels based on systems of complex pseudo-random signals [32].

Despite the fact that a lot of algorithms for generating pseudo-random processes are known, their statistical properties are usually far from the properties of a random signal, so in practice for generation of binary pseudo-random sequences a recursive algorithm is used when, based on a linear recurrence relation and some initial values, a continuous The sequence, each successive member of which is determined from the previous ones. Attempts to adapt for digital algorithms operations on real numbers ended in failure, since replacing the actual number with its approximate value greatly changes the statistics of the obtained sequence. The rounding operation introduces an unpredictable disturbance into the generating algorithm, and the resulting sequence ceases to be statistically independent, and therefore random.

In practical development of multiple-access radio systems with code division of subscribers, an important task is to select the type of coding sequences that possess not only good statistical and correlation characteristics, but also allow them to form ensembles of signals with large volumes on their basis, which provides high structural complexity and confidentiality in transmission information [32].

On the basis of nonlinear dynamic systems, a discrete algorithm is developed that forms a random sequence of integers on the interval [0, 255]. The choice of the algorithm in this form is due to the fact that it can be implemented schematically on a standard eight-bit microprocessor series with a sufficiently high clock frequency (up to 100 MHz and higher). The delay parameter is chosen equal to 16. The initial conditions of the algorithm are determined by specifying a specific combination of 16 eight-bit binary numbers so that the initial point of the dynamical system in the phase space belongs to a strange attractor and completely determines the further behavior of the system. This allows you to uniquely reproduce an identical copy of the generated chaotic signal in any other place and at any time.

By changing the parameters of such a dynamical system and the initial conditions, it is possible to vary the nature of its behavior within a wide range and thereby purposefully control the appearance and properties of the generated chaotic signal. The possibility of obtaining a wide variety of signals depending on the initial data for the same algorithm indicates that it is possible to create in this way large systems of chaotic signals with prescribed necessary statistical properties.

In studying the generating algorithm, special attention was paid to the experimental verification of the absence of regions of regularity and correlations at large times. Theoretical estimation of the probable value of the possible maximum period of the generated signal due to a finite set of elements for the given algorithm gives a value of the order of 1038 symbols. By increasing

the length of the delay or the bit width of the binary numbers, it is possible to further reduce the probability of occurrence of periodicity in the generated chaotic process.

Investigations of the effect of the algorithm parameters on the statistical characteristics of the generated signal made it possible to determine the ranges of the parameters in which the chaotic sequence generated by the algorithm, in its statistical properties, practically coincides with the δ-correlated random process and has a uniform distribution of the probability density of the signal in the entire range of admissible values.

The frequency of appearance of a group of k identical symbols in the binary sequence formed by the algorithm under investigation with subsequent clipping is analyzed. Comparison of the obtained results with the law for an ideal random process, which is a value of 1/2k, showed that they are almost identical.

An investigation of the effect of the initial conditions showed that even a minimal difference in the initial conditions by one bit leads to a complete change in the formed sequence through a number of steps of the order of the delay value, but with the same statistical characteristics, i.e. The new sequence belongs to the same ensemble of the signal system.

To estimate the volume of a system of chaotic signals, selection of segments of binary sequences formed by the algorithm and satisfying the specified correlation properties was carried out. The analysis showed that the ensemble formed is really large, i.e. its volume exceeds the signal base. Its magnitude is several times larger than the volume of the M-sequence signal system, which are now commonly used as coding signals.

Based on the developed generating chaotic algorithm for the formation of a discrete sequence, the model of a digital random number generator was created and investigated.

A block diagram of a digital generator of a chaotic signal realizing one of the chaotic algorithms is shown in Fig. 8. On the output bus of the chaotic signal generator, a numerical sequence of eight-bit binary numbers is generated in the parallel code. To run a chaotic algorithm, you must specify a set of initial conditions, the various versions of which are stored in ROM. When different sets of initial conditions are loaded, various digital random sequences are generated in the generator, which can serve as a basis for realizing the dynamic key exchange mode while encoding information.

The mock-up of a digital chaotic signal generator is functionally composed of a numerical sample device from an array, an annular stack 2, an initial condition setting device 1, and a clock frequency generator 7, 8, 9. Constructively, an eight-bit data bus is used in the layout scheme. This means that a discrete chaotic algorithm is formed using a set of 256 eight-bit binary numbers.

The device of the numerical sample from the array is made on the basis of ROM 3. The use of ROM for sampling discrete values of the chaotic sequence allows us to use the tabular method of calculations when the number of possible discrete numeric values is finite, the deterministic

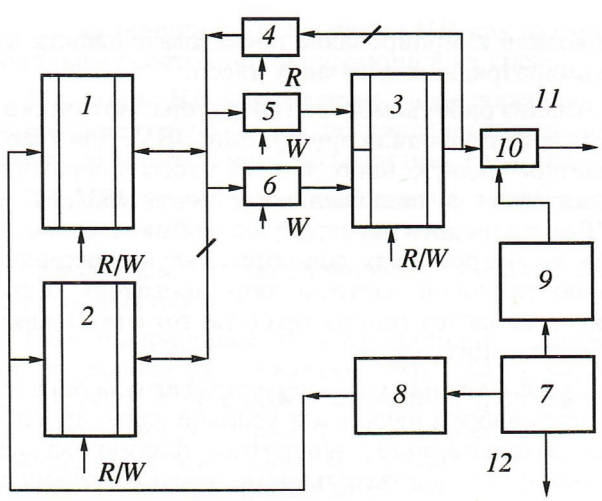

Fig. 8. *Block diagram of a digital oscillator of a chaotic signal realizing a chaotic algorithm: 1 - ROM for storage of initial conditions, 2 - circular stack based on RAM, 3 - ROM for storing the data array, 4, 5, 6 - latch, 7, 8, 9 — clock frequency grid former, 10 — buffer register for signal clipping; 11 - output single-bit bus; 12 - output of the clock generator.* R / W *- control signals. A short transverse line segment marks an eight-bit data bus*

algorithm is known, and therefore it is possible to establish a one- to-one correspondence of a finite number of discrete values to the target space used by the numerical array of ROM. Such a method provides the possibility of a flexible change of the chaotic algorithm by sewing another tabular array of data in the ROM.

The ring stack 1 is a set of shift registers for the operational storage of the data necessary for the operation of the numerical sample device from the array. The ring stack is built on the basis of RAM with the control unit. The device for setting the initial conditions is executed in ROM, which stores sets of initial conditions that ensure the loading of the ring stack at the initial time. The presence of different sets of initial conditions allows the generator of a random digital signal to receive different realizations of a random process. This property makes it possible to implement a controlled dynamic key change mode when encoding digital information. The actual number of all possible keys is limited only by the capacity of this ROM.

The clock frequency generator 7, 8, 9 is designed to synchronize processes on an eight-bit data bus in different generator blocks. The mode of operation of the random number generator is selected by setting the appropriate enabling signal, by which the initial conditions (or the law of dynamic key exchange) are loaded, and then the generator is started in the operating mode of random sequence formation.

To obtain a single-bit binary sequence, which can be used later, for example in phase modulation, clipping of a sequence of eight-bit binary numbers was performed.

The analysis of the operation of the chaotic signal generator was carried out with the help of a computer. For this purpose, the eight-bit data bus of this generator was connected to the parallel port of the IBM PC in the EPP mode (two-way data exchange mode). In this case, the synchronization of the clock frequency of the generator of the grid of the clock frequencies of the generator and the clock cycles of the parallel port was carried out.

When a signal of a certain set of initial conditions was applied to the generator input, a binary sequence was formed on the parallel output bus of the generator, corresponding to the chaotic sequence formed by the algorithm for given initial conditions. Segments of temporary realizations of a discrete random process were recorded in separate files and then a correlation analysis of the received signal system was carried out with the help of a computer.

Experimental studies have confirmed the identity of the software and hardware implementation of the chaotic algorithm. The real speed of the generator was limited by the time of reading the information from the ROM. The results of the analysis of the obtained segments confirmed the high quality of the signals formed from the realizations of the digital chaotic sequence at the output of the generator.

The developed digital random number generator based on a discrete chaotic algorithm is intended as an encoding and decoding device (codec) for radio terminals of a broadband digital communication channel, as well as for encoding information in cryptographic encryption systems. The chaotic algorithm allows to form a system of codes with a large volume, which is a significant advantage over the currently used pseudo-random sequences, and provides high potential inter-channel noise immunity in multi-station communication systems with code division of subscribers. Experimental studies have confirmed the identity of the software and hardware implementation of the chaotic algorithm. The real speed of the generator is limited by the time of reading the information from the ROM.

4. NOISE RADAR AND RADIOVISION

The use of ultra-wideband noise signals in modern radar makes it possible to significantly increase the informativity, accuracy and resolution of measurements [37, 38]. With an

increase in the frequency band of sounding signals over 3 GHz, a spatial resolution of less than 5 cm is achieved for individual reflectors. With such a high resolution, complex targets are recognized and informative radio images are created in noise radar in the microwave and millimeter wave bands with optimal processing of ultra-wideband signals.

In the radar receiver (RLS), the noise signals are coherently compressed in time during correlation processing or in frequency with double spectral processing [39]. As a result of coherent compression and prolonged accumulation of energy of sounding noise signals, a high order of 60 dB or more is achieved in the noise immunity of a radar in the presence of active and passive interference. Noise radar continuously emits electromagnetic waves with a low power spectral density in a very wide frequency band and are therefore characterized by the hiddenness of noise emissions and electromagnetic compatibility with other operating media, including traditional and narrowband systems.

Ultra-wideband probing signals are able to penetrate vegetation and terrestrial cover, as well as artificial obstacles in the form of walls of buildings, concrete and other structures. Ultra-wide-band noise radars make it possible to detect high-resolution objects of military equipment concealed among high forest vegetation, as well as to make remote detection and identification of anti-personnel mines and minefields by inverse reflection and scattering of electromagnetic waves [40]. When sounding with noise signals followed by coherent processing and accumulation of energy of useful reflections, it is possible to detect at low distances insignificant objects with radio-absorbing coatings by increasing their effective scattering surface as the frequency band expands.

For noise radar, the actual task is to develop sources of ultra-wideband noise signals with sufficient radiation power and to develop methods for the optimal processing of such signals. Solid-state and electron-wave autogenerators for the formation of ultra-wideband noise signals with a given power and a controlled spectrum can be made on the basis of advances in the field of dynamical systems with chaotic behavior [41]. Modern devices for coherent convolution of noise and noise-like signals in the form of analog and digital correlators, convolvers, phase demodulators with code control successfully perform correlation processing of probing signals in a frequency band of tens and hundreds of megahertz. Investigations conducted in recent years in the IRE RAS in the field of spectral interferometry have shown the possibility of high-precision radar measurements using noise signals in a frequency band extending up to several gigahertz (and even up to tens of gigahertz). Spatial resolution of noise radars based on spectral interferometry with cepstral processing of ultra-wideband noise signals can reach a fraction of centimeters, which will greatly increase the information content of radar measurements and will enable the construction of detailed radio images for complex and extended objects.

A. Nonlinear scattering effects of radio waves - nonlinear radar

The use in the radar technology of new technologies associated with the use of nonlinear scattering of electromagnetic radiation by various objects allows significantly increasing the amount of information about the environment. The physical basis of such technologies is the effects of nonlinear scattering of electromagnetic waves and the appearance in the object scattered by a field of spectral components that are absent in the field incident on it. The effects of nonlinear scattering allow us to detect various objects against the background of reflections from the surrounding medium when it is probed with electromagnetic waves, and in some cases remotely obtain information about the dynamic processes in the object and its environment. The reason for the appearance of nonlinear scattering is the presence in objects of nonlinear

elements (NEs) with nonlinear electromagnetic properties (imperfect electrical contacts of metal structures, semiconductor elements of electronic means, etc.) [42].

Currently, nonlinear effects are used mainly in two directions: for remote detection of objects with the ability of nonlinear radio wave scattering (NRP), for example, mine explosive devices, camouflaged vehicles and weapon systems, and in the development and investigation of artificial non-linear scatterers HP) - markers - to designate and remote search for objects and people [43].

Among the new areas of research that are of great interest are the following:

1) remote analysis of system dynamics,

2) the simplest artificial HP, as sensors of local states of their environment,

3) the HP system as a means of recognizing moving objects, relaying signals, controlling a certain area of space,

4) systems of remote diagnostics of technical objects and structures,

5) search remote systems for the analysis of rocks.

A "nonlinear" object is usually understood as a passive EMW scatterer, containing discrete nonlinear inclusions whose electrical parameters σ, μ, ε depend on the currents flowing through them. As a consequence, spectral components that are absent in the field incident on it can appear in the signal scattered by the object.

The mechanisms of the appearance of a secondary (scattered) field can be different. This can be seen from the example of the action on HP of quasimonochromatic 3C:

a) HP of a distorting type contains NE with a nonlinear dependence of the current on the applied voltage, which leads to distortions and the appearance in the frequency spectrum of higher harmonics;

b) HP of subharmonic type contains energy-intensive NEs whose presence under certain conditions leads to the appearance of parametric resonance and currents in the scatterer on subharmonics;

c) specially synthesized HP contain NEs capable of creating a secondary field on the basis of the DC component arising in HP under the action of the LC, with the subsequent formation by any set of NEs belonging to HP of any preassigned response to the ES.

Common to all these mechanisms of interaction is the remote acquisition of energy from the EMV source, the presence of an antenna (usually linear), the presence of NEs and the creation of a secondary field with an extended spectrum as a result of their interaction with the ES. As HP can act and non-radiating systems containing active elements to ensure their internal dynamics.

The investigation of the effect of HPP on mechanical systems, radio electronic equipment (REA) and its components for the purpose of their detection is the most studied and mastered in technical terms. As a result of research in this direction, the term "nonlinear radiolocation" appeared. At the present time, the notion of HP as an electrodynamic structure with a finite number of discrete nonlinear inclusions is developed. The influence on the level of the scattered signal of such factors as the depth of immersion of HP in the ground, its humidity, the angular position of HP is estimated. The properties of NEs (metal-oxide-metal structures formed by various metals) in the amplitude, time and frequency regions and the influence of various factors on them are studied. Much of the research is aimed at studying the amplitude, frequency, polarization properties of HP. In particular, it has been established that the amplitude characteristics of HP can be discontinuous functions and there is no unique relationship between the polarizations of the incident and scattered fields, which is determined not only by the configuration of the linear part of the HP, its angular position relative to the field 3C, but also by the direction of the conductivity of the NEs entering in the HP.

The notion that in the nonlinear radar the level of the received signal falls with distance as 1/R6, for nonlinear fields of the second order

and free space needs correction. The amplitude characteristics of HP generally have a quadratic section, linear, and saturation (or even an open). Therefore, the received flux of the nonlinear field vector can be proportional to 1/R2, 1/R4 (as in linear radar) or 1/R6, respectively, and may even increase with increasing R.

Passive respondents are now the area of use of the effects of the ZRP, which has been mastered by production. The first markers were half-wave vibrators loaded on a diode, and could be used, in particular, to detect people in distress. The information volume of their response was one bit. Unlimited lifespan of such respondents, low cost and attractive weight and size characteristics stimulated the development of this direction.

In general, the marker contains an antenna, a transmitter, a receiver and a memory unit. The weight of the marker usually does not exceed several tens of grams, the operating frequency ranges of markers from hundreds of kilohertz to 5 GHz. At low frequencies, their antennas are built into the marker in the form of windings. The marker response can occur both at the frequency of the nonlinear field (NP), and at the frequency 3C or its frequency, independent of the frequency 3C. In the latter case, the DC component that appears on the NE of the marker is used to power the modulator or its own RF generator. An AP can contain an address request. The volume of information read from the labels reaches several hundred bits. The permissible speeds of objects moving around the readers, equipped with marks, reach 300 km/h. It is easy to see that, with restrictions on the duration of the contact time with the tag, the identification range depends on the amount of information that is read, which determines the width of the reader's receiver. The energy distribution between the information volumes of the address request and the label response, the carrier selection, and the location of the mark on the object to be marked is of considerable importance.

Based on this technology, HP-sensors of the state of the environment can be developed with its remote control. The presence of discontinuities in the amplitude characteristics of some HP and small dimensions make it possible to apply them for nondestructive monitoring of the field distribution of the EMW. Such simple artificial HP allow remote fixation of weak perturbations of the stationary electromagnetic field falling on them, caused by changes in the environment surrounding the HP, for example, due to the displacement of objects or living beings. There is the possibility of recognizing "linear" objects moving along the grating from HP. There are known works on the detection of living beings and remote measurement of their physiological parameters on the basis of analysis of the NPs scattered by the surrounding environment by de-energized electronics when EMV falls on them with a sufficient intensity for receiving NP.

It is established that in the system of subharmonic scatterers (GSR) collective effects are possible, manifested in the emergence of a certain hierarchy, when previously excited lasers with an increase in the front of the 3S are able to impose their phase of the scattered signal on other GGRs entering the system. The conditions imposed on 3C and the mutual arrangement of the GDR are established, under which the stochastic reaction of the system to the 3S can in general be converted into a deterministic one. In this case, its "trembling" backscattering diagram acquires a definite fixed form, it becomes possible to regulate the speed of propagation of the excitation and synchronization processes in the system [44].

At present, there are a number of research-related problems, inherent in varying degrees to the above-mentioned areas and requiring attention. These may include the following:

1) issues of recognition of HP,

2) determination of the coordinates of HP,

3) development of processing methods,

4) increasing the efficiency of synthesized HP,

5) studying the effects of ZRP and the possibilities of using them at higher frequencies, which provides more efficient spatial selection of HP and facilitates the formation of more dense EMV flows.

The use of complex STS in nonlinear radar will significantly increase the information content of radar systems.

5. APPLICATION OF CHAOTIC ALGORITHMS FOR PROTECTION, PROCESSING AND TRANSMISSION OF INFORMATION

A. Masking Information with Multimode Chaos in Packet Transmission

Chaotic masking is of interest in the context of packet communication, which is increasingly used in recent times. For example, the introduction of a digital WAP protocol into the GSM standard, which is used in cellular communication systems, implies multimedia support, including the transmission of video signals in real time. The introduction of new telecommunication technologies for packet data transmission GPRS (General Packet Radio Service) and EDGE (Enchanced Data Rates for GSM Evolution) will allow to increase transmission speeds up to 171.2 kbit/s and 384 kbit/s, respectively, but to move to the universal third-generation UMTS communication system (Universal Mobile Telecommunications System) it is necessary to ensure a data transfer speed of at least 2.048 Mbps. To date, GPRS technology is a bridge for a smooth transition from the current types of cellular communications to broadband third-generation strategic systems. At the same time, development of alternative methods of packet information transmission is quite actual, in particular, it is expedient to use waiting chaotic systems with multimode chaos. One of the ways of using such systems is illustrated in the block diagram in Fig. 9, containing a transmitter from elements 1-8 (Fig. 9a) and a receiver from elements 9-16 (Fig. 9b) [45].

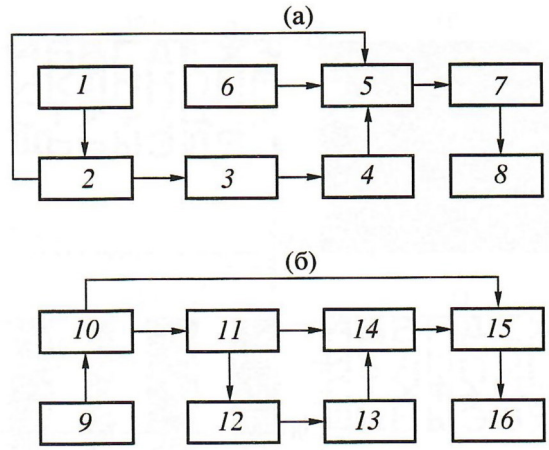

Fig. 9. *Transmitter block diagrams from elements 1-8 (a) and receiver from elements 9-16 (b).*

At the receiving device, oscillations from the antenna 9 are fed to the splitter 10. From one of its outputs (the first), the received oscillations enter the electronic commutator 11, which bypassing the pilot signal is locked, so that the waiting oscillator 13, which is similar to the generator 4, the radio pulse transmitted through the delay line 12, and the chaotic oscillations generated in the transmitter are "cut off". In the switch 11, when the radio pulse is ramped into two equal parts, the branching losses are compensated so that the oscillations of the radio impulse at each of the two outputs are equal to the oscillations of the radio pulse at the input of the commutator. If at the input of the splitter 10 the oscillation process (with loss compensation in the transmission path) is determined by the quantity G z1 (t), then the oscillations Gγ2z1 (t) are realized at its first output (at the input of the switching device 11), where γ2 is the branching factor in the receiver. At its second output, a signal (1 - γ^2) Gz1 (t) appears. After passing the switching device, we have Gγ2 (1 - γ1) f (t), and after the delay in line 12 at time T2 (under the condition T2 = T1) the signal has the form φ2 (τ) = Gγ2 (1 - γ1) f (τ) . As a result of this signal, the generator 13 is excited. In this case, its oscillations x2 (t) are fed to one of the inputs of the adder 14. Another signal input (1 - γ1) γ2Gf (t) is fed to its other input. The total oscillation process, determined by the expression z2 (t) = x2 (τ) + (1 - γ1) γ2Gf (t), falls on one of the inputs

(at the first) of the subtracter 15. On its second input oscillations are fed (from the output of the coupler 10), which are equal to G (l - γ2) z (t). The difference oscillations z (t) = G (l - y2) z1 (t) - z2 (t) act on the detection device 16, from which the output signal is removed after nonlinear conversion, integration and filtration.

In Fig. 10 shows the characteristic power spectra in the transmission of information. In Fig. l0a shows the power spectrum S1 at the output of the device 6 and the power spectrum S3 at the output of the receiver, and in Fig. 10b is the power spectrum of S2 at the output of the amplifier 7. In a numerical analysis of the mathematical model, the generators 4 and 13 were described by nonlinear differential equations with a retarded argument in the characterization of NEs providing a rigid excitation. The transmitted signal s (t) is given (for simplicity and clarity) in the form of a periodic function.

As can be seen (Fig. 10b), the power spectrum at the output of the transmitter reflects the chaotic nature of the oscillations. In this case,

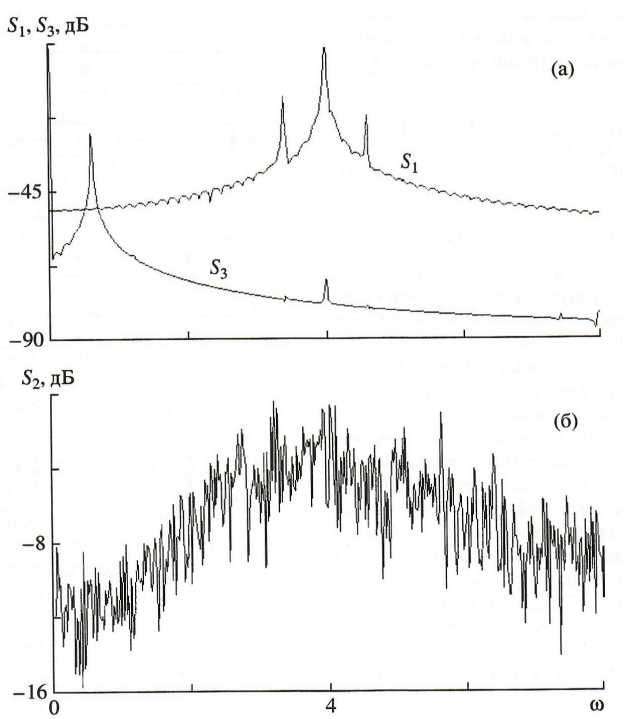

Fig. 10. *The power spectra of the signal in the transmission of information on a flowchart of fig. 9: the power spectrum S1 at the output of the transmitter device 6 and the power spectrum S3 at the output of the receiver 16 (a); power spectrum S2 at the output of transmitter amplifier 7 (b).*

the transmitted regular signal is reliably disguised. In the receiving device, the transmitted signal is clearly allocated (curve S3 in Fig. 9a).

B. Pseudo-holographic coding of information

With the advent of new telecommunication technologies in the development of methods for transferring and storing large volumes of information in digital form, along with the requirements of high transmission speed and the possibility of rapid access, the problem of effective data recovery comes with the inevitable losses in transmission, archiving and long-term storage. Pulse noise in the communication channel during transmission, failures in recording and reading from magnetic and optical media, imperfection of technology, various damage to the working layer during storage - all this leads to losses of both individual bits and whole blocks of information, sometimes very significant. The use and storage of information in electronic form is increasingly used in the modern world. Almost all large libraries and storage facilities transfer their archival funds to digital media. Therefore, the development of special methods of encoding information in the transmission, processing and storage, allowing to ensure the effective restoration of information losses, is of great relevance.

In connection with this, the physical principle of optical holography is interesting (from the Greek holos - all, full and grapho - I write). Optical holography is a method of fixing a phase picture of the wave fields scattered by objects on a photocarrier (hologram) with the aid of a support coherent wave and is essentially an analog coding of images of objects. An important and useful feature of such coding is the fact that, due to the sphericity of the scattered waves, information about each scattering point of the object is evenly distributed throughout the hologram and it becomes possible to fully restore the original image over a small fragment of the hologram with the help of a coherent

radiation (key). Even the irretrievable loss of a significant portion of the hologram does not interfere with the restoration of the whole image during decoding. The deterioration in the quality of the restored image is manifested only in a certain decrease in brightness and contrast.

The most revealing, as in the case of optical holography, is the restoration of a digital image. Obviously, any textual information can also be represented as a graphic.

As a physical model of the digital image to be encoded, we can take a matrix of elements consisting of zeros and ones similar to a bitmap image. In this case, we can assume that the unit corresponds to the black element of the image, to zero - white. Obviously, this way of presenting graphic information can be extended to color images by overlapping several matrices, as is done in color printing or in television. Depending on the resolution, a single pixel element-pixel-can be represented as a single dot or an entire set of pixels.

When transforming a raster matrix by renumbering (mixing) its members in such a way that any compact subset of elements is scattered evenly throughout the matrix field, black and white raster elements are mixed and the image becomes uniformly gray. The inverse single-valued transformation returns all the elements to their places, and the image is restored in its original form. Such a matrix transformation method should ensure a satisfactory reproduction of the image as a whole during decoding, even if part of the transformed matrix is lost. Thus, there is a direct analogy between the proposed digital image coding method and the analog method, known as optical holography.

It should be noted that the restoration of a holistic image over a coded fragment can be performed in various ways, in particular with the aid of the well-known two-dimensional Fourier transform and those analogous to it. However, the mixing of the image elements in this case occurs quite unevenly. It should be noted that encoding methods using the decomposition of image elements with respect to spatial harmonic modes and taking into account the phase relationships between them are analogous even when using a discrete analytical apparatus.

As a model image to be encoded, a simple matrix with a size of 256 x 256 elements is chosen, containing a set of zeros and ones organized in the form of letters of the Russian alphabet (Fig. 11a) [45]. This image has a fairly good contrast. Stirring of the elements of the matrix was carried out using the double permutation method according to the pseudo-random law. To ensure the uniformity of the scattering and the uniqueness of the encoding transformation with the help of the random number generator, a special mixing code was created for each row of the matrix from permutations according to the random law of a complete set of 256 integers of the natural

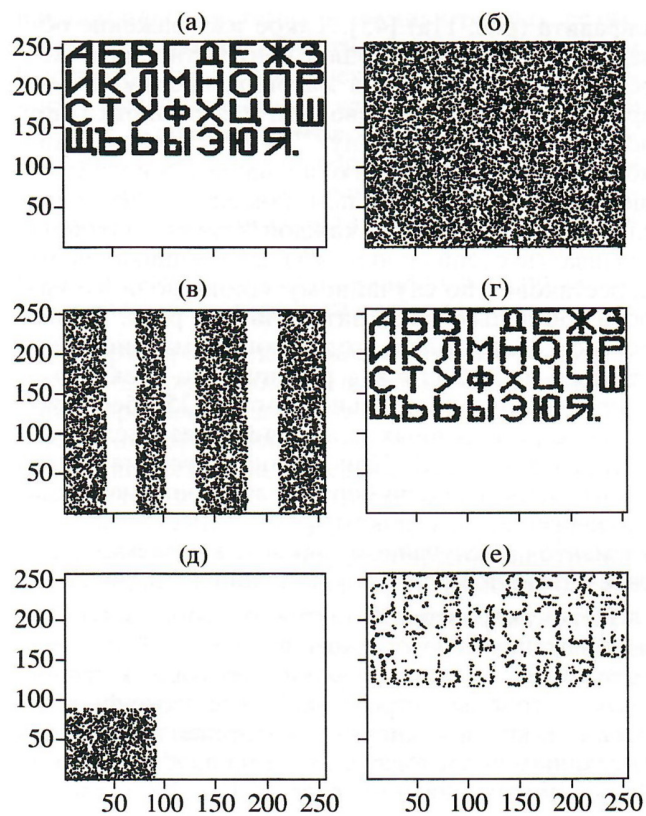

Fig. 11. *An example of pseudo-holographic coding of graphic information: the original image of the Russian alphabet on a matrix of 256x256 elements (a); coded picture after uniform pseudo-random mixing of elements across the entire field of the matrix (b); damaged encoded image (c); reconstructed image by corresponding truncated matrices (r); a fragment of the encoded image (e); the restored image from its fragment (e).*

number. Thus, an encoding matrix consisting of 256 lines with various pseudo-random sequences of 256 randomly intermixed integers from the numerical interval {1, 256} was created. Using this matrix, the original matrix of the image was renumbered by rows by rearranging its elements according to a random law specified by the corresponding row of the coding matrix.

The image matrix thus recomputed was reversed by 90 °. As a result of this rotation, the rows become columns, and the columns become columns. After this, a new coding matrix was formed from the pseudo-random sequences of mixed 256 numbers of the natural number from 1 to 256, and a new mixing was performed. As a result of the second renumbering, there was complete mixing of the elements of the original matrix. Its ij-th element became an lm-th element with probability of the order of 1/2562, i.e. The black and white elements of the image were fairly evenly distributed throughout the entire field of the transformed matrix. The image became a gray square (Fig. 11b).

To perform the inverse transformation, it is necessary to prepare decoding matrices, i.e. Matrices that return the renumbered elements to their original place. The loss simulation of a portion of the coded picture can be simulated in various ways. Replacing in the matrix corresponding to the encoded image, an arbitrary block of elements with zeros, so that the original dimensions of the matrix are preserved, is analogous to a procedure that can be called "whitening". When restoring the original image from the encoded fragment, it does not matter which portion of the encoded image is damaged. In Fig. 11c, 11d shows one of the variants of the corruption of the encoded image: the array of "whitened" columns and the 1/16 fragment of the coded image. The results of restoring the original image for such damage are shown in Fig. 11d, 11e. It is clearly seen that from the surviving fragments of the transformed matrix, it is possible to restore the original picture quite satisfactorily. Naturally, as the area of the matrix undergoing reconstruction is reduced, the image becomes more and more illegible. The obtained results confirm the validity of the analogy between the proposed coding method and the principle of restoring the whole image from the fragment of the hologram.

With the use of additional approximation methods, when reconstructing an image from an encoded fragment, the efficiency of the reduction can be greatly increased. In this case, a priori information on the nature of the image will allow us to choose the most effective method of approximation; For example, halftone images will be well restored with the use of a median spline, and contour (text, drawings, schemes) - using methods that enhance the linear contrast [22].

As shown by numerical experiments, the main requirement for the coding algorithm is to ensure uniform mixing of the individual elements of the information block throughout the entire volume. The second important requirement is unambiguousness when restoring the information block. As a result of the inverse transformation during decoding, the various elements should not be mapped to a single point.

When creating coding matrices providing mixing of image elements by a pseudo-random law, both standard pseudo-random number generators and special programs for generating pseudorandom integers, for example discrete chaotic algorithms described in [21], can be used. It should be noted that with the increase in the volume of information blocks, the efficiency of recovery by fragments strongly depends on the "uniformity" of mixing primary information, so the use of the developed deterministic chaotic algorithms for these purposes can play a decisive role.

With the long-term storage of digital information in electronic form, on magnetic and

optical media, as well as during its transmission through imperfect communication channels, losses of sufficiently large information blocks often occur. The proposed method of coding graphic information allows to significantly reduce such losses, because when restoring the image (decoding), the loss of large blocks is replaced by losses of individual image points that do not affect the integrity of the perception of the overall picture. Note that for the information encoded by the proposed method, various compression methods may be used in the future, which will effectively reduce the information volume.

An additional advantage of the proposed method for encoding digital information is cryptographic stability. The considered operation of mixing matrix elements is essentially encryption with a key, the length of which is equal to the length of the information array. This means that even with the known method of coding, deciphering such an image by a simple search of keys turns into a task beyond the power of modern computer technology. In fact, the number of all possible permutations, even for a small information block (256 elements per line) is 256! ~ 10507. Such a number of possible options for the key modern personal computer qualifies as infinity. Therefore, attempts to unauthorized decryption of such information can be related only to attempts to identify an algorithm for forming a matrix that provides mixing of image elements. Encoded by the proposed method, information can be stored in archives with free access and transmitted through open information channels with the guarantee of maintaining confidentiality.

6. CONCLUSION

Currently, the development of modern information and telecommunication systems and information technologies is primarily associated with the development of software and algorithmic information protection tools for its transmission, processing and storage in computer networks, as well as the rapid growth of personal radio communication systems, a sharp increase in the number of users, with increased mobility of subscribers, with the need to transmit a variety of information.

Prospective directions of using information technologies on the basis of dynamic chaos for transmission, processing, storage and protection of information are considered. Finite-dimensional mathematical algorithms for calculating chaotic signals by the method of reconstruction of nonlinear dynamics in dissipative systems with delay are proposed. A digital generator of chaotic binary codes based on high-speed digital devices was developed. We propose and implement discrete chaotic algorithms for the protection, processing and transmission of information, including graphic information using the pseudo-holographic coding method.

Applied application of information technologies implies the physical implementation of a specific coding process in the transmission, processing and storage of information in telecommunication systems and computer networks. Progress in this area is associated with increased performance and increased noise immunity of information channels. This is primarily due to the need to develop effective channels for information exchange and management of distributed networks and automated systems with remote control, where the price of an error or a partial loss of information can have catastrophic consequences, up to the loss of the entire system.

Using the example of the telecommunication radio terminal of a broadband digital communication channel with spreading, the information technologies of a digital communication channel model with spreading spectrum using encoding chaotic signals were experimentally investigated. It is shown that in such a communication channel, in the transmission, an effective spreading of the

carrier spectrum is realized, transforming it into a noise signal in a wide frequency band. The spreading of the spectrum in the transmission of information provides energy concealment (visibility), and the nature of the noise-like carrier being formed ensures an effective structural concealment of the communication channel. The communication channel implemented on these principles has a high degree of confidentiality, since it is almost impossible to restore the chaotic expanding function and to roll up the broadband signal in an unauthorized reception. The property of mutual orthogonality of chaotic codes allows for statistical separation of broadband signals in a communication channel with multipath propagation with relative delay of rays exceeding the duration of one character of the chaotic code.

The recent trend in the global spread of various open telecommunications systems and the sharp increase in the number of subscribers lead to the need to protect information not only at the level of state bodies, special services or business, but at the level of almost every individual user. In information networks, this problem is mainly related not to the closure of information from unauthorized access (cryptography), but to the loss of information due to low noise immunity of various communication channels. The problem of increasing the noise immunity of communication channels is especially acute in radio relay lines.

Modern integrated circuit technology makes it possible to realize a completely digital radio channel without analog microwave modules, when the microwave carrier, control signals and digital information are formed on the basis of a single frequency grid. This opens up additional opportunities to overcome the technical limitations associated with the need to combine analog and digital units in modern computerized telecommunications channel equipment.

The use of ultra-wideband chaotic signals in modern radar makes it possible to significantly increase the informativity, accuracy and resolution of measurements, which will enable the construction of detailed radio images for complex and extended objects in the microwave and millimeter wave bands. Noise radars with continuous emission in a very wide frequency band are characterized by their hidden functioning and electromagnetic compatibility with other operating facilities, including traditional and narrowband systems.

The rapid development of semiconductor microelectronics and the element base for it has already led to the creation of submicron-sized elements. Further progress in microelectronics will be possible only with the creation of new elements with dimensions of the order of tens and units of nanometers. One of the promising branches of the further development of electronics is molecular nanoelectronics.

When developing molecular electronic devices, a very high degree of integration of individual elements can be realized. The use of such devices as an element base for nanoelectronic circuitry will allow developing digital information technologies of a new generation on a new hardware infrastructure, creating structurally developed neural network systems and cellular automata systems based on the principles of binary and multilevel logic, and developing next-generation telecommunication systems with a large Information capacity, using chaotic signals with large fractal dimension. The complex development of such systems would bring about cardinal changes in the solution of the problem of creating artificial intelligence.

The work was supported by the Russian Foundation for Basic Research (Projects No 03-07-90133, 01-07-90349, 01-02-17529.

REFERENCES

1. Yuri V. Gulyaev, Rostislav V. Belyaev, Georgy M. Vorontsov, Nikolay N. Zalogin, Valerii I. Kalinin, Erast V. Kal'yanov, Vladimir V. Kislov, Vladimir Ya. Kislov, Vladimir V. Kolesov, Evgeny A. Myasin, Evgeny P. Chigin. Dynamic-chaos unformation technologies for

data, transmission and protection. *J. Commun. Techn. El.,* 2003, 48(10):1063-1086.
2. Bogdanov EV, Kislov VY, Myasin EA. Method for generating electromagnetic noise oscillations. *A.S. 1125735 USSR, B.I.*, 1984, No. 43, p. 311.
3. Lorenz EN. *J. Atm. Sci.*, 1963, 20(2):130.
4. Poincaré A. *On curves defined by differential equations*. Moscow, GTTL Publ., 1947.
5. Landau LD. *Dokl. AN SSSR*, 1944, 44 (2): 339.
6. Kislov VY, Zalogin NN, Myasin EA. *J. Commun. Techn.El.*, 1979, 24 (6): 118.
7. Kislov VY. *J. Commun. Techn.El.*, 1980, 25 (8): 1683.
8. Kislov VY, Zalogin NN, Myasin EA. *J. Commun. Techn.El.*, 1980, 25 (10): 2161.
9. Kalyanov EV, Ivanov VP, Lebedev MN. *J. Commun. Techn.El.*, 1982, 27 (5): 982.
10. Kalinin VI, Zalogin NN, Kislov VY. *J. Commun. Techn.El.*, 1983, 28 (10): 2001.
11. Kalinin VI, Zalogin NN, Myasin EA. *Letters to the ZhTF*, 1984, 10 (21): 1311.
12. Anisimova SE, Dmitriev AS, Zalogin NN, and others. *Letters to the ZhETF*, 1983, 37 (8): 387.
13. Dmitriev AS, Kislov VY. *Stochastic oscillations in radio engineering and electronics*. Moscow, Nauka Publ., 1989.
14. Ruell DD, Takens F. *Commun. Math. Phys.*, 1971, 20(3):167.
15. Shuster G. *Deterministic chaos*. Moscow, Mir Publ., 1988.
16. Zaslavsky GM, Chirikov BV. *Physics-Uspekhi,* 1971, 105(1):3.
17. Malinetskiy GG, Potapov AB. *Modern problems of nonlinear dynamics*. Moscow, Editorial URSS Publ., 2000.
18. Dmitriev AS, Panas AI. *Dynamic chaos. New media for communication systems*. Moscow, Fizmatgiz Publ., 2002.
19. Gulyaev SE, Kislov VY, Kislov VV. *Dokl. RAS*, 1998, 359(6):750.
20. Gulyaev SE, Kislov VY, Kislov VV and others. *Radiotekhnika*, 2002, 10: 3.
21. Kislov VY, Kalmykov VV, Belyaev RV, Vorontsov GM. *J. Commun. Techn.El.*, 1997, 42 (11): 1342.
22. Belyaev RV, Vorontsov GM, Kolesov VV. *J. Commun. Techn.El.*, 2000, 45 (8): 954.
23. Kotelnikov VA. *Theory of potential noise immunity*. Moscow, Radio i svyaz Publ., 1998.
24. Takens F. *Lecture, Notes in Mathematics*, 1981, 898:366.
25. Ladyzhenskaya OA. *Dokl. AN SSSR*, 1972, 205(2):317.
26. Farmer JD. *Physica 4D*, 1982, 4(3):366.
27. Mape R. *Lecture Notes in Mathematics*, 1981, 898:230.
28. Kolmogorov AN, Fomin S.V. *Elements of the theory of functions and functional analysis*. Moscow, Nauka Publ., 1972.
29. Kalinin VI. *Proc. 8th Int. Workshop ND & CS. "Nonlinear Dynamics and Complex Systems"*. Sept. 5-7, 2000. Minsk, p. 7.
30. Belyaev RV, Vorontsov GM, Kalinin VI, Kolesov VV. *Tr. IV Int. scientific-techn. Conf. "Perspective technologies in means of communication"*, August 15-17, 2001, Vladimir-Suzdal, c. 212.
31. Shannon CE. *Bell System Techn. J.*, 1948, 27(3):379.
32. Varakin LE. *Communication systems with noise-like signals*. Moscow, Radio i svyaz Publ., 1979.
33. Anisimova SE, Vorontsov GM, Zalogin NN, et al. *Radiotechnika*, 2000, 2:19.
34. Knut D. *The art of computer programming. The resulting algorithms. T.2*. Moscow, Mir Publ., 1977.
35. Kolesov VV, Belyaev RV, Vorontsov GM *J. Commun. Techn.El.*, 2001, 46 (11): 1361.
36. Ushenin A, Reganov V, Nyrkov M. *Electronic Components*, 1998, 5(14):17.
37. Demin VP, Kupriyanov AI, Sakharov AV. *Radio-electronic reconnaissance and radio monitoring*. Moscow, MAI Publ., 1997.
38. Kalinin VI. *Proc. PIERS Workshop on Advances in Radar Methods*, 1998, Baveno, Italy, p. 222.
39. Aksenov Vl, Zalogin NN, Kirillin KL. *Proc. Int. Conf. "Radar 87"*, 1987, London, p. 143.

40. Walton E. *Proc. PIERS Workshop on Advances in Radar Methods*, July 20-22, 1998, Baveno, Italy, p. 141.
41. Kalyanov EV, Kalinin VI, Kislov VY. *J. Commun. Techn.El.*, 2002, 47 (8): 984.
42. Kuznetsov AS, Kutin GI. *Abroad. Radioelectronics,* 1985, 4:41.
43. Babanov NU, Gorbachev AA, Lartsov SV and others. *J. Commun. Techn.El.*, 2000, 45 (6): 676.
44. Gorbachev PA. *J. Commun. Techn.El.*, 1995, 40 (11): 1606.
45. Kalyanov E.V. *J. Commun. Techn.El.*, 2002, 47 (4): 469.
46. Kolesov VV, Vorontsov GM, Zalogin NN. *J. Commun. Techn.El.*, 2002, 47 (5): 583.

DIRECT CHAOTIC COMMUNICATIONS AND ACTIVE RFID TAGS FOR INTERNET OF THINGS AND INTERNET OF ROBOTIC THINGS

Alexander S. Dmitriev, Anton I. Ryzhov, Maxim G. Popov

Kotelnikov Institute of Radioengineering and Electronics of RAS, http://www.cplire.ru
Moscow 125009, Russian Federation

chaos@mail.cplire.ru

Abstract. **The use of ultra-wideband direct-chaotic communications and radio identification tags for the organization of wireless high-speed data transmissons on the Internet of things and the Internet of robotics is considered. Prototypes and models of ultra-wideband transceivers of the 3.0 - 5.0 GHz range are described and presented. It is noted that these transceivers and nodes based upon them are intended for usage in sensor and active networks with arbitrary topology. It removes some of the limitations inherent for a number of other solutions for communication and identification.**

Keywords: **ultrawideband communications, internet of things, radiofrequency identification, direct chaotic communications**

UDC 621.391

Bibliography - 19 references *Received 03.09.2018*

RENSIT, 2018, 10(2):313-322 **DOI: 10.17725/rensit.2018.10.313**

Content

1. INTRODUCTION

The Internet of Things (IoT) is rapidly evolving from the conceptual point of view, extending the scope of applications, searching for and developing suitable wireless technologies. In the last few years an important part of the Internet of things has been realized. It is associated with remote data collection (kilometers and tens of kilometers) of simple data from electric and water meters in housing and communal services and simple management, for example, for electric lighting in cities and on the routes [1 , 2]. On the other hand, direction which defines the concept of the Internet of things as smart houses also continues its growth. Just from these two examples it becomes clear that the requirements to the Internet of things depend on situation and they are very different both in the transmission speed and in the distances to which information is to be delivered. In particular, in smart homes these distances can be up to several dozens meters or up to one hundred meters at maximum. And there are also such areas of the Internet of things as industrial Internet, agriculture, transport, logistics centers, robotics, etc. In [3] the Internet of things specifically highlighted the concept of the Internet of robotics (Internet of Robotic Things - IoRT). It refers to such objects as "... intelligent devices capable of tracking events by combining sensor data from different sources, using local and distributed “intelligence” to determine the best actions, and then to manipulate or monitor the objects in the physical world, and in some cases, to physically move through this world for the action itself... “.

Vivid example for the system of IoRT objects is unmanned automobile transport. According

to some estimates, as early as 2020, around 250 million connected cars will travel the roads around the world [4]. In the next five years, the number of cars equipped with communications equipment will grow dramatically, making connected cars one of the main elements for the Internet of things. Every fifth car in the world will have a wireless network connection with other devices. At the same time wireless communications inside the cars themselves quickly spread from luxury models to middle-class ones.

The article discusses the concepts of IoT and IoRT, the possibilities that can be implemented for the Internet of things with the use of wireless ultrawideband direct-chaotic communication facilities at the physical level [5] and Radio Frequency Identification (RFID) in the range 2.85-10.6 GHz. It also presents experimental prototypes and models of ultrawideband direct-chaotic transceivers and active RFID tags of the 3.0 - 5.0 GHz range with such characteristics. It should be noted that these transceivers and tags are intended for use in sensor and active networks [6] with arbitrary topology, which removes a number of limitations. typical for a number of other solutions. Using adaptive algorithms, it is possible to change the speed and range of transmission in the same network in order to provide solutions for different types of tasks.

2. INTERNET OF THINGS AND "SMART SPACES"

A number of concepts that overlap in meaning, but have their own specific features, are associated with with the Internet of things. To avoid confusion, we begin by clarifying the terminology [7].

In the early 70's, the inventors of the Internet drew in the imagination a world in which networks would connect to each other, becoming a web of interacting systems. By 1973, it became obvious that the main thing was to figure out how to make computers exchange information. By that time were developed various computer networks had been developed, which worked independently of each other. However, the value of all these systems was very limited, since they could not exchange information. To solve this problem, the TCP/IP (Transmission Control Protocol/Internet Protocol) was invented with which made it became possible to connect computers and all kinds of computer networks. The basis of the connected world was laid. Today every device connected to the Internet gets its IP address, and this allows it to connect to other devices.

In the phrase "Internet of things", "things" literally mean things that connect to the Internet and to each other. Each of these connected objects has a unique identification number and IP address. The connection can be made using wires, cables or wireless communication. The Internet of things implies the possibility of moving data needed for process control to any distance - both from another room and from another part of the world.

Within such broad category as the Internet of things, there are some key differences and nuances. Therefore, it is useful to introduce basic definitions.

The term “connected devices" refers to devices that exchange data over a conventional Internet connection, or are connected to a common network, for example, closed or private network. The connected device does not necessarily connect to the Internet of things, but it happens more often. In addition, this connectivity is spreading farther and farther, going beyond computers and penetrating into all corners and corners of the world.

There are two main types of connected devices - they are divided into physical and digital [8]. The first group includes such objects and processes that do not themselves generate or transmit digital data unless special manipulations are made and no changes happened. The second group includes devices that, according to their purpose, are capable of generating data and

transmitting them for future use. Therefore, despite the fact that many physical objects can be tagged using digital technologies, such as passive RFID tags, they are not capable of generating and transmitting any detailed meaningful data.

At the same time, RF identification is the main tool that allows physical devices to enter the digital world via wireless communication channels. RFID tags can be active and passive. Both of them allow nearby located readers to collect data and exchange them with a computer.

Another term related to the Internet of things is "Industrial Internet", concerning machines equipped with sensors that make them "smart". In the field of industrial Internet, data exchange is usually performed in three different ways: machine-machine (M-M, M2M), human-machine (H-M, H2M), and human-smartphone (M-C, M2S) (or other devices, for example, the tablet).

The Internet of things is able to connect together primarily physical objects and items, and also connect them with digital devices, including computers and software applications.

Thus, all devices interact with each other within a group or multi-point configuration and exchange data in real time - often using cloud technologies. When all these machines are connected to people using various computing devices, a completely new conceptual basis arises - the "Internet of everything". The Internet of everything is a more developed and perfect structure, in which the physical and digital worlds merge into a single space.

Currently, most of the data presented on the Internet in the form of text files, messages, audio and photo and video files. The Internet of things collects different new data, unites them in many ways and gives people and machines a broader and deeper understanding of the processes. To do this, you need to give computers their own tools for collecting information so that they can see, hear and smell the world themselves [9]. The Internet of things is able to penetrate into all the nooks and corners, cracks, holes and wormholes existing in an inaccessible for perception, and often an invisible world that extends far beyond the abilities of human organs for sight, hearing, smell and consciousness. It creates new types of networks and systems - completely new routes for data, information and knowledge.

3. REQUIREMENTS FOR WIRELESS COMMUNICATIONS

How the Internet of things works from the communication and network point of view? And what in this sense determines its power as a technology?

Two points are emphasized in [9] concerning the network nature of the Internet of things' power:

- Connecting a separate device increases its power, and often also the value for the user. However, the ability to connect a device to an extensive network - in fact, to the Internet of things - causes technical capabilities to grow exponentially.
- The benefit of connected devices is not the ability to start the engine or adjust the temperature in the house using the smartphone application. The real benefit will come when the whole networks of devices will exchange data and apply them in practice. As a result, the products of technology evolution will make a revolution.

These IoT properties fully comply with the laws for networks that characterize their capabilities. There are three such laws: Sarnov's law, Metcalfe's law and Reed's law [10].

Sarnov's law was formulated with the emergence of radio and television networks in the early 20th century, when the broadcast to multiple receivers came from a small number of transmitting stations. One of the pioneers of broadcasting David Sarnov stated the obvious: "The value of broadcast networks is directly proportional to the number of their listeners and viewers."

The Law of Metcalfe determines the growth of the value of the network in the presence of

connections between its nodes. The total value for the network, where each node is accessible to all other nodes, increases as the square of the number of its nodes. If you have two nodes and the value of each one is one unit, then the value of the network merged from them becomes four. Four interconnected nodes with value of one unit, within the network gain a total value of sixteen units. And the value of hundreds of such nodes is a hundred times a hundred, that is, ten thousand. This mathematical consequences can be expressed economically: the connection of the two networks gives a value significantly greater than the value obtained by adding their values as independent networks.

Reed's law shows that the value of a network increases not as a square, but as an exponent, if it is possible to form arbitrary groups within the network for exchanging information with each other.

What is significant is that the value of a network moves from one category to another as the concept of network expands. Whether growth is due to the gradual addition of consumers or the transparency of the relationships, the degree of expansion is such that it can support new categories of "market invaders", and hence new competitive games.

A similar, expansion-driven value shift can be observed in the history of the Internet. Initially, the use of the Internet was dictated by its role as a network of terminals, which shared selective access to a small number of expensive main hosts. As the Internet grew, its value and use increasingly concentrated around paired exchange of electronic messages, files and so on, increasing its value in accordance with the law of Metcalfe. And with the beginning of the 1990s, the flow of data between teleconferences and Web sites, mailings, and so on began to dominate the Internet, increasing value in accordance with the exponential law for networks with the ability to create groups. Although the functions that prevailed before did not lose their value and did not diminish as the Internet grew, the value and use of services, determined by the prevailing laws of correspondence, grew significantly faster. Therefore, many types of contacts and cooperation outside the Internet have been absorbed by the expanding functions of the Internet, which has become a new sphere of competition.

It is natural that in the early stages of the development of the Internet of things, "objects" will be connected to certain centers-nodes of the network and their direct interaction will be set to a minimum. These objects, except for "things" with active and passive RFID tags, will be sensors, that can collect and transfer some data to the nodes, and actuators, that can transmit control commands to "things". The task of informational interaction between the "things" will arise only when “thing" will need information from other devices to analyze the situation and make some decisions. So such a "thing" should have at least some minimal intellectual resource in the form of, for example, a processor, through which it can carry the analysis.

Although various communication channels, including cable and wires, can be used on the Internet of things, we will be considering radio channels and networks based on wireless transceivers as the most in-demand. Then we can assume that in the first stage of IoT development the most widespread will be wireless local area networks with the topology of the star type, where the transceivers of "things" in the local network interact with a certain node, and the direct interaction between the transceivers inside the local network will be minimal. In this case, the contribution of local networks of Internet of things will grow in proportion to the number of objects connected in these networks. And in the general dependence for potential "strength" of the network, an additional linear factor will appear.

With the growth of the number of "things" in the local network, there inevitably will be a situation in which “things" will begin to interact. For example, it can be an intelligent sensor

network for monitoring certain parameters of a territory, say, a temperature and it can independently estimate the temperature situation in the territory by exchanging data between devices and pass the results of this analysis to the decision node. In this case, the topology of the local wireless network can vary, depending on the location of the sensors and the range of the radio facilities. In general, it would be desirable for the network to allow the implementation of any topology and at the same time to have the capabilities of self-organization. In this case, the contribution of local network for Internet of things will grow in proportion to the square of the number of objects connected in this network. In the general dependence of for potential "strength" of the network, an additional quadratic multiplier will appear.

Finally, if the "things", like the objects of the classical Internet, can participate in the formation of arbitrary groups exchanging information with each other, Reed's law will begin to work and the strength of the network will grow exponentially with the total number of objects on the network.

Is there something specific for the Internet of things and the Internet of robotics depending on the number of objects in them? Formally, as we can see, the same laws as in the classical Internet work here. However, there must be some physical limitations on exponential growth. Indeed, there are at least two such restrictions.

The first thing is related to the cost of nodes in the network. Increase in the number of nodes in the Internet of everything (in the combined classical Internet with the Internet of things) will mainly occur due to the Internet of things. And the growth in the number of objects in it will be determined by economic and technological restrictions stemming from Moore's law. Suppose that the number of objects in the Internet of things is more than 10 times the number of objects in the classical Internet. This can happen in a limited time only if the cost of each IoT object is significantly lower than the cost of equipment in a typical node. Lets say it should decrease by 5-10 times. If this number increases tenfold again, the unit cost should decrease by 5-10 times more. If we assume that the cost of the classical Internet node equipment is $ 500, then an increase in the number of nodes will be 10 times when the node cost is reduced to 50-100 $, and 100 times when the cost decreases to 1-4 $.

The second limitation is related to the physical volume in which nodes for the Internet of things can be placed. Let's take the volume near and inside the Earth, in which all kinds of sensors and objects of the Internet of things can be placed. This volume is equal to the surface area of the Earth, multiplied by the thickness of the layer in which objects can be located. Let, for definiteness, it is equal to 100 m. Then the total volume filled with objects of the Internet will be $h = 5 \cdot 10^7\ km^3 = 5 \cdot 10^{16}\ m^3$.

If we assume that the volume of the usual Internet is about 10 billion, then with a volume of the Internet of everything 100 times more than the classical Internet, the number of objects will be 10^{12}. Or one object at $5 \cdot 10^4$ m^3 - in a cube with a side of about 40 m. Given the strong uneven distribution of objects, their extreme density can reach 1 object per 1 cu. m and above.

4. TECHNICAL COMMUNICATION EQUIPMENT

The technical communication equipment of the Internet of things, the Internet of robotics and the Internet of everything include transceivers, sensors, actuators, tags, readers, storage databases (including cloud databases) and software with a hardware on which it is located. And the capabilities of both individual identification points (nodes) and identification systems as a whole will be determined by the capabilities and characteristics of RFID tags and readers.

Let us briefly consider the main types of radio tags and their characteristics.

We will be primarily interested in wireless communication and radio identification devices operating in the microwave frequency range.

This is due to the potential need to transfer large amounts of data combined with the requirement for small size of the devices themselves (tags) that are required for most mass applications. Ultra-wideband tags should operate in the range from 2.85 to 10.6 GHz and therefore it is important to compare their characteristics with narrowband devices in approximately the same frequency range.

In general there are three types of tags can be used in the Internet of things: passive, semi-passive (semi-active) and active. However, they perform and will perform different functions in the IoT and IoRT due to their technical characteristics. **Table 1** compares the basic properties of active and passive technologies and their capabilities. It can be seen that the main limitations for passive tags are a small range and small amounts of transmitted information. The latter makes it difficult to use passive radio identification to connect devices of the second type - digital devices that generate information or process information while collecting data from sensors. On the other hand, the significantly greater range and data volume capabilities of active RF tags are not free. They are provided by much greater cost of devices and the presence of power source with limited battery life on the tags.

Table 1

Comparison of active and passive RFID technologies

CRITERION	ACTIVE	PASSIVE
Power source of a tag	Internal, on a device	Energy is transmitted from reader through radio channel
Power source on tag	Yes	No
Power availability on tag	Constant	Only during reading
Power availability on tag	Low	High
Strenght of the tag signal on the reader	High	Low
Communication range	Long (up to 100 m and more)	Short or very short (3 m or less)
Number of tags in area	More than 1000 tags for 1 reader, possible to serve 20 tags while moving with a speed more than 100 kmph	Hundreds of tags within 3 meters around reader, can serve 20 tags while moving with a speed 3 kmph or lower
Sensor possibilities	Yes	Limited
Memory capacity available for writing/ reading	High (for example 128 Kb)	Low (for example, 128 bytes)

These circumstances determine now and will determine in the future the scope of application for active and passive radio identification in the basis of the Internet of things. Note that current popularity of active tags is connected mainly with their ability to determine the location of tags with sufficiently high accuracy. Ultrawideband tags and technologies provide the better results for solving such problems and they successfully developing.

With the development of IoT and IoRT technologies, the situation will change in favor of systems that will be required to collect and deliver large amounts of data (at least under peak loads). Such systems will require tags as universal devices that can identify the objects on which they are located, enable to determine their position in space, collect information (for example, from sensors), process it and transmit it to the reader or neighboring nodes. So the tag will be transformed from the narrow purpose device into a universal information and communication node. At the same time, the cost of such devices should gradually decrease, and the battery life should be sufficient to solve the corresponding problems.

Further, as a candidate for the role of such devices, direct chaotic ultrawideband universal transceiver modules capable, among other things, to act as active labels, are considered.

Direct chaotic transceivers [11-13] were created oriented to the standard IEEE 802.15.4a - 2007 [14], which regulates the use of ultra-wideband signals in personal wireless networks at the physical level (Ultra Wideband Personal Area Networks, Physical level). In this standard, direct chaotic signals (chaotic radio pulses) are used as an optional data carrier. In the following years, there was a high level of activity in the UWB communication standards development by the IEEE (IEEE 802.15.4 - 2011, IEEE 802.15.6 - 2012, IEEE 802.15.4f - 2012), the International Organization for

Standardization (ISO) and the International Electrotechnical Commission (IEC) (ISO / IEC 24730-61 - 2013, ISO / IEC 24730-62 - 2013).

The IEEE 802.15.4 - 2011 standard refers to the physical layer of general purpose personal networks, integrating and upgrading the IEEE 802.15.4 - 2006 and IEEE 802.15.4 - 2007 standards. The IEEE 802.15.6 - 2012 standard refers to medical and consumer networks located near the body of a person (body networks). Standards IEEE 802.15.4f - 2012, ISO / IEC 24730-61 - 2013, ISO / IEC 24730-62 - 2013 define the requirements for ultrawideband active radiotags. It is interesting to note that the data transfer rate in the IEEE 802.15.4a-2007 standard is limited to 200 Kbps, but the IEEE 802.15.4-2011 standard created on its basis introduces the transmission rates of 110 Kbps, 850 Kbps, 6.8 Mbps and 27.2 Mbps. The same transmission speeds appear in the ISO / IEC standard 24730-62 - 2013.

After the adoption of the standard for active tags (IEEE 802.15.4f), the first devices appeared on the market provided, among other things, the possibility of high-precision location of labels. These devices include Zebra UWB radio tags and readers [15] and tags from Trackit Systems [16]. Another interesting UWB product is DecaWave's UWB transceiver chip and a transceiver module based on it [17]. The company also supplies a set for development based on the chip.

Note that these practical foreign developments of UWB communications mainly focus on the task of range determination and object localization, while the actual task of data transmission is given less attention. Ultrawideband communication devices based on chaotic radio pulses, in contrast, are mainly designed to solve problems of information transfer and transmission of data streams over networks. Therefore, the requirements for these two areas of UWB wireless communication equipment are significantly different.

5. UNIVERSAL MODULE AND NETWORK NODES BASED ON IT

Considering the development trends of ultrawideband communication, the characteristics of the developed transceivers based on chaotic radio pulses and the experience gained at the Kotelnikov Institute of Radioengineering and Electronics (IRE) of RAS, a universal UWB direct chaotic transceiver module was developed [6], designed to solve a wide range of problems in the field of short range wireless communication.

The developed ultrawideband direct chaotic transceiver module PPM-47 is a small-sized device that can be connected to sensors, actuators, batteries and other components on special boards.

The module structure is shown in **Fig. 1**. It includes an ultrawideband transmitter (UT) unit, an ultrawideband receiver (UR) unit, an antenna, a key (K), and a digital unit (CPU). CPU provides control of data transmission and reception, implements network functions and interface for connection to external devices. Such devices can be sensors or actuators made on separate boards. External devices can be either digital or analog. For the analog ones a built-in analog-to-digital converter of the microcontroller can be used to convert the signal to digital form. The microcontroller used in a transceiver is a high-performance 32-bit STM232L with reduced power consumption. Digital transmission between the microcontroller of the transceiver and external device is carried out via a high-speed SPI interface. The module can provide information transfer between two devices in the point-to-point mode, as well as by the network. In the case of network transmission all control tasks for the network level are provided by the microcontroller of the device itself.

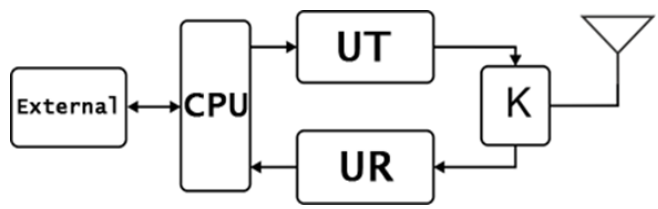

Fig. 1. *Structure of UWB transciever module.*

Structurally, the module is a board of 50x35x6 mm3 size, made on a FR-4 material with a thickness equal to 0.6 mm.

The operating frequency range of the transceiver module is within 3-5 GHz, the physical transmission rate is up to 6 (12) Mbps.

The module can be used independently, without special additional boards or devices, for example, as a base station, connected to a computer or as a relay. It can also be part of sensor and actuator nodes, where sensors or actuators are present with it.

In **Fig. 2***a* shows the base station based on the module. It has a matchbox form-factor and connects via a micro-USB connector to a computer, laptop or smartphone. The device is powered by a micro USB connector. The use of various additional blocks in the form of specialized boards enables the realization of a wide range of devices. For example, such blocks can be: a board with a rechargeable battery, which makes it possible to use the module as a relay (Fig. 2*b*), a board with a disposable battery (Fig. 2*c*), which allows o use the module as the active ultrawideband tag and a board with an acoustic module (Fig. 2*d*).

Relay node - can be used when it is necessary to increase the communication range. Along with the universal module includes a board with the battery. Battery can be charged is via the micro-USB connector (Figure 2*b*).

Active RFID tag - a device that provides identification for the object to which it is attached. An active RFID tag, in addition to the universal transceiver module, includes a power supply board with a 600 mAh lithium battery, which allows the tag to operate autonomously for two years or more (depending on the operating mode). The tag, like the other devices based on the universal module, is placed in a plastic case with the matchbox form-factor(Fig. 2*c*).

Acoustic sensor node - can be used for personal voice communication between people in the office or at home. It can be called a "remote voice". Along with the universal module, it includes a board with a microphone, a speaker, a microcontroller and a battery. The battery is charged via the micro-USB connector. The acoustic sensing unit, like the tag, is placed in a plastic case with the form-factor of a matchbox (Fig. 2*d*).

6. ACTIVE ULTRAWIDEBAND TAG

As an example of a node of a direct chaotic network, let us consider in more detail the active ultrawideband tag.

Different versions of tags are the basis for the concept of the Internet of things and the Internet of everything [18, 19].

The tag based on chaotic radio pulses can work in two modes:

Beacon mode (**Fig. 3***a*). In this case, the label periodically sends the information it contains in the form of packets. The frequency of sending can vary from 0.01 packets per second to 10 packets per second.

Response mode (Fig. 3*b*). Information is sent as a packet in response to a request from an external device, such as a reader.

The tag works in conjunction with the root node (reader). The reader uses the same transceiver module as the tag. This module can work with the internal antenna or with the external

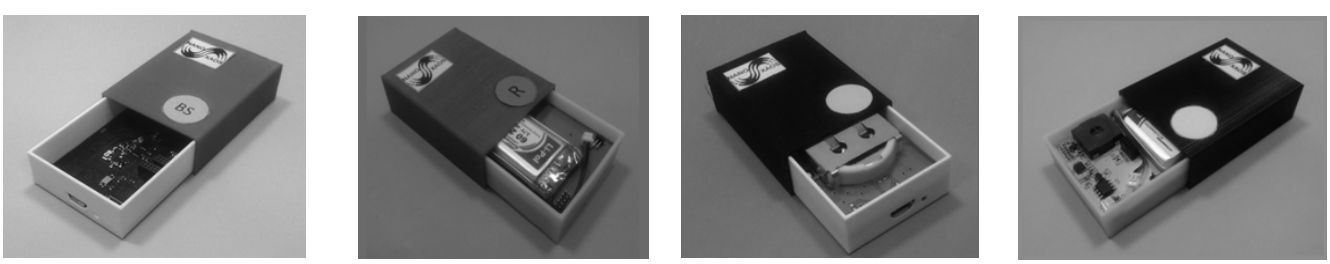

(a) *(b)* *(c)* *(d)*

Fig. 2. *Nodes of active UWB network based on universal module: base station (a); relay node (b); active RFID tag (c); acoustic sensor node (d).*

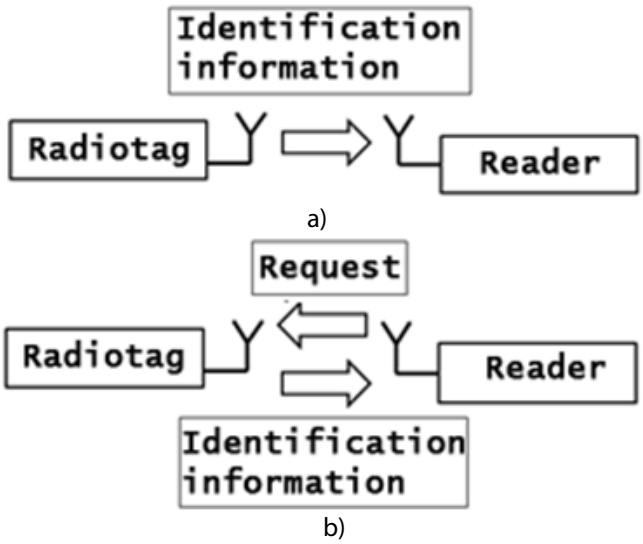

Fig. 3. *Interaction scheme for tags and readers: beacon mode (a); response mode (b).*

one. In the first case, the communication range is up to 30 meters. And if an external directional antenna is used in the reader, the range can be increased up to 100 and more meters.

To ensure long-term battery life, the device implements the system of energy-saving modes.

Short packet length combined with a high transmission rate allows simultaneous operation in the beacon mode for a large number of tags without any coordination. For example, 1000 radio tags with a packet transmission length of 17 microseconds (10 bytes packet size) and packet sending interval of one second will give the probability of collision between packets $\sim 10^{-2}$ in the region of stable reception.

As a power source for the tag a lithium battery CR2450 is used. The battery has an output voltage of 3V and is designed for small values of the output current, 2 mA, at which excess capacity of the battery begins to significantly drop. The transceiver is powered by a voltage of 5 V, and the peak current consumption can be up to 45 mA. Considering these factors, a special electrical circuit is used to power the radio tag. It utilizes capacitors to accumulate the charge in pauses between data transmissions and provides the required current at the time of transmission or reception.

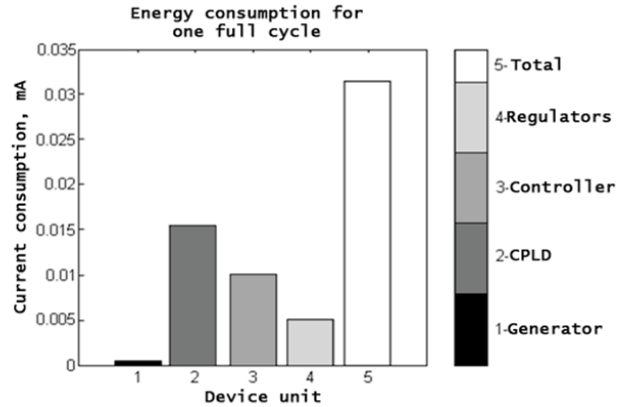

Fig. 4. *Energy consumption of the device: 1 – generator; 2 – CPLD; 3 - microcontroller; power regulators; 4 –* the whole tag.

When the radio tag operates in the beacon mode, it sends a message containing the identification information with some constant period. Then the message can be is received and processed on the reader. The overall duty cycle of the radio tag look like this. For the most of the time of its operating cycle the device is in sleep mode, but it periodically wakes up for the time required to send the packet. Transitions between modes are controlled by the microcontroller. In the sleep mode, the entire periphery of the device, with the exception of the power regulators, is turned off. The microcontroller stops all operations and counts the time until the next packet. At the end, it switches to the operation mode and sequentially turns on all the necessary peripherals. After sending the identification packet, the microcontroller turns off all the peripherals and switches back to the time counting mode until the next packet.

The structure of power consumption with a breakdown by units for the beacon mode with a period of 1 second is illustrated in **Fig. 4.** Calculation of the average power consumption gives a value about 30 μA, with peak consumption at the moment of transmission up to 45 mA.

7. CONCLUSION

Analysis of development prospects for the of Internet Things and the Internet of everything shows that their strength will be determined by the number of "things" that interact at short distances. In order to enable for the value of

the Internet of everything to increase at least proportionally to the square of the number of connected "things", wireless short-range communication networks which can implement any topology and at the same time provide a sufficiently high data transfer rate are needed. In addition, they should be capable of long-term autonomous work, even in situations with a changeable network topology (as in the case of mobile robot groups), and also to work in conditions of increased range for certain cases.

Wireless UWB direct chaotic communication devices meet the above requirements and can provide IoT and IoRT with a wide range of capabilities, so they can be considered as perspective platforms, both for general-purpose nodes and for active RFID tags.

The study was carried out at the expense of a grant from the Russian Science Foundation (project No. 16-19-00084).

REFERENCES

1. Tikhvinsky V, Koval V, Bochechka G. Lora Technology: Prospects of Implementation on IoT Networks. *First Mile*, 2016, 6:43-49.
2. Zhdanov A. "LoRa," Swift "or Sigfox". *Tele-Sputnik,* 2017, 256(2):48-49 (in Russ.).
3. The Internet of Robotic Things. https://www.abiresearch.com/marketresearch/product/1019712-the-internet-of-robotic-things/ (accessed October 12, 2016).
4. Gartner Says By 2020, a Quarter Billion Connected Vehicles Will Enable New In-Vehicle Services and Automated Driving Capabilities. http://www.gartner.com/newsroom/id/2970017 (accessed October 12, 2016).
5. Dmitriev AS, Efremova EV, Gerasimov MY. Multimedia sensor networks based on ultrawideband chaotic radio pulses. *J.Commun. Technol. El.,* 2015, 60(4):393-401.
6. Dmitriev AS Gerasimov MY, Itskov VV, Lazarev VA, Popov MG, Ryzhov AI. Active wireless ultrawideband networks based on chaotic radio pulses. *J.Commun. Technol. El.,* 2017, 62(4):380-388.
7. Greengard S. *The Internet of Things (MIT Press Essential Knowledge series).* Cambridge, Massachusetts, MIT Press Publ., 2015, p 232.
8. Internet of Things vs. Internet of Everything What's the Difference? *ABI Research*, 2014:1-10.
9. Ashton K. That 'Internet of Things' Thing. *RFID Journal*, 2009, https://www.rfidjournal.com/articles/view?4986.
10. Rheingold H. *Smart mobs: The Next Social Revolution.* Cambridge, Basic Books, 2003, p. 288.
11. Dmitriev AS, Efremova EV, Kletsov AV, Kuzmin LV, Laktyushkin AM, Yurkin VY. Wireless ultrawideband communications and sensor networks. *J.Commun. Technol. El.*, 2008, 53(10):1206-1216.
12. Dmitriev AS, Ryzhov AI, Lazarev VA, Mansurov GK, Popov MG, Malyutin NV. Experimental ultrawideband wireless sensor network for medical applications. *J.Commun. Technol. El.*, 2015, 60(9):1027-1036.
13. Dmitriev AS, Efremova EV, Gerasimov MY. Multimedia sensor networks based on ultrawideband chaotic radio pulses. *J.Commun. Technol. El.*, 2015, 60(4):393-401.
14. IEEE Standards Association, «802.15.4a-2007 - IEEE Standard for Information technology-- Local and metropolitan area networks-- Specific requirements-- Part 15.4: Wireless Medium Access Control (MAC) and Physical Layer (PHY) Specifications for Low-Rate Wireless Personal Area Networks (WPANs) Amendment 1: Add Alternate PHYs», 2007.
15. Dart UWB Technology, https://www.zebra.com/us/en/products/location-solutions/dart-uwb/dart-tag.html.
16. Trackit Systems, http://www.thetrackit.com/RTLS.php.
17. Dw1000-product-brief.pdf, http://www.decawave.com/products/dwm1000-module.
18. Gubbi J, Buyya R, Marusic S, Palaniswami M. Internet of Things (IoT): A vision, architectural elements, and future directions. *Future Generation Computer Systems,* 2013, 29:1645-1660.
19. Evans D. The Internet of Things. How the Next Evolution of the Internet Is Changing Everything. *Cisco IBSG, White Paper,* 2011:1-11.

CHARACTERISTICS OF ERROR-CORRECTING SHORTENED BLOCK TURBO-CODES OF ITERATIVE RECEPTION OF INFORMATION

Lev E. Nazarov

Kotelnikov Institute of Radioengineering and Electronics of RAS, Fryazino Branch, http://fire.relarn.ru
1, Vvedensky sq., Fryazino 141190, Moscow region, Russian Federation

Pavel V. Shishkin

Moscow Office of ISS-Reshetnev Compani, http://www.iss-reshetnev.ru
16/37, Mytishchinskaya str., Moscow 129626, Russian Federation

nazarov@sunclass.ire.rssi.ru, shishkin@mail.ru

Abstract. **The focus of paper is directed towards the investigation of the characteristics of error-correcting block turbo-codes which enable communication at relatively low received signal/noise and provide very high power efficiency. Specific feature of investigated turbo-codes is construction with shortened information block for generated error-correcting block-code. According to this the considered shortened turbo-codes have symbol-by-symbol decoding algorithms developed for total class of turbo-codes, namely, decoding algorithms based on modified Chase algorithm. These decoding algorithms with low complexity implementation are iterative and for implementation the channel parameter signal/noise is not required. The resulted characteristics of shortened turbo-codes constructed with usage generated turbo-code (duration of code words, information volume, code rate, error performances) are presented in this paper. The computer simulations for iterative decoding algorithms for the number of turbo-codes with different code rate and information volumes are performed. The results of computer simulations have shown that the investigated shortened turbo-codes are more effective than known convolutional codes with equivalent parameters - the degradation of signal/noise is about 1.85 dB for bit-error 0.00001 for convolutional code with code rate 1/2 concerning the shortened turbo-code based on generated turbo-code with parameters (16384,12769,36).**

Keywords: **error-correcting codes, block product codes, iterative decoding, error performances**

UDC 621.391.01

Bibliography - 12 references
RENSIT, 2018, 10(2):323-328

Received 31.08.2018
DOI: 10.17725/rensit.2018.10.323

Content

1. INTRODUCTION

Interference-free codes are used in digital communication systems in order to increase the reliability of information transmission through interference channels [1]. In the literature, the most known are noise-block block codes with a cyclic structure and convolutional codes, for which algorithms for reception using soft solutions from the output of a demodulator of signals have been developed [1, 2].

Code constructions under the general name block turbo codes constitute an alternative to these codes with respect to probabilistic characteristics and complexity of generation and reception algorithms [3, 4, 5]. These codes are basic for a number of standards, for example, for IESS-15, IESS-315, IESS-316e (Intelsat satellite communication system), for IEEE 802.16 broadband access standard [6].

Block turbo codes are formed on the basis of sequential combination of constituent block codes [3], for these codes algorithms of iterative reception are developed [4]. With the increase in the volume of information blocks of the data of turbo codes and the use of iterative reception algorithms, the

limiting probabilistic characteristics of the Shannon transmission capacity of transmission channels with additive white Gaussian noise (ABGSH) are reached [3].

The class of known constituent codes is limited - block Hamming codes, codes with generalized parity check, low density codes [1, 3, 7, 8] are used. The problem of expanding a number of block turbo codes (BTK) used in the development of digital communication systems for various purposes, for example, with adaptive noise-tolerant transmission modes depending on the efficiency of channel interference, is topical.

The article describes the method of forming an expanded set of BTKs by shortening the information block of the generating turbo code, describes the characteristics of truncated turbo codes, including probabilistic characteristics using the algorithm of iterative reception.

2. PROBLEM STATEMENT

Let C1(n1, k1, d1), C2(n1, k1, d2) be binary block systematic codes whose code words are respectively the rows and columns of the two-dimensional matrix B = (bij; 0 ≤ i <n1; 0 ≤ j> n2) of size n1 × n2 (**Fig. 1**). This matrix is equivalent to the generating matrix for BTK with the parameters n = n1 · n2, k = k1 · k2, R = k / n, d = d1d2 and specifies the structure of code words [3]. Here n, k, R, d are the length of code words, the dimension, the code rate and the minimum Hamming distance of the code.

The algorithms for the optimal reception of signals corresponding to codes are based on the calculation of the set of 2k correlations [9]. For k >> 1, the implementation of these algorithms presents an intractable problem.

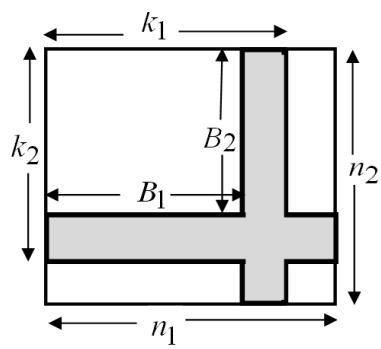

Fig. 1. *The scheme of the codeword of the block turbo code and the truncated turbo code on the basis of the components of the block codes C1(n1, k1, d1), C2(n1, k1, d2).*

Let's describe the algorithm of the iterative reception of the BTK, the essence of which is the decomposition of the optimal reception rule into a set of processing steps corresponding to the constituent block codes, which leads to a significant simplification of the resulting receiving procedure in relation to the optimal reception with a small energy loss [3, 4, 8].

Let A = (aij; 0 ≤ i <k1; 0 ≤ j> k2) be a sequence of information symbols forming a submatrix in the composition of the two-dimensional matrix B = (bij; 0 ≤ i <n1; 0 ≤ j> n2) of the turbo code; Y = (yij; 0 ≤ i <n1; 0 ≤ j> n2) - realization from the output of the signal demodulator; - likelihood ratio of conditional probability densities p (yij | bij = 0) of samples yij; Is the ratio of a priori symbolic probabilities.

In the first stage of the mth iteration, the increments of the a posteriori probabilities for the code symbols bij, j = 0, 1, ..., n1 - 1 for the i-th codeword of the constituent code C1

$$L^{(1,m)}(b_{ij}) = L^{(1,m)}(b_{ij} \mid Y_i^{(1)}, L^{(2,m)}(b_{ij})) - \\ -(L(y_{ij} \mid b_{ij}) + L^{(2,m)}(b_{ij})). \quad (1)$$

Here ; - an implementation in the composition Y, corresponding to the codeword. For the first iteration (m = 1), the condition L(2,1) (bi, j) = L (bi, j) is true.

In the second stage of the mth iteration, similar calculations are performed for increments of a posteriori character probabilities of words of the code C2

$$L^{(2,m)}(b_{ij}) = L^{(2,m)}(b_{ij} \mid Y_i^{(2)}, L^{(1,m)}(b_{ij})) - \\ -(L(y_{ij} \mid b_{ij}) + L^{(1,m)}(b_{ij})). \quad (2)$$

The quantities L(2, m) (bij) are used as a priori information for the first stage of the subsequent (m + 1) iteration L(1, m + 1) (bij) = L(2, m) (bij).

At the last iteration, decisions are made regarding the symbols bij: bij = 0 under the condition L(2, m) (bij | Yi (2), L(1, m) (bij))> 0, otherwise bij = 1.

The estimation algorithm L(bi | Y, L (bi)) is based on the calculation of expression

$$L(b_i \mid Y, L(b_i)) = \ln\left(\frac{\max\limits_{\bar{B}_m : b_{im}=0} \{p(Y \mid B_m)\Pr(B_m)\}}{\max\limits_{\bar{B}_m : b_{im}=1} \{p(Y \mid B_m)\Pr(B_m)\}}\right). \quad (3)$$

Assume that the conditions hold for the code words Bh(i) and Bl(i), respectively. For the AWGN

channel, under the condition that the codewords are equally probable, expression (3) has the form

$$L(b_i|Y, L(b_i)) = C \cdot \left(y_i + \sum_{t=1, t \neq i}^{n} y_t \cdot (-1)^{b_t} \cdot d_t \right). \quad (4)$$

Here dt = 0 if bh, t = bl, t and dt = 1 otherwise, C is a parameter that is constant for all code words. In accordance with the formalism of the iterative method, the second term in (4) is equivalent to the increment of the a posteriori probabilities L(1,m) (bij), L(2, m) (bij) for the constituent codes C1, C2 [3].

The procedure for searching for the code words Bh (i) and Bl (i), i = 0, 1, ..., n-1, requires the following steps [10].

Step 1. Binary "hard" decisions are made regarding the code symbols of the transmitted word B based on the samples of the implementation of Y.

Step 2. A set of error vectors {T} is generated, generating with their help the code words Sj = BTj, j = 1, 2, ..., 2p. The set {T} consists of 2p words containing combinations of errors located in p the least reliable positions of the word B. Here is the addition operation modulo 2.

Step 3. For each of the non-zero words Sj, the reception for block codes C1 or C2 is performed based on the calculation of algebraic error syndromes and a set of code words {D} with a volume not exceeding 2p is formed.

Step 4. The codeword with the greatest correlation between the signals corresponding to the words from {D}, and Y, which is accepted as Bh (i), is determined. A subset of codewords {D} with maximal correlation coefficients that does not contain Bh (i) corresponds to Bl (i) for the symbols bi.

For the symbols bi for which Bl (i) exists in the set {D}, the increment L (ξ, m) (bi), (ξ = 1, 2) is calculated. For the symbols bi for which Bl (i) does not exist in the set {D}, the computation L (ξ, m) (bi) is carried out using the rule L (ξ, m) (bi) = β (-1) bhi, (ξ = 1, 2). Here bhi is the i-th symbol of the code word Bh (i) computed in step 4; β = (E1 - E2) / p. Here, E1, E2 are the minimum and maximum correlation coefficients between the realization of Y and code words from the set {D}.

The expansion of the set of BTKs with variations of their code rates is possible using the shortening method of generating turbo codes by reducing their information volumes.

The essence of the problem to be solved is to describe the method of forming an expanded set of BTKs based on the generating turbo code with a decrease in its information volume, and also to describe the algorithm of iterative reception of these codes and the results of its simulation for a number of generated codes in order to estimate probabilistic characteristics at reception.

3. REDUCED BLOCK TURBO CODES

The shortening method of block turbo codes is based on the reduction in the volume of the information block of the generating turbo code in the formation of code words: the symbols of the code C1, aij; 0 ≤ i <B1, 0 ≤ j <k2 and the code C2, aij; 0 ≤ i <k1, 0 ≤ j <B2 are assumed to be equal to zero. The resulting codeword is shown in Fig. 1, the highlighted color shows the location of zero information and verification symbols of the truncated turbo code with parameters k = B1·B2, n = n1·n2 - (k1 - B1) n2 - (k2 - B2) n1 + (k1 - B1)(k2 - B2).

When forming the code words of truncated turbo codes from the derived series, the procedure for generating a systematic generating turbo code for an input information sequence with a volume of k1 · k2 bits with k1·k2 - B1·B2 zero components and corresponding code words with zero symbols that are not transmitted in channel.

When applying this method on the basis of a generative turbo code with a code rate R, it is possible to form a series of truncated turbo codes with code rates given by the relation

$$\frac{B_2 \cdot B_2}{n_1 \cdot n_2 - (k_1 - B_1)n_2 - (k_2 - B_2)n_1 + (k_1 - B_1)(k_2 - B_2)} \leq R \leq \frac{k_1 k_2}{n_1 n_2}.$$

Here 2 ≤ B1 ≤ k1, 2 ≤ B2 ≤ k2.

The minimum Hamming distance of these codes coincides with the minimum Hamming distance dmin of the generating turbo code. Table 1 shows the parameters k, n and R for a number of truncated turbo codes generated using this technique for generating turbo codes based on block Hamming codes with generalized parity check C1(128,120,4), C2(128,120,4) and C1(128,113,6), C1(128,113,6), in this case B1 = B2 = B.

Code speeds of truncated turbo codes corresponding to the generating turbo code based on the constituent codes C1(128,120,4), C2(128,120,4),

Table 1

Parameters of truncated turbo codes generated using generative turbo codes based on Block Hamming codes with a generalized parity check.

Generating turbo-code	*B*	*n*	*k*	*R*	d_{min}	E_b/N_0, dB
$C_1(128,120,4)$ $C_2(128,120,4)$	0	16384	14400	7/8	16	3.95
	22	900	484	1/2	16	3.10
	36	1936	1296	2/3	16	2.60
	52	3600	2704	3/4	16	2.80
	68	5776	4624	4/5	16	3.10
$C_1(128,113,6)$ $C_2(128,113,6)$	0	16384	12769	4/5	36	3.00
	36	2601	1296	1/2	36	2.25
	66	6561	4356	2/3	36	2.50
	97	12544	9409	3/4	36	2.80

can take the values $1/81 \le R1 \le 7/8$. Table 1 gives the parameters of a series of truncated turbo codes with code speeds of 7/8 (generating turbo code), 1/2, 2/3, 3/4 and 4/5. The code rates of truncated turbo codes corresponding to the generating turbo code based on the constituent codes C1(128,113,6), C1(128,113,6), can take the values $1/256 \le R1 \le 4/5$. Table 1 shows the parameters of a number of truncated turbo codes with code rates 4/5 (generating turbo code), 1/2, 2/3 and 3/4.

When receiving the code words of truncated turbo codes, you can use the iterative algorithm (1) - (4) with the above 4 steps for the generating turbo code. The peculiarity of the reception algorithm is the execution of step 3 - for each of the non-zero words Sj, a trick is used for shortened block codes C1 or C2 based on the calculation of algebraic syndromes and a set of code words {D} is formed, with a volume not exceeding 2p. In this case, error detection and correction is performed for code symbols that are not part of the symbols that are assumed to be zero when generating truncated turbo codes.

4. RESULTS OF MODELING

In **Fig. 2** and **Fig. 3** shows the probabilistic characteristics of the iterative reception algorithms (10 iterations) for truncated turbo codes based on the generative turbo codes considered above. The ordinates represent the error probability values for the information bit Pb, the signal/interference values Eb/N0 are plotted along the abscissa axis. Here, Eb is the energy per information bit, N0 is the spectral density of AWGN (one-sided).

When modeling the iterative algorithms of the turbo codes under consideration, an interval estimate of the probability Pb is made by calculating the frequency w = x/u. Here, x is the number of erroneous solutions in a sequence of independent computational experiments of size u, determined by the size of the confidence interval, the probability Pb, the confidence probability Pd. Under the condition u >> 1, we have [11]

$$P_{äîâ}\left(\left|w-P_á\right|<\alpha\right)\cong 2F\left(\frac{\alpha}{\sqrt{P_á(1-P_á)/u}}\right),$$

$$F(z)=\frac{1}{\sqrt{2\pi}}\int_0^z \exp(-y^2/2)dy.$$

For example, for Pb = 10-5, α = 0.5Pb (confidence interval [0.5Pb, 0.5Pb]) and Pdov = 0.95, the required number of experiments is u = 1450000.

In Fig. 2 shows the probabilistic characteristics when receiving the generating turbo code with the parameters (16384.140000.16) and the code rate 7/8 based on the constituent codes C1(128,120,4), C2(128,120,4) (curve 1) and the derivative of the truncated series turbo codes with code rates 1/2 (curve 2), 2/3 (curve 3), 3/4 (curve 4) and 4/5 (curve 5) for the AWGS channel. Curve 6 corresponds to a convolutional code with a code rate of 1/2 and a code constraint length of 7 [2]. Table 1 lists the corresponding signal / interference Eb/N0 values required to achieve the error probability per bit Pb = 10^{-5} when using these codes.

It is seen that for the generating turbo code (curve 1) with a code rate of 7/8, the error

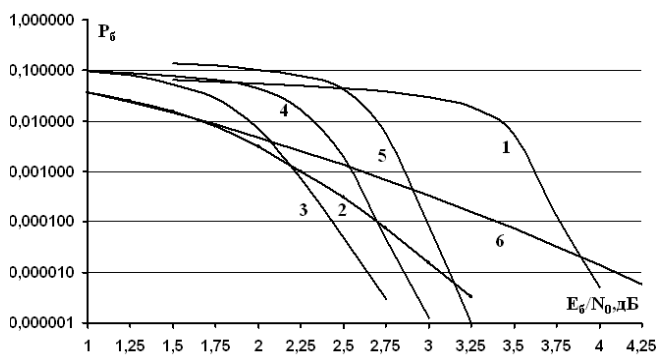

Fig. 2. *The generating torus. 2. Probabilistic characteristics when receiving noise-immune codes: 1 - generating turbo code based on the constituent codes C1(128,120,4), C2(128,120,4); 2 - shortened turbo code with code speed 1/2; 3 - shortened turbo code with code speed 2/3; 4 - shortened turbo code with code speed 3/4; 5 - shortened turbo code with code speed 4/5; 6 - convolutional code with code rate 1/2 and length of code constraint 7.bro-code*

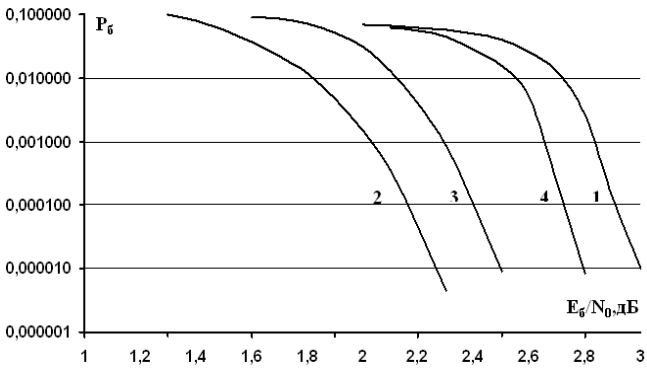

Fig. 3. *Probabilistic characteristics when receiving noiseproof codes: 1 - generating turbo code based on the constituent codes C1 (128,113,6), C2 (128,113,6); 2 - shortened turbo code with code speed 1/2; 3 - shortened turbo code with code speed 2/3; 4 - shortened turbo code with code speed 3/4.*

probability Pb = 10^{-5} is reached with Eb/N0 = 3.95 dB, which differs by only 1.05 dB from the limiting value for the Shannon capacity of the channel under consideration the bandwidth of the ABGS channel for codes with a code rate of 7/8 is achieved at 2.9 dB [2]).

It is also seen that for a shortened turbo code with code speed 1/2 (curve 2), the error probability P_b = 10^{-5} is reached at Eb/N0 = 3.1dB, which determines the energy gain to 1 dB for a given error probability Pb with respect to to a known convolutional code with an equivalent code rate (curve 6). When the error probability decreases, the energy gain values increase.

In Fig. 3 shows the probabilistic characteristics when receiving the generating turbo code with the parameters (16384,12769,36) and the code rate 4/5 based on the constituent codes C1(128,113,6), C1(128,113,6) (curve 1) and the derivative of the truncated series turbo codes with code rates 1/2 (curve 2), 2/3 (curve 3), 3/4 (curve 4) for the AWGS channel. Table 1 lists the corresponding signal/interference Eb/N0 values required to achieve the error probability per bit Pb = 10^{-5} when using these codes.

It is seen that for the generating turbo code (curve 1) with code speed ≈4/5, the error probability P_b= 10^{-5} is reached at Eb/N0 = 3.0 dB, this value differs only by 0.90 dB from the limiting value for the Shannon capacity of the considered channel (the bandwidth of the AWGN channel for codes with a code rate of 4/5 is achieved at 2.1 dB).

For a shortened turbo code with code speed 1/2 (curve 2), the error probability Pb = 10^{-5} is reached at Eb / N0 = 2.25 dB, which determines the energy gain to 1.85 dB for a given value of the error probability Pb with respect to the convolutional code with an equivalent code rate (curve 6 in Fig. 2).

A comparative analysis of the corresponding probabilistic curves in Fig. 2, Fig. 3 and Table 1 shows the presence of an energy gain of up to 0.25 dB for truncated turbo codes with an equivalent code rate for a generating turbo code with parameters (16384,12769,36) and a generating turbo code with parameters (16384,14400,16).

It should be noted that the probabilistic characteristics of the generating turbo code with the parameters (16384,12769,36) with code speed 4/5 based on the constituent codes C1(128,113,6), C1(128,113,6) and the derivative of a number of truncated turbo codes with the code rates 1/2 and 2/3 for AWGS are sufficiently close to probabilistic characteristics (the difference does not exceed 0.2 ... 0.7 dB) of the most effective low density codes recommended for use in satellite communication systems [12].

5. CONCLUSION

The characteristics of noise-resistant block turbo codes are given, the feature of which is that they are formed by shortening the information volumes of the generating turbo codes. This approach extends the class of block turbo codes with a variation of code rates, information volumes and code word lengths. When receiving truncated turbo codes, a modified iterative technique algorithm is developed, which is developed for generating block turbo codes.

For a number of considered generative and truncated block turbo codes, simulation of iterative reception algorithms has been carried out. In particular, it is shown that the energy gain when using a truncated turbo code with a code rate 1/2 with respect to the known convolutional code with an equivalent code rate for the error probability P_b = 10^{-5} reaches 1.85 dB.

The development of effective algorithms for the iterative reception of the considered generating and shortened turbo codes and a comparative analysis of their probabilistic characteristics represents a promising direction of research.

ACKNOWLEDGMENT

This work was supported by the Russian Foundation for Basic Research, project No. 16-07-00746 "Development of the

theory and methods of noise-immune digital communications over nonstationary channels with complex interference".

REFERENCES

1. Peterson W, Weldon E. *Codes that correct errors.* Moscow, Mir Publ., 1976, 594 p.
2. Zyuko AG, Falco AI, Panfilov IP, Banquet VL, Ivashchenko PV. *Immunity and efficiency of information transmission systems*. Moscow, Radio i svyaz Publ., 1985, 272 c.
3. Hagenauer J, Offer E, Papke L. Iterative decoding of binary block and convolutional codes. *IEEE Transactions on IT,* 1996, 42 (2):429-448.
4. Johnson SJ. *Iterative Error Correction: Turbo, Low-density Parity-Check and Repeat-Accumulate Codes*. Cambrige University Press, 2010, 335 p.
5. Nazarov LE, Shishkin PV, Batanov VV. Algorithms for iterative non-coherent signal reception based on serial turbo codes and Walsh signals transmitted over non-stationary channels. *Radiotekhnika i elektronika*, 2016, 61 (4):366-372 (in Russ.).
6. Vishnevsky VM, Lyakhov AI, Portnoy SL, Shakhnovich IV. *Broadband transmission networks*. Moscow, Technosphere, 2005, 592 p.
7. Nazarov LE, Shishkin PV. Investigation of probabilistic characteristics of block turbo codes based on low-density codes of finite geometries. *Journal of Radioelectronics (electronic journal)*, 2018, №5. Access mode: http://jre.cplire.ru/jre/may18/1/text.pdf. DOI: 10.30898 / 1684-1719.2018.5.1.
8. Nazarov LE, Shishkin PV. Characteristics of jam-resistant block turbo codes based on low-density codes. *Information Technology*, 2018, 24 (6): 427-432. DOI: 10.17587/it.24.427-432.
9. Kotelnikov VA. *Theory of potential noise immunity.* Moscow, Gosenergoizda Publ., 1956, 152 p.
10. Pyndiah RM. Near-optimum decoding of product-codes: block turbo-codes. *IEEE Transactions on COM*, 1998, 46(8):1003-1010.
11. Dunin-Barkovsky IV, Smirnov NV. *Theory of Probability and Mathematical Statistics in Engineering.* Moscow, GTTL Publ., 1955, 556 p.
12. Low-Density Parity Check Codes for Use in Near-Earth and Deep Space Applications. Experimental Specification. *CCSDS 131.1-O-2,* 2007, Washington, NASA Headquarters, 44 p.

SEMANTIC FUSION AND JOINT ANALYSIS OF TERAHERTZ AND 3D VIDEO IMAGES BY THE MEANS OF OBJECT-ORIENTED LOGIC PROGRAMMING

Alexei A. Morozov, Olga S. Sushkova, Alexander F. Polupanov, Gennady K. Mansurov, Stanislav K. Paprotskiy, Alexander V. Yanushko, Nadezda G. Petrova, Alexander S. Bugaev

Kotelnikov Institute of Radioengineering and Electronics of RAS, http://www.cplire.ru
11/7, Mokhovaya str., Moscow 125009, Russian Federation

Vyacheslav E. Antsiperov

Moscow Institute of Physics and Technology, http://mipt.ru
9, Institutsky per., Dolgoprudny 141701, Moscow Region, Russian Federation

morozov@cplire.ru, o.sushkova@mail.ru, sashap55@mail.ru, antciperov@gmail.com, gmansurov@mail.ru, s.paprotskiy@gmail.com, yanushko@gmail.com, petrova@cplire.ru, bugaev@cplire.ru

Abstract. **The aim of the work is to create methods and software tools for the terahertz range intelligent video surveillance, that is, for automatic analysis of video images in the terahertz frequency range. Terahertz video surveillance provides unique prospects in the area of public safety; in particular, it allows you to remotely identify weapons and dangerous items hidden under clothing on the human body. However, such characteristics of terahertz video, as low resolution, low contrast, and low signal-to-noise ratio, lead to the need to develop new methods and approaches to automatic video analysis. To understand the terahertz video image, the operator of the industrial video surveillance system usually compares it with images in other frequency ranges (visible or infrared). The comparison of these images of different types helps the operator to interpret the colored and/or one-color spots in the terahertz image in a proper way. In terms of automatic video analysis, this means that the context of the observed events and objects is taken into account, or in other words, a semantic fusion is implemented of the terahertz range video image with video images of other frequency ranges, e.g., near-infrared, visible, etc. The authors consider the semantic fusion of the video images as a critical component of the prospective terahertz intelligent video surveillance technology. A new method of the terahertz video surveillance based on the fusion of the terahertz video with 3D video is proposed. The means of the object-oriented logic programming developed for the semantic fusion of the terahertz and 3D video images are described. The developed method provides a real-time fusion of the terahertz video acquired using the THERZ-7A (Astrohn Technology Ltd) subterahertz scanning device (0.23-0.27 THz) and 3D video data acquired using the Kinect 2 (Microsoft Inc) time-of-flight sensor. The method and software tools for the semantic fusion of the terahertz and 3D video images are developed.**

Keywords: **terahertz video surveillance; 3D video surveillance; intelligent visual surveillance; object-oriented logic programming; Actor Prolog**

UDC 510.663; 519.68:007.5; 519.68:681.513.7; 681.3.06

Bibliography - 83 references *Received 27.08.2018*

RENSIT, 2018, 10(2):329-340 **DOI: 10.17725/rensit.2018.10.329**

Content

1. INTRODUCTION

Terahertz (submillimeter) radiation is electromagnetic radiation with a frequency in the

range of about 300 GHz to 3 Terahertz, i.e. a wavelength of 0.1 to 1 millimeter. The indicated limits of the frequency range are conditional, and many researchers use this term for electromagnetic radiation ranging from tens of gigahertz to 10 terahherts [1-4]. In addition, since terahertz radiation is located on the boundary between infrared radiation and millimeter waves, in many reviews and technical applications they are treated together [5-11]. The term "subterahertz radiation" is also used, if it is necessary to emphasize that we are talking about electromagnetic waves with a frequency of less than one terahertz.

The huge interest of researchers in terahertz radiation is due to the fact that it easily passes through most dielectrics, including plastic, ceramics, brick, wood, cardboard and fabric and is not ionizing. Moreover, terahertz radiation, as well as thermal radiation, is widespread in nature; living organisms are natural sources of terahertz radiation. These properties of terahertz radiation make its use in medicine very attractive [7, 12], archeology, art criticism [9] and, of course, security systems [10, 11, 13-24]. A passive receiver of terahertz waves emitted by a human body allows you to detect dangerous objects and weapons hidden under clothing. Also, active terahertz video surveillance systems including backlighting in the terahertz waveband are being developed [25-27].

Despite intensive research in the field of terahertz video surveillance, it is currently not widely used, with the exception of the security systems of certain buildings and airports. This is due not only to technical difficulties in the generation and reception of terahertz waves (which is reflected, among other things, in the price of the equipment being developed), but also because the equipment currently in use does not allow the full potential of terahertz video surveillance to be fully realized. The resulting terahertz video images are characterized by low resolution, low contrast, low signal-to-noise ratio and a low frame rate. Nevertheless, commercial screening systems have already been created that allow you to reveal remotely and unnoticeably the presence of objects hidden under his clothing.

A typical terahertz video image looks like a set of blurry spots, color or monochrome, depending on the data visualization method used. Simultaneously with the video image in the terahertz frequency range, the screening system displays the image in the visible or infrared frequency range familiar to humans [28, 29] (**Fig. 1**). The terahertz image can be subjected to additional processing in order to increase the contrast and detect abnormal areas [30 34]. This allows a specially trained operator to correctly interpret the terahertz video image and to identify the presence of objects hidden on the human body. This use of terahertz video surveillance, of course, is not optimal. In particular, it gave rise to the opinion that terahertz video surveillance is ineffective for screening passengers at the airport, because the employee managing the CCTV system is easier to use for manual screening of passengers. It is obvious that the mass use of terahertz video surveillance systems will become possible only with the appearance of sufficiently reliable methods of fully automatic analysis of terahertz video images.

The purpose of this work is to create methods and means of terahertz intelligent video surveillance, that is, automatic analysis of video images in the terahertz frequency range. As a basis for the realization of terahertz intellectual video surveillance, the authors consider the semantic merging (comparison) of a terahertz video image with video images obtained on the basis of other physical principles.

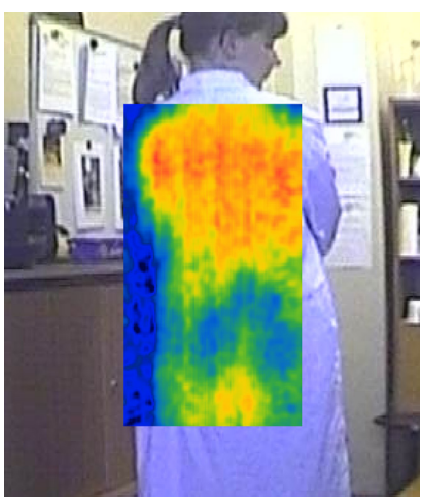

Fig. 1. *An example of a terahertz video image. For the convenience of the video surveillance operator, a terahertz image is placed against the visible. The rainbow color scale was used to display the terahertz data: red corresponds to the brightest areas of the image, blue to the coldest. The TT pistol hidden behind its back on a terahertz image looks like a blue-green spot.*

The article describes the experimental tools of object-oriented logical programming, developed at the Kotelnikov Institute of Radioengineering and Electronics of RAS for solving the problem of semantic fusion of terahertz and three-dimensional video images. Section 2 provides a brief overview of existing projects aimed at combining the possibilities of terahertz and three-dimensional video. Section 3 describes the experimental setup used to test the methods for merging terahertz and three-dimensional video images. In Section 4, the problem of calibrating the measurement system, including the terahertz and time-of-flight cameras, is considered. Section 5 discusses the experimental software developed to implement the terahertz method of intelligent video surveillance, and an example of merging heterogeneous video data.

2. COMBINING THE CAPABILITIES OF THZ AND 3D VIDEO: THE HISTORY OF THE ISSUE

The idea of semantic fusion of video images is that data from different sources of video information are combined into one video image in such a way that the semantic content of some images affects the processing algorithms of others [35, 38]. The simplest example of the semantic fusion of video images in the terahertz and visible ranges can be considered the use of subtraction algorithms in the visible range to understand where a person is, and where the background image, and to distinguish (in different colors) objects found under human clothes and the background image **Fig. 2**).

Of course, the background subtraction algorithm can not distinguish the human body from other moving objects, however, for the operator of the inspection complex, the information obtained is sufficient, because it is able to understand exactly where the person is and what can correspond to those or other spots on the terahertz image. In the case of intelligent terahertz video surveillance for correct interpretation of the image of this information, of course, not enough. To exclude false positives of the system, it is necessary to take into account the data on the person's position in space, as well as on the position of individual parts of his body on the terahertz image. In this paper, we propose to use 3D vision tools for this purpose, namely, a depth map obtained with the Kinect 2 time-of-flight camera and skeletons calculated using the standard Kinekt 2 software.

The combination of three-dimensional machine vision with terahertz video surveillance is an area of intensive research and experimental development. It is customary to distinguish between passive and active terahertz video surveillance. Active terahertz video surveillance is historically associated with such areas as radar and holography [39, 41]. At present, in the field of active terahertz observation, it has been proposed to use the mechanical and digital beam formation [20, 42, 43], terahertz holography [44, 45], time-of-flight terahertz tomography [46], synthesized apertures [47] to obtain information on the three-dimensional surface of the object under study -49], coding apertures [50-54], frequency modulation of the signal [55], antennas from metamaterials [56], etc. In the area of passive terahertz video surveillance, it was suggested to use the fusion of a terahertz image with 3D images, constructed using 3D-sensors based on structured light and lidar [57, 58], as well as data from multi-camera video [59]. Radar data merging with 3D and visible images is also used in active surveillance systems [60, 61].

At present, it is impossible to predict which terahertz video surveillance systems, active or passive, will find the most widespread. Both approaches have their advantages and disadvantages, and, in addition,

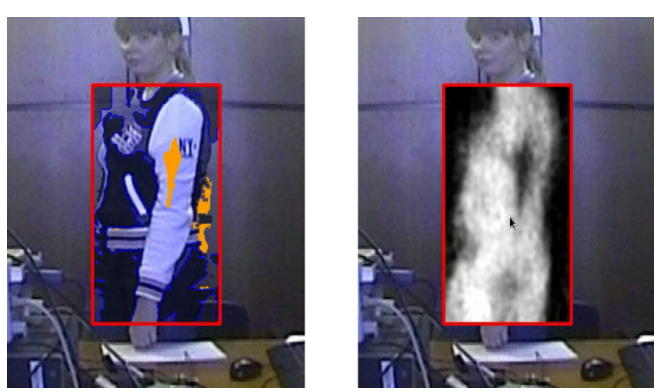

Fig. 2. *An example of the visualization of terahertz data in the industrial inspection complex THERZ-7A (Astrohn Technology Ltd). Software developed by ASoft. On the left is an image in the visible range. Orange marked areas on the human body, where, according to the assumption of the system, some objects are hidden. On the right is an image in the terahertz range, combined with a visible image. The position of the terahertz image relative to the visible image is indicated by a red frame.*

different ways of obtaining terahertz images give different information about the observed objects:

1. It is believed that active systems, theoretically, can provide a terahertz image of a higher quality, because they provide a better signal-to-noise ratio. However, one should take into account that passive systems accept and analyze their own radiation from people and objects (which can be useful, for example, for medical diagnostics); The hidden weapons and objects are clearly visible at the lumen against the background of the human body. Active systems take a reflected terahertz signal; the human body at the same time, as well as the objects hidden under the clothes, create glare that is difficult to interpret. In this situation, the problem of recognition is formulated quite differently.

2. Terahertz radiation, unlike X-ray radiation, is not ionizing and therefore is considered to be safe for humans [62]. At the same time, the widespread use of active terahertz video surveillance systems will inevitably lead to increased electromagnetic pollution of the environment, and this will negatively affect people's health.

3. Active terahertz video surveillance system can be easily detected by electromagnetic radiation, therefore active video surveillance, in fact, ceases to be hidden. Passive systems, at the current level of development, also have drawbacks that prevent them from using for hidden video surveillance, for example, noise from the mechanical system of scanning terahertz radiation.

4. Studies in the field of active systems of terahertz 3D video surveillance are still at the level of experimental installations and prototypes. These systems are still quite cumbersome and inferior to passive terahertz video surveillance systems in terms of frame rate. Nevertheless, in the future such systems can provide information on the form of objects hidden under clothes, which will greatly facilitate their recognition.

5. Separate research areas are terahertz spectroscopy and its use for remote detection of weapons, drugs and explosives. Formally, terahertz spectroscopy systems can be attributed to active systems [16, 24, 63 -65], but they use terahertz radiation of a completely different frequency range. If it is advisable to use subterahertz waves located in the windows for the transparency of clothing (0.1 THz, 0.25 THz, etc.) for tanning clothes, then for terahertz spectroscopy it is necessary to use radiation corresponding to the absorption spectra of the investigated substances (0.5 THz and higher) [65].

To develop and test the method of fusion of terahertz and 3D video images, the industrial passive THERZ-7A THERZ-7A (manufactured by Astrohn Technology Ltd, operating frequency 0.23-0.27 THz) and the Time-of-Flight (ToF) camera of Kinekt 2 (Microsoft Inc). The developed method can also be adapted to the conditions of terahertz illumination. In the case of future industrial terahertz scanning systems scanning 3D surfaces in the terahertz range, the method will require some processing, since the existing algorithms for calculating skeletons of people are trained on video data in the near infrared and visible frequency bands.

3. EXPERIMENTAL INSTALLATION

To conduct experiments with terahertz video surveillance, an experimental setup was assembled, including the industrial THERZ-7A terahertz inspection complex and the Kinekt 2 device (**Fig. 3**). Both devices transmit not one, but several data streams at the same time. The passive terahertz complex transmits a series of terahertz video images with a resolution of 121x207 pixels and a frame rate of 6 Hz (in the proprietary format), as well as an image in the visible range with a resolution of 576x704 pixels and a frame rate of 25 Hz (in MJPEG format). The Kinect 2 device transmits a sequence of three-dimensional frames (coordinates of points in the 3D space) with a frame rate of 30 Hz and a matrix size of 512x424 pixels, a sequence of infrared images also at a frame rate of 30 Hz and a matrix size of 512x424 pixels, a skeleton sequence

(a) (b) (c)

Fig. 3. *An experimental setup that includes a passive terahertz receiver (a), a time-of-flight camera (b) and a calibration board (c).*

of people recognized in the frame 6 people at a time, each skeleton includes up to 25 nodes), a sequence of RGB-frames with a resolution of 1920x1080 pixels and a frame rate of 30 Hz and other information.

During data recording, the devices were connected to different computers, because the capacity (by recording) of the hard drive of one computer is not enough to record in real time the data issued by both devices. Note that the problem with the bandwidth of the hard disk is mainly due to the large volume of 3D data that the Kinekt 2 device provides. In conditions of practical use of the method of semantic fusion of video images, this problem can easily be solved by partial preprocessing and bringing the frequency of three-dimensional frames to the frequency terahertz frames. Computer timers were synchronized before the experiments started, but this does not solve the problem of synchronization of video streams, and later the time shift between frames in different video streams still had to be checked and adjusted manually.

4. CALIBRATION OF THE MEASURING SYSTEM

Before each series of experiments, the experimental setup was calibrated. Calibration of the installation, including a terahertz detector and time-of-flight camera, is a separate technical task. When combining such devices, the same problems arise as when combining three-dimensional vision with a thermal imaging camera [66-68], namely, it becomes necessary to create a special calibration board whose elements will clearly differ in the images obtained with the help of both devices. An additional problem was that the terahertz image has an even lower resolution than what can be obtained with a typical thermal imaging camera. In this case, a small viewing angle of the terahertz camera does not allow to solve the problem by increasing the physical size of the calibration board.

To calibrate the experimental setup, the following approach was developed:

To determine the internal parameters of the optical system of the terahertz complex and its attachment to the time-of-flight camera, we took advantage of the fact that the terahertz image is rigidly tied to the image in the optical range given out

(a) (b)

Fig. 4. *The calibration process of the experimental setup. a) RGB image obtained from the terahertz complex. b) Infrared image obtained from the Kinekt 2 device. For the convenience of moving the calibration board along the crossbar, it is attached using strips of double-sided adhesive tape.*

by the terahertz complex. For calibration, we used RGB images produced by the complex (Fig. 4a), and for experimental records - RGB images combined with terahertz ones (Fig. 1).

The Kinekt 2 device produces infrared images that appear as a by-product in the construction of depth maps (see **Fig. 4**b). This greatly simplifies the task of calibrating the time-of-flight camera, since there is no need to create a relief calibration board visible on the depth map.

For calibration, a standard chessboard pattern measuring 7x10 cells was used, the cell size was 25x25 mm. Dark cells of the board are made of aluminum foil, as this same calibration board is used for thermal imaging [69].

The calibration of the experimental setup includes the calculation of the internal parameters of the optical systems of each of the devices, and then the calculation of the mutual position of the devices and, on the basis of the information on the mutual position, further refinement of their internal parameters. For calculations, the Camera Calibration Toolbox for Matlab software was used [70], in particular, the stereopair calibration algorithm was used to calculate the mutual position of the cameras. The package [70] was developed more than 20 years ago, however, compared to the modern camera calibration package in the Matlab system, it is possible to calibrate a stereopair collected from two cameras with different matrix sizes. Calculation of internal and external parameters of the optical system is an optimization problem, therefore, in order to obtain a stable solution, it is necessary to correctly set limits on the space of values of the parameters

of the model of the optical system. To calibrate the experimental setup, the following limitations were used: to permit the change of the position of the principal point, to take into account two coefficients of radial distortion (out of three possible ones), not to take into account the tangential distortion. To calibrate, up to 45 pairs of calibration images were used (Figure 4), this ensured the accuracy of fitting the model to approximately 0.18 pixels for Kinect 2 and 0.2 RGB pixels for the terahertz complex (**Fig. 5**).

Based on calibration data of the measuring setup, three-dimensional tables of correspondences between the point cloud recorded by the time-of-flight camera and dots on the terahertz image were calculated. In the selected model of the measuring system, the three-dimensional correspondence table is a matrix of 512x424 pixels (the size of the time-of-flight camera matrix) in which the lists of quadratic polynomial coefficients are written to calculate the coordinates on the RGB image produced by the terahertz complex. In each cell of the matrix (i, j) six coefficients p1, p2, p3, q1, q2, q3 are written. The coordinates (x, y) in the RGB image are calculated using quadratic polynomials depending on the reciprocal distance d (i, j) in meters from the time-of-flight camera to the point (i, j) on the surface:

$x = p1\ (1 / d)\ 2 + p2\ (1 / d) + p3,$

$y = q1\ (1 / d)\ 2 + q2\ (1 / d) + q3.$

3D match tables are used for fast (in real time) fusion of video images received from different devices.

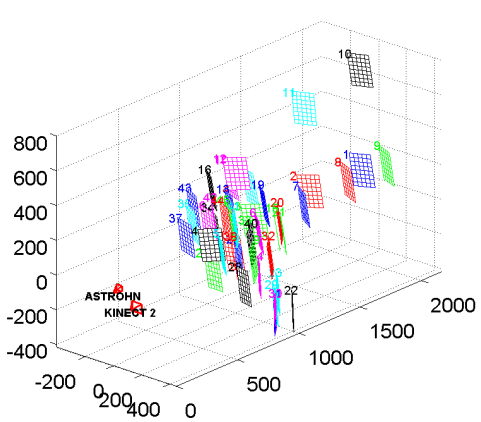

Fig. 5. *The results of the joint calibration of terahertz and time-of-flight cameras as stereo pairs. For calculations, the software package Camera Calibration Toolbox for Matlab [70] was used. Dimensions on axes are in millimeters.*

5. EXPERIMENTAL SOFTWARE

Working with three-dimensional correspondence tables is implemented in the built-in KinectBuffer class of the object-oriented logical language Actor Prolog [71-83]. This class is designed to receive data from the time-of-flight camera of the Kinect 2 device, and also to record and read the created 3D video. A detailed description of the built-in KinectBuffer class can be found in [69].

One of the functions of the built-in KinectBuffer class is the construction of a three-dimensional surface based on a cloud of points and the projection onto this surface of a given texture using a previously prepared correspondence table. We used these tools to merge 3D and terahertz video images in our experiments. The main problem that arises in this way of merging video images is the synchronization of video streams with different frame rates. This problem is complicated by the fact that the frame rate in video streams is not constant. In particular, the frame rate of the skeleton stream produced by the standard SDK of the Kinekt 2 device may not correspond to the frequency of the 3D frames. To solve the problem of synchronization of video streams, a method of "advanced reading" of terahertz video data was developed. This method is implemented in a special built-in class of Actor Prologue Astrohn.

The built-in Astrohn class is designed to produce terahertz and RGB video data from the THERZ-7A device. As well as the built-in KinectBuffer class, the built-in Astrohn class supports data input directly from an external device, as well as recording video data to a file and reading video data from a file. The Astrohn class supports the conversion of terahertz video data into color images. In particular, in the form of color images, terahertz data (using pseudocolours), RGB data transmitted by the terahertz complex, as well as RGB data combined with the current terahertz image can be presented directly. The Astrohn class supports the simplest mode of video frame synchronization, which combines terahertz and RGB images, obtained as close as possible in time. Currently, the Astrohn class supports more than 25 high resolution color scales, including the color scales Aqua, Blackhot, Blaze, BlueRed, Gray, Hot, HSV, Iron, Red (Jet), Medical, Parula, Purple, Green (Rainbow) .

To synchronize terahertz images with three-dimensional video data in the Astrohn class, the method of advanced reading of terahertz video data is realized, the idea of which is as follows. The video data is read from the file and written to the temporary buffer. Each frame of video data is characterized by the time it was received from the device (in milliseconds, in a universal timeline beginning on January 1, 1970). As the buffer is full, data reading is suspended until the program accesses any data frame. You can access the data frame using the built-in predicate retrieve_timed_frame. This predicate checks if there is a frame in the buffer with a given timestamp T, and, depending on the results of the check, performs the following actions:

If two frames with timestamps ti and ti + 1 are present in the buffer, such that ti ≤ T and T ≤ ti + 1, then one of these frames is selected which is closest in time to T. The frame is transferred to the program for processing, in particular , the program receives an asynchronous message frame_obtained, signaling the receipt of the required frame of video data. Reading video data from a file is resumed and continues until the selected frame is in the middle of the buffer. As the buffer overflows, the oldest video frames are discarded.

If the last video frame in the buffer has a timestamp tE, such that tE <T, reading of the video data into the buffer is resumed, and the execution of the predicate retrieve_timed_frame is suspended until a video frame with a suitable timestamp is received.

If the first time frame in the buffer has a timestamp tB, such that T <tB, the execution of the predicate retrieve_timed_frame fails, the logical program rolls back.

The method of advanced reading of video data allows you to adaptively change the speed of reading a video file and synchronize the speed of reading video data received from different devices. The volume of three-dimensional video data obtained with a time-of-flight camera is much higher than the amount of terahertz data, so it is advisable to adapt the control of reading terahertz data, depending on the actually achieved rate of arrival of three-dimensional video frames.

In **Fig. 6** shows an example of a three-dimensional image constructed by merging a point cloud obtained from a time-of-flight camera and a

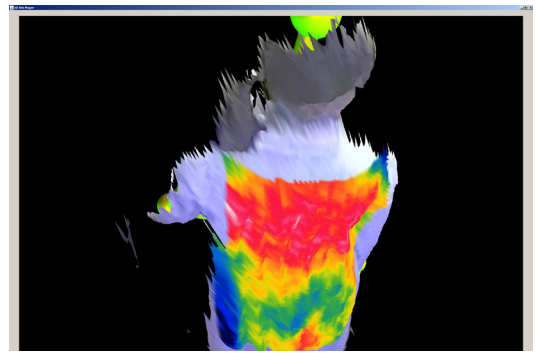

Fig. 6. *An example of a terahertz video image projected on a three-dimensional surface of the human body. The terahertz image is placed against the visible. To display the terahertz data, the same color scale is used as in Fig. 1.*

terahertz image. In **Fig. 7**, the same data is displayed, but the terahertz image is combined with the human skeleton calculated by the standard SDK of the Kinekt 2 device. Using a 3D match table allows you to project a terahertz image onto a three-dimensional surface at a real-time tempo. In particular, the three-dimensional video shown in the figures can be rotated, scaled, or shifted with the mouse directly during playback.

6. CONCLUSION

As a basis for intelligent terahertz video surveillance, a method of semantic fusion of terahertz video with video images obtained on the basis of other physical principles, in particular, with a three-dimensional video image obtained with a time-of-flight camera, is proposed. For experiments with terahertz video surveillance, tools for object-oriented logical programming have been created, namely, built-in classes of the Actor Prolog language for input, recording, reading and synchronizing video streams

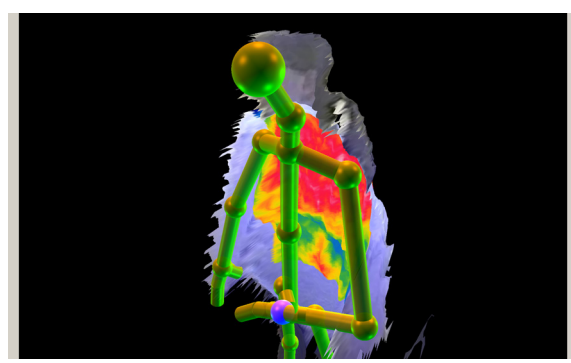

Fig. 7. *An example of a terahertz video image projected on a three-dimensional surface of the human body. The three-dimensional surface is combined with the skeleton, which reflects the position of the head, arms, legs and other parts of the human body relative to the terahertz video image.*

in terahertz and visible frequency ranges, and also three-dimensional video. The experimental verification demonstrated that the developed tools allow in real time to project a terahertz video image onto a three-dimensional surface of a person obtained with a time-of-flight camera. This information can be used by algorithms of automatic analysis to determine the position of a person and certain parts of his body with respect to a terahertz image, which will improve the quality of recognition of objects hidden under clothing. With the help of the developed tools, samples of multi-channel heterogeneous video images of people, weapons and objects were collected, which will later be used to teach algorithms for recognizing objects hidden under clothing.

ACKNOLEDGMENT

The authors are grateful to I.A. Kershneru and R.A. Tolmacheva for participating in ongoing experiments, as well as companies Astron CJSC and ASoft Ltd. for providing equipment for recording terahertz radiation THERZ-7A. The study was carried out with the support of the Russian Foundation for Basic Research (Project No. 16-29-09626-OI).

REFERENCES

1. Vollmer M, Möllmann KP. *Infrared Thermal Imaging. Fundamentals, Research and Applications.* Weinheim, WILEY-VCH, 2010, 612 p.
2. Chan WL, Deibel J, Mittleman DM. Imaging with terahertz radiation. *Reports on progress in physics.* 2007, 70(8):1325.
3. Sethy PK, Mishra PR, Behera S. An Introduction to Terahertz Technology, Its History, Properties and Application. *Intern. conf. on computing and communication,* 2015.
4. Zhu L, Suomalainen J, Liu J, Hyyppä J, Kaartinen H, Haggren H. A Review: Remote Sensing Sensors. In: Rustamov RB, Hasanova S, Zeynalova MH, editors. Multi-purposeful Application of Geospatial Data. *IntechOpen,* 2018, p. 19-42.
5. Sanders-Reed JN. Applications and challenges for MMW and THz sensors. In: Micro- and Nanotechnology Sensors, Systems, and Applications VII. *Proc. of SPIE*, 2015, vol. 9467, p. 94672E.
6. Appleby R, Robertson DA, Wikner D. Millimeter wave imaging: a historical review. *Proc. SPIE Passive and Active Millimeter-Wave Imaging XX*, 2017, vol. 10189, p. 1018902.
7. Sizov FF. Infrared and terahertz in biomedicine. *Semiconductor Physics, Quantum Electronics & Optoelectronics*, 2017, 20(3):273-283.
8. Cherevko AG, Iljin EM, Morgachev JD, Polubehin AI. Analysis of patent activity in the field of advanced radar technology in extra-long infrared wavelength range. *Vestnik SibGUTI*, 2015, 2:164-173 (in Russ.).
9. Jackson JB, Bowen J, Walker G, Labaune J, Mourou G, Menu M, et al. A survey of terahertz applications in cultural heritage conservation science. *IEEE Transactions on Terahertz Science and Technology,* 2011, 1(1):220-231.
10. Kemp MC. A review of millimetre-wave and terahertz technology for detection of concealed threats. *Proc. IEEE 33rd Intern. Conf. on Infrared and Millimeter Waves*, 2008, p. 1-2.
11. Kemp MC. Millimetre wave and terahertz technology for detection of concealed threats – a review. *Proc. IEEE Joint 32nd Intern. Conf. on Infrared and Millimeter Waves*, 2007, p. 647-648.
12. Taylor ZD, Singh RS, Bennett DB, Tewari P, Kealey CP, Bajwa N, et al. THz medical imaging: in vivo hydration sensing. *IEEE transactions on terahertz science and technology*, 2011, 1(1):201-219.
13. Antsiperov VE. Automatic target recognition algorithm for lowcount terahertz images. *Computer Optics*, 2016, 40(5):746-751.
14. Astahov SP, Stroev NN, Sulimski ES. Features of the Software for Design of Research Complex Using Subteraherz Matrix Camera. *Mathematical morphology,* 2015, 14(1) (in Russ.).
15. Kowalski M, Kastek M, Piszczek M, Życzkowski M, Szustakowski M. Harmless screening of humans for the detection of concealed objects. *WIT Transactions on The Built Environment*, 2015, 151:215-223.
16. Angeluts AA, Balakin AV, Borodin AV, Borodin AV, Esaulkov MN, Nazarov MM, et al. Terahertz Spectroscopy and Imaging. *Russian Foundation for Basic Research Journal,* 2014, 83(3):21-36 (in Russ.).
17. Ozhegov R, Gorshkov K, Vachtomin YB, Smirnov K, Finkel M, Goltsman G, et al. Terahertz imaging system based on superconducting heterodyne integrated receiver. In: *THz and Security Applications.* Springer; 2014, p. 113-125.

18. Chrzanowski K. Testing passive surveillance terahertz imagers. *Optica Applicata,* 2013, 43(2):359-371.
19. Trofimov VA, Trofimov VV, Deng C, Zhao Y, Zhang C, Zhang X. Possible way for increasing the quality of imaging from THz passive device. *Proc. of SPIE*, 2011, Vol. 8189:81890L.
20. Cooper KB, Dengler RJ, Llombart N, Thomas B, Chattopadhyay G, Siegel PH. THz imaging radar for standoff personnel screening. *IEEE Transactions on Terahertz Science and Technology,* 2011, 1(1):169-182.
21. Shen X, Dietlein CR, Grossman E, Popovic Z, Meyer FG. Detection and segmentation of concealed objects in terahertz images. *IEEE Transactions on Image Processing,* 2008, 17(12):2465-2475.
22. Semenov A, Richter H, Böttger U, Hübers HW. Imaging terahertz radar for security applications. *Terahertz for Military and Security Applications VI*, 2008, vol. 6949:694902.
23. Kemp MC. Detecting hidden objects: Security imaging using millimetre-waves and terahertz. *IEEE Conference on Advanced Video and Signal Based Surveillance*, 2007, p. 7-9.
24. Federici JF, Schulkin B, Huang F, Gary D, Barat R, Oliveira F, et al. THz imaging and sensing for security applications – explosives, weapons and drugs. *Semiconductor Science and Technology,* 2005, 20(7):S266.
25. Spiegel W, Weg C, Henneberger R, Zimmermann R, Roskos HG. Illumination aspects in active terahertz imaging. *IEEE Trans. Microw. Theory Tech*, 2010, 58(7):2008-2013.
26. Friederich F, Spiegel W, Bauer M, Meng F, Thomson MD, Boppel S, et al. THz active imaging systems with realtime capabilities. *IEEE Transactions on Terahertz Science and Technology,* 2011, 1(1):183-200.
27. Pfeiffer UR, Zhao Y, Grzyb J, Al Hadi R, Sarmah N, Förster W, et al. A 0.53 THz reconfigurable source module with up to 1 mW radiated power for diffuse illumination in terahertz imaging applications. *IEEE Journal of Solid-State Circuits*, 2014, 49(12):2938-2950.
28. Kowalski M, Piszczek M, Palka N, Szustakowski M. The methodology of THz-VIS fused images evaluation. *Photonics Letters of Poland*, 2013, 5(1):32-34.
29. Stroev NN, Sulimski ES. Research of means of multiframes representation for application in systems of radiovision of subterahertz range. *Yugra State University Bulletin,* 2016, (2):17-20 (in Russ.).
30. Trofimov VA, Trofimov VV, Shestakov IL, Blednov RG, Kovalev VY. Effective algorithm based on Fourier transform for the passive THz image quality enhancement. *Image Sensing Technologies: Materials, Devices, Systems, and Applications IV,* 2017, vol. 10209:1020907.
31. Trofimov VA, Trofimov VV. New algorithm for the passive THz image quality enhancement. *Terahertz Physics, Devices, and Systems X: Advanced Applications in Industry and Defense.* 2016, vol. 9856:98560M.
32. Trofimov VA, Trofimov VV, Palka N, Kowalski M. Computer Processing of Images Captured with a Commercially Available THz Camera at Long Distances. *Terahertz and Mid Infrared Radiation: Detection of Explosives and CBRN (Using Terahertz).* Springer, 2014, p. 167-174.
33. Trofimov VA, Trofimov VV, Kuchik IE, Zhang Cl, Deng C, Zhao Ym, et al. Computer processing of image captured by the passive THz imaging device as an effective tool for its de-noising. *Infrared, Millimeter-Wave, and Terahertz Technologies II*, 2012, vol. 8562:856207.
34. Cooper K, Dengler R, Llombart N, Bryllert T, Chattopadhyay G, Mehdi I, et al. An approach for sub-second imaging of concealed objects using terahertz (THz) radar. *Journal of Infrared, Millimeter, and Terahertz Waves*, 2009, 30(12):1297-1307.
35. Ramasamy Ramamurthy S, Roy N. Recent trends in machine learning for human activity recognition – A survey. *Wiley Interdisciplinary Reviews: Data Mining and Knowledge Discovery,* 2018, p. e1254.
36. Vineet V, Miksik O, Lidegaard M, Nießner M, Golodetz S, Prisacariu VA, et al. Incremental dense semantic stereo fusion for large-scale semantic scene reconstruction. *IEEE International Conference on Robotics and Automation*, 2015, p. 75-82.
37. Oliveira L, Nunes U, Peixoto P, Silva M, Moita F. Semantic fusion of laser and vision in pedestrian detection. *Pattern Recognition,* 2010, 43:3648-3659.

38. Lewis JJ, O'Callaghan RJ, Nikolov SG, Bull DR, Canagarajah N. Pixel-and region-based image fusion with complex wavelets. *Information fusion,* 2007, 8(2):119-130.
39. Mittleman DM. Twenty years of terahertz imaging. *Optics express*, 2018, 26(8):9417-9431.
40. Guillet JP, Recur B, Frederique L, Bousquet B, Canioni L, Manek-Hönninger I, et al. Review of terahertz tomography techniques. *Journal of Infrared, Millimeter, and Terahertz Waves,* 2014, 35(4):382-411.
41. Zhang XC. Three-dimensional terahertz wave imaging. *Philosophical Transactions of the Royal Society of London A: Mathematical, Physical and Engineering Sciences*, 2004, 362(1815):283-299.
42. Gao J, Cui Z, Cheng B, Qin Y, Deng X, Deng B, et al. Fast Three-Dimensional Image Reconstruction of a Standoff Screening System in the Terahertz Regime. *IEEE Transactions on Terahertz Science and Technology*, 2018, 8(1):38-51.
43. Nowok S, Herschel R, Zimmermann R, Shoykhetbrod A, Lang SA, Pohl N. 3*D* Imaging System Based on a MIMO Approach at 360GHz for Security Screening. *Proc. 37th PIERS: Progress In Electromagnetic Research Symposium*, Shanghai, China; 2016, p. 671-675.
44. Zhou M. *A Terahertz Holography Imaging System for Concealed Weapon Detection Application*. School of Electronic and Engineering and Computer Science, Queen Mary, University of London, 2017, p. 219.
45. Liu W, Li C, Sun Z, Zhang Q, Fang G. Three-dimensional sparse image reconstruction for terahertz surface layer holography with random step frequency. *Optics letters*, 2015, 40(14):3384-3387.
46. Jun Takayanagi, Hiroki Jinno, Shingo Ichino et al. High-resolution time-of-flight terahertz tomography using a femtosecond fiber laser. *Optics Express,* 2009, 17(9):7533-7539
47. Hao J, Li J, Pi Y. Three-Dimensional Imaging of Terahertz Circular SAR with Sparse Linear Array. *Sensors* (Basel, Switzerland), 2018, 18(8):2477.
48. Rezgui ND, Andrews DA, Bowring NJ. Ultra Wide Band 3D Microwave Imaging Scanner for the Detection of Concealed Weapons. *Proc. SPIE Millimetre Wave and Terahertz Sensors and Technology VII*I, 2015, vol. 9651:965108–1.
49. Gu S, Li C, Gao X, Sun Z, Fang G. Terahertz aperture synthesized imaging with fan-beam scanning for personnel screening. *IEEE transactions on microwave theory and techniques,* 2012, 60(12):3877-3885.
50. Chen S, Luo CG, Wang HQ, Peng L, Deng B, Zhuang ZW. Three-Dimensional Terahertz Coded-Aperture Imaging in Space Domain. *IEEE Access,* 2018, 6:32727-32736.
51. Chen S, Luo C, Wang H, Wang W, Peng L, Zhuang Z. Three-Dimensional Terahertz Coded-Aperture Imaging Based on Back Projection. *Sensors* (Basel, Switzerland), 2018, 18(8):2510.
52. Chen S, Luo C, Wang H, Deng B, Cheng Y, Zhuang Z. Three-Dimensional terahertz coded-aperture imaging based on matched filtering and convolutional neural network. *Sensors* (Basel, Switzerland), 2018, 18(5):1342.
53. Chen S, Luo C, Deng B, Wang H, ID YC. Three-Dimensional Terahertz Coded-Aperture Imaging Based on Single Input Multiple Output Technology. *Sensors*, 2018, 18(1):303.
54. Chen S, Hua X, Wang H, Luo C, Cheng Y, Deng B. Three- Dimensional Terahertz Coded-Aperture Imaging Based on Geometric Measures. *Sensors,* 2018, 18(5):1582.
55. Trontelj J, Sešek A. Electronic terahertz imaging for security applications. T*erahertz, RF, Millimeter, and Submillimeter-Wave Technology and Applications IX*, 2016, vol. 9747:974713.
56. Gollub J, Yurduseven O, Trofatter K, Arnitz D, Imani M, Sleasman T, et al. Large metasurface aperture for millimeter wave computational imaging at the human-scale. *Scientific reports,* 2017, 7:42650.
57. Engström P, Axelsson M, Karlsson M. Microsoft Kinect for THz Sensor Management. *Proc. 3rd Intern. Conf. on 3D Body Scanning Technologies*, Lugano, Switzerland, Hometrica Consulting; 2012, p. 311-319.
58. Engström P, Axelsson M, Karlsson M. Combining structured light and Ladar for pose tracking in THz sensor management. *Signal Processing, Sensor Fusion, and Target Recognition XXII*, 2013, vol. 8745:874515.
59. Axelsson M, Karlsson M, Rudner S. A multi-camera positioning system for steering of a THz stand-off scanner. *Passive Millimeter- Wave Imaging Technology XIV,* 2011, vol. 8022:80220L.

60. Natour GE, Ait-Aider O, Rouveure R, Berry F, Faure P. Toward 3D reconstruction of Outdoor Scenes using an MMW radar and a monocular vision sensor. *Sensors,* 2015, 15(10):25937-25967.
61. Hantscher S, Essen H, Warok P, Zimmermann R, Schröder M, Sommer R, et al. LAOTSE, an Approach for Foreign Object Detection by multimodal netted 2D/3D Sensors. *IEEE Tyrrhenian Intern. Workshop on Digital Communications-Enhanced Surveillance of Aircraft and Vehicles*, 2011, p. 61-64.
62. Angeluts AA, Gapeyev AB, Esaulkov MN, Kosareva OG, Matyunin SN, Nazarov MM, et al. Study of terahertz-radiation-induced DNA damage in human blood leukocytes. *Quantum Electronics*, 2014, 44(3):247.
63. Rahman A, Rahman AK, Rao B. Early detection of skin cancer via terahertz spectral profiling and 3D imaging. *Biosensors and Bioelectronics*, 2016, 82:64-70.
64. Jeunesse P, Schmidhammer U. "On-the-Fly" Monitoring With a Single-Shot Terahertz Time-Domain Spectrometer. *IEEE Sensors Journal*, 2013, 13(1):44-49.
65. Baker C, Lo T, Tribe W, Cole B, Hogbin M, Kemp M. Detection of concealed explosives at a distance using terahertz technology. *Proc. of the IEEE*. 2007, 95(8):1559-1565.
66. Chernov G, Chernov V, Flores MB. 3D dynamic thermography system for biomedical applications. In: *Application of Infrared to Biomedical Sciences*. Springer; 2017, p. 517-545.
67. Rangel J, Soldan S, Kroll A. 3D thermal imaging: Fusion of thermography and depth cameras, robotics and autimation. *IEEE Intern. Conf. on Quantitative InfraRed Thermography*; 2014, pp.2311-2318.
68. Skala K, Lipić T, Sović I, Gjenero L, Grubišić I. 4D thermal imaging system for medical applications. *Periodicum biologorum*, 2011, 113(4):407-416.
69. Morozov AA, Sushkova OS, Petrova NG, Khokhlova MN, Migniot C. Development of Agent Logic Programming Means for Multichannel Intelligent Video Surveillance. *Radioelektronika. Nanosistemy. Informacionnye Tehnologii* (*RENSIT*), 2018, 10(1):101-116.
70. Bouguet JY. Camera Calibration Toolbox for Matlab. Pasadena, U.S., 2015. [Online] Available from: http://www.vision.caltech.edu/bouguetj/calib_doc/htmls/ref.html.
71. Morozov AA, Sushkova OS, Polupanov AF. Object-oriented logic programming of 3D intelligent video surveillance systems: The problem statement. *RENSIT*, 2017, 2(9):205-214.
72. Morozov AA, Sushkova OS. Real-time analysis of video by means of the Actor Prolog language. *Computer Optics,* 2016, 40(6):947-957.
73. Morozov AA, Sushkova OS, Polupanov AF. Towards the Distributed Logic Programming of Intelligent Visual Surveillance Applications. In: Pichardo-Lagunas O, Miranda-Jimenez S, editors. *Advances in Soft Computing, Part II*. Cham: Springer, 2017, p. 42-53.
74. Morozov AA. Development of a Method for Intelligent Video Monitoring of Abnormal Behavior of People Based on Parallel Object-Oriented Logic Programming. *Pattern Recognition and Image Analysis*, 2015, 25(3):481-492.
75. Morozov AA, Vaish A, Polupanov AF, Antciperov VE, Lychkov II, Alfimtsev AN, et al. Development of concurrent object-oriented logic programming platform for the intelligent monitoring of anomalous human activities. *BIOSTEC 2014*, vol. 511 of CCIS, Heidelberg, Springer, 2015, p. 82-97.
76. Morozov AA, Vaish A, Polupanov AF, Antciperov VE, Lychkov II, Alfimtsev AN, et al. Development of concurrent object-oriented logic programming system to intelligent monitoring of anomalous human activities. *BIODEVICES 2014*. SCITEPRESS, 2014, p. 53-62.
77. Morozov AA. Visual Logic Programming Based on the SADT diagrams. *ICLP 2007,* LNCS 4670, Heidelberg, Springer, 2007, p. 436-437.
78. Morozov AA. Development and Application of Logical Actors Mathematical Apparatus for Logic Programming of Web Agents. ICLP 2003, LNCS 2916, Heidelberg, Springer, 2003, p. 494-495.
79. Morozov AA. Logic Object-Oriented Model of Asynchronous Concurrent Computations. *Pattern Recognition and Image Analysis,* 2003, 13(4):640-649.
80. Morozov AA, Obukhov YV. An Approach to Logic Programming of Intelligent Agents for Searching and Recognizing Information on the

Internet. *Pattern Recognition and Image Analysis*, 2001, 11(3):570-582.

81. Morozov AA. Actor Prolog: an Object-Oriented Language with the Classical Declarative Semantics. *IDL-1999,* Paris, France, 1999, p. 39-53.
82. Morozov AA. The Prolog with Actors. *Programmirovanie*, 1994, (5):66-78 (in Russ.).
83. Morozov AA, Sushkova OS. The Intelligent Visual Surveillance Logic Programming Web Site, 2018, Available from: http://www.fullvision.ru.

Radioelectronics. Nanosystems. Information Technologies (abbr. RENSIT)
Certificate El. no. FS77-60275 on 19.12.2014 of the Ministry of Telecom and Mass Communications of Russian Federation, Moscow
ISSN: 2414-1267online. Http://www.rensit.ru. Publisher - Vladimir I. Grachev. 2017, 30 Dec.
Computer printing, page-proofs, graphics, photos of work - the editors RENSIT.